INDSWG – 7/
INDC(IND)*004/G

PROCEEDINGS OF THE

Nuclear Physics And Solid State Physics Symposium 1965

NUCLEAR PHYSICS

CALCUTTA
February 8 – February 13, 1965

ORGANISED BY
PHYSICS ADVISORY COMMITTEE
DEPARTMENT OF ATOMIC ENERGY
GOVERNMENT OF INDIA

C O N T E N T S

NUCLEAR PHYSICS.

Request for copies of this volume

should be addressed

to

Scientific Information Officer,

Atomic Energy Establishment Trombay,

Old Yacht Club,

Apollo Pier Road,

Bombay-1.

India.

P R O G R A M M E

NUCLEAR PHYSICS

11th February, 1965

SESSION I

Chairman : B.V. Thosar

SESSION II

Chairman: D.N. Kundu

---

*Presented by this author.

SESSION III

Chairman : K.K. Gupta

SESSION IV

Chairman : M.K. Banerjee

SESSION VII

Chairman : S.N. Ghosal

SESSION VIII

Chairman ; N.K. Saha.

SESSION IX

13th February, 1965

Chairman: S.P. Pandya

SESSION X

Chairman: Santimay Chatterjee

SESSION XI.

Chairman: E. Kondaih.

BETA-DECAY AND NUCLEAR STRUCTURE

Rolf M. Steffen*
Tata Institute of Fundamental Research, Bombay-5

During the past fifteen years, the development and refinement of nuclear models has been largely based on data involving electromagnetic interactions (e.g. gamma transition probabilities, static magnetic and electric moments, etc.). The clarification of the interaction laws in β -decay and the rapid accumulation of precise β -decay data for allowed and forbidden transitions makes the interpretation of these data in terms of nuclear structure models possible and desirable.

ALLOWED BETA DECAY

Ft-values of medium heavy beta emitters have been explained as effects of the pairing correlation. Saki and Yoshida (1) used experimental ft-values of Gamow-Teller transition of the types $p_{3/2} \longrightarrow p_{1/2}$ in the Ga-Sr region, $g_{9/2} \longrightarrow g_{7/2}$ in the Rh-In region and $d_{5/2} \longrightarrow d_{3/2}$ in the Sb-Nd region to compute the fractional occupation parameters U^2 and V^2. The values obtained with the beta decay data were found to be consistent with the values obtained from (d,p) and (d,t) cross-section data.

The discovery of parity violation in β -decay made measurements of the ratio $X = \langle 1 \rangle / \langle \vec{\sigma} \rangle$ of the Fermi matrix element $\langle 1 \rangle$ and the Gamow-Teller matrix element $\langle \vec{\sigma} \rangle$ by β-γ circular polarization correlation experiments possible. These matrix elements obey the following isotopic spin selection rules:

$$\langle 1 \rangle = 0 \qquad \text{unless} \qquad \Delta T = 0$$
$$\langle \vec{\sigma} \rangle = 0 \qquad \text{unless} \qquad \Delta T = 0,\ 1.$$

---

* Permanent address: Purdue University, Lafayette, Indiana, U.S.A.

Only in the neutron decay and in the beta decay of mirror nuclei is $\Delta T = 0$. Hence in all other beta transitions the Fermi component should vanish if isotopic spin is a good quantum number of the nuclear states involved. The presence of large Fermi components in such transitions would imply that nuclear forces are not charge independent, regardless whether the CVC theory is valid or not. Small Fermi matrix elements may be present if the nuclear forces show a small charge dependence or, for charge independent nuclear forces, if the CVC theory does not hold.

The experimental values of the Fermi matrix element $\langle 1 \rangle$ for several mixed beta-transitions are summarized in Table 1. In all cases the Fermi matrix elements are found to be very small indeed, even for beta transitions in nuclei of fairly large Z. In the latter cases one might expect the isotopic spin concept to be rather poor because of Coulomb effects. Nevertheless, the experiments indicate that the isotopic-spin impurities are surprisingly small even in medium heavy nuclei. Some allowed beta transitions have unusually large ft-values (log ft > 7) indicating that the ordinary allowed matrix elements, especially $\langle \vec{\sigma} \rangle$ are very small. In these cases one might expect that the contributions of second forbidden matrix elements are measurably large. In particular, directional correlations should display small anisotropies caused by the cross terms of the $\langle \vec{\sigma} \rangle$ matrix element and certain second forbidden matrix elements (specially terms containing $\langle \vec{\sigma} \rangle \langle (\vec{\sigma} \cdot \vec{r}) \vec{r} \rangle$ and $\langle \vec{\sigma} \rangle \langle i \gamma_5 \vec{r} \rangle$. Asystematic search for such anisotropies in several hindered allowed beta-transitions revealed that the effects are too small for observation.

The experimental results (2) are summarised in Table 2. The nuclear structure parameter η in the fifth column indicates by what factor the $\langle \vec{\sigma} \rangle$ matrix element is reduced from its "normal" value ("normal" value of log ft= 4.5).

TABLE I

Fermi Matrix Elements in Mixed Allowed β Transitions

isotope	spin parity	log ft	$x = \frac{\langle 1 \rangle}{\langle \sigma \rangle}$	$\frac{\langle 1 \rangle}{10^{-3}}$
F^{20}	2^+	5.0	-0.031 ± 0.072	-6.6 ± 15.3
Na^{24}	4^+	6.1	$+0.011 \pm 0.017$	$+0.7 \pm 1.0$
Al^{24}	4^+	6.1	-0.005 ± 0.063	-0.3 ± 3.8
Ar^{41}	$7/2^-$	5.0	-0.019 ± 0.055	-4.1 ± 11.6
Sc^{44}	2^+	5.3	$+0.052 \pm 0.019$	$+7.7 \pm 2.9$
Sc^{46}	4^+	6.2	$+0.021 \pm 0.006$	$+1.1 \pm 0.3$
Sc^{48}	6^+	5.5	$+0.007 \pm 0.067$	$+0.9 \pm 7.9$
V^{48}	4^+	6.1	$+0.073 \pm 0.042$	$+4.3 \pm 2.5$
Mn^{52}	6^+	5.5	$+0.043 \pm 0.005$	$+5.1 \pm 0.6$
Co^{56}	4^+	8.7	$+0.027 \pm 0.014$	$+0.08 \pm 0.04$
Co^{58}	2^+	6.6	$+0.057 \pm 0.019$	$+1.9 \pm 0.7$
Ag^{110m}	6^+	8.2	$+0.024 \pm 0.033$	$+0.13 \pm 0.18$
Sb^{124}	3^-	7.7	$+0.043 \pm 0.016$	$+0.41 \pm 0.15$
Cs^{134}	4^+	8.9	-0.312 ± 0.028	-0.72 ± 0.07
Eu^{152}	3^-	10.6	-0.048 ± 0.026	-0.016 ± 0.009
Eu^{154}	3^-	9.9	0	0

TABLE II

Higher-Order Effects in Allowed β -Transitions

isotope	Transition	W_o	log ft	η	A_{22} (%)	$A_{22\,exp}$ (%)
F^{20}	$2^+ \longrightarrow 2^+$	11.6	5.0	2	-0.5 (CVC)	-1.05 ± 0.31
Na^{22}	$3^+ \longrightarrow 2^+$	1.69	7.4	+28	± 0.04	-0.18 ± 0.03
Na^{24}	$4^+ \longrightarrow 4^+$	3.15	6.1	± 6	± 0.04	$+0.02 \pm 0.04$
Sc^{46}	$4^+ \longrightarrow 4^+$	1.4	6.2	± 7	± 0.01	$+0.02 \pm 0.04$
Mn^{56}	$3^+ \longrightarrow 2^+$	6.6	7.2	± 22	± 0.5	0.0 ± 0.2
Co^{56}	$4^+ \longrightarrow 4^+$	3.9	8.7	± 126	-3.6 +4.3	-0.1 ± 0.3
Co^{60}	$5^+ \longrightarrow 4^+$	1.4	7.4	± 28	∓ 0.04	-0.02 ± 0.03
Sb^{124}	$3^- \longrightarrow 3^-$	2.2	7.7	± 40	-0.4 +2.2	$+0.2 \pm 0.3$
Cs^{134}	$4^+ \longrightarrow 4^+$	2.3	8.9	± 160	+0.4 -4.8	$+0.1 \pm 0.3$
Eu^{152}	$3^- \longrightarrow 3^-$	2.37	10.8	1400	large	
Eu^{154}	$3^- \longrightarrow 3^-$	2.63	10.9	1600	large	under investigation
Eu^{154}	$3^- \longrightarrow 2^-$	2.1	9.9	500	large	
Tb^{160}	$3^- \longrightarrow 3^-$	1.9	8.1	± 63	-0.4 1	$=1.5 \pm 0.8$

The sixth column gives the anisotropy factor A_{22} of the β-γ directional correlation function

$$W(\theta) = 1 + A_{22} P_2 (\cos\theta)$$

computed from η . The experimental values of A_{22} are listed in the seventh column.

In all cases investigated, the anisotropies were found to be smaller than one percent. This experimental fact indicate, that the nuclear structure mechanism that reduces the allowed matrix elements is also responsible for an appreciable reduction of the second forbidden matrix elements.

FIRST-FORBIDDEN BETA-TRANSITIONS

Recently it has become possible in several cases to extract the individual matrix elements that contribute to first-forbidden beta transitions by combining shape measurement and angular correlation data. The interpretation of these data in terms of various nuclear models may contribute significantly to the understanding of the structure of the nuclear levels involved in beta transitions.

Some typical results for first-forbidden matrix elements are summarized in Table 3. In the beta transitions of Sb^{124}, Eu^{152} and Eu^{154} the tensor type matrix element $\langle B_{ij} \rangle$ plays a dominant role. The possible reasons for the reduction of the vector type matrix elements causing the relative dominance of $\langle B_{ij} \rangle$ are indicated in the last column of Table. 3. In the case of La^{140} the transforming nucleon crosses into a different major shell and therefore the vector type matrix elements are not reduced by j-selection rule effects. In accordance with this picture, the vector type matrix elements are found to be large as compared to $\langle B_{ij} \rangle$. In this case the large ft-value and the forbidden shape of the spectrum is caused by cancellations of the vector type matrix elements.

TABLE III

Matrix Elements in First-Forbidden Beta Transitions

β-Decay	Log ft_c	$\frac{\langle B_{ij} \rangle}{R}$ (10^{-3})	$\frac{\langle r \rangle}{R}$ (10^{-3})	$\frac{\langle i\vec{\sigma} \times \vec{r} \rangle}{R}$ (10^{-3})	$\langle i\vec{\alpha} \rangle$ (10^{-4})	A_{exp}	A_{CVC}	Remarks
Super	5.5	1000	1000	1000	1000			Maximum overlap Configuration mixing
Normal	7.5	200	100	100	100			
Sb^{124}	10.5	14 ± 2	-1 ± 2	-1 ± 1	1.6 ± 0.8	$-0.16\pm$	0.50	$h^-_{11/2} \to g^+_{7/2}$, $d^+_{5/2}$, $d^+_{3/2}$, $S_{\frac{1}{2}}$
Eu^{152}	12.0	2.9 ± 0.4	0.4 ± 0.2	0.4 ± 0.2	2.5 ± 1.1	0.6 ± 0.5	0.58	deformed $\to$ spherical
Eu^{154}	12.7	1.2 ± 0.2	-0.05 ± 0.15	2.3 ± 1.4	0.7 ± 0.5	$-1.4 \pm$	0.60	K = 3
La^{140}	9.1	9 ± 2	32 ± 16	-43 ± 26	81 ± 30	$0.19^{+0.46}_{-0.12}$	0.53	crosses major shell cancellation effect $g^+_{7/2}$ $h^-_{9/2} \to f^-_{7/2}$
Ga^{72}	8.9	90 ± 30	70 ± 50	11 ± 4	170 ± 80	$0.24^{+0.9}_{-0.16}$	0.37	$p^-_{3/2} \to g^+_{9/2}$
Tm^{170}	9.3	13 ± 3	-2.7 ± 0.3	0.5 ± 3	-17 ± 17			
Re^{186}	8.0	-8 ± 1	3 ± 13	18 ± 2	20 ± 90			
Re^{188}	8.6	-5 ± 3	2 ± 6	10 ± 2	20 ± 44			

The conserved-vector-current (CVC) theory predicts the ratio of the $\langle i\vec{\alpha}\rangle$ and the $\langle\vec{r}\rangle$ matrix element (3).

$$\Lambda_{CVC} = \frac{\langle i\vec{\alpha}\rangle}{\langle\vec{r}\rangle/R} = \frac{7}{6}\alpha Z + (W_0 - 2.5)R$$

where R = nuclear radius (in natural units), $\alpha = 1/137$. In those cases, where the experimental data are good enough for computing Λ_{CVC} (e.g. Eu^{152}, Ga^{72}) the agreement between the experimental value of Λ_{CVC} and the theoretical prediction is very satisfactory.

Kisslinger and Wu (4) have shown that the experimental results for the matrix elements in the Sb^{124} β-transition are well explained by considering the particle-hole correlations introduced by the collective motions. These correlations lead to cancellations which result in values of the matrix elements in agreement with experiment.

By combining β-γ directional correlation data on first-forbidden β-transitions and branching ratios the structure of the first excited states of Se^{76}, Sr^{84}, Te^{122} and Xe^{124} was studied by Matumoto et al (5). A detailed analysis of the first-forbidden beta transitions of Tm^{170}, Re^{186} and Re^{188} by Deutsch (6) led to a qualitative understanding of the structure of the nuclear levels involved in these decays.

Recently, β-γ directional correlation measurements involving second excited states of even-even spherical nuclei have become available (7). These data can be compared with those involving first excited states of the same nuclei. The experimental data on Sb^{122}, Sb^{124}, As^{76} and I^{126} show that the matrix element combinations are quite different for the beta transitions to the second excited states as compared to those leading to the first excited states of even-even vibrational nuclei. This experimental fact shows that the coupling of the vibrational modes to the intrinsic modes is considerably different in the first and second excited states of even-even nuclei.

REFERENCES

1. M. Sakai and S. Yoshida, Nuclear Phys. 50, 497 (1964).

2. Z.W. Grabowski, R.S. Raghavan and R.M. Steffen, Phys. Rev. (to be published).

3. J.I. Fujita, Phys. Rev. 126, 202 (1962).

4. L.S. Kisslinger and C.S. Wu, Phys. Rev. (1964).

5. Z. Matumoto et al, Phys. Rev. 129, 1308 (1963).

6. J. Deutsch, in "Nuclear Spectroscopy" (North Holland Publishing Co., Amsterdam, 1964).

7. R.S. Raghavan, Z.W. Grabowski and R.M. Steffen, Phys. Rev. (to be published).

K-SELECTION RULE IN THE β-DECAY OF Tm^{172}

Y.K. Agarwal, C.V.K. Baba and S.K. Bhattacharjee
Tata Institute of Fundamental Research, Bombay

Large retardations of the transition rates in β and γ transitions due to the K forbiddenness have been well known. The β-decay Tm^{172} forms a good example of this selection rule in β-decay. Tm^{172} (K = 2, 2^-) state decays to the 0^+, 2^+ and 4^+ members of the ground state rotational bands by β-transitions β_0, (log ft 8.8), β_2 (log ft 8.7) and β_4 (log ft 10.0) respecitively in addition to transitions to higher excited states. The decay energy is 1870 KeV. β_0 and β_4 are unique first forbidden transitions. The β-transition to the 2^+ state (β_2) can in general have β-decay matrix elements of all ranks λ = 0, 1 and 2. However, rank 0 and 1 matrix elements are forbidden by the K-selection rule since Δ K = 2 in this case. Furthermore, the ratios of λ = 2 matrix elements of β_0, β_2 and β_4 are predicted by Alaga branching ratios (1).

In a case where such a selection rule operates, one can analyse the data on modified B_{ij} approximation. In this approximation, the B_{ij} matrix element is important and the rank λ = 0 and λ = 1 type of matrix elements are approximated by their most important combinations X (λ = 0) and Y (λ = 1). In this approximation, the shape correction factor is given by

$$C(W) = C_A^2 \left| \langle i\, B_{ij} \rangle \right|^2 \left(\lambda_1 p^2 + q^2 \right) + a$$

where
$$a = \frac{X^2 + Y^2}{C_A^2 \left| \langle i\, B_{ij} \rangle \right|^2}$$

Similarly the β-γ directional correlation depends on the ratios X and Y. If one measures the spectral shape and the β-γ directional correlation, one can obtain all the three values X, Y and $\langle B_{ij} \rangle$ coupled with the knowledge of the ft-values. One can now test if X and Y are small as is required by the K-selection rule. Further, one can compare the experimented ratios of B_{ij} matrix elements of β_0, β_2 and β_4 and with the ratios predicted by Alaga selection rules.

The shape correction factors for all the three β-branches β_0, β_2 and β_4 have been measured by Hansen et.al(2). From the shape of β_2, they obtain the limit $a < 1$.

We have made β_2— (79KeV) directional correlation measurements at 6 β energies using the apparatus described elsewhere (3). The directional correlation coefficients were corrected for the first third correlation $\beta_4 - \gamma$ (79 KeV) and due to the compton background of the $4^+ \rightarrow 2^+$ γ-transition of energy 181 KeV. A further correction due to attenuation of the directional correlation due to extranuclear fields was necessary. This correction factor was obtained from measurements on γ-γ cascades in Yb^{172}. The attenuation coefficient so obtained was $G_2 = 0.68 \pm 0.08$. The corrected directional correlation coefficients are given in Table I.

Analysis using both the shape correction factor and our $\beta - \gamma$ directional correlation measurements gave

$$\frac{X}{C_A \langle i\ B_{ij} \rangle} < 0.15 \ ; \qquad \frac{Y}{C_A \langle i\ B_{ij} \rangle} < 0.25.$$

This means that more than 90% of the β-decay takes place by a $\lambda = 2$ type of transition, verifying the K-selection rule. From these limits on X and Y, and using the log ft values, we obtain

$$\left| i \langle B_{ij} \rangle_0 \right|^2 : \left| \langle i\ B_{ij} \rangle_2 \right|^2 : \left| \langle i\ B_{ij} \rangle_4 \right|^2$$
$$= (0.0.76 \pm 0.20) : 1 : (0.052 \pm 0.007)$$

These are in excellent agreement with the values 0.7 : 1 : 0.05 predicted by the Alaga branching ratios.

REFERENCES

1. G. Alaga et. al., Mat. Fys. Medd. Dan. Vid Selsk. 29, No. 9 (1955).

2. P.G. Hansen, Private Communication (1963).

3. S.K. Mitra, Thesis, Banaras Hindu University (1962).

DISCUSSIONS

R.M. Steffen : Was the Kotani formalism used in the evaluation of the data or were exact wave functions used?

C.V.K. Baba: The Rose and Bhalla wave functions are used. Any way, it would make very little difference since only the B_{ij} matrix element is important.

TABLE I

β-γ directional correlation coefficients in the β -decay of Tm^{172} [1790 KeV β- branch (β_2) and γ -79 KeV]

E(KeV)	1010	1110	1210	1310	1420	1550
A_2	-0.04 ± 0.016	-0.075 ± 0.016	-0.110 ± 0.019	-0.104 ± 0.022	-0.094 ± 0.024	-0.122 ± 0.030

THE MAGNETIC MOMENTS OF THE FIRST EXCITED STATES OF I^{127}, I^{131} and Pm^{149}

P.N. Tandon and H. G. Devare
Tata Institute of Fundamental Research, Bombay-5

The ground state of I^{127} is $5/2^+$ corresponding to the $d_{5/2}$ shell model orbital and the first excited state at 59 KeV has the spin and parity assignment $7/2^+$ corresponding to $g_{7/2}$ orbital. This order is reversed in I^{131} where the ground state has the spin assignment $7/2^+$ and the first excited state at 149 KeV, $5/2^+$. In the case of Pm^{149}, the ground state is $7/2^+$ and the first excited state at 114 KeV has the spin $5/2^+$. The Iodine nuclei have only three protons outside the closed shell of 50 and can be expected to be spherical in shape. The Pm^{149} nucleus, on the other hand, has 88 neutrons and can be considered to be on the verge of deformation. It is therefore quite interesting to study the properties of the first excited state of this nucleus. The first excited state in all the three cases has a mean life suitable for the measurement of the g factor by the integral method which we have used. Our apparatus and the method are exactly similar to that described by Manning and Rogers(1) and we use in the following the notation used by them. In this method we select a suitable gamma-ray cascade passing through the level of interest and record the coincidence counts at 135° the source being subjected to a magnetic field at right angles to the plane in which the gamma-rays are detected. If N^+ and N^- are the coincidence counts for two directions of the magnetic field, the quantity $R = \frac{N^+ - N^-}{\frac{1}{2}(N^+ + N^-)}$ is a measure of the rotation of the angular correlation pattern of the gamma-ray cascade. In order to check whether any systematic errors are present, the value of R was measured with the detectors interchanged, i.e., the detector used earlier for the prompt gamma-ray was used for the delayed one and vice-versa. It was verified that this reverses the sign of R without affecting its value. The results of the measurements are given in tabular form.

Nucleus	Cascade Kev	C_2	$T_{\frac{1}{2}}$ n.s	M Kgauss	R	g
I^{127}	355-59	0.206 ± 0.009[2]	1.2[2]	12.8	0.068 ± 0.011	0.77 ± 0.15
I^{131}	452-149	0.043 ± 0.006[2]	0.95[3]	13.3	0.0155 ± 0.0026	1.04 ± 0.24
Pm^{149}	538-114	0.028 ± 0.003[4]	2.52[5]	13.3	0.043 ± 0.003	0.78 ± 0.11

The value of $T_{\frac{1}{2}}$ in the case of I^{127} is considerably smaller than the value 1.8 ns reported by Geiger (6) and used by us in an earlier report (7) on this measurement. Our value is in agreement with the one reported by Jha(8). Recent measurements (9, 10) on the Mossbauer effect in I^{127} show that the observed line is wider than expected on the basis of Geiger's value for the half-life. This width has been attributed to the absorber thickness (10)or to imperfect crystallization in the absorber(9). We feel that the observed width is a genuine effect corresponding to a smaller life time of the state. The Mössbauer effect measurements in I^{127} and I^{129} give quite accurate values of the quadrupole moments of the first excited states and the magnetic moment also in the case of I^{129}(11). It has been pointed out that the quadrupole moments show a linear variation with the addition of pairs of neutrons and it is speculated whether the magnetic moments also show a similar variation (11). The values obtained by us viz., $\mu = 2.71 \pm 0.52$ nm for I^{127} and $\mu = 2.6 \pm 0.6$ nm in the case of I^{131} do not have sufficient accuracy to verify this point.

The single particle estimates for the magnetic moments are 1·72 nm for $g_{7/2}$ and 4.79 nm for a $d_{5/2}$ state. The observed values of μ imply that g_s^{eff}/g_s 0.25 for the $5/2^+$ state in I^{131} and $\frac{g_s^{eff}}{g_s}$ = 0.55 for the $7/2^+$ state of I^{127}. The calculated values taking into account the admixtures of higher seniority configurations(12) are μ = 2.79 nm in the case of $7/2^+$ state of I^{127} and μ = 3.51 nm in the case of $5/2^+$ state of K^{131}. The corresponding values taking into account the collective contributions to these states (12) are μ =2.75 nm and μ= 2.98 nm respectively.

In the case of Pm^{149}, the spin of the first excited state is $5/2^+$ and the magnetic moment μ = 1.94 ± 0.28 nm using the value of the paramagnetic correction β given by Gunther and Lindgren (13). Any possible attenuation of the angular correlation due to internal fields has not been corrected for. The sources used were very dilute solution of $NdCl_3$ in HCl and this correction is not expected to increase the value of μ by more than 10- 15%. Since the Pm^{149} nucleus is likely to have a deformed shape, we may identify the ground state ($7/2^+$) and the first excited state ($5/2^+$) with the [404] and [402] Nilsson orbitals with a value of $\delta \sim 0.05$. This description of the $5/2^+$ state, however, will not give a value of μ in agreement with the observed value. The calculated value for the [402] state is μ = 4.7 nm and is not sensitive to deformation. The observed magnetic moment is more in agreement with the value for a [413] Nilsson state as may be seen from the value of μ =1.8 nm (14) for the ground state of Pm^{151} which has spin $5/2^+$ and can be identified with the [413] Nilsson state. Pm^{151} with 90 neutrons is quite deformed as is clear from the value of the quadrupole moment Q = 1.96. It thus seems that the Pm^{149} nucleus is quite deformed in its first excited state though in the ground state it may have a very small deformation.

REFERENCES

1. G. Manning and J.D. Rogers, Nuclear Physics 15, 166 (1960).
2. S.H. Devare Ph.D. Thesis, University of Bombay (1965).
3. S.H. Devare and H.G. Devare, Proc. Nucl. Phys. and Solid State Phys. Symposium 243 (1964).
4. K.P. Gopinathan, Proc. of the Nucl. Phys. and Solid State Phys. Symposium (1965).
5. W.M. Currie and P.W. Dougan (To be published)
6. J.S. Geiger, Physics Letters 7, 48 (1963).
7. P.N. Tandon and H.G. Devare, Congres International de Physique Nucleaire, Orsay (1964).
8. S.Jha and R. Lenoard, Phys. Rev. (1964).
9. F.De S. Barros, N. Ivantchev, S.Jha and K. Rama Reddy, Phys. Letters 13, 142 (1964).
10. G.J. Perlow and S.L. Ruby, Phys. Letters, 13, 198 (1964).
11. H.de Waard and J. Heberle, Phys. Rev. 136, B 1615 (1965).
12. L.S. Kisslinger and R.A. Sorensen, Rev. Mod. Phys. 35, 853 (1963).
13. C. Gunther and I. Lindgren- Perturbed Angular Correlations- Chapter IV, Edited by E. Karlsson, E. Mathias, K. Siegbahn.
14. B. Budick and R. Marrus, Phys. Rev. 132, 723 (1963).

DISCUSSIONS

N K. Saha: Re. I^{127} excited state lifetime as determined by you and by Geiger what do you think, the large difference is due to?

H.G. Devare: The reason is not clear. Our value is supported also by Jha's measurement.

V.V. Rama Murty: What is the method you have used in determining the lifetime of the level, I mean in I^{127}?

H.G. Devare: The method was the usual time to pulse hight conversion and display of the delayed curve on a multichannel analyzer.

I.M. Govil: What is the retardation factor is the case of I^{127}?

H.G. Devare: The retardation factors in the odd Iodine isotopes are in the region of 150 - 200.

FERMI GAMOW-TELLER MATRIX ELEMENT RATIOS IN ALLOWED BETA TRANSITION IN Eu^{152}, Sb^{124} AND Ga^{72}

S.K. Bhattacharjee, S.K. Mitra and H.C. Padhi
Tata Institute of Fundamental Research Bombay

The measurement of circular polarization of gamma radiation following beta decay has been of great interest because it directly gives the ratio $X = C_V M_F / C_A M_{GT}$ between Fermi and Gamow Teller contributions in allowed beta decays. Combined with knowledge of ft values, one can determine the Fermi and GT matrix elements individually. Except for superallowed transitions, all β decays generally violate $\Delta T = 0$ selection rule in complex nuclei and the Fermi matrix element should be zero, if the isotopic spin is a good quantum number. Following the conserved vector current hypothesis, the only source of M_F is isospin impurity in nuclear wave functions. On this basis the isotopic spin impurity coefficient can be found. We express the isotopic spin impurity coefficient α as

$$\alpha^2 = ft_{SA} / ft_{Fermi} \tag{1}$$

where ft_{SA} is the value for super allowed beta transitions.

The most standard technique of forward compton scattering has been used for measuring circular polarization of gamma rays in our experiments. The measured effect $E = (N_- - N_+) \Big/ \left\{ (N_\mp + N_+)/2 \right\}$ is related to the degree of circular polarization P_C as

$$E = 2 f P_C \langle d\sigma_C / d\sigma_0 \rangle \tag{2}$$

where f is the fraction of polarized electrons in the scatterer and $\langle d\sigma_C / d\sigma_0 \rangle$ is the efficiency (ratio of polarization sensitive and polarization insensitive cross sections). The circular polarization of gamma rays following β decay is

$$P_C = A (v/c) \cos\theta \tag{3}$$

where v is the velocity of beta particles and θ is the angle between a β particle and the accompanying gamma ray. A is the asymmetry parameter. In a $3^-(\beta)\,3^-(\gamma)2^+$ cascade which is the type we have investigated

$$A = \frac{1}{6} \qquad \frac{1 - 4\sqrt{3}\,X}{1 + X^2} \tag{4}$$

An experimental determination of A leads to the value of X. We have measured the beta-gamma circular polarization correlation in the following transitions.

1) 700 keV beta group and the 780 keV cascade gamma ray in Eu^{152}

2) 620 keV beta group and the 1690 keV cascade gamma ray in Sb^{124}

3) 960 keV beta group and the 2215 keV gamma ray in Ga^{72}.

All these decays are of the type $3^-\,(\beta)\,3^-\,(\gamma)2^+$. The measurrd effects (corrected for chances, γ-γ background and transmission) and asymmetry coefficients are shown in Table I. The ratio X is determined graphically from the values of A using Eqn. (4). In column 7 of Table 1, the isopin impurity coefficient α, calculated using Eqn. (1) is shown. It can be seen that the impurity coefficients are quite small even in a nucleus in the region A = 152.

TABLE I

Source	Measured effect %	A	$X = \frac{C_V M_F}{C_A M_{GT}}$	log ft	$M_F \cdot 10^3$	$\alpha \cdot 10^3$
Eu^{152}	0.65 ± 0.08	0.15 ± 0.02	0.02 ± 0.02	10.9	$(5.5 \pm 5.5) \times 10^{-3}$	$2.2 \pm 2.2 \times 10^{-3}$
Sb^{124}	1.53 ± 0.15	0.30 ± 0.03	-0.12 ± 0.03	7.7	1.3 ± 0.03	0.53 ± 0.13
Ga^{72}	-0.78 ± 0.25	-0.13 ± 0.04	0.26 ± 0.04	6.2	15.5 ± 2.2	6.3 ± 0.9

NUCLEAR FISSION AS A MARKOV PROCESS

R. Ramanna, R. Subramanian and Raju N. Aiyer
Atomic Energy Establishment Trombay, Bombay.

It has been shown in a previous publication (1) that the mass distribution in fission can be obtained by assuming a random transfer of nucleons between the two sides of the fissioning nucleus and the asymmetry in thermal fission is due to the shell configuration formed during the process.

This theory has now been extended by treating fission as a Markov process. The transition matrix is obtained from experimental data and from ground state properties of nuclei. By associating an energy transfer with each nucleon transfer, the deformation energy-mass curve has been obtained from the transition matrix. The gap in this curve at the symmetry point is shown to be due to proton transfers.

The number of steps required to achieve the experimental mass distribution is shown to be of the order of 500 while the number of proton transfers required to produce the observed energy gap is approximately 70. This implies that the proton transfers cease early in the fissioning process which justifies the assumption of the polarisation of protons to the ends of the fissioning nucleus and hence the formation of a symmetry axis early in the fissioning process.

Further, it is observed, that the threshold energies for all heavy nucleides lie between 5 to 7 MeV. If the threshold energies for fission is defined as the energy required to start the random motion this will be the same for all heavy nucleides and of the order of the binding energy of a nucleon.

Assuming that not more than one nucleon is transferred in any given step the transition matrix is given by

$$P_{ij} = \begin{bmatrix} P_{oo} & P_{o1} & 0 & \cdots\cdots & & \\ P_{10} & P_{11} & P_{12} & 0 & \cdots\cdots & \\ 0 & P_{21} & P_{22} & P_{23} & \cdots\cdots & \\ \cdots & \cdots & \cdots & \cdots & \cdots & \cdots \\ 0 & 0 \ldots\ldots & P_{m,m-1} & P_{m,m} & P_{m,m+1} & \ldots \\ \cdots & \cdots & \cdots & \cdots & \cdots & \cdots \end{bmatrix} \qquad (1)$$

where $P_{m,m+1}$ denotes the probability that the configuration on one side with mass m will increase its mass by one nucleon in any given step.

$P_{m,m-1}$ denotes the probability that the configuration on one side with mass m will decrease its mass by one nucleon in any given step.

$P_{m,m}$ denotes the probability that the configuration with mass m will remain unchanged in any given step (staying probability).

If the mass distribution has reached equilibrium before scission then one has

$$X_{m-1}\, P_{m-1,m} + X_m\, P_{m,m} + X_{m+1,m}\, P_{m+1m} = X_m \quad \ldots\ldots \quad (m = 0,1,2 \ \ldots h) \qquad (2)$$

Also since

$$P_{m,m-1} + P_{m,m} + P_{m,m+1} = 1 \quad \ldots\ldots \qquad (3)$$

one has

$$\frac{X_m}{X_{m+1}} \qquad \frac{P_{m+1,m}}{P_{m,m+1}} \quad \ldots\ldots \qquad (4)$$

The diagonal elements cannot be fixed from eq.(4). From shell effects and ground state stability conditions it can be shown that the diagonal elements are very close to the actual mass distribution as shown in Fig.1. The transition matrix so obtained was raised to various powers and these are

Fig. 1. The continuous curve gives the actual mass distribution (2)

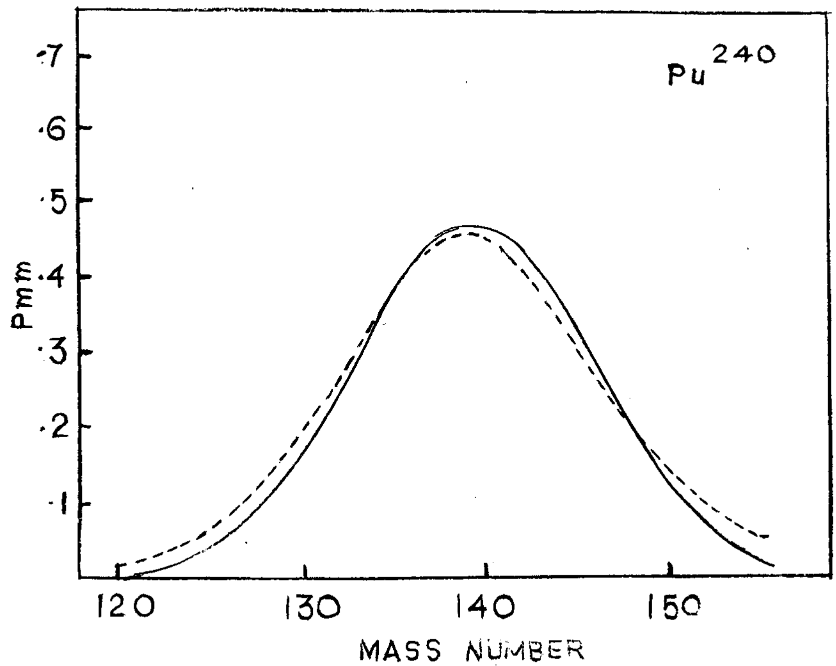

FIG.1

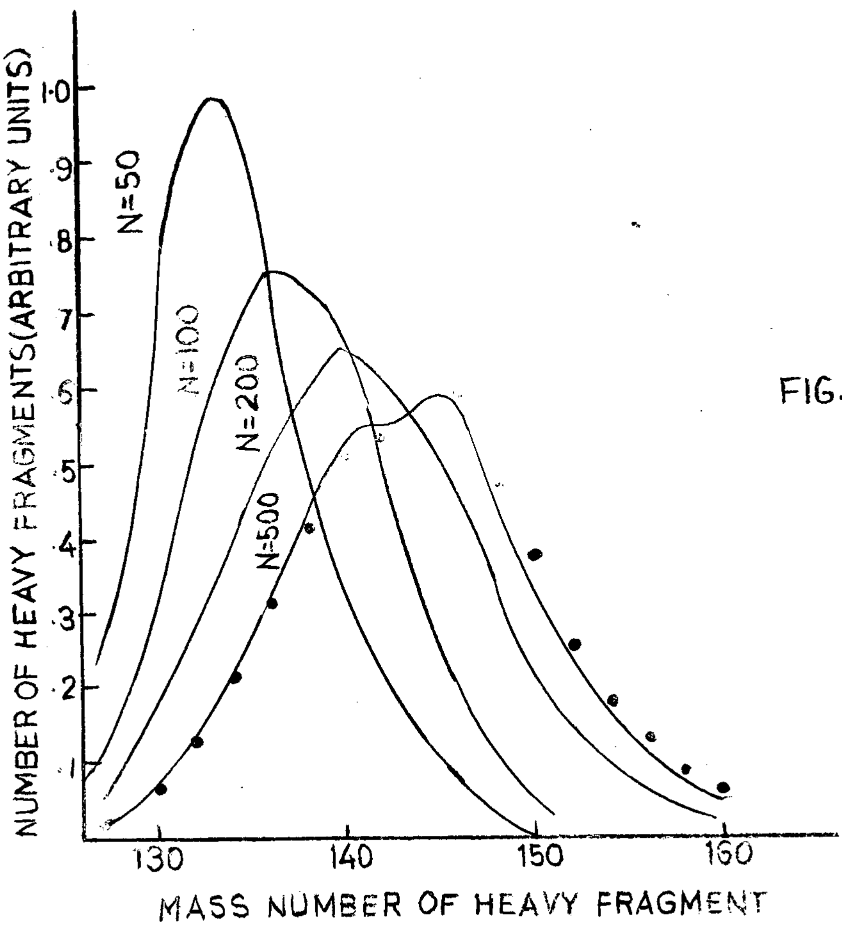

FIG.2

shown in Fig. 2. for Cf^{252}.

DEFORMATION ENERGY AND MASS

It is assumed that with each nucleon transfer certain energy is also transferred and the whole of this energy goes to the deformation energy of the fragment. If the average deformation energy for each mass has reached equilibrium before scission then one has

$$P_{m,m+1} X_m (E_m + \epsilon_{m,m+1}) + P_{m+1,m+1} X_{m+1} E_{m+1} + P_{m+2,m+1} X_{m+2} (E_{m+2} - \epsilon_{m+2,m+1}) = X_{m+1} E_{m+1} \quad \ldots (5)$$

where E_m is the average deformation energy of the fragment of mass m and $\epsilon_{m,m+1}$ is the change in the binding energy when a fragment goes from state m to state m+1.

From eq. (5) using eq.(4) one gets

$$R_{m+1} = P_{m+1,m}/P_{m+1,m+2} = (E_{m+2} - E_{m+1} - \epsilon_{m+2,m+1}) / (E_{m+1} - E_m - \epsilon_{m,m+1}) \quad (6)$$

which gives the relation

$$E_{m+1} - E_k = \sum_{p=k}^{m} \epsilon_{p,p+1} + (E_{k+1} - E_k - \epsilon_{k,k+1}) [1 + R_{k+1} + \cdots + R_{k+1}R_{k+2}\cdots R_m] \quad (7)$$

Knowing $\epsilon_{m,m+1}$ and any two values of E_m the deformation energy mass curve can be generated. The curve obtained for $\epsilon_{m,m+1} = 0$ for U^{236}, Pu^{240} and Cf^{252} and $\epsilon_{m,m+1} = -1$ MeV are shown in Fig. 3.

The order of magnitude of the energy gap produced by the proton transfers can be calculated in the following way.

Let E_H denote the average energy transferred with a proton from a fragment with higher Z to a fragment with lower Z and E_L the average energy for the inverse process. If N_p be the total number of proton transfers and 2Z the charge difference between the two fragments, the loss

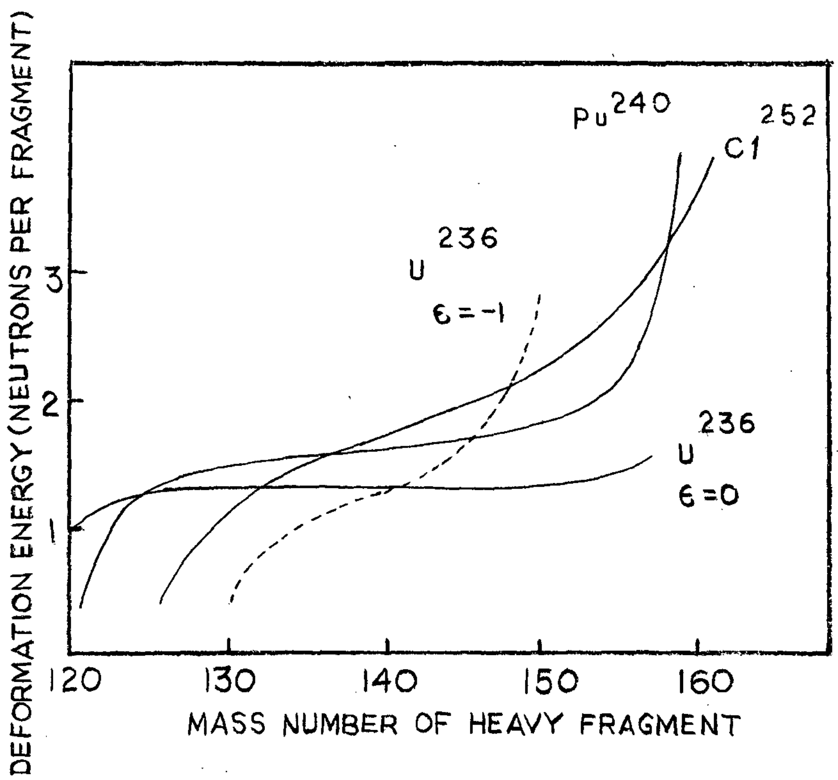

FIG.3.

Fig. 4 (a). The continuous lines give the values of R_m for Pu^{240} for the case where the probabilities $P_{m,m}$'s are given by the actual mass distributions and the dotted lines are for calculated values of probabilities $P_{m,m}$.

Fig. 4 (b). The probabilities $P_{m,m-1}$ (denoted by P_L) and $P_{m,m+1}$ (denoted by P_R)

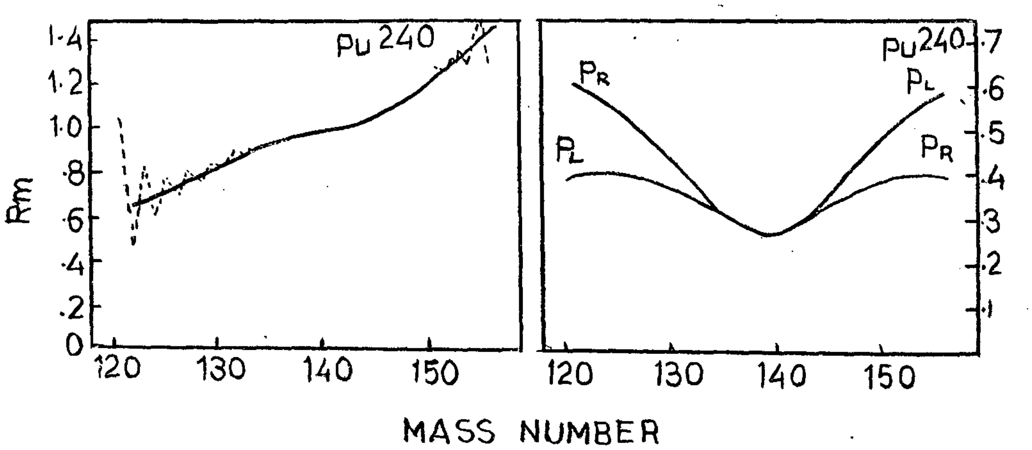

FIG.4

FIG.4(a) FIG.4(b)

for emitting and absorbing a neutron respectively for Pu^{240} as determined from mass data. (2)

in the energy of the fragment with higher Z is

$$\tfrac{1}{2}\,(N_p - Z)\,E_H - \tfrac{1}{2}\,(N_p + Z)\,E_L$$

The corresponding light fragment gains an equal amount of energy. At the symmetry point since Z = 0 the difference in energy between the two fragments is $N_p \;(E_H - E_L)$

$E_H - E_L$ can be shown to be equal to 0.6 MeV which gives N_p as 70 to obtain the observed energy gap of 40 MeV.

Even if the time between proton transfers is much larger than for neutrons, the small number of proton transfers cease early in the process to account for charge polarisation.

REFERENCES

1. R.Ramanna, Phys. Letters 10, 321 (1964).

2. J.C.D. Milton and J.S. Fraser, Can. J. of Phys. 40, 1626 (1962).

3. J.S. Fraser, J.C.D. Milton, H.R. Bowman and S.G. Thompson, Can. J. of Phys. 41, 2080 (1963).

DISCUSSIONS

A.K. Ganguly: If the mass yield curves are prior to neutron evaporation or if neutron evaporation can disturb the curves?

R.Ramanna: The No. of neutron emitted prior to scission is about 10% and to this extent it can change the masse distribution up to scission. But as these distributions are measured latter they will have to take into account the neutron emission.

A.K. Ganguly: Does the theory take into account that the fission process does not give any positron emitters?

R. Ramanna: Such emission is from the fragments and does not come into the fission process.

J. Premanand: What is the dimensionality of the stochastic matrix?

R. Ramanna: 35 rows and columns.

J. Premanand: Is the stochastic matrix time independent?

R. Ramanna: It is the mean for the process from T = 0 to scission.

J. Premanand: What is the reason for choosing the P_{oo} to be the probability for equal mass fission products?

R. Ramanna: Intution shows that when shell configurations are formed the tendency is for it to stick and not change and hence it seems resonable to assume that the staying probabilities depend on shell effects.

P. Mukherjee: What is the effect of nucleon correlation on your P_{o1}, P_{o2} etc.?

R. Ramanna: It will be to reduce time of fission as higher unit transfer will hasten the process.

LONG RANGE ALPHA PARTICLE EMISSION IN THE FISSION OF U^{235} BY 3 MeV NEUTRONS

V.A. Hattangadi, T. Methasiri*, D.M. Nadkarni
R. Ramanna and P. N. Rama Rao
Atomic Energy Establishment Trombay

To study the mechanism of emission of the long range alpha particles in fission, investigations have been carried (1) out in the fission of U^{235} by 3 MeV neutrons to obtain the energy spectrum and the angular distribution of long range alpha particles with respect to the incident neutron direction. 3 MeV neutrons were used because second chance fissions are energetically impossible and do not complicate the angular distribution.

EXPERIMENTAL ARRANGEMENT AND METHOD

The experimental arrangement is shown in Fig.1. The three solid state detectors were used to detect the long range alpha particles emitted in coincidence with fission fragments. The fission fragments were detected by scintillations produced in Xe gas and were observed by a photomultiplier tube. The detector D_1 was placed close to the target so as to detect all the alpha particles emitted in the backward hemisphere. Two detectors D_2 and D_3 were used to detect the alpha particles emitted at 0° and 90° with respect to incident neutron beam. The alpha particles were detected with an angular resolution of $\pm$ 18°. The Xe gas pressure was about 2/3 atm. which was sufficient to stop the fission fragments and natural alpha particles from reaching D_2 and D_3. The uranium target was made by electroplating U^{235} on an Al backing of thickness 10 mg/cm^2. The thickness of uranium coating was about 1 mg/cm^2 over an area of about 2 cm^2. The Al backing

---

* IAEA Fellow on leave of absence from the Office of the Atomic Energy for Peace, Bangkok, Thailand.

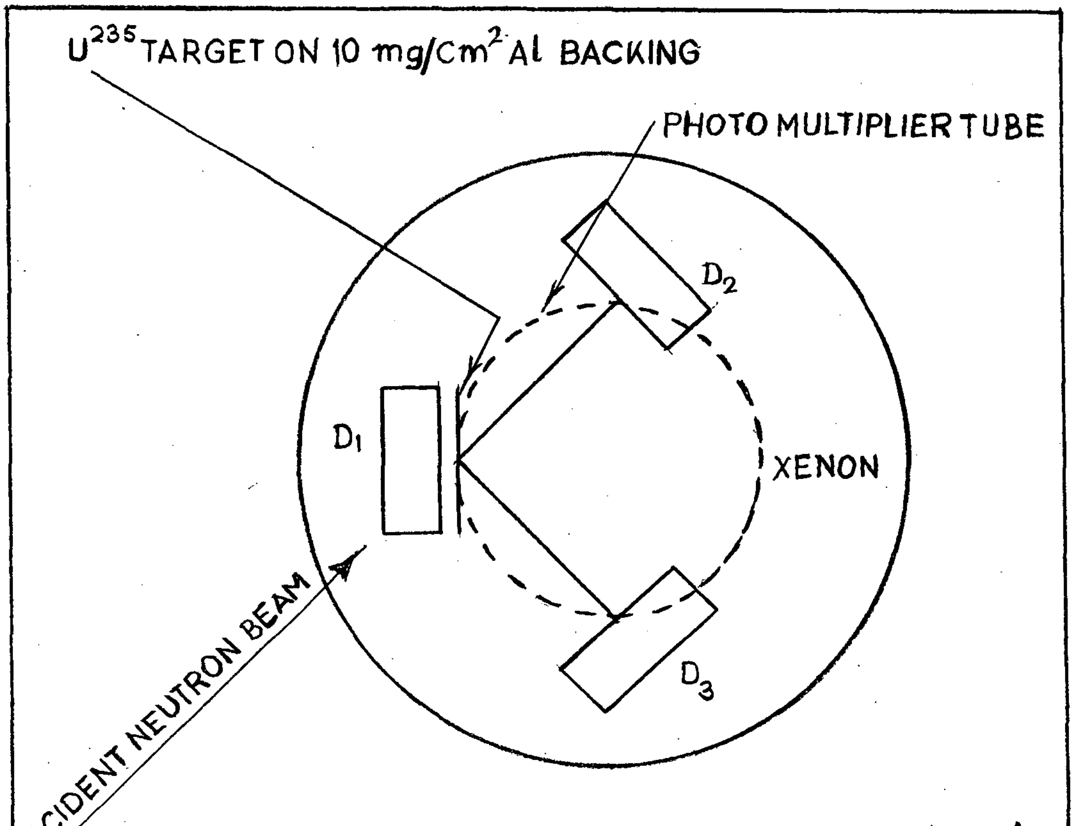

U^{235} TARGET ON 10 mg/Cm^2 Al BACKING
PHOTO MULTIPLIER TUBE
D_2
D_1
XENON
INCIDENT NEUTRON BEAM
D_3

FIG. 1

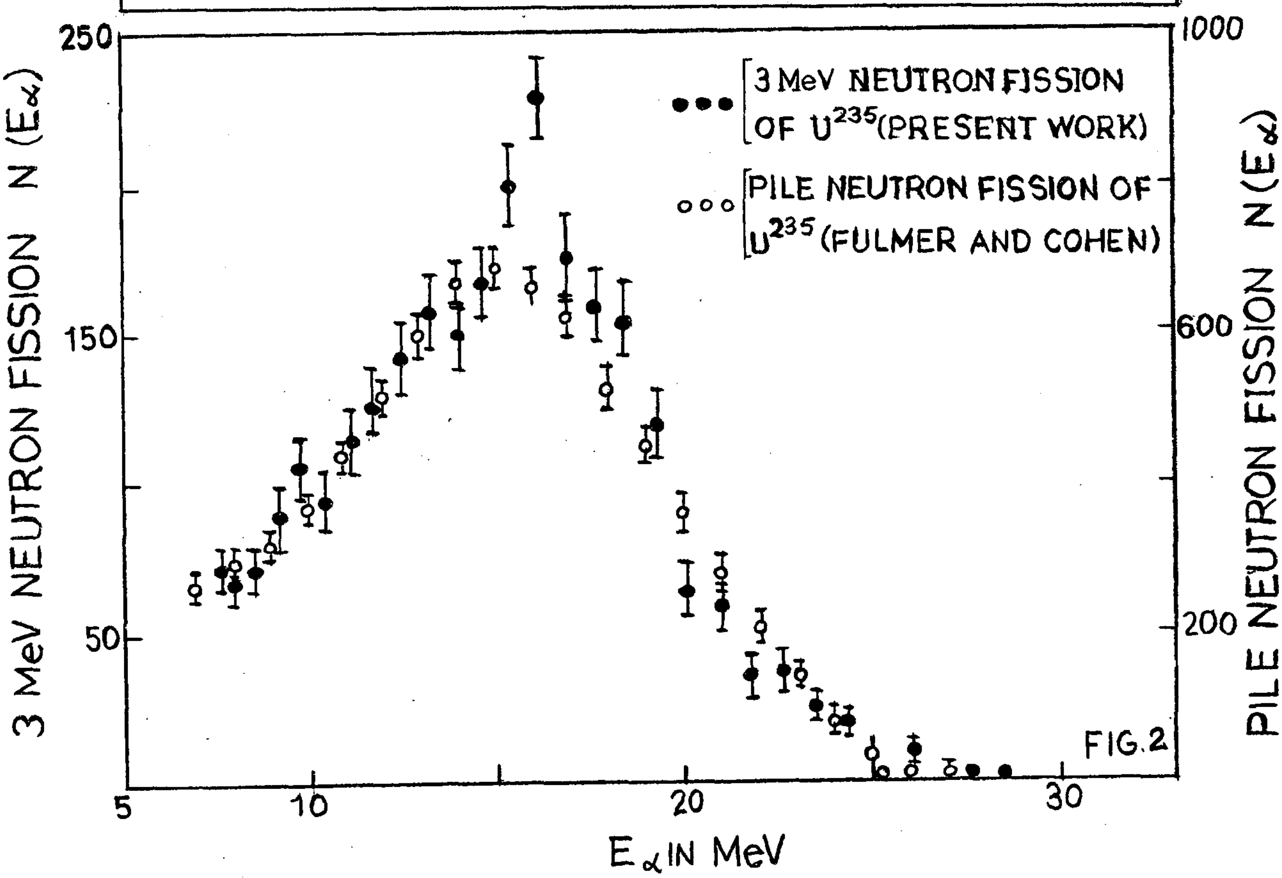

3 MeV NEUTRON FISSION N (E$_\alpha$)
PILE NEUTRON FISSION N(E$_\alpha$)
3 MeV NEUTRON FISSION OF U^{235}(PRESENT WORK)
PILE NEUTRON FISSION OF U^{235} (FULMER AND COHEN)
250
150
50
1000
600
200
5
10
20
30
E$_\alpha$ IN MeV

FIG. 2

was of sufficient thickness to stop fission fragments and natural alpha particles from reaching D_1. 3 MeV neutrons were produced by $T(p,n)\,He^3$ reaction using a 5.5 MeV Van de Graaff generator. Three charge sensitive preamplifier and amplifier systemswere used to amplify the pulses from the detectors and were recorded by a 400 channel analyser.

RESULT AND DISCUSSION

The anisotropy $\left(N_\alpha(0°) / N_\alpha(90°) \right)$ was found to be 1.32 ± 0.12 and is in agreement with that predicted by the statistical theory (2). According to this theory the angular distribution of evaporated particles is given by

$$N(\theta) = 1 + \frac{\alpha^2 \overline{I^2}\,\overline{\ell^2}}{2} \cos^2\theta$$

where $\overline{I^2}$ is the average angular momentum of the compound nucleus,

$\overline{\ell^2}$ is the average angular momentum of evaporated particles,

$\alpha = \hbar^2/2JT$, where J and T are the moment of inertia and temperature of the compound nucleus respectively. $\overline{I^2}$ and $\overline{\ell^2}$ were calculated using the sharp cut-off approximation and α was calculated using the value of K_0^2 obtained from an analysis of angular distribution of fission fragments (3). The expected anisotropy is of the order of 10–25% depending on the value of r_0 to which parameter this value is very sensitive.

The energy spectrum of the alpha particles has been corrected for loss in Al and is shown in Fig.2 together with that in the case of thermal neutron fission of $U^{235}(4)$. The spectrum of particles evaporated from a nucleus is given by:

$$N(E)\,dE = \text{Const}\; E\,\sigma_c(E)\,\omega(E^* - E)\,dE$$

where $\sigma_c(E)$ is the cross-section for the inverse reaction, E^* is the excitation energy of the compound nucleus, and $\omega(E^* - E)$ is the level density of residual nucleus. The nuclear temperature T is given by

$$\frac{1}{T} = \frac{d}{d(E^* - E)}\left[\ln \omega(E^* - E)\right]$$

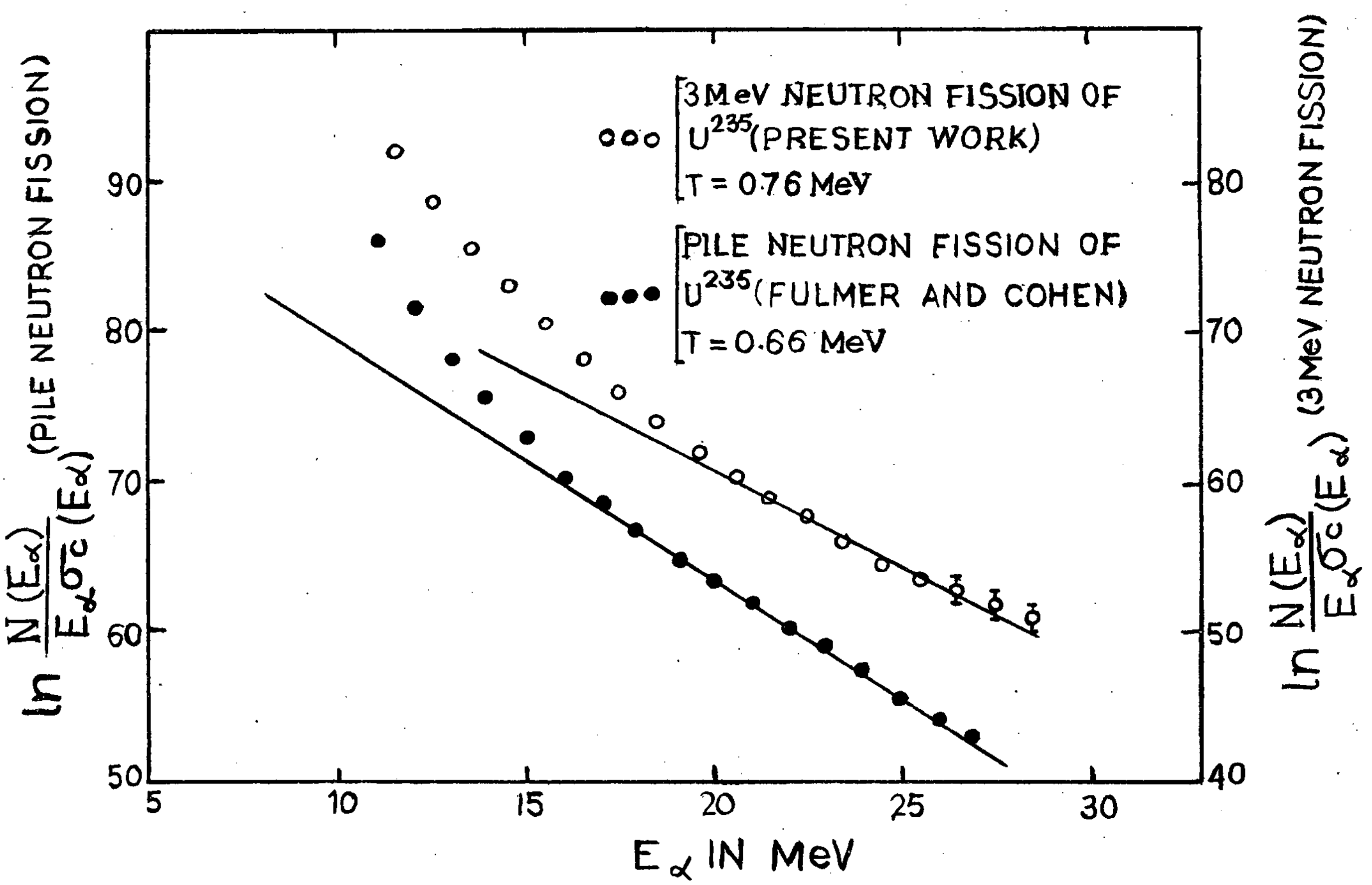

3 MeV NEUTRON FISSION OF
U^{235} (PRESENT WORK)
T = 0.76 MeV
PILE NEUTRON FISSION OF
U^{235} (FULMER AND COHEN)
T = 0.66 MeV
$\ln \frac{N(E_\alpha)}{E_\alpha \sigma_c(E_\alpha)}$ (PILE NEUTRON FISSION)
$\ln \frac{N(E_\alpha)}{E_\alpha \sigma_c(E_\alpha)}$ (3 MeV NEUTRON FISSION)
E_α IN MeV

FIG.3

and can be obtained by plotting $\ln[N(E)/\sigma_c(E)E]$ vs E using the numerical calculations of $\sigma_c(E)$ for a spherical nucleus with r_0 = 1.2 fermis, it was found that the high energy part of the alpha spectra in 3 MeV and thermal neutron fission of U^{235} correspond to temperatures of 0.76 ± 0.04 and 0.66 ± 0.03 MeV respectively.(Fig.3) The peak of the alpha particle spectrum in 3 MeV neutron fission of U^{235} was found be at a slightly higher energy compared to that in the thermal fission of U^{235} (4) and also the width of the spectrum in the former case was found to be smaller. These differences are probably due to the relative higher temperature in the former case. The relative probability of binary to ternary fission is found to increase with excitation energy of the compound nucleus and is in agreement with the results of previous measurements.(5) This increase may be due to a competion between the modes of evaporation of alpha particles and neutrons in the fission process.

The results of the present investigation support the hypothesis that the long range alpha particles are evaporated from the compound nucleus prior to scission(6).

REFERENCES

1. N.A. Perifilov, Yu. F. Romanov and Z.I.Saloveva, Soviet Physics Uspekhi 3, 542 (1961).
2. T. Ericson and V. Strutinski, Nucl. Phys. 8, 284 (1958).
3. J.E. Simmons and R.L. Henkel, Phys. Rev. 120, 198 (1960).
4. C.B. Fulmer and B.L. Cohen, Phys. Rev. 108, 370 (1957).
5. R-A.Nobles, Phys. Rev. 126, 1508 (1962).
6. R. Ramanna,K.G. Nair and S.S. Kapoor, Phys. Rev., 129, 1350 (1963).

DISCUSSIONS

Dr. Ramanna (Comment).

I would like to point out that the K_0^2 used from angular distribution data is a clever way of evaluating α_0^2, but whether we can use this K_0^2 in ternary fission is doubtful as the angular distribution changes in ternary fission.

Nadkarni: That is true and it is therefore of interest to measure more accurately the anisotropy of fragment angular distributions in ternary fission.

VARIATION OF FISSION THRESHOLD AND THE FISSION FRAGMENT MASS DISTRIBUTION

D. M. Nadkarni
Atomic Energy Establishment, Trombay

The measurements of kinetic energy distribution and the correlation of mass asymmetry and angular anisotropy of fission fragments in 4 MeV neutron fission of U^{235} (1) have been utilised here to understand the mechanism of mass division in fission.

The total kinetic energy distribution of fission fragments in the mass ratio region of 1.00 to 1.11 showed a second peak appearing at an energy of about 125 MeV together with the main peak at 163 MeV. This feature was found to be more pronounced for fragments emitted in the 0° direction with respect to the incident neutron direction compared to that in the 90° direction. It was observed that the symmetric fragments have lower average kinetic energies, emit more neutrons and have relatively higher anisotropy compared to the asymmetric fragments. These observations are in agreement with the hypothesis that the fission process is a two mode process one leading predominantly to symmetric fragments and the other to asymmetric fragments (2).

However, the observed correlation of angular anisotropy and mass asymmetry of the fission fragments in the 4 MeV neutron fission of U-235 (1) shows that the fission is a many-mode process, division into each mass ratio being a mode in itself having a different set of kinetic energy, excitation energy and the fission threshold. Here an attempt has been made to understand the mechanism of mass division in fission using the results of correlation of mass asymmetry and angular anisotropy.

It will be assumed here that the mass distribution depends on the saddle point state of the fissioning nucleus and does not change appreciably during the descent from saddleto scission. The compund nucleus U-236 is excited to a level $E^* = B_N + E_N$ where B_N and E_N are the binding energy of the neutron to the nucleus and kinetic energy of the neutron respectively. The compound nucleus then makes transitions to various saddle point states corresponding to division into various mass ratios. For division into two freshly formed fragments at the saddle point there will be a particular threshold energy E_{th} and the excitation energy of the resulting system being $E^* - E_{th}$. The fragment mass yield is given by the transition rate:

$$W(M_H/M_L;\ E_{th}) = \text{Const.}\ |\langle f|O|i\rangle|^2 \omega(E^* - E_{th})$$

where $\langle f|O|i\rangle$ is the transition matrix element and $\omega(E^* - E_{th})$ the density of states for mass division M_H/M_L. As the matrix element is not known, to obtain relative mass fragment yields it will be assumed to be same for all final states. The mass yield is therefore, proportional to the density of states. Considering the nucleus to be Fermi gas, the level density is

$$\omega(E^* - E_{th}) \sim \text{Const. exp}\left[2\{a(E^* - E_{th})\}^{\frac{1}{2}}\right] \quad (1)$$

In the case of 4 MeV neutron fission of U^{235}, $(E^* - E_{th})$ for various mass ratios can be obtained using the value of anisotropy $\left[N(0°)/N(90°)\right]$ for each mass ratio (M_H/M_L) (1). On the statistical theory of angular distribution of fission fragments (3),

$$N(0°)/N(90°) = 1 + 1/2\ (I_m/2K_o)^2 \quad (2)$$

where I_m is the maximum total angular momentum of the fissioning nucleus and K_0^2 is the average of K^2. In the region of interest to us here the relation between K_0^2 and $(E^* - E_{th})$ has been empirically determined (4) to be of the form

$$K_0^2 = B_1 + B_2\ (E^* - E_{th}) \quad (3)$$

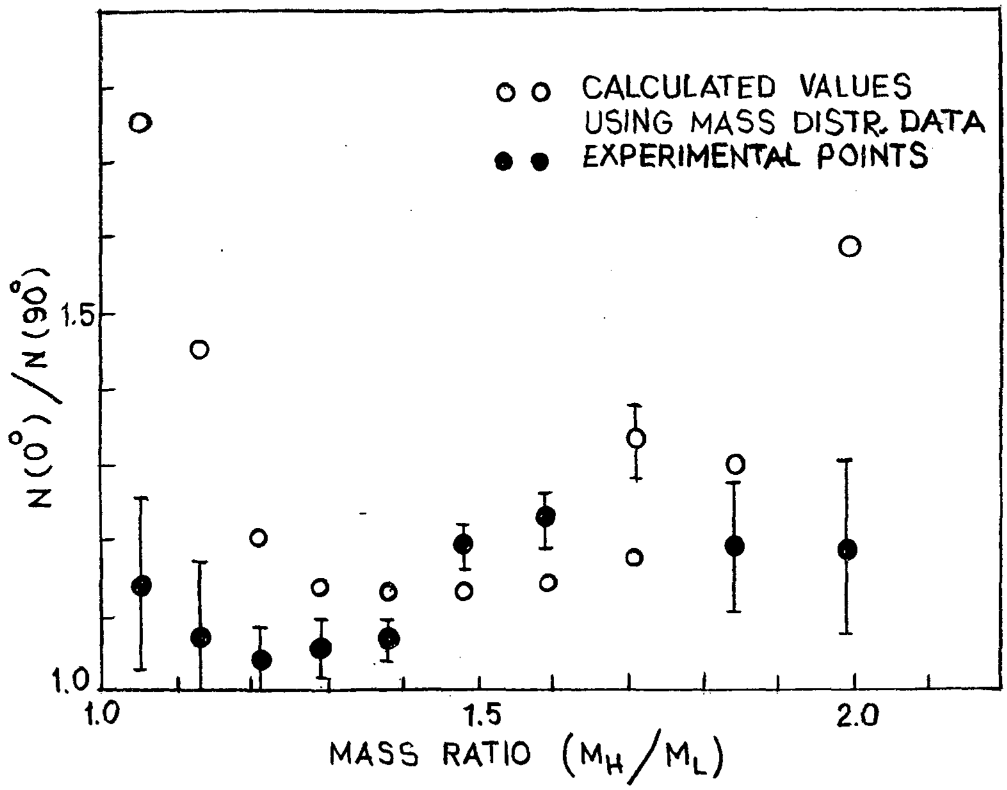

CALCULATED VALUES
USING MASS DISTR. DATA
EXPERIMENTAL POINTS
$N(0^\circ)/N(90^\circ)$
1.5
1.0
1.0
1.5
2.0
MASS RATIO (M_H/M_L)

Fig.1.

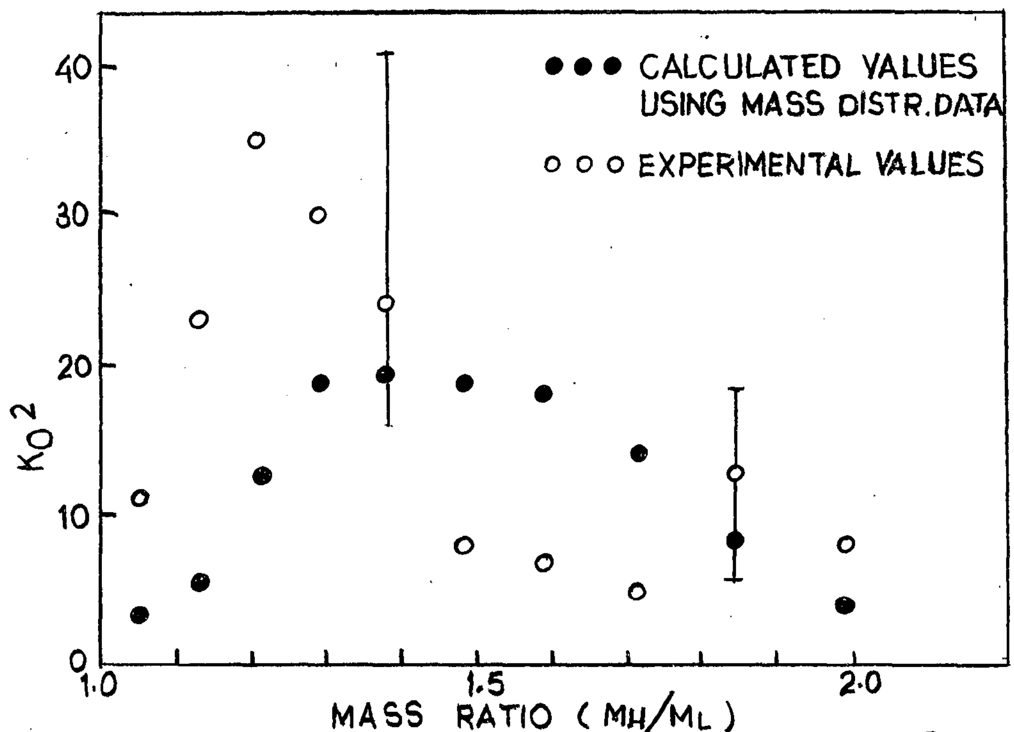

CALCULATED VALUES
USING MASS DISTR.DATA
EXPERIMENTAL VALUES
$K_0{}^2$
40
30
20
10
0
1.0
1.5
2.0
MASS RATIO (M_H/M_L)

Fig.2.

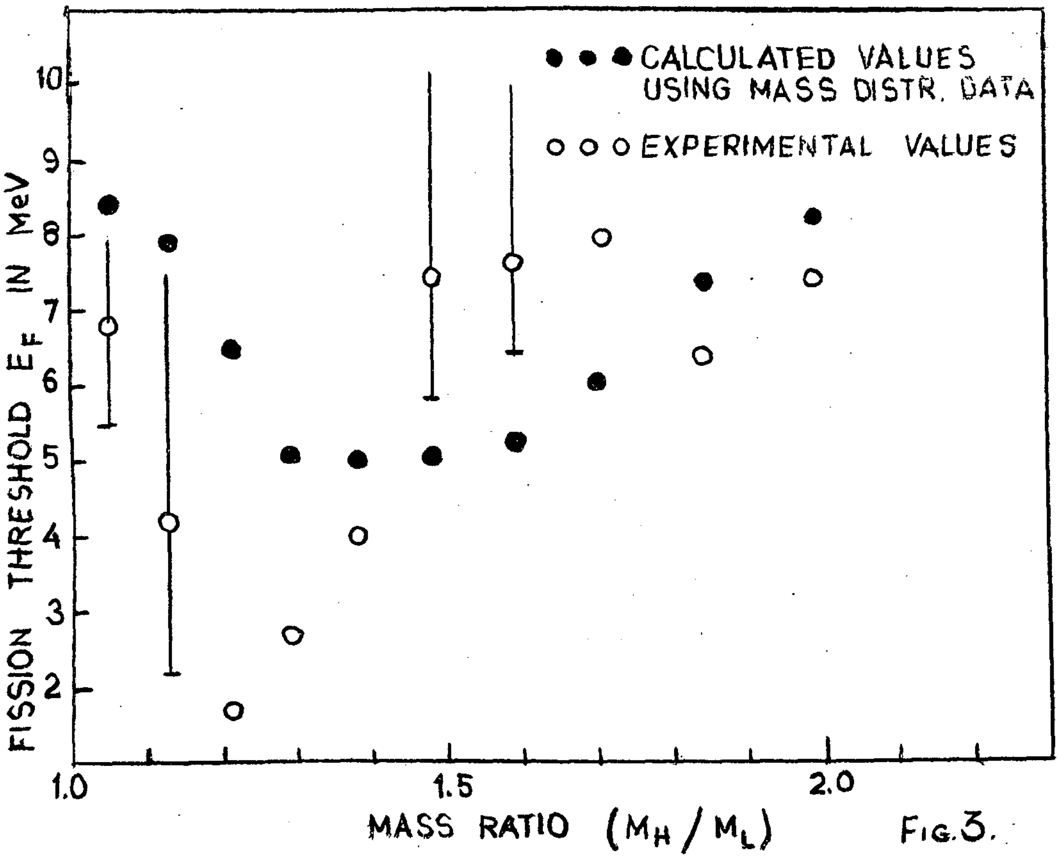

CALCULATED VALUES USING MASS DISTR. DATA
EXPERIMENTAL VALUES
FISSION THRESHOLD E_F IN MeV
MASS RATIO (M_H/M_L)

FIG. 3.

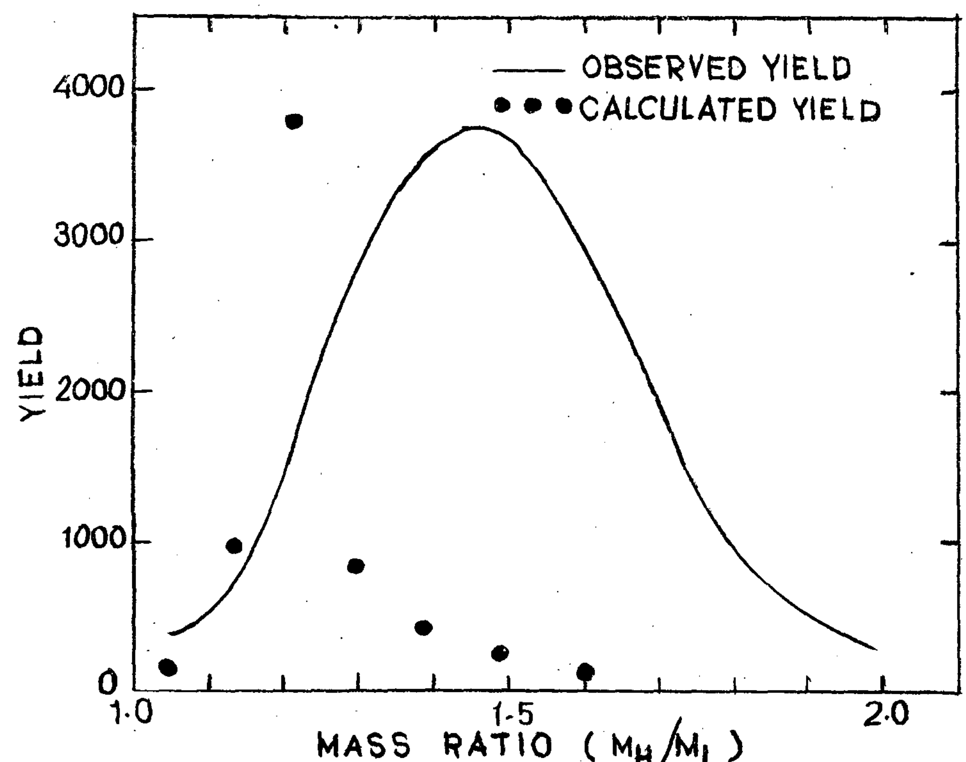

OBSERVED YIELD
CALCULATED YIELD
YIELD
MASS RATIO (M_H/M_L)

FIG. 4.

where $B_1 = 6.1 + 1.9$ and $B_2 = 4.7 + 0.39$. Using Eqns. (2,3) K_0^2, $(E^* - E_{th})$ and E_{th} were calculated for each mass ratio. For each mass ratio the average value of a was estimated using Lang's modification of Newton's formulation (5)

$a = 0.0748(\bar{j}_n + \bar{j}_p + 1) A^{2/3}$ where $\bar{j}_n$ and $\bar{j}_p$ are the effective values of the angular momentum of neutrons and protons near the fermi level (6). This estimate of a is not strictly correct as the available excitation energy may not be equally distributed among the fragments in any mass ratio. The fragment mass yield calculated thus shows a peak in the mass ratio region 1.2 - 1.25 and a peak to valley ratio of the order of 50 compared to the observed mass distribution with a peak around 1.4 - 1.5 and a peak to valley ratio of about 20. However, the statistical error in the measured anisotropy and the approximations made about the energy dependence of K_0^2 and the level density parameter introduce considerable errors in the calculated yields. The agreement between the calculated and the measured mass distribution could be improved when more precise data on the correlation of anisotropy and asymmetry of fission fragments and nuclear level density parameter and other fission parameters become available.

On the other hand the observed mass distribution can be used to compute $(E^* - E_{th})$, E_{th}, K_0^2 and anisotropy using eqn (1) - (3). It was found that the trend of variation of these parameters calculated using the mass distribution data and observed correlation of anisotropy and asymmetry are similar [Fig. (1) - (4).]

In spontaneous and slow neutron fission the symmetric fission is sub-barrier and the yield of symmetric fragments calculated using the barrier penetration formula of spontaneous fission is too low compared to the measured symmetric fragment yield. This probably indicates that the symmetric fragmentsare formed by a passage of the fissioning nucleus through an asymmetric saddle point with subsequent dynamic effects which give a tendency towards symmetric shape(7). Thus one cannot completely rule out some sort of dynamic effects which influence the mass distribution, at least in low energy fission. The present simplified calculations indicate a possible mechanism of mass division in fission.

REFERENCES

1. S.S. Kapoor, D.M. Nadkarni, R. Ramanna and P.N. Rama Rao, Phys. Rev.(1964)
2. A. Turkevitch and J.B. Niday, Phys. Rev. 84, 52 (1951).
3. I. Halpern and V. Strutinski, Proc. Second Inter. Conf. Peaceful Uses of Atomic Energy, Geneva (1958).
4. J.E. Simmons and R.L. Henkel, Phys. Rev. 120, 198 (1960).
5. D.W. Lang, Nucl. Phys. 26, 434 (1961).
6. T.D. Newton, Can. J. Phys. 34, 804 (1956).
7. S.A.E. Johansson, Nucl. Phys. 22, 529 (1961).

A STUDY OF THE Ne (n, p) REACTION AT $E_n = 14.1$ MeV

E. Kondaiah and R.K. Patell
Tata Institute of Fundamental Research, Bombay 5.

A preliminary report is given here on a study of the Ne (n, p) F reaction induced by 14.1 MeV neutrons, for which no data are known to have been published. An Allan type camera(1), lined with 2 mm thick graphite was filled with natural neon gas at a pressure of 1 atm. and exposed to the neutron beam. The reaction products were recorded in an Ilford K2, 400μ nuclear emulsion, placed at the centre of the camera, and shielded from the direct neutron beam by a 50 cm brass bar. An identical exposure with hydrogen served as a standard in the cross-section determination, and another exposure, under vacuum, served as the background.

The plates were developed by the temperature development method, using Amidol developer, and treated for shrinkage inhibition. An area of 5 mm x 4 mm at the centre of the plate was scanned; only those tracks originating at the surface and having a dip angle between 2° and 10° were accepted. Due to the camera geometry, larger dip angless ($>$ 10°) tend to distort the angular distribution. The space angle and energy of each track was calculated and corrected for the divergence of the neutron beam, and for energy loss through the gas target. Due to the extended target geometry the energy resolution was poor; at a proton energy of 8 MeV, uncertainty in energy is $\pm$ 0.5 MeV, and at 2 MeV, it is $\pm$ 1.5 MeV for neon, in the hydrogen exposures the uncertainty was $\pm$ 0.15 MeV and $\pm$ 0.3 MeV respectively. The CDC 3600 computer was used to analyse the data.

ANGULAR DISTRIBUTION

The chief character of the angular distribution for the energy region

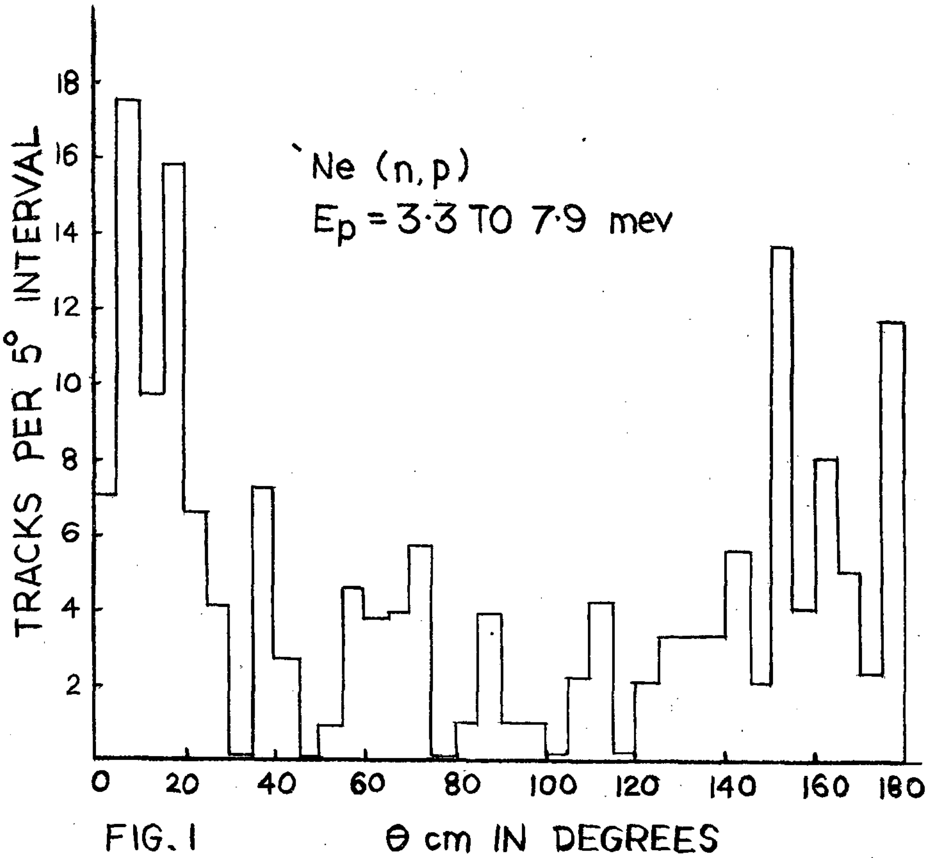

TRACKS PER 5° INTERVAL
18
16
14
12
10
8
6
4
2
Ne (n, p)
Ep = 3·3 TO 7·9 mev
0
20
40
60
80
100
120
140
160
180
θ cm IN DEGREES

FIG. 1

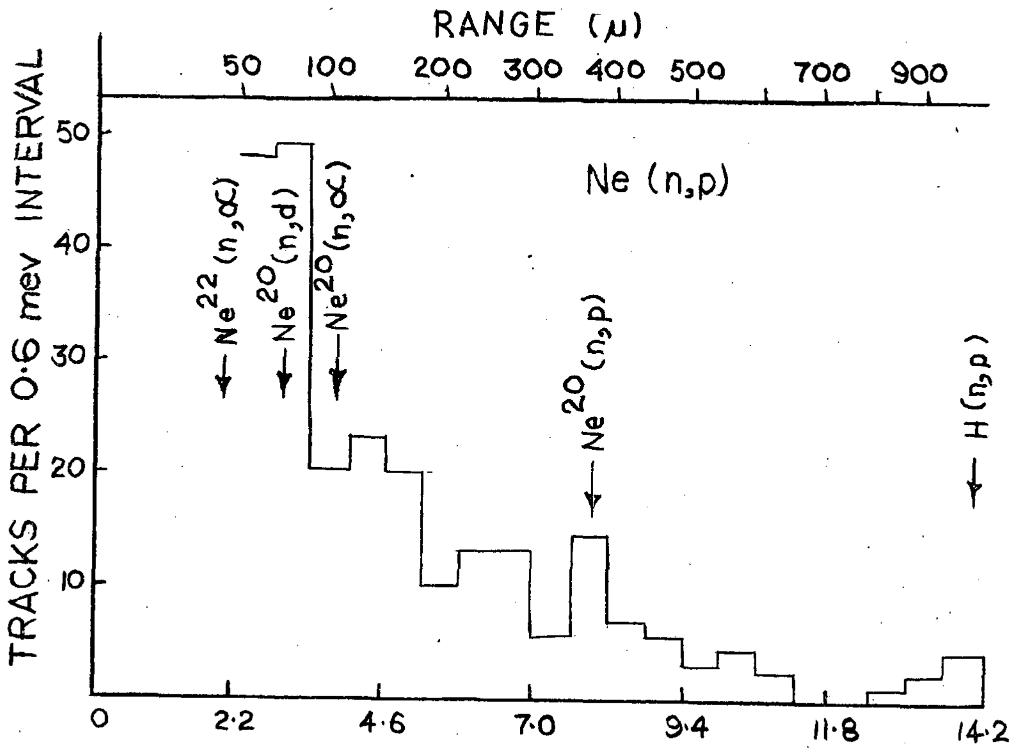

RANGE (μ)
50
100
200
300
400
500
700
900
TRACKS PER 0·6 mev INTERVAL
50
40
30
20
10
Ne (n,p)
Ne22 (n,α)
Ne20 (n,d)
Ne20 (n,α)
Ne20 (n,p)
H (n,p)
0
2·2
4·6
7·0
9·4
11·8
14·2
Ep mev

FIG. 2

$3.3 \geqslant E_p \geqslant 7.9$ MeV (Fig.1) is symmetry around 90° centre of mass angle, with strong forward and backward peaking, indicating the prevalence of a compound process. The distribution of tracks corresponding to $2.2 \geqslant E_p \geqslant$ 3.2 MeV, which also includes contributions from the Ne (n,α) O and Ne (n, d) F reactions, is isotropic in the centre of mass system.

ENERGY DISTRIBUTION

Fig. 2 shows the energy distribution in the laboratory system of all charged particles from the neon exposure. The cut-off at E_p = 2.2 MeV is due to absorption in the gas target. The tracks beyond 7.9 MeV, which are less than 10% of the total number of tracks, are presumably from the water vapour impurity. The arrows indicate the positions of the ground states of the corresponding residual nuclei. In the region E_p = 3.3 MeV to 7.9 Mev only Ne (n, p) F protons are present.

CROSS-SECTIONS

The cross-section, for $E_p \geqslant 3.3$ MeV, was estimated to be $\simeq$100 mb assuming a total cross-section of 660 mb (2) and a differential cross-section of 52 mb/st for the H(n,p) standard.

REFERENCES

1. D.L. Allan, Nuclear Physics 6, 464 (1958); 10, 348 (1959).

2. M.D. Goldberg et al, B.N.L. 400 (1962).

DISCUSSIONS

V.K. Deshpande: Could you comment further on how you conclude that the reaction proceeds via compound nucleus formation?

R.K. Patell: We have not made any theoretical fits yet; however, we can assume it is a compound nuclear process because the angular distribution is symmetric around θ_{CM} = 90° and an analysis of the energy spectrum assuming statistical theory to hold gave the nuclear temperature as 1.8 MeV, which is quite reasonable.

V.K. Deshpande: What is the energy of excitation in the compound nucleus?

R.K. Patell: About 21 MeV.

Ca^{40} (n,α) Ar^{37} ANGULAR DISTRIBUTION AT En =4.7 MeV

S.M.Bharathi, U.T. Raheja, B. Lal, P.N. Tiwari and E. Kondaiah
Tata Institute of Fundamental Research, Bombay

A gas proportional counter telescope, which has been described earlier (1), with slight modifications was used to study the energy and angular distribution of alpha particles arising from Ca^{40} (n,α) Ar^{37} reaction at En = 4.7 MeV. A Ti -Tr target bombarded with 5.5 MeV protons in the Van de Graff accelarator at Trombay was used as the source of neutrons.

The $\frac{dE}{dX}$ spectrum of alphas from the counter nearer the source, gated by the coincidence pulse derived from both the counters was observed on a TMC 400 channel analyser. The energies of alpha particles giving rise to the observed pulse heights, could be assessed by means of standard range-energy curves (2).

$\frac{dE}{dX}$ pulse height spectra were obtained at angles 0°, 30°, 60°, 120° 180°. Fig.1. shows a typical $\frac{dE}{dX}$ spectrum, taken at 30° to the neutron beam. This shows three groups which are seen at other angles also. The intensity at back angles is not sufficient to identify the groups. Hence these intensities were estimated by adding up the counts from appropriate channels. Table I helps to identify the groups of levels in Ar^{37} corresponding to the three groups A. B and C. From the table it is seen that group A comprises of ground state alphas, group B consists of alphas leading to first and second excited levels, while group C includes alphas leading to their, fourth and fifth levels of Ar^{37}. Individual levels could not be resolved due to the limited resolution due to the target thickness and the counter.

Figure 2,3 and 4 give the angular distribution of A, B and C respectively. From these figures, it can be seen that $\frac{\sigma 0°}{\sigma 180°} \cong 3,1$ and 0.2 for groups A,B and C respectively. This means, the forward to backward intensity falls of as the energy of the outgoing alphas decreases. Further

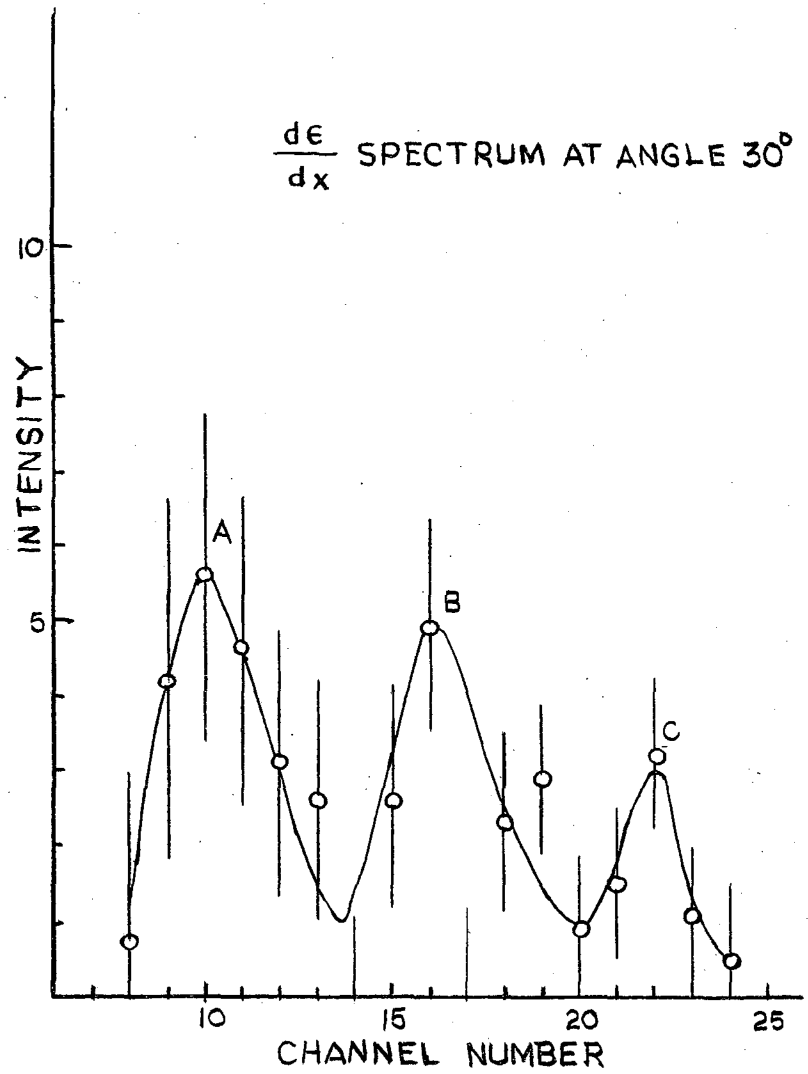

$\frac{d\epsilon}{dx}$ SPECTRUM AT ANGLE 30°
INTENSITY
10
5
A
B
C
10
15
20
25
CHANNEL NUMBER

FIG.1

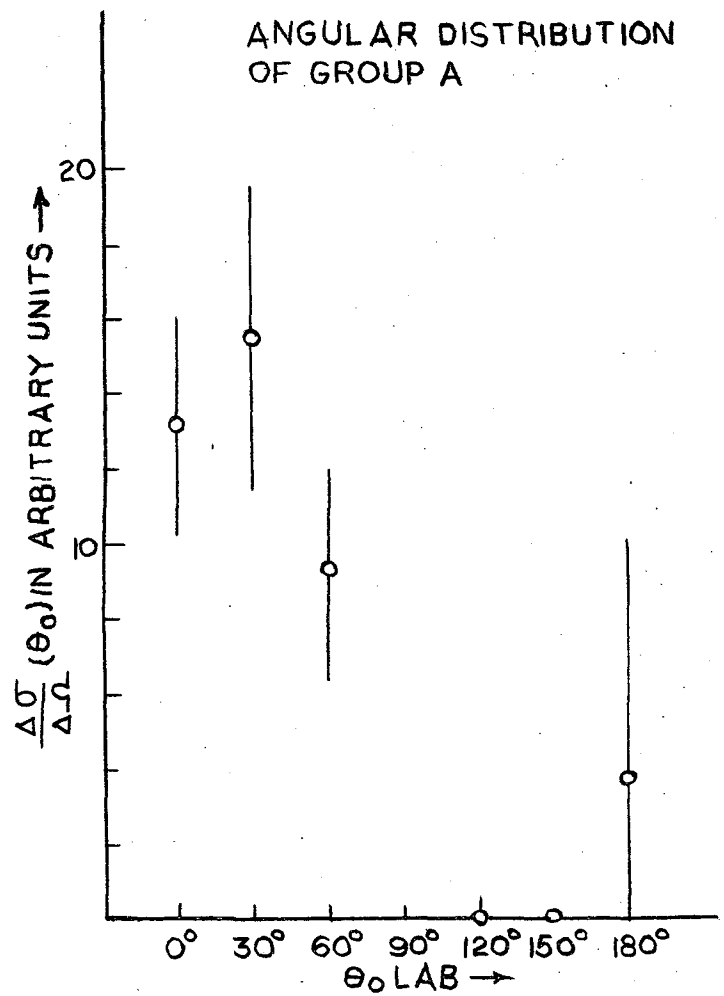

ANGULAR DISTRIBUTION
OF GROUP A
$\frac{\Delta\sigma}{\Delta\Omega}(\theta_0)$ IN ARBITRARY UNITS →
20
10
0° 30° 60° 90° 120° 150° 180°
θ_0 LAB →

FIG.2

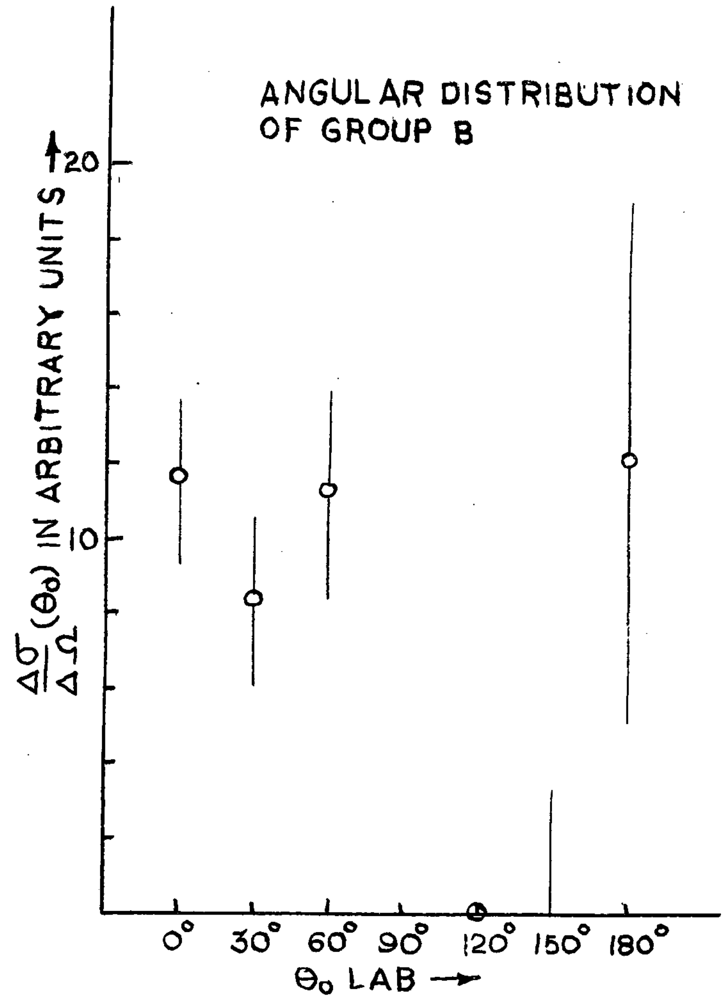

ANGULAR DISTRIBUTION OF GROUP B
$\frac{\Delta\sigma}{\Delta\Omega}(\theta_0)$ IN ARBITRARY UNITS
20
10
0° 30° 60° 90° 120° 150° 180°
θ_0 LAB

FIG. 3

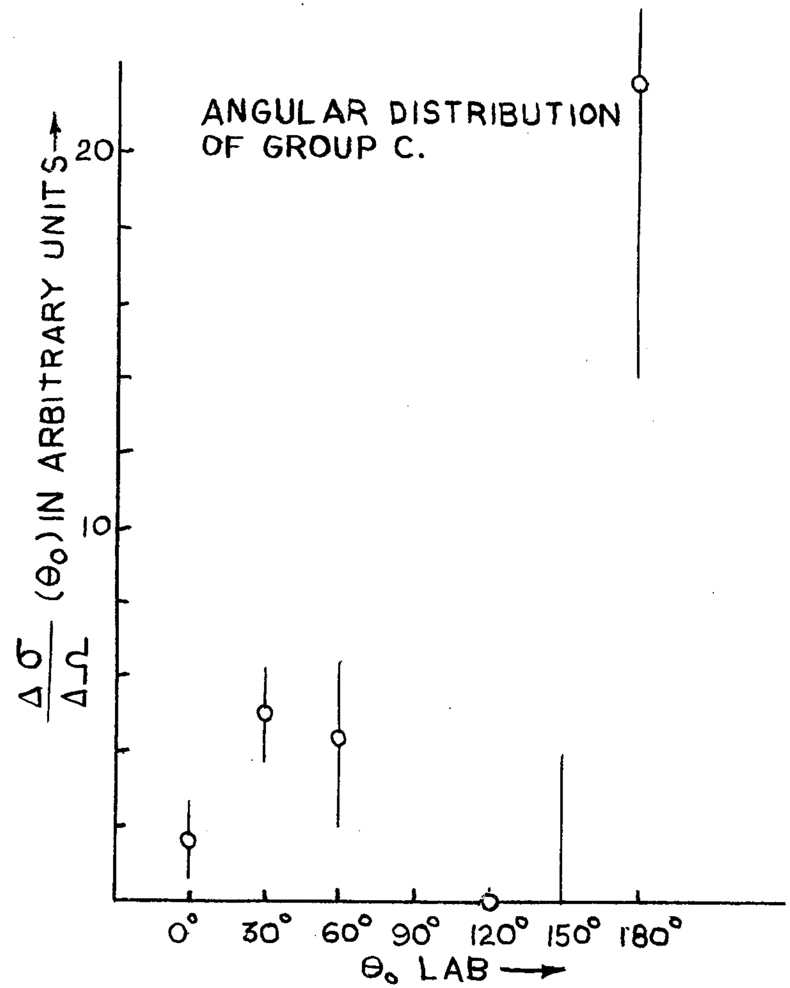

ANGULAR DISTRIBUTION OF GROUP C.
$\frac{\Delta\sigma}{\Delta\Omega}(\theta_0)$ IN ARBITRARY UNITS
20
10
0° 30° 60° 90° 120° 150° 180°
θ_0 LAB

FIG. 4

work is in progress to improve the statistics.

REFERENCES

1. U.T. Raheja and E. Kondaiah, Proc. Nuclear Phys. Symposium 255 (1963).

2. M.S. Livingston and H.A. Bethe, Rev. Mod. Phys. 9, 245 (1937).

TABLE I

Angle	Levels of Ar^{37}	Calculated E_α (from Q value) leading to level in column II after connecting for the target thickness (2.2 mg/cm^2)*	E_α observed (peak position)	Group
0°	0	5.6 ± 0 . 6	6.25±1.0	A
	1	4.32 ± 48	4.95±0.79	B
	2	4.16 ± 0.46		
	3	3.58 ± 0.40		
	4	3.43 ± 0.38	3.5±0.53	C
	5	3.32 ± 0.36		
30°	0	5.53 ± 0.64	6.25±1.25	A
	1	4.25 ± 0.47	4.5±0.45	B
	2	4.08 ± 0.45		
	3	3. 5 ± 0.39		
	4	3.37 ± 0.37	3.0±0.4	C
	5	3.25 ± 0.36		
60°	0	5.36 ± 0. 6	5.5±0.4	A
	1	4.09 ± 0.45	4.14±0.45	B
	2	3.91 ± 0.44		
	3	3.39 ± 0.37		
	4	3.20 ± 0.37	3.4±0.37	C
	5	3.08 ± 0.34		

* The errors mentioned here are the estimated errors due to the effective target thickness.

DISCUSSIONS

P. Mukherjee: Is it possible to use a solid state detector to better Advantage?

C. Badrinathan : There are certain disadvantages with solid state detectors (1) the back-ground is usually much larger. (2) The thickness of the dE/dX detector needed for these energies is only about 10-20 microns, and so is quite difficult to achieve with silicon. (3) Finally the life of these detectors is limited by radiation damage.

A.K. Ganguly: What was the actual counts to background counts ratio of the spectrometer used?

S.M. Bharathi: The actual counts to background ratio depends on the target and the angle. To give you a rough idea, for the case discussed here this is $\sim$ 25%.

H. Bakhru: What was the target thickness, area, angular spread in the measurement and the recording time at each angle in the experiment?

S.M. Bharathi : Target thickness was 2.2mg/cm^2 and of diameter $\frac{1}{2}$". The maximum scattering angle between the direction of the neutron striking the target at a point and the the direction of alpha particle emitted from that point was as much as 23°. Recording time was about 180μ amp hrs.of the proton beam of the Van de Graff.

ANALYSIS OF THE ANGULAR DISTRIBUTION FOR $O^{16}(n,\alpha)\ C^{13}$ REACTION AT 14 MeV

M.L. Chatterjee,
Saha Institute of Nuclear Physics, Calcutta

EXPERIMENTAL STUDIES AND RESULTS

To study the angular distribution of (n,α) reaction on O^{16}, a thin Mylar ($C_{10}O_4H_8$) film was positioned between two Ilford K2 plates with their emulsion surfaces in contact with the film. The experimental arrangement resembled that of I. Kumabae et al (8). The whole plate assembly was bombarded with 14 MeV neutrons.

Fig. 1 shows the distribution of alpha particles against the excitation energies of the residual nucleus C^{13} as well as the Q-values. In a proper scale the states of Be^9 are also shown. Since Mylar contains both carbon and oxygen in appreciable quantities, the α's coming out of bombardment of the Mylar film arise from $O^{16}(n,\alpha)\ C^{13}$ as well as $C^{12}\ (n,\alpha)\ Be^9$ reactions. The distribution shows two peaks - one in the neighbourhood of Q -value - 6.0 MeV and the other in the region of - 8.0 MeV.

In the region of Q value about - 6.0 MeV, which correspond to about 4 MeV excitation of the residual nucleus C^{13} , there is overlap (9) between the states 3.68 MeV and 3.85 MeV of C^{13} and the ground state of Be^9, since Q value for the $C^{12}\ (n,\alpha)\ Be^9$ reaction leading to the ground state Be^9 is -5.7 MeV. Hence for the analysis of the angular distribution for the O^{16} $(n,\alpha)\ C^{13}$ reaction in the region of 4 MeV excitation of C^{13}, a broad range of Q values namely between - 5.0 MeV to -7.0 MeV has been chosen. The entire contribution from the $C^{12}\ (n,\alpha)\ Be^9$ reaction leading to the ground state falls in this region. The angular distribution for the ground state group

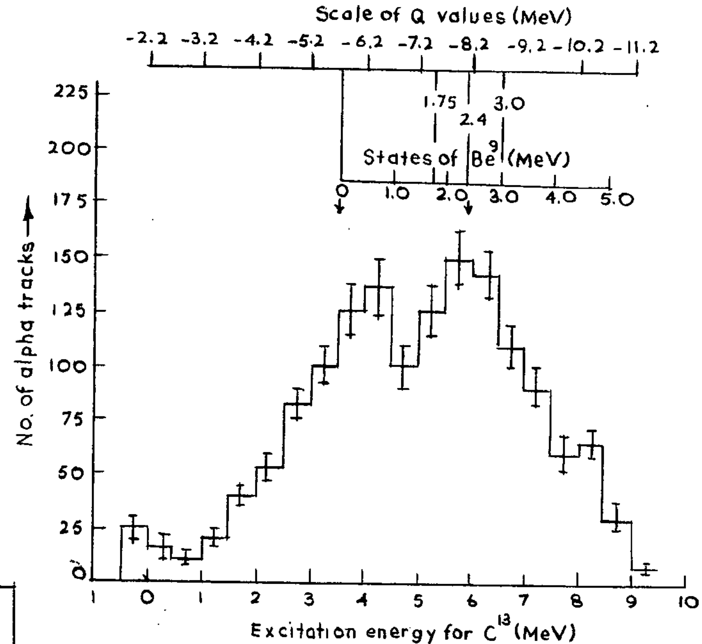

FIG.1

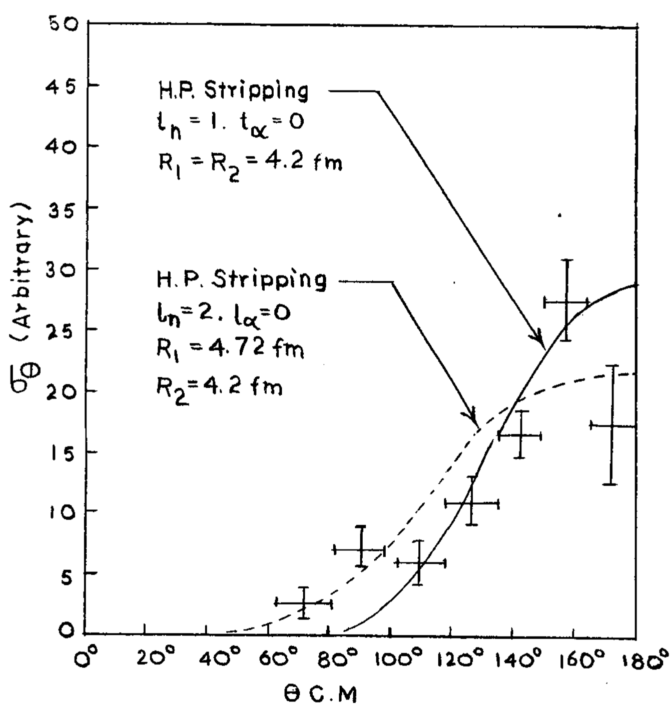

FIG.2

FIG.3.

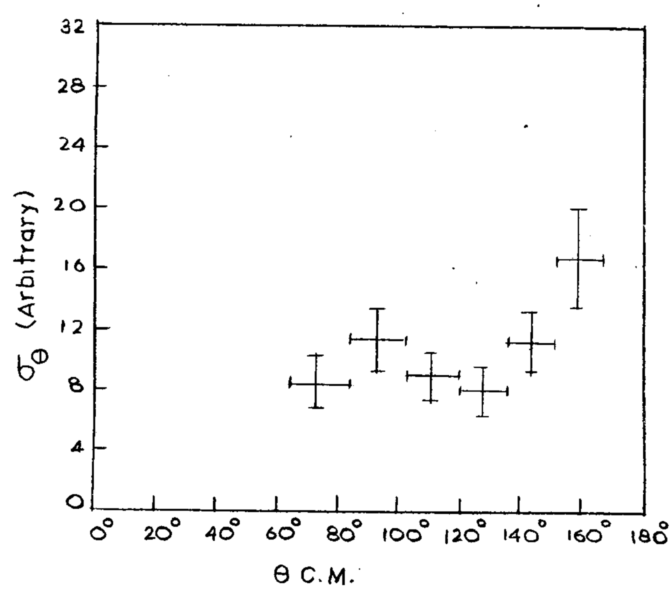

of alphas from C^{12} (n,α) Be^9 reaction is known (4,5) and the contributions are subtracted out to obtain the angular distribution in the region of 4 MeV excitation of C^{13} (Fig. 2.).

In the range of Q values between -7.0 and - 9.0 MeV there can be appreciable overlap (9) between the states at 5.51 and 6.10 MeV of C^{13} and 1.75, 2.40 and 3.0 MeV of Be^9. Of these states of Be^9, the contribution from the 2.4 MeV state is the most prominent (5). Fig. 3 shows the angular distribution in this region after proper subtraction of the contribution from C^{12} (n,α) Be^9 (2.4 MeV) reaction.

THEORETICAL FITS FOR THE ANGULAR DISTRIBUTION AND DISCUSSIONS

The angular distribution in the region of 4 MeV excitation of C^{13} (Fig.2) shows that the distribution is peaked in the backward direction in the neighbourhood of 160° c.m. The backward peaking indicates that the reaction is chiefly governed by the heavy-particle stripping mechanism. The angle dependent part in the differential cross-section is taken into account according to the following formula (7,10) assuming the heavy-particle stripping to be the mechanism operative:

$$\sigma(\theta) \approx |RE_1|^2 |RE_2|^2$$

where $RE_1 = \frac{1}{q_n^2+\beta_n^2}\left[q_n R_n j_{\ell_n-1}(q_n R_1) + C_{\ell n}(\beta_n R_1)\, j_{\ell_n}(q_n R_1)\right]$

$$RE_2 = \left[q_\alpha R_2\, j_{\ell_\alpha-1}(q_\alpha R_2) + C_{\ell\alpha}(\beta_\alpha R_2)\, j_{\ell_\alpha}(q_\alpha R_2)\right]$$

where q_n and q_α are the momentum transfers of the neutron and the α - particle, respectively

$$\beta_n^2 = 2M_{nc}\epsilon_{nc}\ ,\quad \beta_\alpha^2 = 2M_{\alpha c}\epsilon_{\alpha c}$$

where ϵ_{nc} and $\epsilon_{\alpha c}$ are the binding energies of the neutron and alpha particle in the residual nucleus and the target respectively; M_{nc} and $M_{\alpha c}$ are the reduced mass of the systems consisting of core plus neutron and core plus alpha, respectively; l_n is the orbital angular momentum of the captured neutron in the residual nucleus and l_α is the orbital angular momentum at which the alpha-particle leaves the target; R_1 and R_2 are the cut-off radii at which the capture of the neutron and the emission of the alpha-particle has taken place;

$$C_l(\beta R) = -i\beta R \left[h^{(1)}_{l-1}(i\beta R) \Big/ h^{(1)}_{l}(i\beta R) \right]$$

where h_l denotes Hankel function of order l.

In Fig. 2 the solid curve shows the fit with $l_n = 1$ and $l_\alpha = 0$ and the dotted curve with $l_n = 2$ and $l_\alpha = 0$. From the two fits it seems that the distribution in the region of 4 MeV excitation of C^{13} might be due to the combined contributions from two levels of opposite parities. There is actual experimental evidence (9) for the existence of two close levels at 3.68 MeV ($3/2^-$) and 3.85 MeV ($5/2^+$) in the C^{13} nucleus.

Cindro et al also observed backward peaking in the $O^{16}(n,\alpha)C^{13}$ recation (2). For the 3.7 MeV excitation of C^{13}, Lillie (3) observed peaks both in forward and backward hemispheres. The forward peaking has not been observed in the present work. The backward peaking observed both in Figs. 2 and 3 indicates that heavy-particle stripping probably is the chief mechanism that governs $O^{16}(n,\alpha)C^{13}$ reaction. In the calculation of theoretical fits PWBA has been used. For better fits DWBA calculations should be pursued.

REFERENCES

1. B.Sen. Nucl. Phys. 41, 435 (1963).

2. N. Cindro, I. Slaus, P. Tomas and B Eman, Nucl. Phys. 22, 96 (1961).

3. A.B. Lillie, Phys. Rev. 87, 716 (1952).

4. M.L. Chatterjee and B. Sen Nucl. Phys. 51, 583 (1964).

5. R.A. Al- Kital and R.A. Peck Jr., Phys. Rev. 130, 1500 (1963).

6. V.I. Ostroumov and R.A. Filov, JETP (Soviet Physics) 10, 459 (1960).

7. M.A. Nagarajan and M.K. Banerjee, Nucl. Phys. 17, 343 (1960).

8. I. Kumabae et al., J. Phys. Soc. Japan 13, 129 (1958).

9. F. Ajzenberg - Selove and T. Lauritsen, Nucl. Phys. 11, 1 (1959).

10. Tsuyoshi Honda and Haruo Ui, Prog. Thor. Physics. 25, 613 (1961).

DISCUSSIONS

V.K. Deshpande

Comment: The inverse reactions C^{13} (α,n) and Be^{9} (α, n) have been studied at Rochester. Many sharp peaks are observed in the yield curve in the case of C^{13} spin and parities assume for these levels have been checked by studying, angular distributions. The $C^{13}(\alpha,n)$ reaction therefore seems to proceed via compound nuclear mechanism.

M.L. Chatterjee: Yes, the studies of reverse reactions like C^{13} (α, n) and Be^9 (α, n) are very important so far as the reciprocity is concerned. In this connection I would like to refer to the work of Kjell and Nilsson (Arkiv for Physiks Vols 21,22,23) where they have also studied (α, n) reactions on Li^7, Be^9 C^{13}, at several alpha energies ranging between 9.8 to 13.5 MeV. In their results they also find different types of angular distribution for the different groups of neutrons. But in some cases strong asymmetry about 90° c.m is observed. In the $C^{13}(\alpha, n)$ reaction, at least for certain states of O^{16} they have attempted to fit the distribution in terms of knock-on and h.p. stripping. Your results indicate that $C^{13}(\alpha, n)$ reaction seems to proceed via Compound nucleus. But the (n,α) studies in recent years at 14 MeV in the light nuclei region indicate the presence of direct and exchange effects. Of course to reconcile with the reciprocity relation, the (n,α) studies need be persued at different neutron energies.

V.K. Deshpande

Comment: An estimate of the absolute cross-section on the basis of Heavy Particle stripping would probably show a discripancy of an order of magnitude or more with this experimental data.

M.L.Chatterjee: It is difficult to evaluate absolute cross-sections from direct and exchange reaction theories. The only basis of the attempt to interpret the present results in terms of h.p.stripping is that in the light nuclei (especially in C^{12} and O^{16}) there are enough evidence for the existence of He^4 Clusters. On this ground on can expect high c.f.p. for He^4 in O^{16}.

B.K. Jain

Question: Why do you anticipate H.P. Stripping contribution predominent in $O^{16}(n,\alpha)$? It may be just possible that ordinary stripping with DWBA analysis may give the fit.

M.L.Chatterjee: Yes, that may be possible. Our analysis here is restricted by the PWBA and hence the conclusion also. But unless one makes thorough DWBA calculations for both pick-up and heavy particle stripping including absolute evaluations, one cannot in any way rule out the importance of h.p. stripping. In the light nuclei region the presence of He^4 Clusters seem more favourable than He^3. On this basis one can expect the exchange process like h.p. stripping will be more probable than direct pick-up as an He^3. However one cannot be very sure of it unless the complete matrix is evaluated.

Regarding DWBA calculations in the light nuclei region there is one basic difficulty. As Hodgson points out (Proc. of Conf. on Dir Int. and Nuclear Reaction Mechanism held at Padua) that the conditions for the validity of the optical model are frequently not satisfied for light nuclei. So if the elastic scattering data be analysed with this model, the optical parametres show marked fluctuations with energy and from nucleus to nucleus. So the choice of the proper optical parametres becomes very crucial.

FINE STRUCTURE IN THE MASS DISTRIBUTION OF THE FISSION PRODUCTS FROM THE FAST NEUTRON FISSION OF U^{238}

C.K. Mathews
Radiochemistry and Isotope Division
Atomic Energy Establishment Trombay
Bombay

Isotopic abundances of the elements xenon, cesium, barium, cerium, neodynium and samarium formed in the fast (fission spectrum) neutron fission of U^{238} have been measured using the mass spectrometeric method. These ratios were normalised with respect to each other through isobaric nuclides and isotope dilution to obtain the relative yields of isobaric chains in the heavy mass region. By normasizing the heavy mass yields to 100%, the absolute fission yields of twenty isobaric chains in the 130-154 mass range were determined.

Fine structure in the cumulative yields vs.mass curve for the fast neutron fission U^{238} is discussed along with those for the slow neutron fission U^{233} and U^{235}. It is concluded that while most of the fine structure arises from the variation in the neutron emission probabilities as a function of the mass of the fragment, some of it could be the result of shell effects in the fission act itself. The origin of this latter effect is discussed in terms of a modified Whetstone model.

DISCUSSIONS

D.M. Nadkarni: The excitation energy of the nucleus involved here seems to be high enough where one cannot use the Universal curve of Terrel for correcting the observed mass distribution. However, in the 4 MeV fission of U^{235} we found that the fine structure still persists even if we use the relation $\nu_L = \nu_H = \nu_T/2$. In the present case however it is not clear if one could used a definite $\nu(M)$ distribution.

C.K. Mathews: The only point I have made is that sharp variation in the neutron yield curve could give rise to appreciable fine structure in the cumulative mass distribution. Terrel's curve was not used for any quantitative deductions.

R. Ramanna: It seems that the Terrell's Universal Curves have not been established (Ref. recent USSR work by Apati et al), the curves corrected for prompt emission therefore is not reliable. Besides the time of flight work does not show any peaks. I therefore feel any theoretical interpretation of the fine structure at this stage is not justified. However it is possible to include the fine struc. effect and the statistical theory I discussed this morning.

C.K. Mathews: I have mentioned in my paper that Terrel's curve is not accurate and any deductions based on it are not to be taken seriously. Time-of-flight measurements do show fine structure, however small.

N.N. Ajitanand: Were there any corrections applied due to experimental dispersion, inherent in the Mass spectrometer method?

C.K. Mathews: There was no need to do this. The only background contributions at a particular mass number defined by an e/m arise from $\frac{\frac{1}{2}e}{\frac{1}{2}m}, \frac{2e}{2m}, \frac{3e}{3m}$ ---etc and hydrocarbon background. The former is extremely small because of the very low probability of second ionization as well as association and the latter can be made negligible, by eliminating all hydrocarbon sources.

SELF-CONSISTENT CALCULATIONS OF NUCLEAR STRUCTURE

M.K. Pal
Saha Institute of Nuclear Physics, Calcutta.

It is a rather enigmatic fact that self-consistent calculations of nuclear structure are of very recent origin, while the nuclear shell model has by now become an old subject. However, after, the initial reluctance to undertake such calculations was over-come, progress has been achieved in strides. In the hands of structure physicists the self-consistent method has already taken a highly sophisticated shape; the pairing effects have been incorporated in the conventional Hartree-Fock (HF) type theory and the result is the so-called Hartree-Fock-Bogoliubov (HFB) theory. It is true that there are yet a few unsolved problems, namely the inclusion of the full neutron-proton correlation effects, or the modification of the formation to include polarisation on effects in odd nuclei. But one would like to assess the present growth in the subject as highly satisfactory in terms of our basic understanding of the elementary modes of excitation of the nucleus; and hope that a satisfactory solution of the unsolved problems within the frame-work of the self-consistent theory would evently emerge with time.

Although the main emphasis in this talk will be on the self-consistent calculations of nuclear structure, I would neverthless like to include in the review a few other non-self-consistent work in this field which are of sufficient importance to deserve mention. Since I found it difficult to fit these "self-consistently" into the self- consistent theme of this talk, I thought I would first deal with them as a few isolated topics on nuclear structure and then pass on to the description of the self - consistent calculations.

The first work I would like to talk about, is by A.B. Volkov (1) from Copenhagen. This is a variational calculation for the shape of lp-shell nuclei. The isotropic harmonic oscillator wavefunctions for the ls- and lp-shells are deformed, to start with through the prescription $x \longrightarrow ax$, $y \longrightarrow ay$, and $z \longrightarrow bz$. The parameters a and b can obviously be related to the nuclear radius, and the deformation parameter ϵ. Since x and y co-ordinates are scaled equally, and z differently, the deformation that has been put into the wavefunctions has a spheroidal symmetry. The two-body potential, used in the calculation of the energy, is of Gaussian shape, and has a "soft core" repulsive part having Wigner plus Majorana exchange dependence. Since the nuclear radius itself is a variational parameter in these calculations, to the use of realistic two-nucleon interaction becomes very essential. The parameters of the two-body potential described above were, therefore, determined carefully by reproducing the size and binding energies of He^4 and O^{16}, and the average (singlet and triplet) values of the effective range and scattering length. The calculated ground-state energies for several nuclei are shown in Fig. 1 as a function of the deformation ϵ. It is seen that the minimum of the energy in each case occurs at a significantly large nonzero value of the deformation. It is rather disturbing that, contrary to our naive belief, even such light nuclei should show marked deformations in the ground state. However, the following findings leave scope for a revision of these results: it is found that the equilibrium deformation gets reduced, firstly with a decrease in the amount of Majorna exchange intraction, and secondly by taking the lp orbitals to have a larger spatial extent than the ls-orbital. In view of the fact that the two-nucleon potential used in this work has not been tested by fitting a wide range of two-body data, and the fact that

1p-orbitals are certainly less bound than the 1s-orbital, the equilibrium deformations calculated by Volkov may not be quantitatively very reliable.

The second work, I want to mention, is on the excited levels of O^{16}. Although the ground state of this nucleus correspondsto the closed 1p-shell and hence has a spherical shape, there is an extensive experimental evidence that the excited states of this nucleus form several well-marked rotational bands (Fig.2). This means that the closed-shell spherical shape is not a very stable one; nucleus has a rather soft structure, which gets deformed with a little bit of excitation energy. There have been some theoretical attempts to interpret the rotational spectra of O^{16} with the help of shell-model wavefunctions classified by the SU_3 group. The original idea behind suchwork is that of Elliot (2), and has been applied to the O^{16} states by Brink and Nash (3) and by Borysowicz and Sheline (4). The spectra obtained by the latter workers are also shown in Fig. 2. We will have occasion, later on in this lecture, to comment on the use of wavefunctions belonging to pure SU_3 symmetry for the explanation of collective rotational states.

The third work, I have inmind, has to do with the magnetic moments of odd nuclei. After the old work a Arima and Horie (5) and of Blinstoyle (5) nothing much was done in this field for a long time. Recently there has been a revival of interest with the availability of experimental data on the magnetic moment of excited states of nuclei. With this new breakthrough in the experimental techniques, it has been fashionable to try to reproduce the magnetic moments in terms of two parameters, which follow from a rather crude core-polarisation model. One writes the magnetic moment as

$$\underset{\sim}{\mu} = (g_s)_{eff}\, \underset{\sim}{\sigma} + g_l\, \underset{\sim}{l}$$

where g_l is the gyromagnetic ratio due to orbital angular momentum $\underset{\sim}{l}$ and $(g_s)_{eff}$ is that the due to spin $\underset{\sim}{\sigma}$. A fit to the experimental data gives a

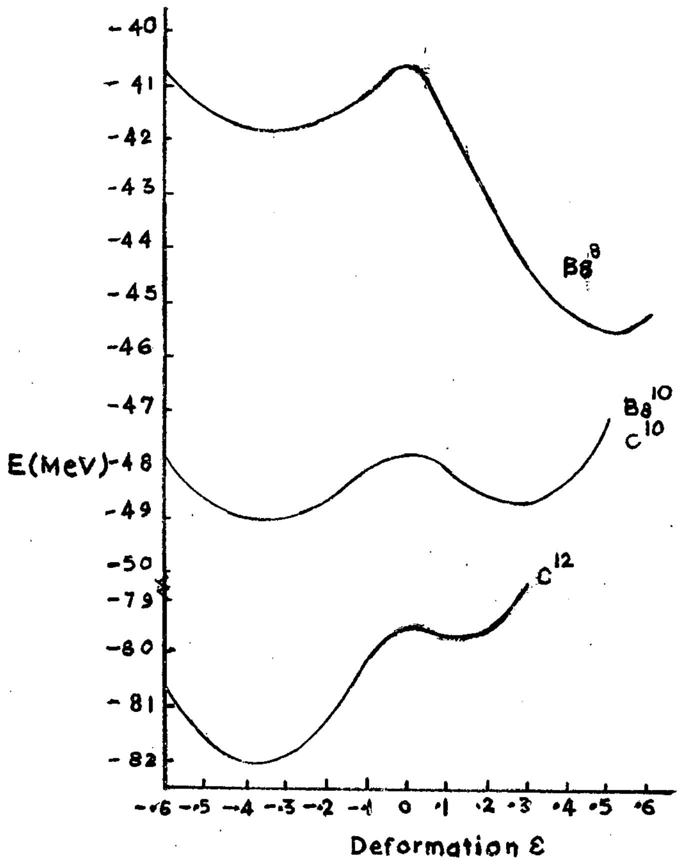

Fig. 1.

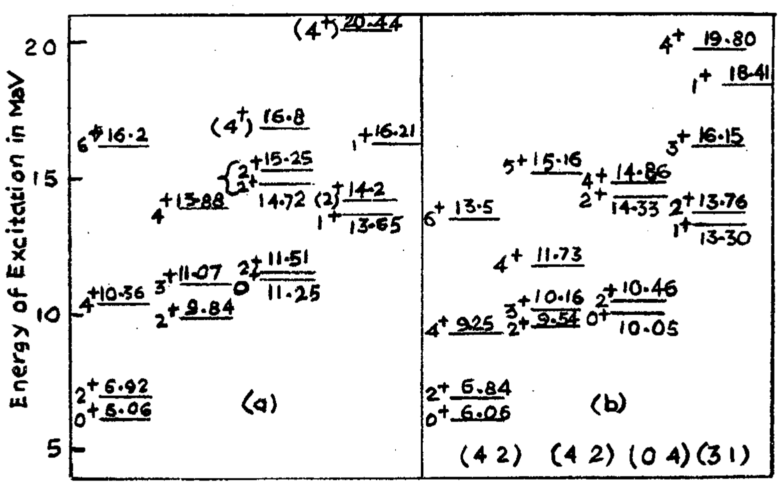

Fig 2.

Experimentally observed rotational bands of 0^{16} (left half of the diagram), together with the theoretical results of ref.4 (right half) using the SU_3 symmetries (42), (04) and (31).

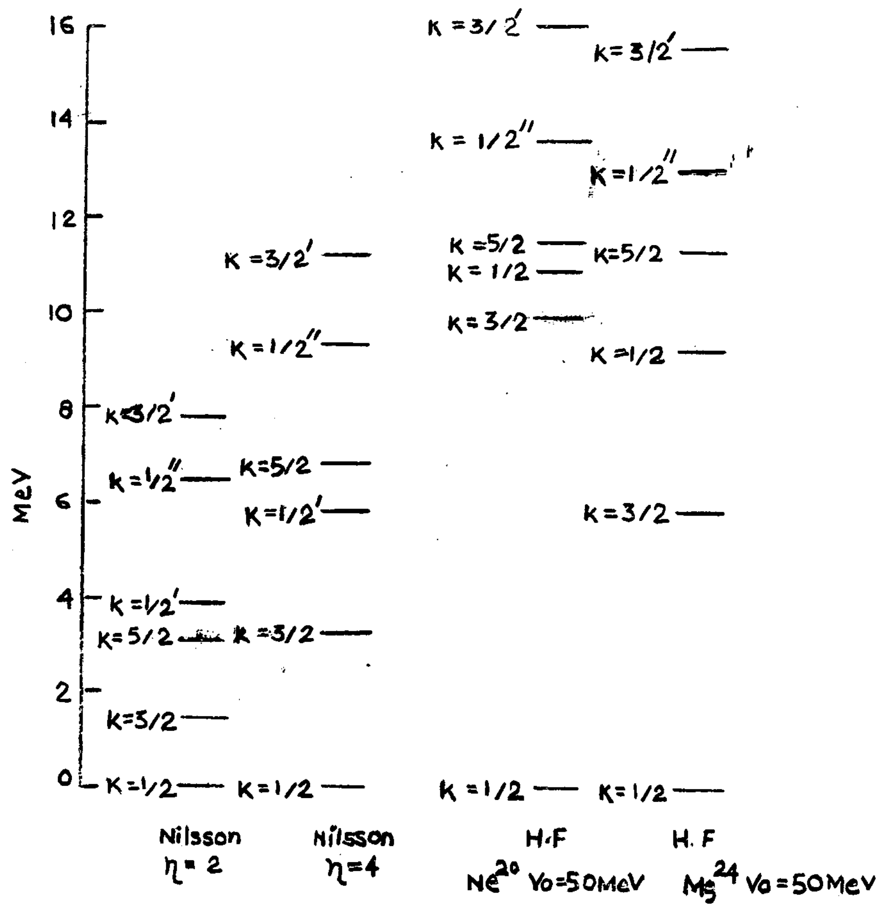

Fig. 3.

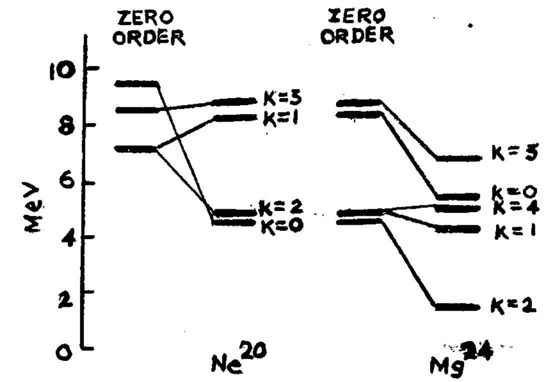

Fig. 4.

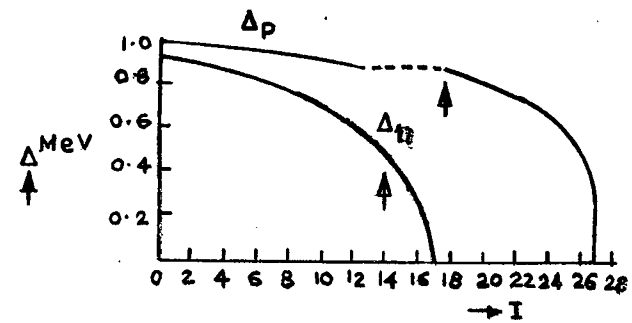

Fig. 5.

$(g_s)_{eff}$ which is, in most cases, quite different from the intrinsic nucleon gyromagnetic ratio, $(g_s)_{intr}$. This is to be expected because the use of $(g_s)_{intr}$ in place of $(g_s)_{eff}$ means driving at the schmidt values of the magnetic moments, which are well-known to be very much off from the experimental values. The departure of $(g_s)_{eff}$ from $(g_s)_{intr}$ is attempted to be understood in terms of the polarization of the core through spin-dependent two-nucleon interactions. The use of a rather crude picture of the core-polarization [see, for example, Bodenstedt and Rogers (6)] leads to additional contributions to the magnetic moment, over and above the intrinsic moment and the moment due to orbital angular momentum. Thus $(g_s)_{eff}$ is the resultant of these extra moments due to core polarization and the intrinsic moment:

$$(g_s)_{eff}\, \underset{\sim}{\sigma} = (g_s)_{intr}\, \underset{\sim}{\sigma} + \delta g_s\, \underset{\sim}{\sigma} + g_p\, (Y^2 \cdot \underset{\sim}{\sigma})^1 \quad (1)$$

Here δ_{gs} and g_p are the two parameters (dependent on core-polarization), mentioned earlier, and $(Y^2, \underset{\sim}{\sigma})^1$ is a tensor of rank unity obtained by compounding the spherical harmonic Y^2 with $\underset{\sim}{\sigma}$. Apart from some calculation done by Migdal (7), which is not very transparent to the present reviewer, there have been no other detailed calculations, based on structural models, of the parameters δ_{gs} and g_p; so far only the experimentalists have been trying to check the feasibility of interpreting the data in terms of the above two parameters. The possibility of including core-polarization effects in the self-consistent theories will be discussed later later on.

The last isolated topic I would like to touch upon, concerns a volume of work of the Talmi-type in the Zr-region. In this type of work one determines the matrix elements of two-nucleon interactions from observed spectra, and then uses these to calculate more complicated cases. The calculations are feasible in regions of nuclei where pure jj-coupling configurations could be attributed to the observed states. ${}_{40}Zr^{90}_{50}$ is taken to have a closed shell structure. The next proton and neutron added to this nucleus go respectively to the $1g_{9/2}$ and $2d_{5/2}$ orbitals. The low-lying levels of the corresponding nucleus ${}_{41}Nb^{92}_{51}$ thus arise from the angular momentum coupling in the configuration $(1g_{9/2})_p \; (2d_{5/2})_n$. In the same way the low-lying levels of ${}_{41}Nb^{93}_{52}$ will correspond to the configuration $(1g_{9/2})_p \; (2d_{5/2})^2_n$. In particular the ground state of Nb^{93}, with angular momentum $J = 9/2$, will arise from states like $\left| (1g_{9/2})_p \, , \, 2d_{5/2})^2_n \; J' : J = 9/2 \right\rangle$, where the two neutrons have coupled to an angular momentum J', which has then coupled with the $(1g_{9/2})_p$ to give rise to the resultant $J = 9/2$. According to the simple seniority idea the lowest state is expected to have $J' = 0$, i.e. the seniority zero state for the neutron pair. However, one can do a better job than this. Making use of the n-n interaction matrix elements and n-p interaction matrix elements from the observed spectra in Zr^{92} and Nb^{92} respectively, one can set up the interaction matrix with the basic states given above and then diagonalise the matrix, and thus find the lowest state wavefunction in the form: $\sum_{J'} C_{J'} \times \left| (1g_{9/2})_p \, , \, (2d_{5/2})^2_n \; J' : J = 9/2 \right\rangle$. This calculated wave-function can be tested with the help of the experimental spectroscopic factors for the transitions to the different levels of Nb^{92} reached in the pick-up reactions (p,d) or (d,t) on Nb^{93}. In fact the observed ratios of the spectroscopic factors are very much in disagreement with the assumption of a pure lowest-seniority ($J' = 0$) state for Nb^{93}; on the other hand the detailed wavefunction with nonvanishing $C_{J'}$ for all the possible J' , calculated as explained above, gives a surprisingly good agreementwith the pick-up data. The experiment was done at Oak Ridge and the interpretation is due to Sweet, Bhatt and Ball (8).

In the same region of nuclei Pandya (9) has done a very clever analysis of the experimental spectra of Nb^{92} in terms of Slater integrals $F^{(k)}$. The calculated values of $F^{(k)}$ are then compared with those expected from potentials of the form: (1) $V_0 + V_1 \underset{\sim}{\sigma_1} \cdot \underset{\sim}{\sigma_2}$ and (2) $V_0(1+\alpha \underset{\sim}{\sigma_1} \cdot \underset{\sim}{\sigma_2})$. The first form goes over to the second when the radial shapes of V_0 and V_1 are taken to be the same. From Pandya's analysis in terms of $F^{(k)}$ it is concluded that V_0 and V_1 have very closely the same radial shape, i.e. form (2) of the potential is quite justifiable, and the value of the parameter is found to be about 0.155 in close agreement with what people generally use. It is also found that the ratios of the later integrals are very different from what one would expect from a zero-range potential; that is to say, one must use a finite range potential in the calculations. Although the work done in the Zr^{90} region is quite voluminous, only the above two pieces of work have been selected for the purpose of this review to give a representative idea as to the power of the Talmi-type approach when applied to the suitable regions of nuclei with suitable minor modifications, if necessary of the lowest seniority wave-functions.

I shall now give an account of the self-consistent calculations. The basic concepts in the HF theory will be sketched first with a view to introducing the terminologies that are used in this field. In this short review it is hardly possible to go into the details of the method which are available these days in several treatise (10) on the subject. We start with the Hamiltonian in its second-quantised form in terms of the creation and destruction operators $C^{\dagger}_{\alpha}, C_{\beta}$ etc. for the single-particle states α, β etc.:

$$H = \sum_{\alpha\beta} \langle \alpha | T | \beta \rangle C^{\dagger}_{\alpha} C_{\beta} + \frac{1}{2} \sum_{\alpha\beta\gamma\delta} \langle \alpha\beta | v | \gamma\delta \rangle C^{\dagger}_{\alpha} C^{\dagger}_{\beta} C_{\delta} C_{\gamma}$$

where T is the single-particle kinetic energy, and $\mathcal{V}$ the two-nucleon interaction potential. The Hartree-Fock calculation is based on the assumption of a ground state Ψ_0, taken in the form of a determinant, in which the N-nucleons under consideration are ascribed N single-particle states. The calculation then strives to determine a single-particle Hamiltonian self-consistently for which the N occupied states in Ψ_0 are the lowest N states (satisfying Pauli exclusion principle). The expectation value of H with respect to Ψ_0, to be denoted by $\langle H \rangle$, contains $\langle c_\alpha^+ \quad c_\beta \rangle$ and $\langle c_\alpha^+ \; c_\beta^+ \, c_\delta c_\gamma \rangle$. The first one is the matrix element $\rho_{\beta\alpha}$ of the single-particle density operator ρ :

$$\rho_{\beta\alpha} = \langle c_\alpha^+ c_\beta \rangle$$

The HF-method, being based on a single-particle picture, attempts to approximate the more complicated expression $\langle c_\alpha^+ \; c_\beta^+ \; c_\delta \; c_\gamma \rangle$ in terms of the matrix elements of ρ, the single-particle density, as follows:

$$\langle c_\alpha^+ c_\beta^+ c_\delta c_\gamma \rangle \approx \langle c_\beta^+ c_\delta \rangle \langle c_\alpha^+ c_\gamma \rangle - \langle c_\alpha^+ c_\delta \rangle \langle c_\beta^+ c_\gamma \rangle$$
$$= \rho_{\alpha\beta} \, \rho_{\gamma\alpha} - \rho_{\delta\alpha} \, \rho_{\gamma\beta}$$

This approximation is known as the HF factorization. The single-particle wave-functions and energies are then determined by requiring that $\langle H \rangle$ be a minimum with respect to variations in the single-particle wave-functions in Ψ_0. This minimisation programme is found to be equivalent to diagonalising the single-particle HF Hamiltonian $\Gamma \equiv T + V$ where V is defined in terms of the matrix elements of $\mathcal{V}$ as follows:

$$\langle \alpha | V | \gamma \rangle = \sum_{\beta\delta} \langle \alpha\beta | \mathcal{V} | \gamma\delta \rangle_{Exch.} \rho_{\delta\beta}$$

Since the single-particle HF potential V depends on ρ, ie. the choice of Ψ_0, it is clear that the diagonalisation of Γ has to be carried out self-consistently.

Since the Hamiltonian that is being diagonalised in the HF programme is a functional of ψ_0, one cannot expect ψ_0 to contain the symmetry of the starting Hamiltonian H. In fact the Hartree Fock potential V may quite often be deformed in order that the absolute minimum of $\langle H \rangle$ is secured through the HF self-consistent programme. In nuclear calculations it is customary not to try forms of V which have the most general kind of deformation; one very often restricts oneself to spheroidal symmetry. The ψ_0 that results from such calculations has a good projection quantum number, called the band quantum number K, and is generally a mixture of states of various total angular momentum J consistent with the given K. States of good J can be projected out of ψ_0 by suitable angular momentum techniques and then the expectation values of H for such states can be calculated in a straightforward manner. Thus one obtains the energies of the different angular momentum levels corresponding to a given intrinsic function ψ_0. In the language of the crude collective model what one is doing is the calculation of the energies of the different rotational states belonging to a rotational band.

The same programme is sometime achieved by calculating the rotational moment of inertia I and then using the formula $(\hbar^2/2I)\, J\,(J+1)$ to calculate the rotational energies. It does not necessarily follow that the two ways of computing the rotational energies would lead to identical results. The moment of inertia again is calculated by several different methods not necessarily yielding equal values. The first method due to Skyrme, called the variational method, has recently been revived by Levenson (11). The method which is most popular in this field is based on the concept of a cranking of the nucleus with angular velocity ω about an axis (say X) perpendicular to the symmetry axis Z. The cranked Hamiltonian is given by $H - \omega J_x$. In the adiabatic approximation, i.e. small ω, the ωJ_x part of the cranked Hamiltonian can be treated as a perturbation, and thus the perturbed wave function ψ corresponding to the cranked Hamiltonian can be very easily written down, and then the identity: $\langle \psi | J_x | \psi \rangle \equiv I\omega$, determines the moment of inertia I. The resultant formula for I was first derived by Inglis and is popularly known as the cranking model formula. Even within the cranking model it is possible to do a beter job in determining I by using the time-dependent equation for the cranked density function ρ (t); this has been done by Thouless and Valatin (12) whose equations lead to the cranking model formula for I if certain terms containing γ are neglected.

If ωJ_x were not treated as a perturbation and one did a HF calculation with the cranked Hamiltonian, one would obtain a HF function ψ (ω) which is dependent on ω. Such a ψ (ω) will obviously have mixed bands through the ωJ_x term in the Hamiltonian. It is pertinent to ask the following question: can the HF solutions of the cranked Hamiltonian be better variational functions that the HF solution of the uncranked case? The variational problem, in this generality, has been investigated by Thouless and Peierls (13).

After the initial HF calculation has been done for the lowest intrinsic function, it is possible to carry out calculations for the excited intrinsic functions by promoting particles from the occupied states to unoccupied states above Fermi-sea. The residual interaction has to be diagonalised in such a calculation among the various possible hole-particle states. This is sometimes referred to as the Tamm-Dancoff(TD)type calculation. It is possible to incorporate the effects of correlations being present in the ground state in such calculations for the excited intrinsic states by a method, well-known in the theory of plasma oscillations of an electron-gas by the name random-phase approximation or simply RPA.

Before sketching the modifications leading from the HF to the HFB theory, I would like to describe the results of some HF type calculations by Levinson and collaborators (14) in the 2s-1d shell. Spheroidal symmetry was imposed in these calculations, and the resultant single-particle levels for several nuclei are shown in Fig. 3. What is noticeable in these results is the large gap between occupied and the unoccupied levels. This is a very happy feature and lends confidence in one's mind in the success of the HF - method and the subsequent RPA calculation for the excited intrinsic states. This gap, which is a result of the self-consistent programme, is markedly absent from the spectra obtained non-self-consistently in the Nilsson model with a spheroidal deformed potential. The calculation of moments of inertia by the variational formula of Skyrme gives rise to the following difficulties: although in the case of Ne^{20} one obtains a fairly well-defined minimum in the calculated curve from which one can read off the moment of inertia, the minimum in Mg^{24} is rather flat and thus does not admit of a precise theoretical prediction. The rotational levels calculated from the projected wave functions and from the cranking model formula agree fairly well. The results of the RPA calculations for the excited intrinsic states are shown in Fig. 4 together with the zero-order positions of the holeparticle states. As is expected RPA gives rise to significant changes from the zero - order situation. The changes are very well-marked with respect to transition probabilities also.

It would be pertinent here to stress the basic points made in a work by Banerjee and Tewari, which is going to be reported in this symposium. I choose to do so, at the risk of repition, because the results of this direct diagonalisation calculation give adequate support to the applicability of HF method in the 2s, 1d shell. This work starts by diagonalising the energy matrices with the SU_3 wave functions as basis. It is found that the resultant wave functions for the various angular momenta are very closely the results of projection out of the same intrinsic wave-function. The latter, however, is a very much mixed state, containing mixture of various bands and SU_3 symmetries. But despite this complicated structure, it satisfies the test of a determinantal wave function: $\rho = \rho^2$, ρ being the single-particle density matrix calculated with this intrinsic wave function, to an accuracy of one percent. The mixture of bands in this wave function suggests that it is the HF solution of a cranked Hamiltonian. The mixture of various SU_3 symmetries tells us that the goodness of collective wave functions in the 2s, 1d shell does not have much to do with the goodness of wave functions classified by the SU_3 group. Because of the preliminary version of the SU_3 work by Elliott in the 2s, 1d shell, people were prone to believing the latter fact; this belief is reflected in the attempts on the excited states of O^{16} mentioned earlier.

I shall now describe the HFB self-consistent theory, where the effects of nucleon -nucleon pairing are incorporated. As is well-known, in the theory of pairing one works in terms of a variational wave-function Ψ_0 that does not conserve the number of particles. In the expression $\langle c_\alpha^\dagger \; c_\beta^\dagger \; c_\delta \; c_\gamma \rangle$ one, therefore, has to consider now the new possibility $\langle c_\alpha^\dagger \; c_\beta^\dagger \rangle \langle c_\delta \; c_\gamma \rangle$

over and above the particle-conserving terms $\langle c^{\dagger}_{\alpha} \quad c_{\gamma}\rangle \langle c^{\dagger}_{\beta} \quad c_{\delta}\rangle$ and $-\langle c^{\dagger}_{\alpha} \quad c_{\delta}\rangle \langle c^{\dagger}_{\beta} \quad c_{\gamma}\rangle$ used earlier in the HF theory. The quantities $\langle c_{\delta} \quad c_{\gamma}\rangle \equiv K_{\delta\gamma}$ define the elements of the pairing matrix K . As a result of this new term the expectation value $\langle H\rangle$ now contains the matrix elements of pairing potential, defined by:

$$\langle\alpha|\Delta|\beta\rangle \equiv \sum_{\gamma\delta} \langle\alpha\beta|v|\gamma\delta\rangle_{\text{even}} K_{\delta\gamma}$$

The minimisation of $\langle H\rangle$ can now be achieved by diagonalising self-consistently a supermatrix W given by

$$W = \begin{pmatrix} \bar{\Gamma} & \Delta \\ -\Delta & -\bar{\Gamma} \end{pmatrix}$$

where $\bar{\Gamma} = \Gamma - \lambda 1$, Γ being the HF Hamiltonian, and λ the chemical potential, which has to be determined by requiring the particle number to be produced on the average. Denoting an eigen vector of this matrix by $\begin{pmatrix} U \\ V \end{pmatrix}$, one is led to the quasi-particle operators $a^{\dagger}_{i}$ defined as follows:

$$a^{\dagger}_{i} = \sum_{\alpha} (U_{i\alpha} C^{\dagger}_{\alpha} + V_{i\alpha} C_{\alpha})$$

The quasi-particles correspond to elementary excitations of the single-particle type in odd nuclei. In even-even nuclei the elementary excitations correspond to two-quasiparticle excited states; in particular the residual long-range quasi-particleinteractions (usually assumed to be a quadrupole-quadrupole interaction) may produce a coherent mixture of the two quasi-particlestates showing collective characteristics. This coherent state corresponds to the phonon-mode of excitation in the language of the crude vibrational model.

The general equations for the self-consistent calculation become much simplified if one assumes that the pairing potential Δ is given rise to by an idealised two-body pairing interaction v_p, which has constant matrix elements G connecting paired states of the type $|jm, \ j\,\bar{m}\rangle$ to $|j'm', \ j'\,\bar{m}'\rangle$. The bar on the top of the projection quantum number specifies the time-reversed of the corresponding state. The self-consistent programme then splits up into two parts: in the first part one calculates the self-consistent wave-function and energies of $\bar{\Gamma}$, and then in the second part one does the BCS simple pairing theory with these self-consistent states. The quasi-particle operators, in this simple theory, are given by

$$a_i^+ = u_i \ c_i^+ \ \mathcal{v}_i \ c_{\bar{i}}$$

where $\bar{i}$ is the time-reversed of the state i, which is a self-consistent state of $\bar{\Gamma}$. $\mathcal{v}_i^2$ has the simple interpretation as the probability of the state i being occupied.

The ground state of the system is represented as

$$\Psi_0 = \prod_i \left[u_i - v_i \, c_i^+ c_{\bar{i}}^+ \right] |0\rangle$$

where $|0\rangle$ is the closed-shell core state, and the state lable i runs over the self-consistent states calculated in a representation of the levels in the unfilled shell. Ψ_0 has the property

$$a_i \Psi_0 = 0$$

that is to say it is the vacuum of the quasi-particles. The result of creating a quasi-particle in the state k is given by

$$\Psi = a_k^+ \Psi_0 = c_k^+ \prod_i{}' \left\{ u_i - v_i c_i^+ \ c_{\bar{i}}^+ \right\} |0\rangle .$$

The prime on the top of the product sign means that the factor corresponding to the state k is now absent. Thus the one quasi-particle state is simply the corresponding particle state coupled with a core-state, which is "blocked" in the sense that the given particle-state is completely excluded from the core. This structure of the one-quasi-particle state implies that the magnetic moment of the quasi-particle is the same as that of the particle. Thus, the quasi-particle theory, although it considers the intra-shell configuration mixing effects through the short-range pairing interaction, fails to cause any improvement to the Schmidt values of the magnetic moments. Kisslinger and Sorensen (15) considered the mixing of the one-quasi-particle state with those obtained by coupling a quasi-particle to the one-phonon state. The extra magnetic moment, thus obtained, is, however, quite insignificant compared to what is needed by the experimental data in most cases. They had, therefore, considered the mixing of other suitable configurations through an additional δ-function interaction. However, the quasi-particle formalism, as sketched so far, contains a severe limitation that forces it to miss the largest correction to the Schmidt values of the magnetic moment. This is the core-polarization effect mentioned earlier, and the reason the quasi-particle theory misses it is due to the naive use of time-reversal invariance. One does not calculate in this theory the quasi-particle transformation for the time-reversed states separately. Time reversal invariance is tacitly assumed and then the time-reversed quasi-particle is obtained simply by changing the operators appropriately. The coefficients u_i, v_i are real and hence do not change. While this is a justified procedure for the even nuclei, for an odd nucleus it is not so. The extra core nucleon has a definite angular momentum projection quantum number, and the core-nucleons having opposite projections will interact differently with it. This means that the quasi-particle transformation properties for equal and opposite projections should now be quite different. A suitable modification of the pairing theory for odd nuclei, taking into consideration this core-polarisation effect, is under consideration at the moment, and detailed results will be reported elsewhere.

Chan and Valatin (16) have recently published the results of their calculation on the variation of the nuclear energy gap with increase in the rotational energy. The original work was due to Mottelson and Valatin (17), where the authors pointed out the similarity between the effect of applied magnetic field on the energy gap in the metallic superconductors, known as Meissner effect, with that to be expected in the case of nuclear energy gap as a result of the rotation of the nucleus. The rotational motion sets up a Coriolis interaction ωJ_x, which opposes the pairing effect and thus effectively reduces the energy gap. In the recent paper by Chan and Valatin detailed second-order calculations have been made of this effect. As a result of the rotation, the pairing matrix K changes from its static value, and the second order change in K indeed gives rise to a reduction in the value of Δ, the energy gap. Fig. 5 shows the results obtained by these authors. The value of angular momentum at which Δ disappears, marks the reaching of a rotational energy value beyond which the intrinsic state has changed from a superconducting $(\Delta \neq 0)$ to a normal state ($\Delta = 0$). This value of angular momentum, therefore, gives a cut-off to the rotational band built on the superconducting ground-state configuration. With the availability of the data in the heavy-ion experiments on rotational levels of large angular momenta these ideas will very soon be tested quantitatively in many nuclei.

Finally, a few words about the treatment of neutron-proton correlations in HFB theory. What is available at the present day is a set of perturbation calculations (15) of the neutron-proton interaction with the neutron and proton quasi-particle states; no mixing of neutron proton states has been taken into account while setting up the quasi-particles in terms of particles.

Such procedures have been justified by the authors by limiting the applicability to nuclei where neutrons and protons are filling up significantly different levels. The immediate extension of such calculations would be to mix the neutron proton states while setting up the HFB equations and then obtain the mixed quasi-particle states. If a residual interaction has to be diagonalised it can then be done with these mixed quasi-particles. Such an HFB theory will treat the n-n, p-p, and n-p pairing on the same footing. At the present moment computer programmes of this type are being set up by several groups, including the group at this institute and, I hear, by the people at the Tata Institute. These new programmes use finite-range central, tensor, spin-orbit interactions etc., and in this sense mark an improvement over the pioneering work by Baranger and Kumar (18) where the authors used the idealised pairing plus quadrupole interaction. The work in reference 18 has already given us a lot of understanding on the equilibrium shape of nuclei.

One major problem, however, remains unsolved. Neutrons and protons, present simaltaneously in an unfilled shell, will give rise to a lot of correlation effects in α-like groups. Such four-particle correlations are never taken care of by the HFB theory, which is essentially a linear theory connecting the single particle operators to quasi-particle operators. Bloch and Messiah (19) have shown, in general, that this kind of a linear theory always corresponds to pair-wise correlated states. Various people (20) have tried to treat the four-particle correlations of neutrons and protons, but with no great success. There are two possibilities which immediately appeal to one's mind: the first is to develop a particle-conserving theory in terms of a variational function having the appropriate four-particle and pair structure; the second is to use the commutator method of setting up the HFB equation in the following extended sense. The commutators of H with the particle creation and destruction operators, when suitably linearised, give rise to the HFB linear equations. If the triple terms in the particle operators are retained at this state, then the set of equations has to be completed by again evaluating the commutator of H with the triple product of particle operators. This last expression will contain higher order product of operators, and the chain of equations has to be terminated at a suitably chosen step to obtain a closed set of equations to be solved. Although the methods are easily understood, when described in this way, a practical execution of all the steps involved are extremely cumbersome. One has to wait and see how things develop in this field in the future.

REFERENCES

1. A.B. Volkov, Phys. Letters 12, 119 (1964).
2. J.P. Elliott, Proc. Roy. Soc. 245, 128, (1958).
3. D.M. Brink and G.F. Nash, Nucl. Phys. 40, 608 (1963).
4. J. Borysowicz and R.K. Sheline, Phys. Letters 12, 219,(1964).
5. A. Arima and H. Horie, Progr. Theor. Phys. (Kyoto) 12, 623 (1964); R.J. Blinstoyle, Proc. Phys. Soc. (London) 66, 1158 (1953).
6. E. Bodenstedt and J.D. Rogers ('Perturbed Angular Correlations' Published by the North-Holland publishing company, 1964).
7. A.B. Migdal, Nucl. Phys. 57, 29 (1964).
8. R.F. Sweet, K.H. Bhatt and J.B. Ball, Phys. Letters 8, 131 (1964).
9. S.P. Pandya, Phys. Letters 10, 178 (1964).

10. M. Baranger, 'Theory of Finite Nuclei' ("Cargese Summer Lectures, 1962" published by W.A. Benjamin, Inc.); M.K. Pal, 'Theory of Nuclear Structure' (Lectures delivered at the centre for advanced studies in physics and Astrophysics, Department of Physics, University of Delhi, Cyclostyled notes, November, 1964).

11. C.A. Levinson, Phys. Rev. 132, 2184 (1963).

12. D.J. Thouless and J.G. Valatin, Nucl. Phys. 31, 211 (1962).

13. R.E. Peierls and D.J. Thouless, Nucl. Phys. 38, 154 (1962).

14. I.Kelson and C. A. Levinson, Phys. Rev. 134, B269 (1964); W.H. Bassichis, C.A. Levinson and I. Kelson, Phys. Rev. 136, B380 (1964).

15. L.S. Kisslinger and R.A. Sorensen, Revs. Mod. Phys. 35, 853 (1963).

16. K.Y. Chan and J.G. Valatin, Phys. Letters 11, 305 (1964).

17. B.R. Mottelson and J.G. Valatin, Phys. Rev. Letters 5, 511 (1960).

18. M. Baranger and K. Kumar, see M. Baranger, Ref. 10 and rapporteur's talk at the International Congress on Nuclear Physics, Paris (2-8 July 1964).

19. C. Bloch and A Messiah, Nucl. Phys. 39, 95 (1962).

20. B.H. Flowers and M. Vujicic, Nucl. Phys. 49, 586 (1963); B. Bremond and J.G. Valatin, Nucl. Phys. 41, 640 (1963); M. Baranger, Phys. Rev. 130, 1244 (1963).

DISCUSSIONS

M.M. Bajaj : Can you explain the physical concept of the coupling between the particle and phonon excitations occuring in the theory of Kisslinger and Sorensen? Please clarify the idea of phonon excitation: How do they arise?

M.K. Pal: The phonom excitation is a coherent superposition of two quasi-particle excitations. It is called a phonon because such an excitation very roughly looks like the addition of a Boson to the ground state.

The origin of all couplings in structure theory is the basic two-nucleon effective interaction one starts with. As one goes along in the structure theory and changes the language from particle to quasi-particle, and then from coherent superposition of two quasi-particle states to a phonon, the effective two-body interaction one started with can also be side by side recast in the new language. The particle-phonon coupling arises as a consequence of this. I am afraid it is difficult to be more physical than this.

S. Das Gupta: If one tries to follow the iterative procedure in the Hartree-Bogolinbov theory (as one usually does in the Hartree-Fock) a trouble arises because of the no. of particles changes at each iteration. Do you know of any easy way to get around this problem?

M.K. Pal: I am afraid, such difficulties have to be faced squarely in the numerical computations. There is no way to byepass the trouble, at least not that I know of, or could think of right now. The chemical potential λ has to be fixed at each stage of iteration to produce the right number of particles on the average.

S.Das Gupta : What is the definition of ϵ in the slide you show from Volkov's work?

M.K. Pal: Although Volkov does not define it in his paper, it is quite easy to guess what it would be. ϵ would correspond to writing a, b as a constant times the faction $(1 + 1/3\epsilon)$ and $(1 - 2/3\epsilon)$, for example. In other-words the difference of b and a, divided by either of them or some kind of mean value is related to ϵ.

S. Das Gupta: Is it possible that a Hartree-Fock calculation for the excited state could show deformation and would it be orthogonal to the ground state then(also obtained by HF)?

M. K. Pal : It is certain that HF calculations for the excited states would show deformation in most cases. If you have the O^{16} case in mind, then I must say one should try it rather than doing single-minded SU_3 that I showed on the slide. As to the second part of your question the state obtained by HF for the excited state will not automatically be orthogonal to that obtained for the ground state. They will basically correspond to different Hartree-Fock Hamiltonian T + V, through the different deformation of the potential V.

M. K. Banerjee: I wish to comment that even the Wigner force has a large contribution to the spin polarisation effect. It arises due to the dependence of the two-particle interaction matrix element on the two-particle J. In Tewari's calculation he finds noticeable spin polarisation effect.

M.K. Pal : Yes, it is true. However, the contribution to the magnetic moment from core-polarisation will be larger from spin-dependent, rather than spin-independent interactions, particularly interaction of the kind $\underset{\sim}{\sigma_1} \cdot \underset{\sim}{\sigma_2}$, $\underset{\sim}{\tau_1} \cdot \underset{\sim}{\tau_2}$ where $\underset{\sim}{\sigma}$ and $\underset{\sim}{\tau}$ are respectively the spin and isobaric spin operators.

GROUND-STATE CORRELATIONS AND THE THEORY OF ONE-AND TWO-PHONON STATES

Ram Raj and Y.K. Gambhir
Saha Institute of Nuclear Physics, Calcutta

The description of one-phonon state based on microscopic theory in the first Random-Phase Approximation (R.P.A.) was very successfully given by Baranger (1) and others. In this method one introduces the pair creation (annihilation) operator $A^{+J}_{M}(ab)$ $(A^{J}_{M}(ab))$ for quasi-particles in the angular momentum states 'a' and 'b' coupled to a total angular momentum J with projection M defined by

$$A^{+J}_{M}(ab) = \sum_{\alpha\beta} \begin{bmatrix} a & b & J \\ \alpha & \beta & M \end{bmatrix} a^{+}_{\alpha} a^{+}_{\beta}$$

The notation $[\ \ ]$ denotes a Clebsch-Gordan coefficient.

One then evaluates the comm utators $[H, A^{+}_{M}(ab)]$ and $[H, A^{J}_{M}(ab)]$ whose structure after linearisation is of the form

$$\begin{aligned}[H, A^{+J}_{M}(\mu\nu)] &= (E_\mu + E_\nu) A^{+J}_{M}(\mu\nu) + \frac{1}{2}\sum_{ab} \Big[G(ab\mu\nu J)\{u_a u_b u_\mu u_\nu \\ &+ v_a v_b v_\mu v_\nu\} + 2F(ab\mu\nu J)\{u_a v_b u_\mu u_\nu + v_a u_b v_\mu u_\nu\}\Big] A^{+J}_{M}(ab) \\ &+ \frac{1}{2}\sum_{a,b}\Big[2F(ab\mu\nu J)\{u_a v_b v_\mu u_\nu + v_a u_b u_\mu v_\nu\} - G(ab\mu\nu J) \\ &\{u_a u_b v_\mu v_\nu + v_a v_b u_\mu u_\nu\}\Big](-1)^{J-M} A^{J}_{-M}(ab)\end{aligned}$$

where E's are unperturbed quasi-particle energy, v_a^2 and u_a^2 represent the probability of occupancy and non-occupancy of the state 'a'. $G(ab\mu\nu J)$ and $F(ab\mu\nu J)$ are the particle-particle and holeparticle matrix elements. According to Baranger:

1) For Quadrupole. Quadrupole force, $G(ab\mu\nu J)$ is smaller than $F(ab\mu\nu J)$ and therefore it can be neglected.

2) For realistic force, one must include $G(ab\mu\nu J)$ as well.

Numerical calculations have been done for Ni- isotopes using Quadrupole.Quadrupole and Gaussian forces for the residual interaction between quasi-particles. The effect of the inclusion of $G(ab\mu\nu J)$ and ground-state correlations has also been investigated. The results are given below:

Energy (MeV) of the first 2^+ state in Ni- isotope:

1) Potential -Quadrupole.Quadrupole

Strength X = 1.9 (K.S. Value[2]) = 1.85

Nucleus	Without correlation		With correlation		Experimental value
	F	F+G	F	F+G	
$_{28}Ni^{58}$	1.46	1.46	1.43	1.42	1.45
Ni^{60}	1.69	1.55	1.59	1.47	1.33
Ni^{62}	1.76	1.54	1.61	1.46	1.17
Ni^{64}	1.82	1.55	1.70	1.50	1.34
Ni^{66}	1.98	1.68	1.94	1.66	—
	2) Potential Gauss		Range = 1.75 f		VO = 55 MeV
$_{28}Ni^{58}$		1.17		1.11	
Ni^{60}		1.33		1.31	
Ni^{62}		1.39		1.38	
Ni^{64}		1.44		1.43	
Ni^{66}		1.53		1.53	

The above results with Quadrupole.Quadrupole show that the inclusion of $G(ab\mu\nu J)$ plays the same role as ground state correlations as they push the states down and there is very little difference between the two results as for as energies are concerned. Also the results with Gaussian potential show that the groundstate correlations have practically no effect as for as energies are concerned.

The extension of the above method for two-phonon states in the second random-phase approximation has been suggested by Pal and Mitra (3).

Following Pal and Mitra, a closed set of equations has been derived in general by evaluating $[H, A^{+J}_{M}(ab)]$ and $[H, (A^{+J_1}(ab) A^{+J_2}(ab))_M]$ and retained only the terms of the type A^+, A^+A^+ and AA. Detailed study of the above equations has been made and one encounters the following difficulties.

The basis in two-phonon space in general are redundant and not orthonormal. This point has also been discussed in a recent paper by Savoia (4) et.al. They have also given a prescription to remove these difficulties which in general is very difficult to apply and at the same time they have not done any numerical calculation. A numerical calculation without removing these difficulties for Cd^{114} has been done by Tamura and Udagawa (5). They have made some artificial modification in their calculation discussed in the paper and still their results do not agree well with the experiment.

Although the R.P.A. is quite satisfactory for the description of one-phonon states but is opened to severe criticism for the two-phonon states. Therefore, one may legitimately doubt about the reliability of the results obtained for the two -phonon states and is not sure whether one is gaining anything by doin this or not. Hence it is worthwhile to carry out calculations with a method which is less accurate in principle but is not open to such criticism.

A new method which is being suggested here is the Tamm - Dancoff (T.D) approximation in which all the four quasi-particle states are treatedby simple shell model calculation which in turn, automatically insures the independent and orthogonal wave-functions with non-redundant basis.

The region in which we are interested contains three levels, therefore the following types of configuration will appear in general:

1) j^4
2) $j^3 j'$
3) $j^2 j'^2$
4) $j^2 j' j''$

Only the H_{22} part of the interaction Hamiltonian (i.e. the part which conserves the number of particle) will contribute in this case and its matrix element in two particle states has in general the form

$$\langle j_1 j_2 J | H_{22} | j_3 j_4 J \rangle = G(j_1 j_2 j_3 j_4 J)\{u_{j_1} u_{j_2} u_{j_3} u_{j_4} + v_{j_1} v_{j_2} v_{j_3} v_{j_4}\}$$
$$+ F(j_1 j_2 j_3 j_4 J)\{u_{j_1} v_{j_2} u_{j_3} v_{j_4} + v_{j_1} u_{j_2} v_{j_3} u_{j_4}\} + (-1)^{j_1 + j_2 - J}$$
$$\times F(j_2 j_1 j_3 j_4 J)\{v_{j_1} u_{j_2} u_{j_3} v_{j_4} + u_{j_1} v_{j_2} v_{j_3} u_{j_4}\}$$

The above method does not take into account the ground-state correlations but one can take this into account by considering the mixing of zero and two quasi-particles by picking up the appropriate part of the interaction Hamiltonian. There are some technical difficulties in this part of the calculation of matrix elements but we are trying to overcome them.

REFERENCES

1. M.Baranger, Phys. Rev. 120, 957(1960).
2. L.S.Kisslinger and R.A. Sorensen, Mat. Fys.Medd. Dan.Vid. Selsk. 32, No.9 (1960).

3. D.Mitra and M.K. Pal, Phys. Rev. Lett., 1, 153 (1962)

4. M. Savoia, J. Sawicki and A. Tomasini, Nuovo Cimento Serie. X. 32, 991 (1964).

5. T. Tamura and T. Udagawa, Nuclear Physics 53, 33 (1964).

STRUCTURE OF Pr-ISOTOPES

Y.K. Gambhir and Ram Raj
Saha Institute of Nuclear Physics, Calcultta

Well known Bardeen (1) -Bogoliubov (2)-Belyaev (3) treatment of the pairing correlations is applicable only for the pairing force i.e. the force in J = 0 state. In single closed shell nuclei having identical nucleons in the unfilled shell this method gives fairly good results (4). But in the case where both neutrons and protons are present in the unfilled shell there is a comparable force in J = 1 and T = 0 state in addition to the J = 0 state interaction. The method for this general case has been developed by Bremond and Valatin(5) and by Pal and Goswami (6). In the latter method one ends up with four coupled Hartree-Bogoliubov equations in the neutrons and proton creation and annihilation operators. The diagonalisation of the coefficient matrix gives the energy and transformation of quasiparticles.

In the nuclei where outermost neutrons and protons fill different major shells, the J =0, T = 1 force does not exist between neutrons and protons and it can be shown from the general formalism that the lowest order effect of this n-p interaction (J = 1, T = 0) is to keep the equations of the pairing model for identical nucleons unaltered in form, only the single particle energies to be used in these equations are to be modified through the contributions from n-p interaction which is practically the same as the perturbation treatment of n-p interaction.

The perturbation treatment is described by Pal and Mitra (7). The Hamiltonian is written as

$$H = H_n + H_p + H_{np}$$

where H_n and H_p are the pairing model Hamiltonians for the neutrons and protons respectievely and H_{np} is the n-p interaction.

After carrying out the Bogoliubov transformation and grouping the identical terms one gets the following familiar pairing model equations

$$1 = \frac{G_p}{2} \sum_{ap} (2ap+1) \left[(\varepsilon_{ap} - \lambda_p)^2 + \Delta_p^2 \right]^{-1/2} \tag{1}$$

and

$$Z = \frac{1}{2} \sum_{ap} (2ap+1) \left[1 - \frac{(\bar{\varepsilon}_{ap} - \bar{\lambda}_p)}{\sqrt{(\bar{\varepsilon}_{ap} - \lambda_p)^2 + \Delta_p^2}} \right] \tag{2}$$

where

$$\bar{\varepsilon}_{ap} = \varepsilon_{ap} + \sum_{bnJ} \frac{(2J+1)}{(2ap+1)} \langle ap\, bnJ | V | ap\, bn J \rangle V_{bn}^2$$

with similar equations for neutrons.

The suffix p and n specify the protons and neutrons respectively other symbols have their usual meaning.

For δ - function potential $\bar{\varepsilon}$ becomes

$$\bar{\varepsilon}_{ap} = \varepsilon_{ap} + \sum_{bn} (2bn+1) V_{bn}^2 F_0 (ap\, bn) \tag{3}$$

where

$$F_0 (ap\, bn) = \frac{1}{16\pi} (3V_t + V_s) \int_0^\infty R_{ap}^2 R_{bn}^2 r^2 dr \tag{4}$$

It is evident from reference (7) that only the monopole term of the δ- function will contribute to $\bar{\varepsilon}$ i.e. the part which can be considered along with the average spherical field in which neutrons and moving.

Results for odd-Pr isotopes:-

The ground state of Pr^{141} is $5/2^+$ measured from paramagnetic resonance (8) and from atomic beam magnetic resonance (9) and the first excited state is $7/2^+$ at 142 KeV. While in Pr^{143} the ground state is $7/2^+$ in accordance with the direct measurement (10) and the first excited state is $5/2^+$ at 57 Kev. The ground state spin of Pr^{145} is $7/2^+$ and no data is available for its excited state.

If one solves the pairing model equations with appropriate modification due to the odd no. of protons with the values of ϵ_{ab} single particle energies from K. S and fixing G the pairing strength to reproduce the 142 KeV. Separation between $7/2^{+}$ and $5/2^{+}$ using this value of G for Pr^{143}, requires fantastically large X the strength of δ -function potential, to get the reversal i.e. $7/2^{+}$ as the ground state, ofcourse the variation of G has little effect. Thus the right thing on our disposal is the single particle energy E of d5/2 state. If one treats this as a parameter one gets various sets of E and G for the 146 kev separation in Pr^{141}. The reversal of ground-state in Pr^{143} with the reasonable values of X will narrow down the choices of these sets. This automatically gives $7/2^{+}$ the ground-state of Pr^{145}. Due to lack of time we could not do these extensive calculations. In the present situation the following results are being reported for one particular set.

	K.S.Values (MeV)		Our Values (MeV)			Ground state	First excited state	Separation (meV)	
Nucleus	G	E	G	E	X			Theor	Expt
Pr^{141}	.17	1.0	.13	.65	-	$5/2^{+}$	$7/2^{+}$	.149	.142
Pr^{143}	.17	1.0	.13	.65	10	$7/2^{+}$	$5/2^{+}$	.049	.057

Results for odd-odd isotopes (Pr^{144}) :-

For odd-odd isotopes like Pr^{144} one will be required in the next higher order of approximation, to diagonalize the residual part of the n-p interaction using near lying quasi-neutron, quasi-proton states as well.

The present calculation for Pr^{144} involves the following approximations with the above values of the parameters:-

1) All the three outermost neutrons are in the 2 f 7/2 shell, this assumption can be justified from the single particle level spectra beyond the shell

closure at 82.

2) It is follows from the assumption (i) that the quasi-neutron and neutron states in this case are identical.

3) Quadrupole-Quadrupole force has been used in calculating the residential part H_{np}.

We have considered the following quasi-neutrons and quasi-proton configurations in the diagonalisation work

(1) $(2f_{7/2})^{3}_{7/2}\, g_{7/2}$ (2) $(2f_{7/2})^{3}_{7/2}\, d_{5/2}$

The results thus obtained one compared with that of experiment below:

Expt.

Energy (MeV)	Spin
.133	1^-
.100	2^-
.080	1^-
.053	3^-
0	0^-

Theoretical

Energy (MeV)	Spin
	1^-
.202	3^-
.138	2^-
.079	1^-
0	0^-

It is clear that 0^- first 1^- and the 2^- states are approximately reproduced. As is expected from the experience of shell model that the 3^- state cannot be brought down with such a simple minded force. The second 1^- state has gone too high. One should not be disheartened to see the above agreement because we have not exhausted all the possibilities of various sets for E, G and X.

REFERENCES

1. Bardeen, Cooper and Schreiffer, Phys. Rev., 108, 1175 (1957).

2. N.N. Bogoliubov, JETP., 34, 58 (1958).

3. S.T. Belyaev, Mat. Fys. Medd. Dan. Vid. Selsk., 31, No. 11 (1959).

4. L.S. Kisslinger and R.A. Sorensen, Mat. Fys. Medd. Dan. Vid. Selsk., 32, No. 9 (1960).

5. B. Bremond and J.G. Valatin, Nucl. Phys., 41,640 (1963).

6. M. K. Pal and A.Goswami, Unpublished, D. Phil. Thesis (1963) Calcutta University of A. Goswami.

7. M. K. Pal and D. Mitra, Nucl. Phys. 42, 221 (1963).

8. R.W. Kedzie, M. Abraham and C.D. Jeffries, Phys. Rev., 108, 54 (1957).

9. H. Lew, Phys. Rev., 91, 619 (1953).

10. B. Budick, R. Marrus, W.M. Doyle and W.A. Nierenberg, B. Budick and others, Bull. Am. Phys. Soc. 7, 477 (1962); Phys. Rev. 135, B1281 (1964).

11. K.P. Gopinathan, M.C. Joshi and E. A. S. Sarma, Phys. Rev. 136, 5B1247 (1964).

THE NILSSON AND THE SELF-CONSISTENT MODELS FOR NUCLEAR DEFORMATIONS

M. R. Gunye and S. Das Gupta
Tata Institute of Fundamental Research
Bombay

INTRODUCTION

Till very recently, the Nilsson Model(1) has been almost always used to predict equilibrium deformations in nuclei (2 to 6). The starting point is the one-body Hamiltonian.

$$\frac{p^2}{2m} + \frac{1}{2} m \omega_1^2 (x^2+y^2) + \frac{1}{2} \omega_z^2 z^2 - c\, \underset{\sim}{l} \cdot \underset{\sim}{s} - d\, \underset{\sim}{l}^2 \tag{1}$$

where

$$\omega_\perp^2 = \omega^2(\delta)\left[1+\frac{2}{3}\delta\right]; \quad \omega_z^2 = \omega^2(\delta)\left[1-\frac{4}{3}\delta\right]$$

and $\omega(\delta)$ is fixed by imposing the condition of volume conservation of the equipotential: $\omega_x \omega_y \omega_z = \omega_0^3$. Here ω_0 is the frequency at zero deformation. The quantities c and d are constants. To calculate the equilibrium deformation, one first solves eqn. (1) for many values of δ, i.e., obtain eigenvalues $\mathcal{E}_\nu(\delta)$. At each deformation one fills up the lowest levels with the given number of nucleons in a nucleus, taking care to satisfy the Pauli principle. The value of δ which minimizes $\sum_{\text{occupied}} \mathcal{E}_\nu(\delta)$ gives the equilibrium deformation. No distinction between closed shells and unfilled shells is made and the summation in $\sum_{\text{occupied}} \mathcal{E}_\nu(\delta)$ runs over particles both within the closed shells and outside. It has been suggested before(5) that the inclusion of particles within the closed shells plays an important role in determining the equilibrium deformation.

An alternative method was suggested by Belyaev (7). The Hamiltonian to solve is

$$\frac{p^2}{2m} + \frac{1}{2} m \omega_0^2 r^2 - \chi q \left[2z^2 - x^2 - y^2\right] - c\, \underset{\sim}{l} \cdot \underset{\sim}{s} - d\, \underset{\sim}{l}^2 \tag{2}$$

where the quadrupole moment Q must be determined self-consistently

$$\sum_{\text{occ.}} \langle 2z^2 - x^2 - y^2 \rangle = Q \tag{3}$$

The quantity χ is a measure of nuclear polarizability and is ultimately related to the two-body interaction. The energy is given by

$$E(Q) = \sum_{\text{occ.}} \langle \frac{p^2}{2m} + \frac{1}{2} m \omega_0^2 r^2 - C \underset{\sim}{\ell} \cdot \underset{\sim}{s} - d \underset{\sim}{\ell}^2 \rangle - \frac{1}{2} \chi Q^2 \tag{4}$$

If there are several values of Q which satisfy eqn. (3), then that value of Q which gives the minimum energy E(Q) determines the equilibrium deformation.

FORMULATION OF THE PROBLEM

Baranger and Kumar (8) (referred to hereafter as BK) have made extensive use of the self-consistent formalism to calculate equilibrium deformations and find that this method works equally well as the Nilsson model. BK solve eqns.(2), (3) and (4) only for particles outside the closed shells. The particles within the closed shells are also presumably deformed (9,10) but the effect of this, it is hoped, is taken care of by properly renormalizing the value of χ . No such renormalization is possible in the Nilsson model, and as we shall show, the core must be taken into account explicitly. Therefore there appears to be clear distinction between the two models. It is our purpose here to compare the predictions of the two models and especially to find out if the results of the self-consistent model would change if the core were taken into account explicitly.

COMPARISON OF THE TWO MODELS AND DISCUSSION

The simplest case to compare is deformations in a single j-shell(14). Here the results are similar; oblate ($\delta < 0$, $Q < 0$) in the beginning of a shell and prolate ($\delta > 0$, $Q > 0$) at the end.

The next thing to consider is an anisotropic harmonic oscillator. In the Nilsson Model

$$H = \frac{p^2}{2m} + \frac{1}{2} m \omega_\perp^2 (x^2+y^2) + \frac{1}{2} m \omega_z^2 z^2$$

We calculate equilibrium deformations in the N= 4 shell, first without taking into account the filled N = 0 to 3 shells. For even systems, the result is that for particle numbers n = 2, 4, 6 prolate shapes are preferred. For n = 8 to 28, oblate shapes are preferred. We then include the core of N = 0 to 3 shells. Now n = 2 to 12 are prolate and n = 14 to 28 are oblate.

When doing the corresponding calculation in the self-consistent model, an interesting phenomenon appears. Eqns.(2),(3) and (4) may be regarded as arising from a Hartree-Fock calculation of a two-body force $V(ij) = -\chi(2z_i^2 - x_i^2 - y_i^2)$. The exchange term is neglected. To obtain the self-consistent solutions, choose a parameter D, solve

$$H = \frac{p^2}{2m} + \frac{1}{2} m\omega_0^2 r^2 - D(2z^2 - x^2 - y^2)$$

and use the solutions of this Hamiltonian to calculate the energy expectation value

$$E(D) = \sum_{occ.} \left\langle \frac{p^2}{2m} + \frac{1}{2} m\omega_0^2 r^2 \right\rangle - \frac{1}{2}\chi \left(\sum_{occ.} \langle 2z^2 - x^2 - y^2 \rangle \right)^2 \qquad (5)$$

and the quadrupole moment $Q = \sum_{occ.} \langle 2z^2 - x^2 - y^2 \rangle$

A self-consistent solution is found whenever $D = \chi Q$. The allowed range of $D/m\omega_0^2$ is from -.5 to +.25. However so long as $\chi > 0$, E(D) can be made as low as one wants it to be by taking $D/m\omega_0^2$ arbitrarily close to though less than .25 (or arbitrarily close to but greater than -.5). This is because

$$Q = \sum_{occ.} \frac{\hbar}{m\omega_0} \left[\frac{2n_z+1}{(1-\frac{4D}{m\omega_0^2})^{1/2}} - \frac{n_\perp + 1}{(1+2D/m\omega_0^2)^{1/2}} \right]$$

and this tends to ∞ as $(.25 - D/m\omega_0^2) \to +0$. The first term in eqn. (5) tends to ∞ but the second term to $-\infty^2$. Therefore a lower value of the energy than that corresponding to the lowest self-consistent solution can always be found. This apparent paradox is arising from the unreasonable form of the force $V(ij) = -\chi (2z_i^2 - x_i^2 - y_i^2)(2z_j^2 - x_j^2 - y_j^2)$ which can tend to $-\infty^2$ as $z_i^2,\ z_j^2 \longrightarrow \infty$ with $y_i^2\ x_i^2,\ y_j^2\ \ x_j^2$ finite. However at $D/m\omega_0^2$ close to .25 or -.5 the self-consistency condition is not satisfied and for very large deformations the schematic force does not make much sense.

If we start from a small value of χ, then the curve E(D) of eqn.(5) against $D/m\omega_0^2$ looks as in fig. 1 a. We have chosen to illustrate a case where the prolate shape is favoured over the oblate; a_1, a_2, a_3, a_4 and a_5 are the five self-consistent solutions; a_1, a_3 and a_5 are maxima; a_2 and a_4 are minima. At all of these points $D = \chi Q$ is satisfied. Increasing χ gives rise to the situation in fig. 1b and further increase leads to fig. 1c, where no self-consistent solution can be found for $D > 0$.

We now come back to the problem of finding out prolate and oblate deformations in the N = 4 shell. An indeterminacy arises because the answer may depend on the value of χ. The value of χ can further be determined self-consistently. (For this, see ref. 9,10, 3). In calculations of BK and Kisslinger and Sorensen (11), χ is not determined self-consistently. Hence we have varied the value of χ from 0 to a maximum value when the self-consistency condition cannot be satisfied for $D > 0$. We find that as the N = 4 shell fills up, n = 2 to 14 are always prolate; n = 16 to 28 are usually oblate although for large values of χ, n = 16, 18 and 20 can become prolate. The above results are true whether we consider just the N = 4 shell or the N = 0 to 4 shells together.

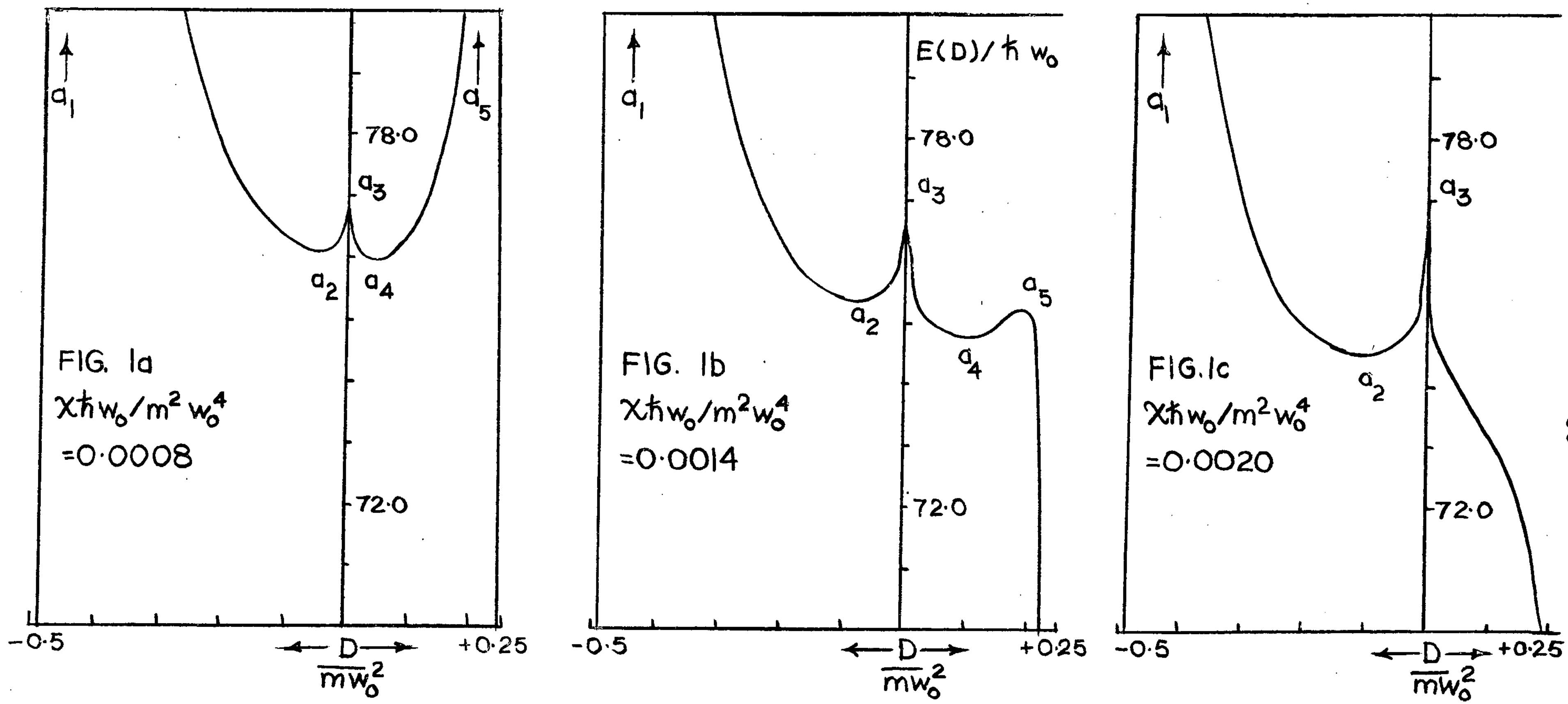

FIG. 1a
$\chi\hbar w_0/m^2 w_0^4$
$=0{\cdot}0008$
a_1 a_2 a_3 a_4 a_5
78·0
72·0
−0·5
+0·25
D/mw_0^2
FIG. 1b
$\chi\hbar w_0/m^2 w_0^4$
$=0{\cdot}0014$
$E(D)/\hbar w_0$
a_1 a_2 a_3 a_4 a_5
78·0
72·0
−0·5
+0·25
D/mw_0^2
FIG. 1c
$\chi\hbar w_0/m^2 w_0^4$
$=0{\cdot}0020$
a_1 a_2 a_3
78·0
72·0
−0·5
+0·25
D/mw_0^2

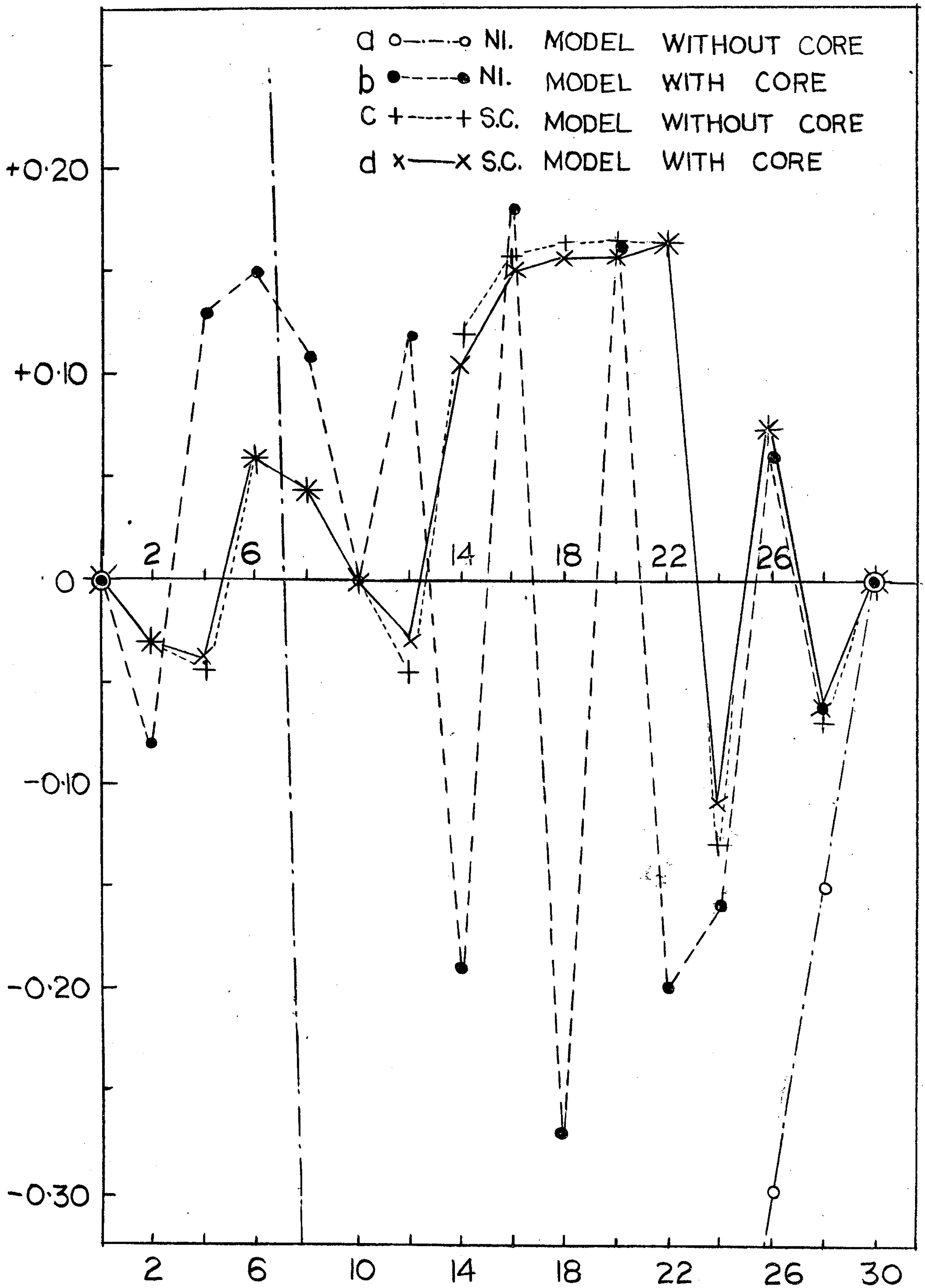
a o-·-·-o NI. MODEL WITHOUT CORE
b ●------● NI. MODEL WITH CORE
c +-----+ S.C. MODEL WITHOUT CORE
d x——x S.C. MODEL WITH CORE
+0·20
+0·10
0
-0·10
-0·20
-0·30
2
6
10
14
18
22
26
30

This suggests that the results of the self-consistent method and the Nilsson model will be similar but only if the core is included in the Nilsson model. Further, the inclusion of the core is unimportant in the self-constent method.

One would like to know if these conclusions would go through in a realistic calculation and this is what we consider next. Following Nilsson(1) we put C = $.1\hbar\omega_0$ and = .0225 $\hbar\omega_0$ in eqn.(1) for the N = 4 shell. We use the method of appendix A of Nilsson's paper (1) for both the Nilsson and self-consistent models, taking care to solve the deformation dependent part exactly. The method has always been used in calculating equilibrium deformations (2 to 6). The other method suggested by Nilsson does not ascribe any quadrupole moment to the closed shells and this appears to be inconsistent with experimental findings (9,10). The Nilsson model results for the N = 4 shell are given by curves a and b of fig.2. Without the core, only n = 2 to 6 are prolate and n = 8 to 28 are oblate (curve a). With the core, there are 7 prolates, 6 oblates and 1 spherical (curve b). Note also that the deformation changes drastically after the core is included. Curve c in the same figure corresponds to a self-consistent calculation for the N = 4 shell without the core. We have shown the result for $\chi\hbar\omega_0/m^2\omega_0^4$ = .0012 which is taken from BK (Note that our definition of $\chi = 5/16\pi\ \chi$ BK). Curve d is obtained when N = 0 to 4 shells are considered together. We have chosen to show the results for $\chi\hbar\omega_0/m^2\omega_0^4$ = .00085. We see that the pattern does not change when the core is included in the self-consistent method. We find that there does not exist one to one correspondence between the Nilsson model predictions and the self-consistent model predictions as the particles fill up the shell; but there is an overall agreement in the number of prolates and oblates (8 prolates, 5 oblates and 1 spherical in the self-consistent model). We have checked that with reasonable variations in the value of χ this sort of rough agreement continues. Further the agreement is obtained only if the core is included in the Nilsson model.

REFERENCES

1. S.G. Nilsson, Mat. Fys. Skr. Dan. Vid. Selsk. 32, No. 16 (1956).

2. B.R. Mottelson and S.G. Nilsson, Mat. Fys. Skr. Dan.Vid. Selsk., 1, No. 8 (1959).

3. D.R. Bes and Z. Szymanski, Nuclear Physics 28, 42 (1961).

4. T.D. Newton, Canad. J. Physics 38, 700 (1961).

5. S. Das Gupta and M.A. Preston, Nuclear Physics 49, 401 (1963).

6. M.R. Gunye, S. Das Gupta and M.A. Preston, Physics Letters 13, 246(1964).

7. S.T. Belyaev, Mat. Fys. Skr. Dan. Vid. Selsk. 31, No 11 (1959).

8. M. Baranger and K. Kumar, Physical Review Letters, 12, 73 (1964).

9. B.R. Mottelson, The Many-Body Problem (Dunod, Paris 9159) p.283.

10. B.R. Mottelson, Nuclear Spectroscopy (1960 Varenna Summer School Lectures Academic Press, 1962) p. 44.

11. L.S. Kisslinger and R.A. Sorensen, Reviews of Modern Physics 35, 853 (1963).

12. Z. Szymanski, Nuclear Physics 11, 454 (1959).

13. M. Baranger and K. Kumar, Private communication; calculations with renormalized value of have been completed for rare-earth and other nuclei and are to be found in the thesis by K. Kumar, Carnegie Institute of Technology (1963).

14. M. Baranger and K. Kumar, Contract Number 760 (15) NRO 24-439, Office of Naval Research.

CALCULATION OF EXCHANGE STRIPPING AMPLITUDES

Anand Kumar
Saha Institute of Nuclear Physics, Calcutta.

It is possible to estimate the probability of finding the last neutron and proton in a nucleus in a deuteron state from (d,n) or(n,d) reactions under favourable circumstances. In a (d,n) reaction the ratio of the exchange and the direct amplitutdes depends, among other factors, on the ratio

$$\lambda = \frac{\text{Deuteron width in the final nucleus x Neutron width in the target nucleus.}}{\text{Proton width in the final nucleus}} \quad (1)$$

An estimate of this ratio can be obtained if the exchange amplitude is not very small and if we employ a reliable theory for the analysis of the reacting angular distribution. We have used the Direct reaction theory using Born approximation and plane waves for the description of the initial and final states(1). Undoubtedly a more reliable estimate can be obtained by the use of 'Distorted Wave Born Approximation', in fact, that we shall discuss subsequently. For an investigation of the effect the following two experiments (2,3) (i)Be^9(d,n) B^{10} (ii) O^{16}(n,d) N^{15} were preferred in view of a prominent backward peaking. It seems that the fits are satisfactory and there is a large amount of h.p.s. present, refer figure 1. Let us give a name to the above ratio extracted in this manner as 'the experimental value'. The ratio of width obtained in this manner was compared with predictions based on the shell model of the nucleus. The single particle widths are given directly by the chosen single particle wave-functions and the fractional parantages. The deuteron width was obtained as follows: the product of the wave-functions of the last neuteron and the last proton may be rewritten in terms of the relative and centre of mass coordinates of these particles. Multiplying the product with a suitable deuteron wave-function, in our case it is of the hulthen type, and integrating the overlap over the relative coordinate one obtains the wave-function of the deuteron moving about the rest of the nucleus. The width can be obtained once this wave-function is known. The overlap integral, of course, is a measure of the situtation that the last neuteron and proton look like a deuteron. This overlap is found to be very large, 94% for n=0, let us call it 'In'. Finally the deuteron width can be written as:

$$\nu_{Ld} = \frac{R^{3/2} \langle \text{core, deuteron} | \} \text{ final} \rangle \sum_{n,N_L} \langle n_1 l_1, n_2 l_2; Ld | n L, N L, L d \rangle I_n \Phi_{NL}(R)}{[\sum_{nN} | \langle n_1 l_1, n_2 l_2; Ld | n 0, N Ld, Ld \rangle |^2 \; I_n^2}$$

where, 'R' is the cut-off radius, second term is a coefficient of fractional parantage, first term within the sum is the Talmi coefficient and $\Phi_{NL}(R)$ stands for the oscillator wave-function. The use of oscillator w.fs. necessarily reduces the width. The reason is that the oscillator w.fs. are damped more strongly than Exp(-Beta x R) which is the true asymptotic tail. In view of this, phenomenonlogically, we retain the coefficient of expansion in (2) but replace $\Phi_{NL}(R)$ by the square-well w.fs. having the same 'L' and number of nodes. This improves the width by a factor nearly seven-halves. Also admixtures of other configuration e.g., $1\text{-}p^2 + \alpha\, 1\text{-}d^2$, does not make significant contribution and also the change in width is very slow with α-variation.

Shell-model prediction and the experimental value

$\lambda_{S.M.} = 0.241$; $\lambda_{Expt} = 0.249$

for the first experiment are in fair agreement, which gives us an idea of the influence of the correlations on the deuteron width. In view of large size of the deuteron this is most certainly a long range correlation in nature. For experiment, too, the two estimates differ by an order of magnitude and thus a reliable evidence on correlation can not be obtained. The answer lies in a D.W. B.A. calculation.

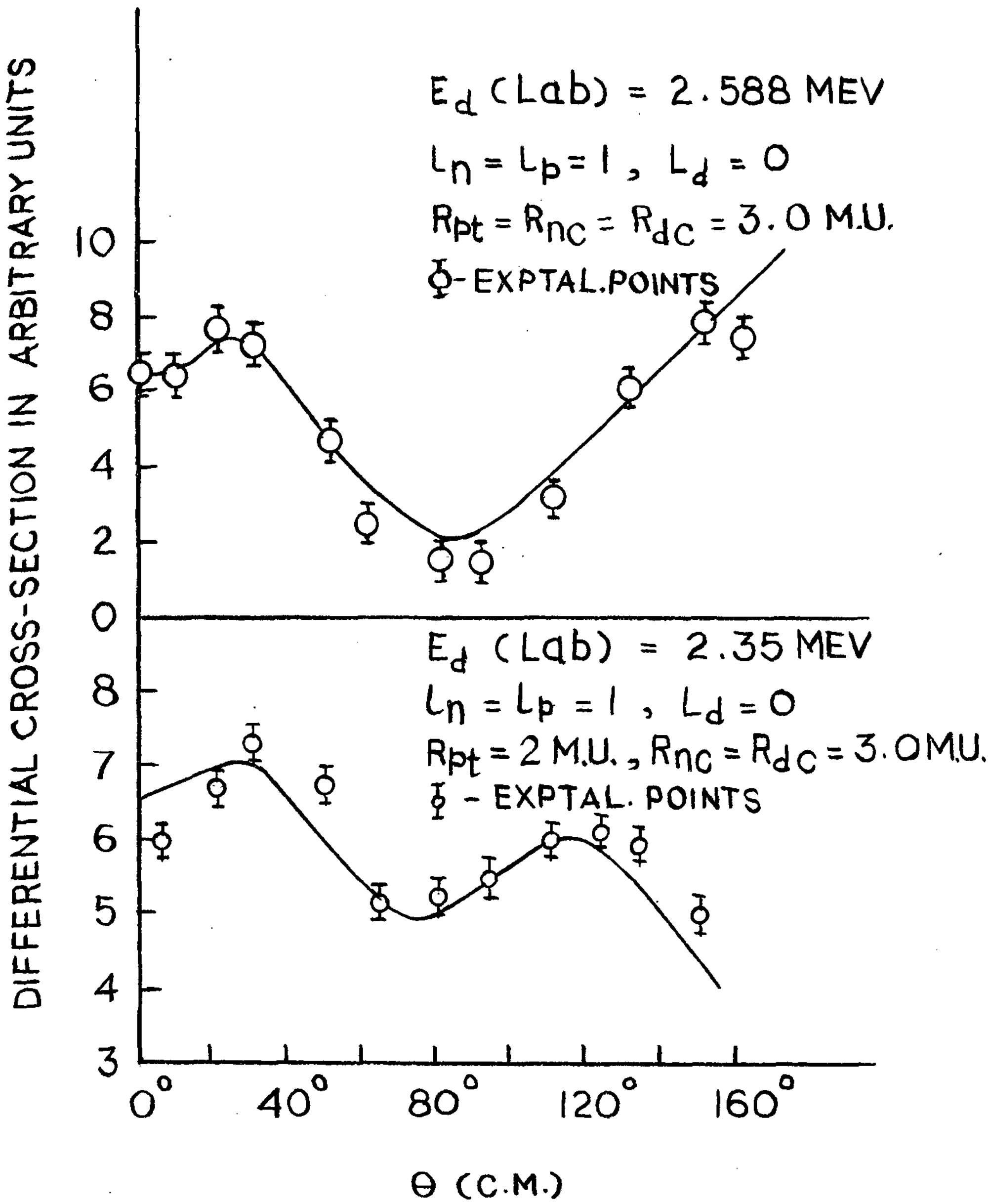

FIG. 1. ANGULAR DISTRIBUTIONS OF THE GROUND-STATE NEUTERONS IN THE REACTIONS (1) $Be^9(d,n)B^{10}$ AND (2) $N^{15}(d,n)O^{16}$. THE FULL CURVE SHOWS THE THEORETICAL PREDICTION.

Stripping amplitude in a D.W.B.A. can be written as:

$$T_{d.n} = \langle \chi_f(-\vec{K}_f, \vec{r}_f)\, \Phi(r_{BC}) | V(r_{AB}) (1 - \sum_{j=1}^{N} P_{jA} - P_{AB}) | \Phi(\vec{r}_{AB})\, \chi_i(\vec{K}_i, \vec{r}_i) \rangle .$$

In general, we have followed the notations of (6,7). Antisymetrizer (term in the parenthesis) breaks 'Tdn' into a direct and a exchange-amplitude, in the later the role of the projectile and the target is reversed compared to the former. So far no realistic (ie, finite-range) calculations have been made. They have calculated 'Tdn' only with a zero-range - approximation. This is a very poor approximation in treating the 1-p shell exchange term due to the fact that the bound-state with $\ell=1$ is not peaked near the origin. All the recent attempts (4,5) to perform a realistic calculation suffer from the asymptotic approximation on the bound-states. Apparently these attempts seem to be as refinements on the zero-range-force (Z.R.F.) calculations but we have shown in the following that both the approximations are equivalent and give rise to same value of the amplitude. Therefore once again we cannot treat exchange in 1-p shell with only such refinements. T(Z.R.F) follows if one substitutes the following expn.in (3)

$$V(r_{AB})\, \Phi(\vec{r}_{AB}) = V_0\, \delta(\vec{r}_{AB}) = V_0\, \delta[\alpha(\vec{r}_f - \delta\vec{r}_i)] = V_0\, \delta\left(\frac{1}{\gamma}(\vec{r}_i - \vec{r}_{BC})\right)$$

$$T(Z.R.F.) = \int \chi_f(-\vec{K}_f, \delta\vec{r}_i)\, \Phi^*(\vec{r}_{BC})\, \chi_i(\vec{K}_i, \vec{r}_i)\, d^3 r_i \qquad (4)$$

We can write now T(F.R.F.) if we replace the scattering states by their inverse Fourier-transforms and suitably arrange the continuum states, as

$$T(F.R.F.) = \int e^{-i\vec{q}_A \cdot \vec{r}_{AB}}\, V(r_{AB})\, \Phi(\vec{r}_{AB})\, d^3\vec{r}_{AB} \int e^{i\vec{q}_c \cdot \vec{r}_{BC}}\, \Phi^*(\vec{r}_{BC}) \times \chi_f(\vec{q}_f)\, \chi_i(\vec{q}_i)\, d^3\vec{r}_{BC}\, d^3 q_i\, d^3 q_f \qquad (5)$$

where, $\vec{q}_A = \vec{q}_f - \gamma\vec{q}_i \quad , \quad \vec{q}_c = -\delta\vec{q}_f + q_i$

First integral in T(F.R.F) reduces to a constant if we factor out the potential in the manner done in (6) and make the asymptotic approximation for $\Phi(\vec{r}_{AB})$. While the second integral can be made to reduce to (4) if we integrate on $\vec{q}_i, \vec{q}_f$ and rearrange the various terms. Thus the equivalence is settled. The equivalence also follows for other choices of $\Phi(\vec{r}_{AB})$ should the first integral be a constant reducible.

N. Austern et.al. (7) treatment; they have given a suitable plan for a full realistic calculation. However, gk(ri,rf) defined in their paper as,

$$g_K(r_i, r_f) = \int_{-1}^{+1} d(\cos\theta) \frac{\phi_l(r_{BC})}{r^l_{BC}} V(r_{AB}) \frac{\Phi_{l'}(r_{AB})}{r^{l'}_{AB}} P_K(\cos\theta) \tag{6}$$

are hard to evaluate unless some subtle assumptions are made on the potential and the bound-states. We find that the situation can be simplified and the domain of applicability can be extended if one can exploit the point of discontinuity of the potential and locate out the contributing region in which all the net points give a finite value to the functional. For a square-well potential this was taken up for a substantial r_{AB} and r_{BC} variation. Basing on this we have analysed the second experiment. To have a qualitative view we have restricted only to nine partial waves and distant net points. Although the fit is not so good, yet the agreement between width-ratios improves and also the h.p.s. is small. It seems that a calculation with more net points will give a clear evidence on this point. Results are in progress.

Computation was taken up on C.D.C. 3600, T.I.F.R., Bombay.

REFERENCES

1. M.A. Nagarajan and M.K. Banerjee, Nucl. Phys. 17, 341 (1960).
2. B. Richard and G.E. Owen, Phys. Rev. 120, 369 (1960).
3. J.L. Weil and K. W. Jones, Phys. Rev. 112, 1975 (1953).
4. A. Dar, et.al., Phys. Rev. 131, 1732 (1963).
5. Fernando B. Morinigo, Phys. Rev. 133, B65 (1964).
6. M.K. Banerjee, Nuclear Spectroscopy, Part B, Ed. F.A. Selove, A.P.
7. N. Austern, et.al. Phys. Rev. 133, B3 (1964).

A DISTORTED WAVE BORN APPROXIMATION CALCULATION FOR (He^3 ,p) REACTIONS

B. K. Jain and N. Sarma
Nuclear Physics Division
Atomic Energy Establishment Trombay
Bombay

INTRODUCTION

The study of single nucleon stripping and pick up reactions involving deuterons has given extremely important information regarding the structure of nuclei. Many of the original limitations of the theory were removed by more realistic formulations such as the use of distorted wave Born approximation theory and the inclusion of finite range interactions and spin orbit effects. Information regarding single particle configuration mixing and spectroscopic factors is now available for many nuclei. Much more valuable data regarding nuclear configurations can be obtained from the study of two-nucleon stripping reactions such as (He^3,p) and (He^3,n). Here two particles are captured into the target nucleus and the interaction between the two captured nucleons is important. Investigation of two nucleon interactions in a nucleus, as for example the proton-proton correlation in (He^3,n) reactions and the proton-neutron correlation in (He^3,p) reactions can be made by measurements on two-nucleon stripping. Plane wave Born approximation theories have been moderately successful in determining level spins but spectroscopic factors cannot be obtained from such a naive theory . The DWBA theory developed for deuteron induced reactions has been used in some cases for the analysis of He^3 stripping, but this is necessarily approximate. A theory for (He^3,n) reactions has been given by Henley and Yu(1) and for (t,p) reactions by Rook et al. (2).

We now report on our work on a distorted wave Born approximation theory for (He^3,p) reactions.

THEORY

A. General considerations

In distorted wave Born approximation theory the effect of absorption and scattering (such as compound nucleus and elastic scattering processess) on the incident and emergent waves is taken into account by using optical potentials for the entrace and exist channels. In the calculation ofthe cross-section there are two potentials, the optical potential and the potential responsible for the direct interaction. Using these potientials, the matrix element T is given by the Gell-mann and Goldberger relation(3).

$$T=\langle \psi_f(\boldsymbol{\xi}_f)\, e^{i\mathbf{k}_f\cdot\mathbf{r}_f} \,|\, U_f(\mathbf{r}_f) \,|\, \psi_i(\boldsymbol{\xi}_i)\, \chi_i^{(+)}(\mathbf{k}_i, \mathbf{r}_i)\rangle + \langle \psi_f(\boldsymbol{\xi}_f)\, \chi^{(-)}(\mathbf{k}_f, \mathbf{r}_f) \,|\, V_f \,|\, \Psi\rangle \tag{1}$$

U_f and V_f are the optical potential and the residual interactions respectively in the final state channel. $\psi_f(\boldsymbol{\xi}_f)$ and $\psi_i(\boldsymbol{\xi}_i)$ are the internal wave-functions of the outgoing and incoming channels; $\chi_i^{(+)}$ and $\chi_f^{(-)}$ are the elastic scattering wavefunctions for the entrance and exit channels using outgoing and incoming scattered waves as the boundary conditions. Ψ is the wave-function that has only direct interaction degrees of freedom. To use the Born approximation, we assume further that the initial and final state channels are determined primarily by the optical potentials. The direct interaction is treated as a perturbation and hence the approximation can be made:

$$\Psi \approx \psi_i(\boldsymbol{\xi}_i)\, \chi_i^{(+)}(\mathbf{k}_i, \mathbf{r}_i) \tag{2}$$

where ξ_i are the collective internal coordinates. The transition matrix, T then becomes the amplitude for the direct interaction in distorted wave Born approximation theory.

$$T=\langle \psi_f(\boldsymbol{\xi}_f)\, \chi_f^{(-)}(\mathbf{k}_f, \mathbf{r}_f) \,|\, V(\boldsymbol{\xi}_f, \mathbf{r}_i, \mathbf{r}_f) \,|\, \psi_i(\boldsymbol{\xi}_i)\, \chi_i^{(+)}(\mathbf{k}_i, \mathbf{r}_i)\rangle \tag{3}$$

$\underset{\sim}{K_i}$, $\underset{\sim}{K_f}$ and $\underset{\sim}{r_i}$, $\underset{\sim}{r_f}$ are the initial and final channel wave and position vectors respectively.

The differential cross-section can then be expressed in terms of the amplitude T, by calculating the incoming and outgoing currents.

$$\frac{d\sigma}{d\Omega} = \frac{M_i^* M_f^*}{(2\pi\hbar^2)^2} \frac{\underset{\sim}{K_f}}{\underset{\sim}{K_i}} \frac{1}{(2J_i+1)(2J_p+1)} \sum |T|^2 \tag{4}$$

The summation is carried out over the projections of the intrinsic spins of the outgoing and incoming particles. J_p is the spin of the projectile.

B. Application to (He^3,p) reactions:

For (He^3,p) type direct reactions, neglecting the excitation of the core, we can write the interaction V in (3) as $V_{np}' + V_{pp}'$.

Since nuclear core excitations are neglected, the final state wave-function is just that of the captured neutron-proton pair bound to the target nucleus. It is, therefore, written:

$$\psi_f(J_f,M_f) = \sum_{\substack{t_i' J_i' J t \\ \nu_i' M_i' \mu \\ j_1 j_2}} B_{t_i' t_f t}(j_1 j_2 J, J_i' J_f)(J_i' J M_i' \mu / J_i' J J_f M_f)(t_i' t \nu_i' 0 / t_i' t t_f \nu_f) \; \psi_i(J_i', M_i') \, \phi_J^{\mu}(\underset{\sim}{r_n}\, \underset{\sim}{r_p}) \, \rho_t^0(n,p) \tag{5}$$

where j_1, j_2 are single particle states of the shell model, t_i, t_f and t are the isopins of the initial and final nuclei and the transferred neutron proton pair respectively. $B_{t_i' t t_f}(j_1 j_2 J, J_i' J_f)$ is the c.f.p for a neutron-proton pair in the final nucleus state with the given quantum numbers. The wave -function $\phi_J^M(\underset{\sim}{r_n}, \underset{\sim}{r_p})$ can be expanded in terms of their centre of mass and relative motion wave function using Talmi coefficients(5).

Assuming the interaction V to be spin-isopin independent central potential of Gaussian form, and carrying out the trivial integrations, we get for the transition matrix

$$\sum|T|^2 = \frac{V_0^2}{b}(2J_f+1)\sum_{\substack{LSJ\\M}}\frac{1}{(2L+1)}\left|\sum_{j_1j_2}B_{t_it t_f}(j_1j_2\,J\,J_i\,J_f)\,H(10NL,n_n l_n\,n_p l_p L)\times\right.$$
$$\left.T(j_1j_2J;LSJ)\times(t_i t\,\nu_i 0|t_i t t_f \nu_f)(\tfrac{1}{2}\tfrac{1}{2}\tfrac{1}{2}-\tfrac{1}{2}|\tfrac{1}{2}\tfrac{1}{2}t\,0)\,I\right|^2 \quad (6)$$

where

$$I = \int \chi_{K_f}^{(-)*}\left(\xi + \frac{A}{A+2}R\right)\phi_L^{M*}(R)\,\phi_0^0(r)\left[\exp\{-\beta^2(\xi + r/2)^2\} + \exp\{-\beta^2(\xi - r/2)^2\}\right]\times$$
$$\chi_{K_i}^{(+)}(\xi/3 + R)\,\phi_{He}(\xi, r)\,dr\,dR\,d\xi \quad (7)$$

$\phi_L^M(R)$ and $\phi_0^0(r)$ are the oscillator potential wave functions

$$\phi_0^0(r) = \sum_{k=0}^{n-1} C_{nk}\left(\frac{\alpha^2}{2}\right)^k r^{2k} e^{-\alpha^2 r^2/4} \quad (8)$$

where C_{nk} is given by the expansion of Laguerre polynomials, and $\alpha = 2M\omega/\hbar$ is the oscillator constant.

Substituting (8) in (7) then integrating over r,

$$I = 2\pi^{3/2} N_{He}\sum_{k=0}^{n-1}(-1)^k C_{nk}\left(\frac{\alpha^2}{2}\right)^k \frac{\partial^k}{(\partial f^2)^k}\frac{1}{f^3}\int \exp(-g^2\xi^2)\,\chi_{K_f}^{(-)*}\left(\xi + \frac{A}{A+2}R\right)\times$$
$$\phi_L^{M*}(R)\,\chi_{K_i}^{(+)}(\xi/3 + R)\,dR\,d\xi \quad (9)$$

where $f^2 = \frac{1}{4}(\beta^2 + 3\gamma^2 + \alpha^2)$, $g^2 = \gamma^2 + \beta^2 - \beta^4/4f^2$

γ and β are the Gaussian widths for the He^3 wavefunction and interaction V.

On the assumption that χ_i and χ_f are independent of ξ we obtain

$$I = 2\pi^3 N_{He}\sum_{k=0}^{n-1}(-1)^k C_{nk}\left(\frac{\alpha^2}{2}\right)^k \frac{\partial^k}{(\partial f^2)^k}\frac{1}{f^3}\,\frac{1}{g^3}\int \chi_{k_f}^{(-)*}\left(\frac{A}{A+2}R\right)\phi_L^M(R)\,\chi_{k_i}(R)\,dR \quad (10)$$

The integral in this equation is evaluated numerically.

Substituting eqn. (6) in (4) one obtains the expression

$$\frac{d\sigma}{d\Omega} = \frac{M_i^* M_f^*}{(2\pi\hbar^2)^2}\frac{K_f}{K_i}\frac{V_0^2(2J_f+1)}{(2J_i+1)(2J_{pt}+1)}\sum_{\substack{LSJ\\M}}\left|\sum_{\substack{j_1j_2\\t}} B_{t_it t_f}(j_1j_2\,J\,J_i\,J_f)\times T(j_1j_2J,LSJ)\right.$$
$$\left.H(10NL;n_n l_n n_p l_p,L)(t_i t\,\nu_i 0|t_i t t_f \nu_f)\times(\tfrac{1}{2}\tfrac{1}{2}\tfrac{1}{2}-\tfrac{1}{2}|\tfrac{1}{2}\tfrac{1}{2}t\,0)\,I\right|^2$$

selection rules are

$$J_f = J_i + L + S, \qquad \pi_f = (-1)^L\,\pi, \qquad S=0, t=1 \text{ OR } S=1, t=0$$

The cross section shows that the contributions of different L's are incoherent while those of different j's are coherent. Therefore those L value contributions which are small may be neglected without any serious error. The j coherence shows that the cross section is very sensitive to correlations existing in the nucleus. This may produce states, (low lying in general) which will contain mixtures of different single particle levels. Two nucleon stripping can be used to investigate these states and the crosssection to these will be large if the phases are additive.

REFERENCES

1. Ernest M. Henley and David U.L. Yu Phys. Rev. 133, B 1445 (1964).

2. J. E. Rook and D. Mitra Nuclear Phys. 51, 96 (1964).

3. Gell-Mann and Goldberger Phys. Rev. 91, 398 (1953).

4. T.A. Brody and M.Moshinsky Tables of Transformation Brackets (Institute of Physics, University of Mexico 1960).

5. M.E. Rose, Elementary Theory of Angular Momentum, Chapter XI.

MAGNETIC MOMENT OF THE 129 KEV STATE IN Tm^{171*}

Y.K. Agarwal, C.V.K. Baba and S.K. Bhattacharjee
Tata Institute of Fundamental Research, Bombay

The magnetic moment of the 129 KeV ($7/2^+$) state in Tm^{171} which is a member of the rotational band built on (411) $K = \frac{1}{2}$ Nilsson state has been determined by an integral method to be 0.94 ± 0.18 n.m. This has been measured by perturbing the 296-124 KeV γ-γ directional correlation by an external magnetic field of 21.5 kg. The magnetic properties of the (411) $K = \frac{1}{2}$ band have been analysed using the known data on the rotational states in this band. The results are compared to those of Tm^{169} which has a similar $K = \frac{1}{2}$ rotational band.

---

* The details can be found in:

Y.K. Agarwal et al., Physics Letters 14, 214 (1965).

CONFIGURATION MIXING AND INDEPENDENT PARTICLE MOTION

S. N. Tewari
Saha Institute of Nuclear Physics, Calcutta

In the past the calculational limitations of the shell model have confined its applications to the special regions of the periodic table near closed shells. However, under stimulation of collective ideas, several important advances have been made and to mention a very significant development among them, which is pertinent for our discussion, is Elliott's SU_3 classification of many particle states. This scheme has certainly simplified the job as has been demonstrated by the calculations of Banerjee, Levinson and Meshkov (2) and by Elliott and Harvey (3) in the s-d shell nuclei. However, their work at the same time showed that even though the SU_3 representation is extremely useful, it is not quite good enough for the quantitative treatment of nuclear spectra if one just takes the lowest SU_3 state. A calculation on Na^{22} has been done by us where we have allowed for the mixing of all possible SU_3 symmetries. The interaction used is the following:

$$H_{int} = \sum_{i<j} V(r_{ij}) + g_{l^2} \sum_i l_i^2 + g_{ls} \sum_i l^i \cdot s^i + \sum_{i<j} V(r_{ij})\, \sigma_i \sigma_j$$

$$\text{where. } V(r_{ij}) = V_0 \exp(-r/a)/r/a \;, \quad V_0 = -45 \text{ MeV} \quad a = 1.37 \times 10^{-13} \text{ cm}$$

$$g_{l^2} = 0.2 \text{ MeV}, \quad g_{l.s.} = 2.2 \text{ MeV}$$

The interaction has been made reasonable by producing the level orderings of Na^{22}. It is interesting to note that the energy of the first excited state with J =1 as obtained by us is 0.581 MeV while the experimental value for the same is 0.593 MeV. However our aim was not to produce the exact energy spectra of Na^{22}, but to study the features of wave-functions obtained by using a reasonable interaction. The wave-functions are obtained by diagonalizing the energy matrices in the representation

$$\Psi^J_M = \sum_i a^J_i \, P^J_M \, \Phi_i \, ([f](\lambda\mu)\epsilon\kappa\sigma)$$

Where Φ_i's form the basis of SU_3 representation. The quantum number $[f]$ describes the symmetry under space permutations. Associated with $[f]$ are the isotopic spin T and spin S. The quantum numbers ($\lambda\mu$) distinguish the diffirent SU_3 representations within $[f]$ while within each $(\lambda\mu)$ the states are further distinguished by quantum numbers ϵ and κ (where refers to ϵ max). σ is the spin projection quantum number on the body fixed symmetry axis. The matrix elements were calculated by the method of Banerjee and Levinson (4). There are various selection rules which govern the admixture of the SU_3 states. It is in fact because of these selection rules that one finds an intrinsic wave-function. The discussion of all such features have been given in our work reported elsewhere (5).

The remarkable feature about the wave-function is that they are all, to an extremely good order, the results of projections, out of the same intrinsic wave-function i.e. we can now write

$$\Psi^J_M = P^J_M \sum_i a_i \, \Phi_i \, ([f](\lambda\mu)\epsilon\kappa\sigma)$$

This feature is demonstrated in the Fig. 1 where a_i's are plotted against J for the different Φ_i's occuring into the admixed wavefunction. The different Φ_i's have been labelled by K which in Fig. stands for K + σ. This is the so-called band quantum number. For convenience the remaining quantum numbers excepting K have been chopped up. One observes that the dependence of a_i's on J is extremely weak for the same band terms. For the band mixing terms the dependence is still weak for the most important band mixing terms i.e. for the terms with K = 2. For K =0 and 1 the dependence is really large. But the amplitude of these terms in the admixed wave-function is extremely small and hence our assertion as above about the existence of intrinsic wave-function is fully justified for the low angular momentum state i.e at least upto J = 5.

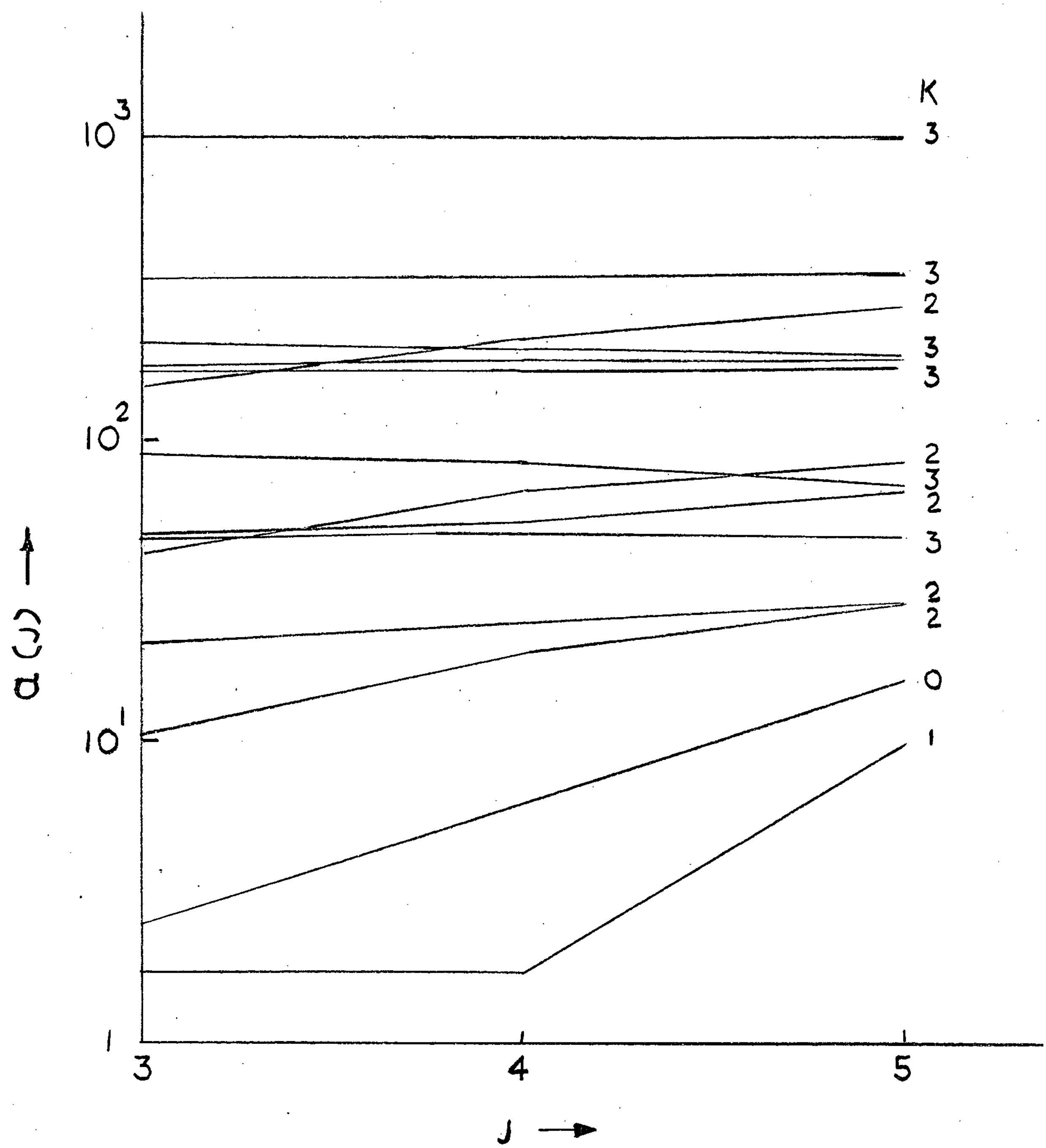

Fig 1.

Density matrices have been set up for J = 3 and J = 4. For J = 5 it is under calculation. The results are tabulated as follows:

J	$tr.\rho_p$	$tr.\rho_m$	$tr.\rho_p^2$	$tr.\rho_m^2$	$\frac{tr(\rho_p-\rho_p^2)}{2tr\,\rho_p}$	$\frac{tr(\rho_m-\rho_m^2)}{2tr\,\rho_m}$
3	3.00000	3.00000	2.93987	2.93842	1%	1%
4	3.00000	3.00000	2.93186	2.93097	1.1%	1.1%
5	Yet	to	be	calculated.		

ρ_p is the density matrix calculated by neglecting the band mixing terms in the wavefunction.

ρ_m is the density matrix calculated with all the terms in the wave-function. Looking down at the numbers in the last two columns which measure the deviation from the single determinantal character of the wave-function one concludes that the intrinsic wave-function is a single determinant to the order of 99%. Thus our calculation gives adequate support to the applicability of H.F. method in the 2s-1d shell. The comparison of the numbers in the last two columns brings forth two extremely significant conclusions which are stated as follows:

1) The impurity in the single determinantal character measures the configuration mixing where by configuration we imply the following:

$$\Phi_{\text{arbitrary}} = a_1\Phi_1 + a_2\Phi_2 + \cdots\cdots$$

where Φ_1, Φ_2 etc. are single determinants and they can be connected by scattering involving at least two particles. The configuration mixing thus implies that the intrinsic state is not just the independent particle motion but there is some residual correlation. Since the numbers in the last two columns compare to an extremely good order the residual correlation is, therefore, presumably due to short angular range correlation.

2) Since the band mixing is small, it suggests that the band admixed wave-function can be adequately described (to order of 99%) by taking the cranked wave-function as the Hartree-Fock solution.

Following the above suggestions ie the pure wavefunction is a Hartree-Fock soln. and the band admixed wavefunction is the cranked solution of Hartree-Fock we would like to point out that the variational wave-function as suggested by Peierls and Thouless(6) under some simplifying condition can be written as projection out of an intrinsic wave-function which is almost a single determinant and preseumably a cranked wavefunction. In pointing out so our aim is to emphasize that impurity in the single determinantal character of the wave-function as calculated above can not be taken care of by introducing some extra degrees of freedom of the type of Peierls and Thouless(6) in the wavefunction. Presumably, we would like to emphasize once more, it is due to short angular range correlation.

Peierls and Thouless write the wave-function in the form

$$\Psi^J_M = \int d\Omega \int_0^\infty \omega \, d\omega \, G(\theta, \varphi, \chi, \omega) \, \Phi(\theta, \varphi, \chi, \omega)$$

$$= \int d\Omega \int_0^\infty \omega \, d\omega \, G(\theta, \varphi, \chi, \omega) \, e^{i\omega\Theta} \, \Phi(\theta\varphi\chi)$$ under the condition of the small range of the angular velocity where Φ is obtained by H.F. method.

$$\int d\Omega = \int_0^\pi \sin\theta \, d\theta \int_0^{2\pi} d\varphi \int_0^{2\pi} d\chi$$

Where θ, φ, χ are the Euler angles for a rigid body fixed to the symmetry axis and the direction of the angular velocity ω imparted round an axis 1^r to the symmetry axis. Taking the above as the variational wave-function they derived, from the minimisation condition, a differential eqn. for the weight function G. Under the limit of small coupling between J and ω the soln. for G can be written $D^J_{MK}\omega^K e^{-\mu\omega^2/2}$ where μ is some parameter. Hence Peierls and Thouless wave-function becomes:

$$\Psi^J_M = P^J_M \int_0^\infty \omega\, d\omega\, e^{-\mu\omega^2/2} e^{i\omega\theta}\, \Phi(0.00)$$
$$= P^J_M \{ (e^{i\alpha_K\theta + \beta_K\theta^2 \cdots})\, \Phi\, (0\,0\,0) \}$$

where θ is a single particle hermitian operator $\alpha_K, \beta_K \cdots$ constants. Now let us agree to identify this intrinsic wavefunction i.e. the wave-function within curly bracket with out band admixed wave-function. Then it follows that the measure of the important term for the band mixing which is proportional to $\langle\theta^2\rangle$ is 2%. Now since the term most important for causing the impurity in the single determinantal character is proportional to $\langle\theta^4\rangle$, the impurity is of the order of .04 percent. However, in doing so we must justify the identification which will be taken up sometimes in future. For the present the motivation was its attractive simplicity.

We have tried to explain the first excited with J =1 by R.P.A. over the ground state. We write

$$\Phi^{J=0} = \sum C_{ij}\, a_i^{+} a_s\, \Phi^{J=3}$$

now
$$\langle \Phi^{J=1} | \Phi^{J=1} \rangle = 1 = \langle \Phi^{J=3} | c^{+}c | \Phi^{J=3} \rangle$$
$$= \langle \Phi^{J=3} | [\tilde{c}, c] | \Phi^{J=3} \rangle$$
$$= tr\, [\tilde{c}, c]\, \rho$$

The quantity $tr[\tilde{c},c]\rho$ has been calculated and its value turns to be 0.88 instead of 1 implying there by that the R.P.A. is not a good approximation. However, we would refrain from making a firm statement at the present and the question is still occupying our full attention.

REFERENCES

1. Proc. of Royal Soc., 245A, 128, 562. (2). Phys. Review, 130, 1064.

3. Proc. of Royal Soc. 272A, 557. (4). Phys. Review 130, 1036.

5. Proceedings of Low energy nuclear physics symposium (India) 1964.

6. Nuclear Physics, 38, 154.

SYSTEMATICS OF l -FORBIDDEN M_1 TRANSITION

I.M. Govil and C.S. Khurana
Muslim University, Aligarh.

INTRODUCTION

In many of the odd mass nuclei near filled shells, it has been found that there exists a state close to the ground state which differ in orbital angular momenta (l) by two units e.g. $g_{7/2} \rightleftharpoons d_{5/2}$, $s_{1/2} \rightleftharpoons d_{3/2}$, $p_{3/2} \rightleftharpoons f_{5/2}$ It is found that between these two states the γ-ray transition is mostly of M_1 character. The shell model describes these states very accurately but it fails to explain the existance of M_1 transition. Since the magnetic dipole moment operator does not change the orbital angular moments of the two wave functions involved, the states assigned by the shell model should not differ in angular momenta in the case of M_1 transition. Indeed it is found that these transitions are retarded by a large factor but still they are found to have a finite value. It is therefore, expected that these transitions are caused by the breakdown of the l-forbiddenness due to some other effects of nuclear dynamics. We have studied these transitions taking a large number of data to investigate the possibility of some systematic trend of these transitions.

RESULTS AND DISCUSSIONS

Fig. 1 shows the experimental values of the matrix elements plotted on a logarthimic scale. The matrix elements (μ^2) were calculated from the experimental half-life (τ_γ) using the following formula:

$$\mu^2_{exp.} = \frac{(2j_i+1)\times 10^{13}}{0.419\,\tau_\gamma E_\gamma^3}$$

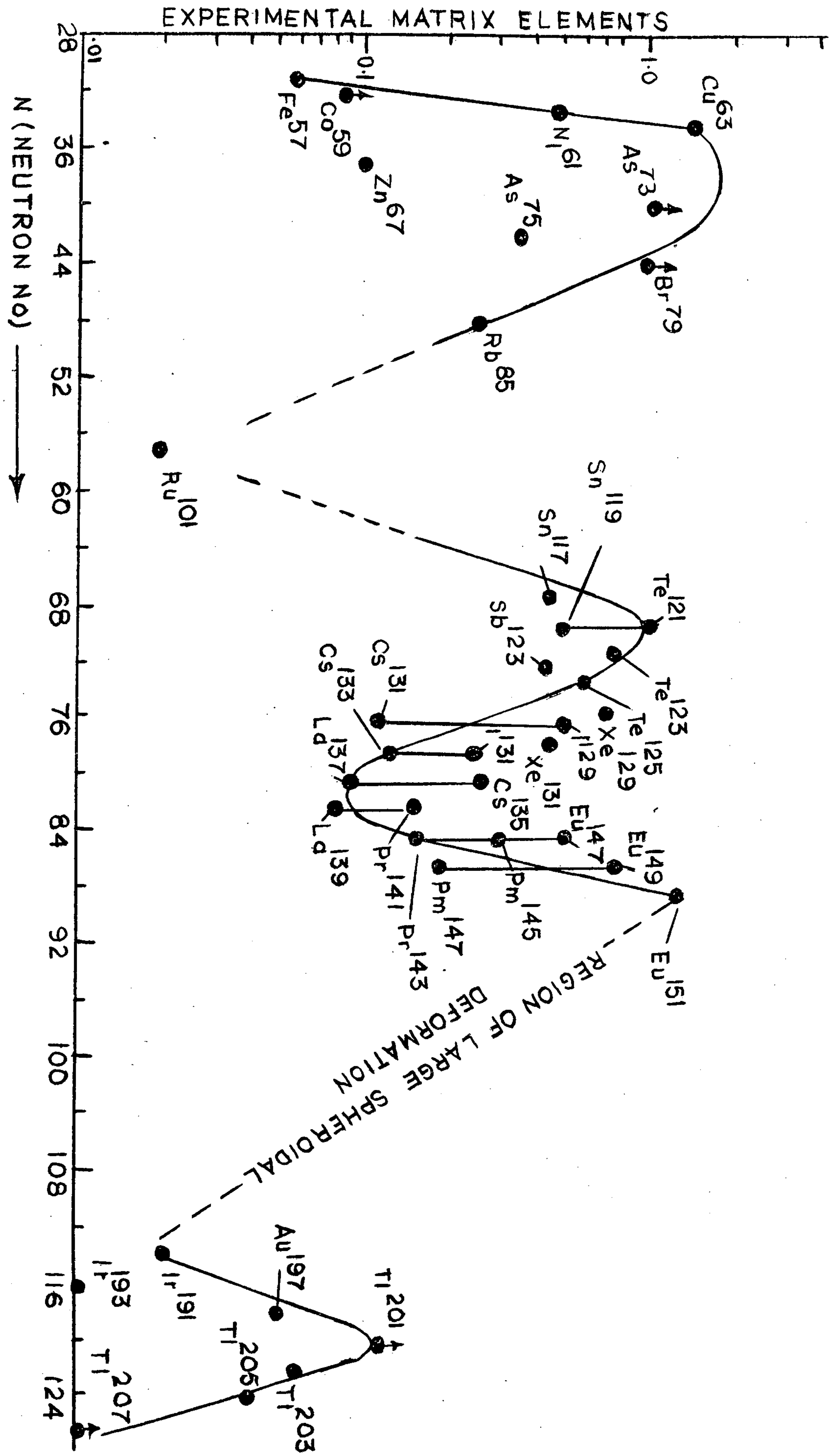
EXPERIMENTAL MATRIX ELEMENTS
.01
0.1
1.0
N (NEUTRON No)
28
36
44
52
60
68
76
84
92
100
108
116
124
Cu63
Ni61
Co59
Fe57
As73
As75
Zn67
Br79
Rb85
Ru101
Sn119
Sn117
Te121
Sb123
Te123
Te125
Cs131
Cs133
Xe129
I129
I131
Xe131
La137
Cs135
Eu147
Eu149
La139
Pr141
Pm145
Pm147
Pr143
Eu151
REGION OF LARGE SPHEROIDAL DEFORMATION
Au197
Tl201
Ir191
Ir193
Tl205
Tl203
Tl207

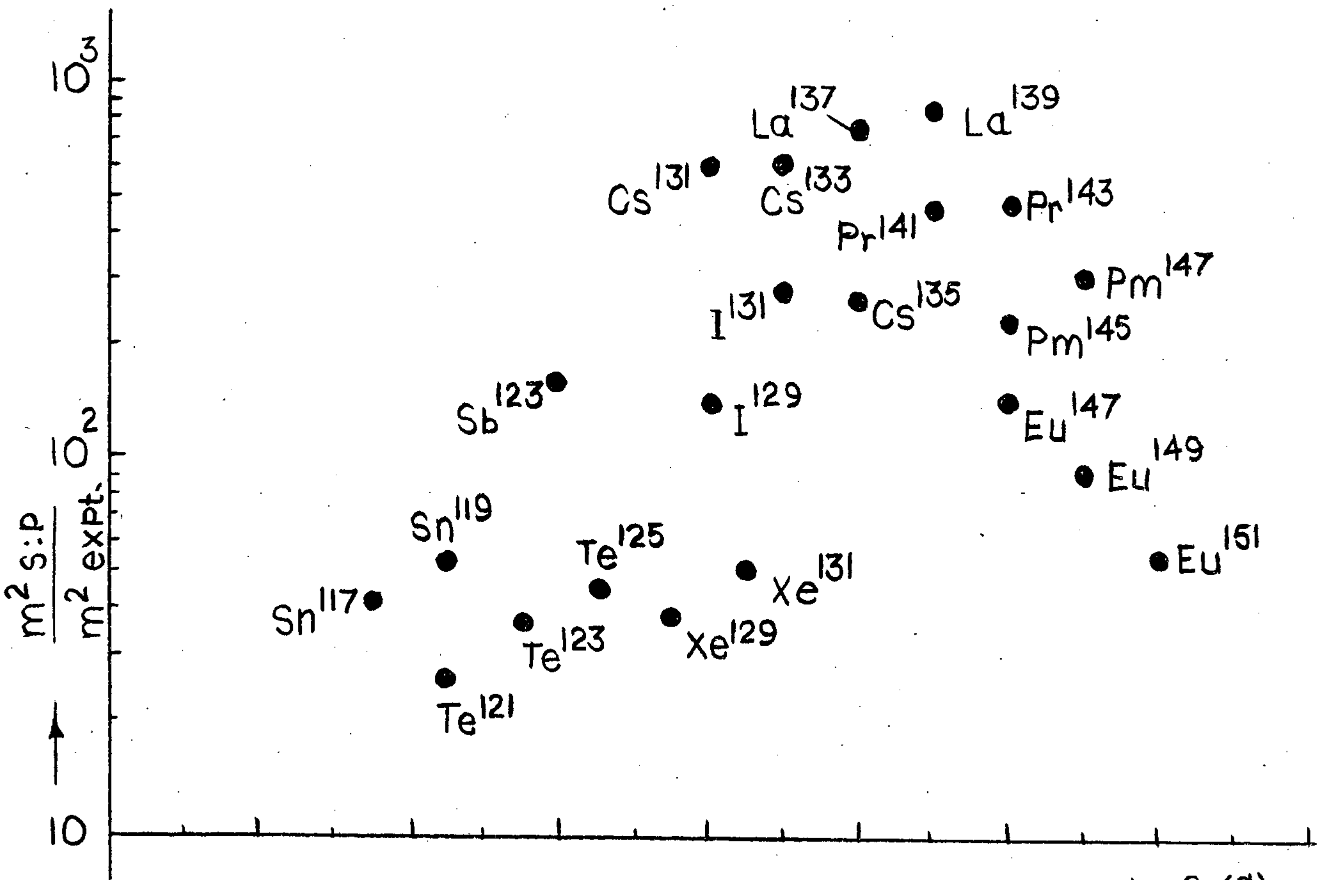

Fig. No. 2-(a)

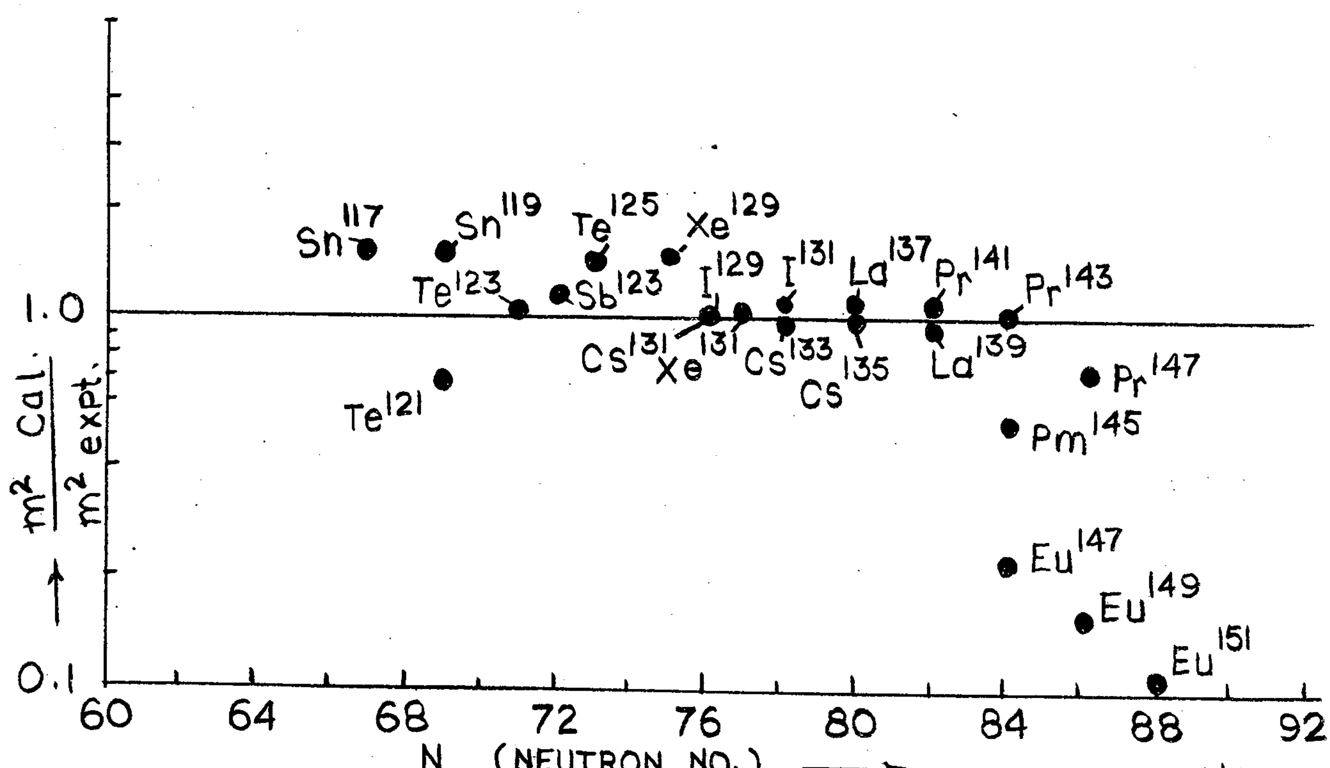

Fig. 2-(b)

where E_γ is the radiative transition energy and J_i is the angular momentum of the initial state. The points with the same neutron number are joined by a straight line. The solid line through the points is an arbitrary line. It is drawn to see if there is any special trend. Though it is not very conclusive, the plot shows some shell effect corresponding to the magic numbers at 28, 50, 82 and 126. At these magic numbers the observed value of the matrix element drops by a large factor. In the region $28 \leq N \leq 50$ the l-forbidden M_1 transition takes place between $p_{3/2} \rightleftharpoons f_{5/2}$ and the matrix element increases as we go away from the magic number 28 of neutrons till it attains a maximum value around N-44 (Br^{79}) after which the value starts falling down. A similar trend is reproduced more clearly in the region $50 \leq N \leq 126$, where the transition takes place between $s_{1/2} \rightleftharpoons d_{3/2}$ (odd neutron nuclei) and $d_{5/2} \rightleftharpoons g_{7/2}$ (odd proton proton nuclei). The value of matrix element at N = 69 corresponding to Te^{121} is ~ 1 while it drops by a factor of ten at the magic number N=82 correspon-ding to La^{139}. The same situation arises again at N=126 in the case of Thallium isotopes. The trend is also supported if we observe the change in matrix element for a given Z and increase the neutron number. If with the addition of a pair of neutrons the nucleus approaches towards magic num-ber (N=82) the value of the matrix element shows a downward trend. Examples of this effect are Te 121-Te 123- Te 125, Xe 129-Xe 131, I^{129}- I^{131} wheareas if the addition of a pair of neutrons takes the nucleus away from the magic number the behaviour is reversed i.e. the increase in neutron number increase the matrix element which is evident from the pairs Pr^{141}- Pr^{143}, Eu^{147} - Eu^{147} - Eu^{149} - Eu^{151}. The pairs Cs^{131} - Cs^{135} and Pm^{145}- Pm^{147} are exceptions to this general trend.

Similarly if we look for the variation of μ^2 with proton number number for a fixed value of N, the same regularity as mentioned above is observed e.g. the pairs $_{53}I^{129}$ - $_{55}Cs^{131}$, $_{53}I^{131}$ - $_{55}Cs^{133}$ and $_{55}Cs^{135}$ - $_{57}La^{137}$ show a general downward trend of matrix element with the increase in Z, while the pairs $_{57}La^{139}$ - $_{59}Pr^{141}$, $_{59}Pr^{143}$ - $_{61}Pm^{145}$ - $_{63}Eu^{147}$ show a rise in the value of the matrix element. The exception is met with the pair $_{50}Sn^{119}$ - $_{52}Te^{121}$ which is probably due to the reason that closed shell of Z =50 plays some role in reducing the matrix element. The low value of matrix element in the case of Sn^{117} may also be explained on the same basis.

To see if this effect is really the shell effect we have plotted in fig.2(a) the ratio of m^2 s.p/m^2 exp. (or retardation factor) for these ℓ-forbidden M1-transitions in the region $50 \leq N \leq 126$. It is evident that the retardation is much above unity and lies between the values of 40 and 800. The minimum value of 40 is for nuclei away from the magic number and maximum value is for nuclei at the magic number N = 82. This discrepancy is explained on the basis that, since at magic number the state are truely represented by the shell model wave functions, the magnetic dipole transition between two such states which differ in orbital angular momenta is strictly forbidden and hence a larger deviation of the matrix element is expected.

Fig. 2 (b) shows the plot of m^2 cal/m^2 exp. where the m^2 cal. are the calculated values from the Arima's theory based on configurational mixing. It is striking to note that the ratio has been brought down to a value around unity for a large number of nuclei. For nuclei with magic number of neutrons or near to them there always exists a configuration which yields a value very near to the experimental value. This indicates that the picture of congigurational mixing is very satisfactory at magic numbers, which further supports the shell model, since the zeroth order wave functions assumed in the so called Arima's theory are the shell model wave functions which are less perturbed by the other effects of nuclear dynamics only at the magic numbers. The smooth decrease of the ratio μ^2 cal./μ^2 exp. for N $\geqslant$82 clearly indicate that the effect of collective motion of the nucleons starts playing part in perturbing the seroth order wave funtions and thus the observed matrix element can no longer be explained by the configurational mixing.

IMAGINARY PART OF THE NUCLEAR OPTICAL POTENTIAL AT LOW ENERGIES

M.Z. Rahman Khan and Israr Ahmed
Department of Physics, A. M.U.. Aligharh (U.P)

During the last few years considerable effort has been made to obtain information about the radial distribution of the imaginary part of the nuclear optical potential from phenomenological analysis of low energy data (e.g. 1-4). However, the conclusions reached are not completely reliable. Although surface-peaked imaginary distributions give a slightly better over all fit to the low energy data, yet most of these potentials fail to account for the generally low values of the S-wave strength functions in the valley between 3S and 4S size resonances. This is specially disconcerting since strength functions are known to be one of the best means for the study of the radial distribution of the imaginary part of the optical potential at low energies. The situation is actually worse for it has been strongly indicated by Z.R. Khan that the experimental values are probably much higher than the actual values (3).

Recently, however, Z.R. Khan (5) has shewn that it is possible to secure any desired low values for the calculated strength functions in the region $A \approx 95$ by properly choosing the width and location of a surface-peaked imaginary distribution of appropriate strength. Unfortunately, the presently available S-wave strength function data have so much scatter that fits can be obtained for a variety of surface-peaked imaginary distributions. A fairly detailed consideration of this situation is presented here.

All phenomenological analyses, which have attempted to obtain the imaginary distribution, have assumed the constancy of all optical parameters except the radius. The validity of this assumption is clearly questionable. A possible dependence of optical parameters on shell closures was suggested as early as

1959 by Lane et.al.(6).

Recently Lane and Stamp (7) have expressed the view that reliable information about the imaginary distribution can be obtained by analysing the data for individual nuclei over a small energy range. We have briefly discussed the information about the radial distribution of the imaginary part of the optical potential that would be obtained from such an analysis.

We use a distorted wave approximation employing square well wave functions as the zero order solution. The departure of the imaginary part from a uniform distribution is treated as a perturbation. This approximation is satisfactory at low energies where the imaginary part is small. The use of square well wave functions in the distorted wave treatment seems a fair approximation for diffused real part provided the imaginary distribution does not lie too far out in the surface region. In any case only qualitative remarks have been made and it seems plausible that these would remain largely unaltered for a realistic situation.

THEORETICAL CONSIDERATIONS

Consider a complex potential which has as its real part a fixed square well of radius R and depth V_o. Let the imaginary part have an arbitrary distribution W(r) confined within the real part. Corresponding to any given partial wave, an equivalent uniform depth is obtainable, which, for that partial wave, is completely equivalent to the actual imaginary distribution. The S-wave equivalent depth $\overline{W}_0$ (R) is given by (3).

$$\overline{W}_0(R) = \frac{\int_0^R W(r)\sin^2 kr\,dr}{\int_0^R \sin^2 kr\,dr} \qquad (1)$$

Where K is the wave number inside the real part of the potential.

Let W(r) be of constant strength W_s in a region of width δ so situated that the outer side of the imaginary distribution is at a distance η from the outer boundary of the square well. Eq. (1) then gives

$$\overline{W}_0(R) = \frac{W_s\,\delta}{R\left(1-\frac{\sin 2KR}{2KR}\right)}\left[1-\left\{\sin 2K(R-\eta)-\sin 2K(R-\eta-\delta)\right\}/2K\delta\right] \cdots (2)$$

The P-wave equivalent depth for the same W(r) is given by (3)

$$\overline{W}_1(R) \approx \frac{W_3\delta}{R}\left[1+\left\{\sin 2K(R-\eta)-\sin 2K(R-\eta-\delta)\right\}/2K\delta\right] \qquad (3)$$

If R_1 and R_2 are the radii of two nuclei, one exhibiting a S-waves resonance and the other a P-wave resonance at low energies then eq. (2) gives

$$\frac{R_1\overline{W}_0(R_1)}{R_2 W_0(R_2)} = \frac{1-\left\{\sin 2K(R_1-\eta)-\sin 2K(R_1-\eta-\delta)\right\}/2K\delta}{1+\left\{\sin 2K(R_1-\eta)-\sin 2K(R_1-\eta-\delta)\right\}/2K\delta} \qquad (4)$$

which after rearrangement gives

$$\frac{\sin K\delta}{K\delta} = \frac{1-W}{1+W}\sec 2K(R_1-\eta-\delta/2) \qquad (5)$$

where

$$W = R_1\overline{W}_0 R/R_2 W_0(R_2) \approx \frac{\overline{W}_0(R_1)}{\overline{W}_0(R_2)}$$

Clearly when w differs significantly from unity, (experimental data indicate that w is between(5 and 10) the maximum value δ_{max} of δ corresponds to sec 2k $(R_1-\eta-\delta/2)=1$ or -1 according as $w<1$ or >1. The δ_{max} can then be obtained from a plot of $\frac{\sin K\delta}{K\delta}$ against $K\delta$.

Taking w = 10 we have calculated $\overline{W}_0(R)$ for the nuclei lying between A =55 and 95 for three values of δ; δ_{max}, $1/2\,\delta_{max}$ and zero (δ-function). Values of the parameters are given in the fig. captions.

It may be pointed out that for a given w(w$\gg$1) the curve corresponding to a given δ can also be obtained by taking as the imaginary part a certain uniform plus a suitably located surface- peaked distribution of width smaller than δ . The uniform part is maximum when the surface-peaked distribution is a δ-function.

From the curves it may be seen that the S- wave data for the nuclei in the immediate neighbourhood of A$\approx$55 and 95 can be fitted by a variety of surface-peaked distributions. When appropriately located the widths of the surface-peaked distribution may be taken anywhere between zero(δ-function) and δ_{max}. These distributions, however, differ in their predictions of the S-wave properties of nuclei lying between the two extremes A$\approx$55 and 95. Unfortu-

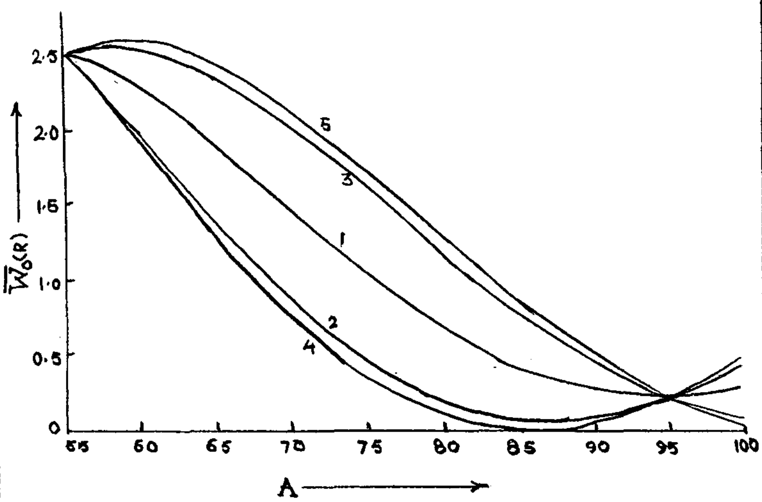

$\bar{W}_o(R)$ for the nuclei lying between A = 55 and 95 V_o = 42.6 Mev.

R = $1.45A^{1/3}$fm. curve 1 : $k\delta_{max}$ = 1.07, $k\eta$ = 2.61, W_S = 10.10 MeV

curves 2 and 3: $\frac{1}{2}$(k δ_{max}) $k\eta$ = 2.61 and 3.14

respectively, W_s = 20. 2 MeV.

curves 4 and 5 δ-function, $k\eta$ = 2.83 and 3.44 ,

W_s = 10. 81 and 10. 8 MeV.respectively.

nately the accuracy of the presently available data is such that it can hardly be of significant help in distinguishing between most of these distributions.

However, we like to point out the interesting fact that the values of the location parameter η differ only a little for the different distributions considered here. The difference, even in the extreme situation, is only about 30% of the periodicity of η (the period being π/K). The situation for w =5 is not very different. It is however, clear that if w is close to unity the uncertainty in location would become complete. Thus no matter what the actual distribution fits in the neighbourhood of A $\approx$ 55 and 95 would give a fairly good idea of the location parameter.

For a reliable determination of the width it is clearly necessary to have very accurate data for a large number of the intermediate nuclei. It may be pointed out that even if the S-wave strength function data are measured with nearly such accuracy as to determine an almost unique δ, it is clear, from what has already been said, that equivalent fits would be obtained by taking as the imaginary part a suitably located surface peak of any width smaller than δ plus a certain uniform distribution.

Now we shall briefly discuss the information about the radial distribution of the imaginary part of the optical potential that can be obtained by analysing the low energy data for individual nuclei.

The ratio of S- to P-wave equivalent depths for a nucleus of radius R, having a surface-peaked imaginary distribution of the type considered earlier is given by

$$\frac{\overline{W}_0(R)}{\overline{W}_1(R)} \approx \frac{1-\left\{\sin 2k(R-\eta)-\sin 2k(R-\eta-\delta)\right\}/2k\delta}{1+\left\{\sin 2k(R-\eta)-\sin 2K(R-\eta-\delta)\right\}/2k\delta} \qquad (6)$$

It then follows that the data for an individual nucleus can always be fitted by a suitably located surface-peaked imaginary distribution whose width may be chosen any where between zero (δ- function) and δ_{max}.

It is clear that the data can also be fitted by an imaginary part consisting of a uniform distribution plus a suitably located surface peak.

Useful information from such a study would be obtained only if the ratio of the equivalent depths turns out to be significantly different from unity, for otherwise the data would be equally fitted by a uniform distribution and a variety of surface-peaked distributions. It is, therefore, crucial to examine the dependence of the ratio of the equivalent depths on small changes in the radius. Unfortunately, at present we do not have the result of this investigation.

CONCLUSIONS

Obtaining fits to S-wave strength function data for spherical nuclei is no problem provided we agree to treat the location of the imaginary distribution as a variable parameter. The problem rather, is that, at present due to large uncertainties in the data, fits can be obtained by a vast variety of imaginary distributions.

REFERENCES

1. F. Perey and B. Buck, Nuclear Physics 32,353 (1962).
2. H. Fiedeldey and W.E. Frahn, Nuclear Physics 38, 686 (1962).
3. M.Z. Rahman Khan, Nuclear Physics 41 629 (1963).
4. A.P.Jain, Nuclear Physics 50, 157 (1964).
5. M.Z. Rahman Khan, to be published
6. A.M. Lane, J.E. Lynn, E. Melkonian, and E.R. Rae, Phys. Rev. Lett. 2, 424 (1959).
7. A.M. Lane and A.P. Stamp, Nuclear Physics 57, 444 (1964).

B.K. Jain: Can you please make it a bit more explicit what is form of W you have assumed?

Israr Ahmed : Our imaginary distribution $W(r)$ is of constant strength W_s in a region of width δ so situated that the outer side of the imaginary distribution is at a distance η from the outer boundary of the square well.

TRITON PARAMETERS WITH REALISTIC POTENTIALS

B.S. Bhakar and A.N. Mitra
University of Delhi
Delhi

We present here the results of exact evaluation of certain triton parameters of experimental interest, by regarding triton as a 3-body problem. The potential model chosen for the purpose is the so-called separable potential, in terms of which the threebody problem can be exactly formulated (1). The results for the binding energy with central forces have been known for some time. The present calculations include the non-trivial effect of tensor forces on the binding energy and the probabilities of various angular momentum states.

The complete formulation of the problem was given some time ago by one of us recently (2). The potentials considered for the numerical evaluation are those given by Yamaguchi (3) and Naqvi (4), denoted in the following table by suffixes and N respectively; C and T denote the (triplet) central and tensor forces respectively; S stands for the singlet N-N force and C^{eff} is the effective s-wave force in the ^1S_o state given by Yamaguchi (3).

The figures show that while an effective central force leads to over-binding, the mere C-part of the total C +T potential gives insufficient binding. Inclusion of tensor forces improves the results considerably. In this respect, the Naqvi force $(C + T)_N$ seems to give a value nearer to experiment than Yamaguchi's $(C + T)_Y$. This is particularly interesting if the hard core effects in this formalism are indeed small, as Tabakin (5) has recently found.

The percentage probabilities P_L of various states given in the table also show the expected trend, viz., an overwhelmingly [3] S-state, with small [2,1] S and D states, and a negligible P-state.

TABLE I

Potential	B.E. (MeV)	[3] P_o	[2,1]	P_o P_1	P_2
$C^{eff} + S_Y$	12.189	99.19	0.81	0	0
$C^{eff} + S_N$	11.819	99.04	0.96	0	0
$C_N + S_N$	7.036				
$(C+T)_Y + S_Y$	10.40	93.412	1.285	0.023	5.280
$(C+T)_Y + S_N$	9.951	94.055	0.850	0.021	5.073
$(C+T)_N + S_N$	8.850				

REFERENCES

1. A.N. Mitra, Nuclear Phys. 32, 529 (1962).
2. B.S. Bhakar, Nuclear Phys. 46, 572 (1963).
3. Y.Yamaguchi, Phys. Rev. 95, 1628, 1635 (1954).
4. J.H. Naqvi, Nuclear Phys. 36,578 (1962).
5. F. Tabakin, Phys. Rev. 137, No. 1B (1965).

DISCUSSIONS

M.K. Pal: I just want to ask a question for the sake of my own enlightenment. Well, how refined are the present day non local potential, for example Naqvi's one, with respect to fitting the two-body data including polarisation?

A.N. Mitra: Well, to the best of my knowledge, the parameters given by Naqvi (Nucl. Phys. 36, (1962) plus Tabakin's hard core potential, give a rather realistic representative of the 2-body data (scattering and bound states), including finer effects like magnetic and quadrupole moments.

S.P. Pandya: Perhaps the charge and magnetic moment form factors may be a test for your wavefunctions.

A.N. Mitra: Yes. The difference between the magnetic form factors of H^3 and He^3 depends on $(2,1)P_o$. Schiff's original estimate was 4%, but most other analyses have yielded 0.8 - 1.2%.

NUCLEON-NUCLOEN CORRELATION IN L = 0 STATE

S.B. Khadkikar
Tata Institute of Fundamental Research, Bombay-5

The "pairing" Hamiltonian with pairing interactions G_1 in L = 0, S = 0, T = 1 and G_2 in L = 0, S = 1, T = 0 state has the following form

$$H = \sum \epsilon_{\ell\lambda} a^{+}_{\ell m\lambda} a_{\ell m\lambda} + \frac{1}{4} \sum_{(\lambda,\ell\ell',mm')} G(\lambda_1\lambda_2,\lambda_1'\lambda_2') a^{+}_{\ell-m\lambda_1} a^{+}_{\ell-m\lambda_2} a_{\ell'-m'\lambda_2'} a_{\ell'm'\lambda_1'} \qquad (1)$$

where λ is the spin-isopin index $= (S_z \delta_z)$. $G(\lambda_1\lambda_2, \lambda_1'\lambda_2')$ in (1) is given in terms of G_1 and G_2 by (2)

$$\left.\begin{aligned} G(1\bar{1},1\bar{1}) &= G(2\bar{2},2\bar{2}) = \tfrac{1}{2}(G_1+G_2) \\ G(1\bar{1},2\bar{2}) &= G(2\bar{2},1\bar{1}) = \tfrac{1}{2}(G_1-G_2) \end{aligned}\right\} S_z = T_z = 0 \qquad (2)$$

where the values of $\lambda = 1, 2, \bar{1}, \bar{2}$ are

$$1 \equiv (+,+); \quad 2 \equiv (+,-) \quad \bar{1} \equiv (-,-) \quad \bar{2} \equiv (-,+)$$

The phase $(-)^m$ has been absorbed in redefinition of $a_{\ell-m}$ and $a^{+}_{\ell-m}$.

The Hamiltonian (1) we want to treat in the Bogoliubov variation method.

OUTLINE OF THE METHOD

Using Wick's theorem we can write H in terms of the contractions and normal products of operations a^{+}, a in the variational state. We define density matrix ρ and the pairing tensor t in terms of the contractions,

$$\rho_{\nu\nu'} = a^{+}_{\nu} a_{\nu} \qquad \text{and} \qquad t^{*}_{\nu\nu'} = a^{+}_{\nu} a^{+}_{\nu}$$

and

$$H = H_0 + H_1 + H_2$$

where H_0 is the fully contracted term and H_2 contains only the normal product of the interaction which we would not consider.

$$H_1 = \sum \tilde{\epsilon}_{\ell\lambda\lambda'} :a^{+}_{\ell m\lambda} a_{\ell m\lambda'}: + \frac{1}{2} \sum w^{\ell}_{\lambda_1\lambda_2} :a^{+}_{\ell m\lambda_1} a^{+}_{\ell-m\lambda_2} + \frac{1}{2} \sum w^{*\ell}_{\lambda_1\lambda_2} : a_{-m\lambda_2} a_{\ell m\lambda_1}:$$

where $\tilde{\varepsilon}_{l\lambda\lambda'} = \varepsilon_{l\lambda}\delta_{\lambda\lambda'} + \sum G(\lambda\lambda,\lambda'\lambda')\,\rho_{l\lambda,\lambda'} - g_\lambda \delta_{\lambda\lambda'}$

$$w^l_{\lambda_1\lambda_2} = \tfrac{1}{2}\sum G(\lambda_1\lambda_2,\lambda_1'\lambda_2')\,t^l_{\lambda_1'\lambda_2'}$$

The chemical potentials g_λ are introduced to take into account the non-conservation of number of either kind of nucleons.

We now introduce, following C. Bloch(1) the matrices R and K

$$R \equiv \begin{pmatrix} \rho & t \\ t^+ & 1-\tilde{\rho} \end{pmatrix} \quad , \quad K \equiv \begin{pmatrix} \tilde{\varepsilon} & w \\ w^+ & \tilde{\varepsilon} \end{pmatrix} \tag{4}$$

The invariance of commutation relations gives the condition

$$R^+ = R \quad , \quad R^2 = R \tag{5}$$

and the variational principle is expressed

$$[K, R]_- = 0 \tag{6}$$

Eigenvectors of R with the eigenvalue 0 (1) should also be eigenvectors of K with the eigenvalue W (-E).

SOLUTION OF EQUATIONS (5), (6) for (3)

We make a choice of pahses such that ρ is real symmetric and t is imaginary antisymmetric.

$$\rho = \tilde{\rho} = \rho^+ \; , \quad t = -\tilde{t} = t^+ \tag{7}$$

t has six parameters and ρ has 10. These parameters can be chosen as multiplying constants to the complete set of 16 Hermitian matrices 1, $\gamma_\mu, -i\gamma_5, i\gamma_\mu\gamma_\nu, \gamma_\mu\gamma_5$ where γ_μ, γ_5 anticommute. The condition (5) led to a solution of the form

$$t = \vec{A}\cdot\vec{\Gamma}_1 + \vec{B}\cdot\vec{\Gamma}_2 \, , \quad \rho = \nu + \eta\,(\vec{A}\cdot\vec{\Gamma}_1)(\vec{B}\cdot\vec{\Gamma}_2) \tag{8}$$

where A_i, B_i are the six parameters in t ; Γ_1 is $(\gamma_1\cdot\gamma_3, i\gamma_1\gamma_3)$ and Γ_2 is $(i\gamma_2\gamma_4, \gamma_2\gamma_5, \gamma_4\gamma_5)$ with the standard representations for γ_4 and $\gamma_5 = i\gamma_1\gamma_2\gamma_3\gamma_4$. ν and η are determined by $\sum_i |A_i|^2$ and $\sum_i |B_i|^2$ through the condition $t^2 = \rho - \rho^2$.

Expressions for $\tilde{\varepsilon}$ and w are obtained using (8), (2) and (3).

We drop superscript l for $\vec{A}$ and $\vec{B}$ for convenience.

$$\tilde{\mathcal{E}} = \mathcal{E} + \frac{g_1+g_2}{2} + \frac{3}{2}\nu(G_1+G_2) - \frac{1}{2}\eta(G_1+G_2)(\vec{A}\cdot\vec{\Gamma}_1)(\vec{B}\cdot\vec{\Gamma}_2)$$
$$+\eta(G_1-G_2)[(A_1 0 0)\cdot\vec{\Gamma}_1][(B_1 0 B_3)\cdot\vec{\Gamma}_2) - \eta(G_1-G_2)$$
$$[(0 A_2 A_3)\cdot\vec{\Gamma}_1][(0 B_2 0)\cdot\vec{\Gamma}_2] + \frac{g_1-g_2}{2}[(100)\cdot\Gamma_1][(100)\cdot\Gamma_2]$$

and

$$w = [(G_1 a_1, G_2 a_2, G_2 a_3)\cdot\Gamma_1)] + [(G_1 b_1, G_2 b_2, G_1 b_3)\cdot\Gamma_2]$$
$$\equiv (\vec{\Delta}_1\cdot\vec{\Gamma}_1) + (\vec{\Delta}_2\vec{\Gamma}_2) \tag{9}$$

where $a_i = \sum_l (2l+1) A_i^l$, $b_i = \sum_l (2l+1) B_i^l$

DISCUSSION OF THE VARIATIONAL CONDITION (6)AND DIAGONALISATION OF K

The variational conditions are given by (10), (11)

$$\vec{\Delta}_1\times\vec{A} = [(G_1-G_2)\eta^2|B|^2(A00) + \frac{g_1-g_2}{2}(B_1 00)]\times\vec{A}$$
$$\vec{\Delta}_2\times\vec{B} = [(G_1-G_2)\eta^2|A|^2(B_1 0 B_3) + g_1-g_2/_2(A_1 00)]\times\vec{B} \tag{10}$$

which have solutions

$$\vec{\Delta}_1 = x\vec{A} + (G_1-G_2)\eta^2|B|^2(A_1 00) + \frac{g_1-g_2}{2}(B_1 00)$$
$$\vec{\Delta}_2 = y\vec{B} + (G_1-G_2)\eta^2|A|^2(B_1 0 B_3) + g_1-g_2(A_1 00)$$

$$(\vec{B}\cdot\Gamma_2)(\vec{A}\times\vec{\Delta}_1)\cdot\vec{\Gamma}_1 + (\vec{A}\cdot\vec{\Gamma}_1)(\vec{B}\times\vec{\Delta}_2)\cdot\Gamma_2^2 = (G_1-G_2)$$
$$[(\vec{A}\times(A_1 00)]\cdot\vec{\Gamma}_1(B\cdot\Gamma_2) - (\vec{A}\cdot\vec{\Gamma}_1)(\vec{B}\times(0 B_2 0))\cdot\Gamma_2] + \frac{g_2-g_2}{2\eta}$$
$$[(\vec{A}\times(100))\cdot\Gamma_1(100)\cdot\Gamma_2) + (100)\cdot\Gamma_1(\vec{B}\times(100))\Gamma_2]] \tag{11}$$

X and Y which can be found by diagonalisation of K must satisfy the following conditions.

$$G_2\sum_l \frac{(2l+1)}{x^l} = 1, \quad G_2\sum_l \frac{(2l+1)}{y^l} = 1$$

It is seen clearly that $\vec{\Delta}_1$ and $\vec{\Delta}_2$ are coupled through the remaining conditions in (10); and (11) are the additional constraints on the choice of $\vec{A}$, $\vec{B}$. We shall consider the various solutions later.

We now make a remark about the diagonalisation of K. $[\tilde{\mathcal{E}}, \omega]_- \neq 0$ in general, and the diagonalisation of the (8x8) K matrix cannot be reduced to that of 4 x 4 matrices and one has to use wider group of unitary matrices than that of $\vec{T}_1 \vec{T}_2$ which is R_4,

We shall now consider two cases in which $[\tilde{\mathcal{E}}, \omega] = 0$ and are easily solved as $\sim$ ($G_1 = G_2$) terms in $\tilde{\mathcal{E}}$ are automatically annulled.

i) $\eta = 0$ which implies $N = Z$, $\vec{A} = 0$ or $\vec{B} = 0$ and $g_1 = g_2$. Condition (10) then gives for $\vec{B} = 0$ is following.

$$G_1 \sum \frac{(2\ell+1)}{\chi^\ell} = 1 \qquad A_2 = 0 \qquad A_3 = 0 \qquad \text{OR}$$

$$G_2 \sum \frac{(2\ell+1)}{\chi^\ell} = 1 \qquad A_1 = 0$$

where one of the correlations should break down. Or, if $G_1 = G_2 = G$

$$G = \sum \frac{2\ell+1}{\chi^\ell} = 1 \tag{12}$$

where $\chi^\ell = -2E^\ell = -2\sqrt{(\tilde{\mathcal{E}}^\ell)^2 + |\Delta_1|^2}$

E^ℓ is the quasi-particle energy.

The number of particles (n) is given by

$$n/4 = \sum_\ell (2\ell+1)(E^\ell - \tilde{\mathcal{E}}^\ell)/2E^\ell \tag{13}$$

This is the case considered by Flowers and Vujcic (2).

ii) $g_1 = g_2$ which implies $\frac{\partial E_g}{\partial N} = \frac{\partial E_g}{\partial Z}$ where E_g is the ground state energy and neutrons and protons are occupying same levels (low mass nuclei). The choice $A_1 = 0$, $B_2 = 0$ satisfies all the equations (10), (11) in this case. We get

$$[|\Delta_1| - |\Delta_2|] \sum_\ell \frac{(2\ell+1)}{2E^\ell_\mp} = \frac{|\Delta_1|}{G_2} \mp \frac{|\Delta_2|}{G_1} \tag{14}$$

These are the two gap equations where $E_\mp$ is given by

$$E^\ell_\mp = \sqrt{[\mathcal{E}^\ell + \frac{g_1+g_2}{2} + \frac{3}{2}\nu^\ell(G_1+G_2) \mp \frac{1}{2}\eta^\ell(G_1+G_2)|A||B|]^2 + (|\Delta_1| \mp |\Delta_2|)^2} \tag{15}$$

where $|A^\ell| = \frac{|\Delta_1| + |\Delta_2|}{2E^\ell_+} + \frac{|\Delta_1| - |\Delta_2|}{2E^\ell_-}$

$$|B^\ell| = \frac{|\Delta_1| + |\Delta_2|}{2E^\ell_+} - \frac{|\Delta_1| - |\Delta_2|}{2E^\ell_-} \tag{16}$$

and $\nu^\ell = \left[2 - \sqrt{1-4(|A|+|B|)^2} - \sqrt{1-4(|A|-|B|)^2}\right]/4$

$$\eta^\ell |A||B| = \left[-\sqrt{1-4(|A|+|B|)^2} + \sqrt{1-4(|A|-|B|)^2}\right]/4$$

The number of nucleons ($N+Z$) given by .

$$\sum (2l+1)\nu^{l} = \frac{N+Z}{4} \tag{17}$$

Our results (14) through (17) are more general than those obtained by P. Vogel, (3) in that we have found out the exact contribution to the single particle energies.

iii) Case $g_1 \neq g_2$ would require dropping of ($G_1 - G_2$) proportional terms in $\tilde{\mathcal{E}}$ as equations (10), (11) become incompatible. This case is being further investigated.

REFERENCES

1. Lectures on Nuclear Many-Body Problem by C. Bloch (Tata Institute of Fundamental Research, 1962).
2. B.H. Flowers, M. Vujicic, Nuclear Phys. 49, 586 (1963)
3. P. Vogel, Phys. Letters 10, 314 (1964).
4. M.K. Pal and M.K. Banerjee, Phys. Letters 13, 155 (1964).

RECENT RESULTS IN FAST NEUTRON REACTIONS

Aparesh Chatterjee
Calcutta University and Saha Institute of Nuclear Physics
Calcutta

INTRODUCTION

Ever since Bernard Cohen (1) did his Ph.D. dissertation on fast neutron induced reactions, a vast amount of experimental data has accumulated during the last 15 years. The activation technique in Cohen's experiments has been followed in the later extensive studies (2) in Chalk River, Arkansas and Aldermaston. Lillie (3) used a clound chamber to study the 14 MeV neutron reactions in light nuclei, but this method has practically been superceded by nuclear emulsion work (4) at Harwell, Rhode Island, and other places. Measurements with GM Counter-telescope systems were initiated by Ribe (5) and has often been used in angular distribution measurements parallelly with emulsions. This technique has lately been promoted into a very powerful tool with the happy development of scintillation counters and solid state detectors. Ingeneous combinations of phosphors, silicon detectors and gas proportional counters are now being used to do very elegant and beautiful experiments.

We shall mainly consider reactions induced by neutrons of energy E_n above 10 MeV upto about 20 MeV.. In the lower energy region (1 to 10 MeV) we only mention two experiments; (i) the (n,n') reactions at Los Alamos and (ii) the systematic work at 3-8 MeV initiated by Late T.M. Bonner at Rice University. Most of these data remain to be assimilated, understood, and systematized.

Instead of thorough survey, we shall discuss a few selected topics covered by recent experiments.

REACTIONS IN VERY LIGHT NUCLEI

The p-H and n-H scattering experiments furnish a vast amount of data on nuclear forces. Very light nuclèi containing only a few nucleons are therefore hoped to suppliment our knowledge on nucleon-nucleon interactions in presence of other nucleons, on charge dependence (if any) and on the nature of 3-body and many body forces. The ^1S scattering length, for instance, is highly sensitive to the charge dependence hypothesis. The photo- and inverse-disintegration processess, similarly, tell us something about electromagnetic nuclear field interactions and about the d-and t- widths.

Recent experiments in Zagreb(6) using counter telescope systems at $E_n = 14.4$ MeV with 2-dimensional analyzers have given the p $(n,d)\gamma$ and $d(n,t)\gamma$ cross-sections to be $\sim 30\mu$ b. Assuming the validity of the Siegart theorem, and that the initial state is described by adequate phase parameters for n-H and n-D interactions, one can have an estimate for the d-and t- widths.

A similar experiment(6) with the D(n,p)2n reaction (the break-up reaction into 3 bare nucleons) has recently been done by measuring the desired proton spectrum at 4°. The theoretical analysis is a difficult 3-body problem in its full complexity. Without invoking any detailed model, it can be shown that

$$d^2\sigma/dE\,d\Omega \propto \left[k'k''/(1+k'^2a^2)\right]a^2 \tag{1}$$

where a is the ^1S nucleon-nucleon scattering length, k' is the relative wave number of two strongly interacting nucleons in the final state, and k'' is the relative k of the third particle with respect to the centre of mass of the two strongly interacting particles. At the high-energy peak shown in Fig. 1, the two strongly interacting neutrons are recoiling backward in the CM system with low relative momentum (the proton goes forward). Since the (virtual) binding energy of the di- neutrons E_{nn} and the n-n scattering length a_{nn} are related, one gets a measure of a_{nn}. The experimental result is $a_{nn} = 21.7 \pm 2.0$ fm; the theoretical estimate, assuming charge symmetry, is -27 ± 1.4 fm.

Sayres et al (7) have studied the $He^3(n,n)He^3$ elastic scattering, the $He^3(n,p)T$ and $He^3(n,d)D$ reactions with monokinetic neutrons at 5 energies between $E_n = 1$ to 17.5 MeV by using a He^3 -filled proportional counter. The elastic scattering experiment was designed to discriminate between to forms of potential interaction, viz., Serber exchange and symmetrical exchange. The total ($\sigma_d + \sigma_p$) reaction cross-section was found to be $\sim$200 mb and it was concluded that the influence of the charge exchange reaction was important.

REACTIONS IN LIGHT, MEDIUM WEIGHT, AND HEAVY NUCLEI

A logical next step is to treat the light nuclei (8), but there are difficulties associated with generalizations in selected mass regions. We therefore make a few observations on all nuclei. The available information is mostly on total cross-sections in different reaction channels; isomeric and isotopic cross-section data exist in many cases, and occasional additional information on the energy spectra and angular distribution of the emitted particles is available. The data are mostly of the poor energy resolution type. Recent experiments with improved techniques, however, are more ambitious, and have given more detailed results on the excitation functions, energy spectra and angular spectra.

DIRECT INTERACTIONS AND COMPOUND NUCLEAR DECAYS

We conveniently divide fast neutron reactions into the above two categories as the two limiting cases. The distinction comes from the interaction times scales involved (10^{-23}S and 10^{-15}S in the two extremes) and from the number of nucleons taking part in the neutron-nucleus interactions. In general, both types of interactions are simultaneously present in a chosen target nucleus. Following Feshbach, one can also think of interactions resulting from the intermediate structures (gateway states).

Estimates of the compound nuclear magnitudes of cross-sections are in principle straightforward. The form of the level density of the two-fermion nuclear system is well known (9). In practice, however, one make drastic simplifying assumptions. For example, the inverse cross-section at a given excitation is usually taken to be the same as that of the ground state with little theoretical justification; another difficulty arises from our lack of detailed knowledge of the structural effects expected from compound nuclear reactions at high excitation energies. Thus the usual experimental estimates of the (i) compound nuclear cross-sections and (ii) relative magnitudes of compound nuclear and direct effects are often doubtful. It is hoped that the situation will improve with the recent attempts to include the nuclear structure effects properly.

14 MeV (n,d) REACTIONS

As an example of a reaction which proceds entirely through direct interactions, we note the recent experiments(10) in Milan in Fig. 2. The curve above for $Ni^{58}(n,d)\ Co^{57}$ has been fitted in shape with distorted wave Born calculations after Satchler. The table below compares the absolute experimental and theoretical cross-sections at 15° in the last two columns for the f-shell target nuclei listed column 1 with their appropriate spectroscopic factors given in column 2. Remarkable agreement between the two sets of

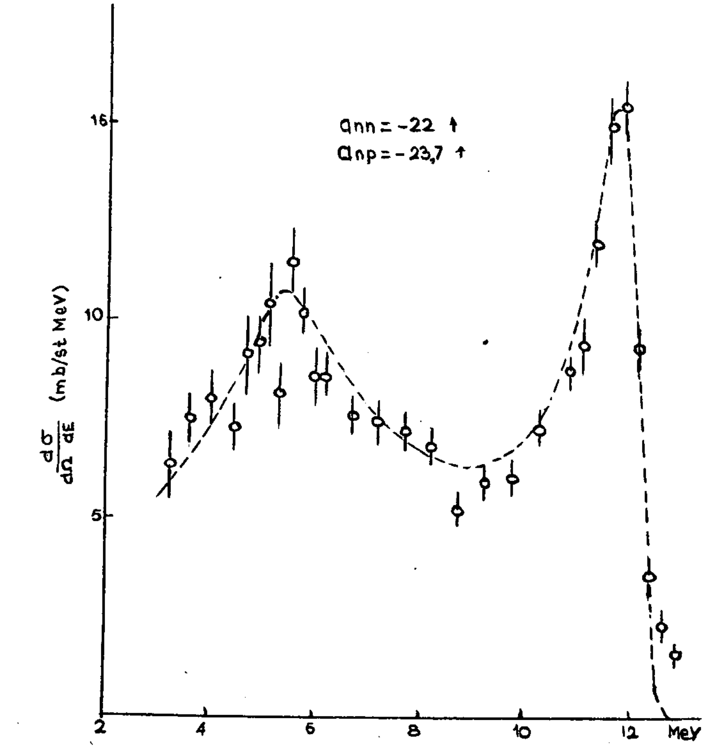

A fit to the measured spectra at 4° with $A^2 = 1/20$, $B^2 = 1/46$ $\alpha = 90°$
$a_{nn} = -22$ F, and $a_{np} = -23.7$ F.

Fig. 1.

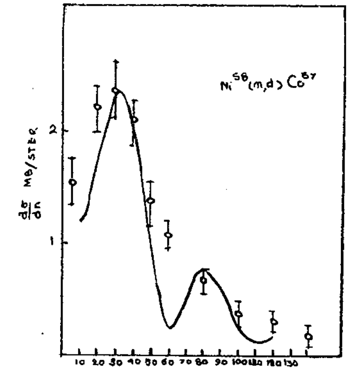

Angular distribution for the $Ni^{58}(n,d)Co^{57}$ reaction compared with a theoretical DWBA calculation for $l_n = 3$

TABLE I

COMPARISON OF EXPERIMENTAL ABSOLUTE CROSS SECTIONS FOR (n,d) REACTION AT 15° WITH THEORETICAL PREDICTIONS ON BASES OF SHELL MODEL WITH jj COUPLING

Neutrons	Shell Model Reduced Width (calculated)	$\bar{\sigma}$ (15°) theo	$\bar{\sigma}$ (15°) Exper.
Sc^{45}	1	0.23	≤ 0.30
V^{51}	0.75	0.21	0.48 ± 0.005
Cr^{54}	4	1.19	1.11 ± 0.1
Mn^{55}	2.5	0.14	0.36 ± 0.07
Fe^{54}	6	1.78	≤ 1.36
Fe^{56}	6	1.84	1.15 ± 0.1
Co^{59}	0.25	0.06	0.15 ± 0.05
Ni^{58}	8	2.16	2.84 ± 0.3
Ni^{60}	8	2.46	1.90 ± 0.2

Fig. 2

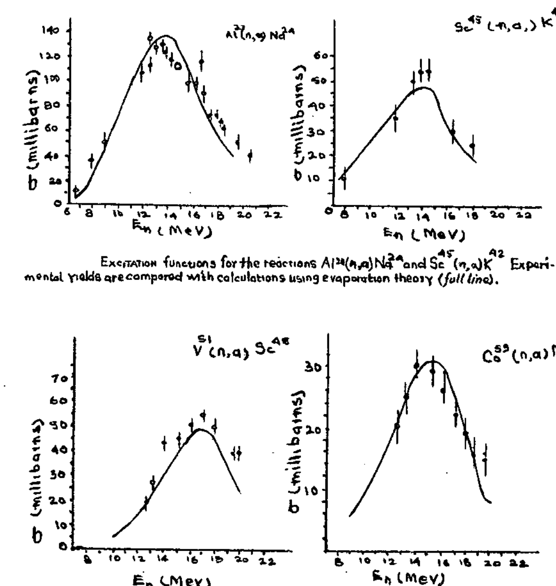

Excitation functions for the reactions $Al^{27}(n,\alpha)Na^{24}$ and $Sc^{45}(n,\alpha)K^{42}$. Experimental yields are compared with calculations using evaporation theory (full line).

Excitation functions for the reactions $V^{51}(n,\alpha)Sc^{48}$ and $Co^{59}(n,\alpha)Mn^{56}$. Experimental yields are compared with calculations using evaporation theory (full line).

Fig. 3

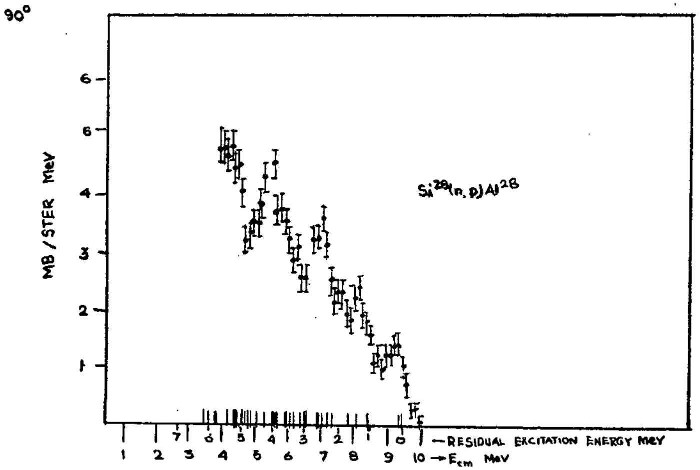

Proton spectrum from the $Si^{28}(n,p)Al^{28}$ reaction

Fig. 4.

Fig. 6.

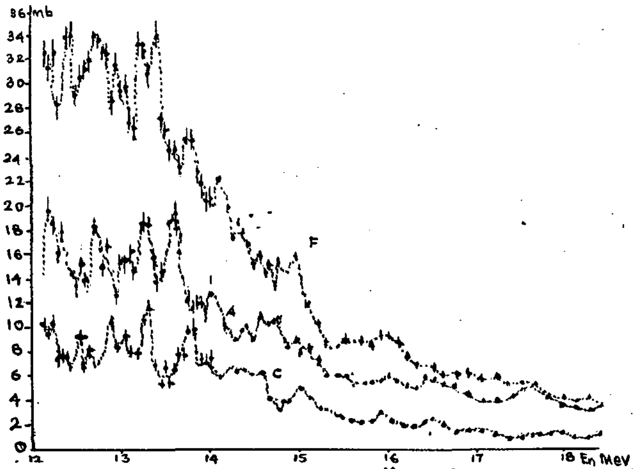

Experimental Excitation functions for three $Si^{28}(n,\alpha)Mg^{25}$ groups showing statistical fluctuations A, ground state, C, 2d Excited state F, 5th, 6th and 7th excited states unresolved[20])

Fig. 5

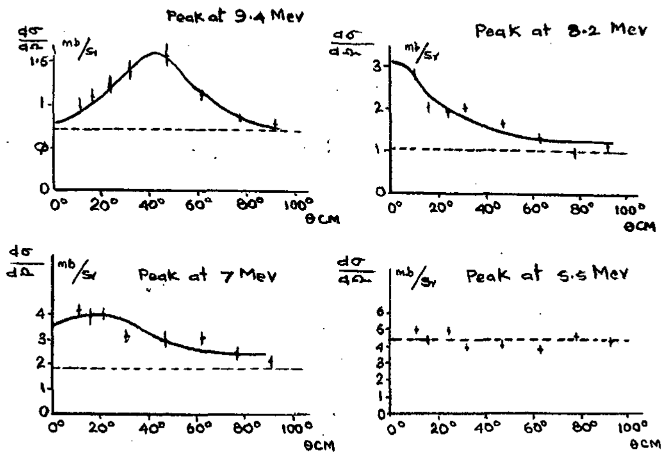

Angular distribution of protons emitted in $Si^{28}(n,p)Al^{28}$

—Angular distributions of prominent proton peaks observed for the $Si^{28}(n,p)Al^{28}$

Fig. 7.

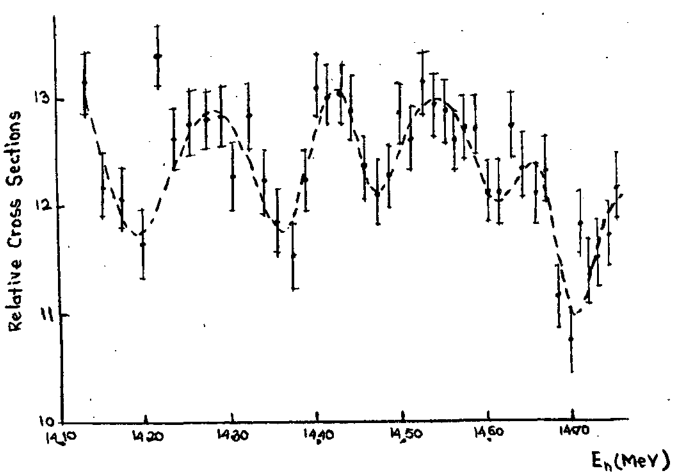

cross-sections is obtained on the assumption that the transferred angular momentum $l = 3$ comes from that of the picked-up proton from the $f_{7/2}$ state for f-shell nuclei.

EXCITATION SPECTRA OF (n,α) REACTIONS

As a contrast to the (n,d) reactions, it is believed that the fast neutron (n,α) reactions proceed entirely through the compound nucleus formation and subsequent evaporation. Recent experiments (11) have shown a good fit in absolute magnitudes and shapes for the excitation functions between $E_n = 7$ and 20 MeV for nuclei in the mass 27 to 59 region (Fig.3) by using the evaporation theory and optical transmission factors.

(n,p) REACTIONS

These reactions are examples where the direct and compound nuclear effects are generally mixed. From the measurement of energy spectra, it is believed that direct effects are stronger in light and heavy nuclei, while compound nuclear decays are more significant in medium weight nuclei. The direct (n,p) effects are similar to that of stripping. Figs. 4 and 5 show the energy spectra and angular spectra for different peaks (12) in the Si^{28} (n, p) Al^{28} reaction at $E_n \sim 14$ MeV. In Fig. 4, the few prominent proton group peaks at high residual excitations are clearly seen. Angular distributions of these peaks show diffraction patterns in Fig. 5; the distribution is isotropic at lower excitations but marked anisotropies are found at higher excitations.

REACTION SYSTEMATICS

In the earliest days of fast neutron reaction work, the attempts at systematization showed that a simple-minded compound nuclear evaporation approximation was not adequate and that it was necessary to include the direct effects. Recent experiments and systematic studies, however, clearly show the desirability of incorporating the known nuclear structure informations in both types of reaction mechanisms.

(a) Levkovskii-Gardner trend

Levkovskii (13) has shown that in a few cases of 14 MeV (n,p) reactions, the isotopic cross-section trends follow a definite pattern. Using a semi-empirical cross-section equation with 6 adjustable parameters, a thorough analysis by Gardner (14) has established an isotopic cross-section relationship of the form

$$R = \sigma(n,p)_{Z,A\pm m} / \sigma(n,p)_{Z,A} \sim x^{\mp m} \tag{2}$$

where m = 1,2, ..., and x has a value close to 2.

In case of (n,α) reactions, it was observed (15) that a similar relationship holds.

$$R' = \sigma(n,\alpha)_{Z,A\pm 2n} / \sigma(n,\alpha)_{Z,A} \sim \gamma^{\mp n} \tag{3}$$

where n = 1,2, ..., and γ varies from 4 to 1.7 from light to heavy nuclei.

(b) Shell Effects

These have been observed (16, 17, 18) in (n,α) and (n,p) reactions with fast neutrons in the form of distinct minima for all positions of proton shell and sub-shell closures. It has been possible to make a semiquantitative estimate of these effects (16) by using the simple Bloch-Rosenzweing model of combinatorial nuclear structure and by using a shift-function f_s to describe the shell-dependent form of the level density at the excitation energy U' :

$$U' = U + f_s \tag{4}$$

Recently, Bormann (19) has qualitatively analysed the (n,2n) shell effects.

FLUCTUATION PHENOMENA

When the level widths Γ in a compound nucleus are much greater than the level spacings, the levels are thoroughly mixed. Ericson (20) has shown that coherent contribution from different levels gives rise to interference effects between various levels, and the excitation function fluctuates with an width $\sim\Gamma$. From the statistical assumption, the fluctuation amplitude is given in terms of the square root of the mean square deviation as

$$A = \left[(\sigma-\bar{\sigma})^2\right]^{1/2}/\bar{\sigma} \tag{5}$$

and the fluctuation width is obtained from the correlation function

$$f(\varepsilon) = \left[\sigma(E_n+\varepsilon)\,\sigma(E_n) - \bar{\sigma}^2\right] \tag{6}$$

averaged over an interval of many fluctuations.

Experiments with medium resolution ($\Delta E_n \sim 50$ KeV) give typically $\Gamma\sim$ 50 -150 KeV (compound nuclear lifetimes $\sim 10^{-20}$ S) and $A\sim5\%$ of $\bar{\sigma}$ for light and medium weight nuclei. Fig. 6 gives the first experimental evidence (21) of these Ericson fluctuations between 12 and 18 MeV in Si^{28} (n,α) Mg^{25} reaction using a silicon detector target. Fig. 7 shows that even the simple activation technique[22] in Al^{27} (n,p) Mg^{27} shows these fluctuations.

REFERENCES

1. B.L. Cohen, Phys. Rev. 81, 184 (1951).
2. E.B. Paul and R.L. Clake, Can. J. Phys. 31, 267 (1953); R.W. Fink et.al., Phys. Rev. 112, 1950 (1958); 118, 242 (1960); Nucl. Phys. 8, 139 (1958); Phys. Rev. 115, 989 (1959); Nucl. Phys. 15, 326 (1960); Phys. Rev. 125, 297 (1962); R.F. Coleman et. al., Proc. Phys. Soc. 73, 215 (1959); Barry et al., Proc. Phys. Soc. 74, 632 (1959); C.S. Khurana and H.S. Hans, Nucl. Phys. 13, 88 (1959); S.K. Mukherjee et al., Proc. Phys. Soc. A77, 508 (1961); B.Mitra and A.M.Ghose, NP Symp, Chandigarh and this Symp.

3. A.B. Lillie, Phys. Rev. 87, 716 (1952).

4. G.M. Frye, Jr., Phys. Rev. 93, 1086 (1954); 103, 308 (1956); D.L. Allan, Proc. Phys. Soc. A70, 195 (1957); Nucl. Phys. 10, 348 (1959); Nucl Phys. 24, 274 (1961); R.A. Peck. Jr., Phys. Rev. 106, 965 (1957); Peck et al., Phys. Rev. 106, 976 (1957); Nucl Phys. 9, 273 (1958); 10,418 (1959) Bull, Am, Phys. Soc. 4, 287 (1959); Phys. Rev. 115,993 (1959); 123, 1378 (1961); 125, 1011 (1962).

5. F.L. Ribe, Phys. Rev. 87, 205 (1952); 103,741 (1956); 106, 767 (1957); Ribe and Seagrave 94, 934 (1954).

6. M. Cereneo et al., Phys. Rev. 124, 1947 (1961); 124, 1923 (1961); Phys. Lett. 6, 356 (1961); Nucl. Phys. 43, 254 (1963).

7. A.R. Sayres et al., Phys. Rev. 122, 1853 (1961).

8. S.S. Vasil'ev et al., DAN SSSR 119, 914 (1957); Sov. Phys. Doklady 3, 354 (1958); Benveniste et al., Nucl Phys. 19, 52 (1960); Bormann et al, Z. Naturforsch. 16a, 444 (1961); 15a, 22 (1960); Z. Phys. 166, 477 (1962) 174, 1 (1963); E. Kondaiah et al., Nucl. Phys. 5, 346 (1958); V. Verbinsky et al., Phys. Rev. 108, 779(1957).

9. T. Ericson, Advances in Phys. 9, 425 (1960).

10. L. Colli et al., Nuovo Cim. 20, 94 (1961); Ilakovac et al., Phys. Rev. 128, 2739 (1962).

11. L. Colli et al., Nuovo Cim. 21, 966 (1961); 20, 928 (1961); De Juren et al., Phys. Rev. 127, 1229 (1962); Gabbard and Kern, Phys. Rev. 128, 1276 (1962); Butler and Santry, Can. J. Phys. 41, 372 (1963).

12. See refs. 4 (Peak) and 11 (Colli).

13. V.N. Levkovskii, JETP 31 360 (1956); 33, 1520 (1957);45, 305 (1963).

14. D.G. Gardner, Nucl. Phys. 29, 373 (1962); Gardner and Poularikas, Nucl. Phys. 35, 303 (1963).

15. A. Chatterjee, Nucl. Phys. 47, 511 (1963).

16. A. Chatterjee, Nucl. Phys. 49, 686 (1963); 60, 273 (1954); Phys. Rev. 134, B374 (1964).

17. D.G. Gardner and Y.W. Yu, Nucl. Phys. 60, 49 (1964).

18. S.Notorrigo and P. Cuzzocrea, unpublished (private communication).

19. M. Bormann (1964) unpublished (private communication).

20. T. Ericson, see ref. 9 and Phys. Rev. Lett. 5, 430 (1960); Varenna Summer School (1961).

21. L. Colli et al., Phys. Lett. 1, 120 (1962); 2, 12(1962); Nucl Phys. 43, 529 (1963).

22. N. Cindro et al., Physics. Lett. 6, 205 (1963).

DISCUSSIONS.

M.K. Banerjee: Can we look at slide 6 again? It appears that some peaks are well correlated while some are not. Well, if we believe that the Feshbach gateway state model is good, then these peaks are the reflection of the spread of the width of the gateway state among a few adjacent levels. Since the distribution is still quite narrow, it is possible that sharp selection rules may be operative for the transition to the various low lying ground states. Transition to some levels may be allowed while that to some others may not be allowed. This will produce an apparent lack of correlation.

M.K. Mehta: (to M.K. Banerjee) Is it possible to measure angular distributions on the structures which are due to "gateway" states which you mentioned and get some information about the spin and parity of the state; You mentioned that these states are very sharply defined and the transition is to a sharply defined state, so this should be possible.

Paresh Mukherjee: (to M.K. Banerjee) Such angular correlations between a selective event and the peak have been done, and they seem to be related with the final state quantum numbers.

A.S. Divetia: Regarding the D(n,p) 2n reaction, I would like to comment that a method complimentary to the method at Jugoslavia, of measuring the proton energy spectrum, is being tried out at Rice University. The attempt is to measure the two neutrons in coincidence; this is more difficult experimentally, but more complete information is obtained.

A. Chatterjee: I agree that this is the right thing to do. I shall be glad to hear more about the results of this experiment at Rice University.

E. Kondaiah: In fig.1, the two peaks differ in width very much. What is the explanation for this difference?

A. Chatterjee: The lower energy peak near 5.5 MeV corresponds to the proton and one neutron moving forward with a low relative momentum, the other neutron recoiling backwards. It is experimentally difficult to separate the break-up protons from elastically scattered deuterons and from protons originating from elastic neutron scattering on hydrogen in the deuterium target as a contaminant. Various corrections are also needed in the observed energy spectra. With decrease of energy, the importance of n-p final state interaction increases.

N. Nath: I wish to make a comment about the energy range one chooses for averaging the cross-section in the Ericson type of fluctuations in the excitation function. It is very essential that one chooses the proper range for averaging, otherwise it may be difficult to conclude whether the fluctuations observed are truly of the Ericson type. Angular distribution measurements in the region of a "fluctuation peak probably provides a more definite answer".

V.K. Deshpande: There are cases known in charged particle induced reactions where the total cross-section shows structure in its energy variation but the angular distributions are insensitive to the energy variation. Normally one would expect the angular distributions to be far more sensitive due to their dependence on phase relations. The He^3, n and He^3, p reactions on C^{12} show this behaviour.

SYSTEMATIC MEASUREMENTS OF (n,p) CROSS SECTIONS AT 14.8 MeV

B. Mitra and A.M. Ghose
Nuclear Physics Laboratory, Bose Institute
Calcutta

Accurate values of (n,p) cross sections of light nuclei for 14.8 MeV neutrons have been determined by adopting the following procedure to eliminate or reduce systematic errors associated with many of the previous investigations.

(1) Neutron energy spread ΔEn has been limited by (i) using a thin target (ii) keeping incident deuteron energy confined in the range of 100 to 125 Kev and (iii) placing samples for irradiation not too close to the target ($\Delta\theta \sim \pm$ 30°). Reaction kinetic computations of Benveniste and Zenger (1) show that the maximum values of ΔEn as $\sim \pm$ 100 Kev around En = 14.8 MeV for Ed = 100 Kev. The r.m.s spread of ΔEn is still smaller.

(2) Quantitative dependence of the data on the monitor counting rate has been eliminated to obviate the effects of varying amounts of γ-rays, slower neutrons etc. produced when different samples are irradiated. A long counter and a heavily biased plastic scintillation counter have been used only to check the constancy of flux during one particular irradiation.

(3) The crosssections have been measured relative to σ_{std} = Cu^{63} (n,2n) Cu^{62} cross-section because (i) the values of σ_{std} are known as a function of En and (ii) samples are available in pure form. Combining the results of Ferguson and Thompson (2) and Glover and Weigold (3) we have adopted the value of σ_{std} as 530 $\pm$ 25mb.

(4) Neutron flux and beta counter have been calibrated by using σ_{std}. The difference in the geometries of the standard and the sample has been

experimentally measured by determining apparent cross section of copper powder and foils in the sample geometry position.

(5) Samples, in the form of powder or foil, were contained in a graphite sample holder because, of all available materials in the laboratory irradiated, graphite showed minimum residual activity.

(6) Purity of samples were checked by noting the consistency of measured cross sections of the same nuclei in several chemical forms as well as by checking the half lives of the reaction products.

(7) Using a line frequency scaler and a switching device which starts it as soon as R.F. supply in the ion source is turned off, error in timing was reduced to $\pm$ 20 milliseconds.

(8) Error in β - ray counting has been reduced by using a relative β-counting method developed by us. The method is based on the results of Bayhurst and Prestwood (4) who have shown that the efficiency of detection ϵ in a good geometry end-window counting experiment (with same sample thickness) is a smooth function of the average energy $\bar{E}_\beta$ of the electrons. We have shown that these data can be represented, for $\bar{E}_\beta > 0.1$ Mev, by an equation of the type

$$\epsilon = a(1 - e^{-b \bar{E}_\beta})$$

Since we are only interested in the relative efficiency, we can set

$$\epsilon_{rel} = 1 - e^{-b \bar{E}_\beta}$$

The value of b is determined by measuring apparent specific activity induced in copper foils of varying thickness. The accuracy of the method was checked by determining ϵ_{rel} for Al(n,p)β-rays.

Experimental arrangements have been described in a previous report and will be published elsewhere.

The values of cross-sections determined by us is shown in table I. The error shown are probable errors composed quadratically out of counting errors, errors in the standard cros section, errors in β-counting etc. We have also included predicted values from statistical model calculations of Erba et al (5), Gardner's semiempirical calculations (6) and Levkovski's empirical computations(7). The results of a few other experimenters are also shown there.

It will be noted that we have only considered half-lives in the range of a few seconds to several minutes. Experiments on shorter and longer half-lives will be considered in future reports.

REFERENCES

1. J. BenVeniste and J. Zenger, (UCRL) 4266; 1954.
2. Fergusson and Thompson, Phys. Rev. 18, (1960)228.
3. R.N. Glover and E.Weigold, Nuc.Phys., 29,(1962) 309.
4. Bayhurst and Prestwood, Nucleonics, 17, (1959) 82.
5. E. Erba, U.Facchini, E.Saetta-Menichella, Nuov. Cim., 22,(1961) 1237.
6. D.G. Gardner, Nuc. Phys., 29, (1962) 373.
7. V.N. Levkovskii, Sov.Phys. JETP, 18,(1964), 212.
8. J. Kantele, Bull. Am. Phys. Soc., 6, (1961) 252.
9. K.W. Seemann and W.E. Moore, Bull. Am. Phys. Soc. 6, (1961) 237.
10. J.A. DeJuren et al., Phys. Rev. 127, (1962) 1229.
11. J.Kantele and D.G. Gardner, Nuc. Phys., 35, (1962) 353.
12. E.B. Paul and R.L. Clarke, Can. J. Phys, 31, (1953) 372.
13. C.S. Khurana and H.S. Hans, Proc. 4th Symp., Low Energy Nuc. Phys, Bombay, (1960) 297.
14. S.K. Mukherjee et al., Proc. 4th Symp., Low Energy Nuc. Phys, Bombay, (1960) 189.

15. S.K. Mukherjee et al., Proc. Phys. Soc. 77, (1961) 508.

16. D.L. Allen, Nuc. Phys. 24, (1961) 274.

17. A.V. Cohen and P.H. White, Nuc. Phys. 1, (1956) 73.

18. R.S.Scalan and R.W. Fink, Nuc. Phys. 9, (1958) 334.

19. A. Poularikas, (Ref. Gardner Ref. No. 6)

20. D.M. Chittenden, (Ref. above).

TABLE I

(n,p) Cross sections of nuclei in 14 MeV range

(in millibarns)

Nucleus	Computed values			Experimental values	
	Erba et al	Gardner	Levkovskii	Present work	Previous wofks
O^{16}	-	64	80	40.1 ± 2.7	39 ± 4 [8] 34 ± 6 [9] 41.8 ± 2.3 [10] to 34.1 ± 1.8 38.2 ± 5 [11]
F^{19}	-	40	21	23.3 ± 2.2.8	16.5 ± 2 [8] 14.3 ± 2.5 [11] 135 ± 50 [12]
Na^{23}	51	64	44	41.8 ± 3.8	40 ± 5 [13] 29 ± 2 [14] 21 ± 3 [15] 34 ± 16 [12] 50 ± 20 [16]
Al^{27}	81	87	72	97 ± 10	77 ± 8 [14] 87 ± 8 [8] 82 ± 10 [11] 53 ± 5 [12] 115 ± 14 [13]
Si^{28}	251	240	240	222 ± 15	220 ± 60 [12] 157 ± 17 [13] 246 ± 28 [16]
Cl^{37}	-	53	30	21.3 ± 2.1	39 [17] 33 ± 7 [12] 25 ± 2 [18]
V^{51}	16.4	40	42	24.7 ± 2.2	53 ± 5 [19] 27 ± 5 [12] 23 ± 7 [16]
Cr^{52}	54	96	84	82.8 ± 5.8	78 ± 12 [12] 67 ± 10 [16] 83 ± 9 [20] 103 ± 12 [13] 105 ± 11 [14]

CROSS SECTION OF THE REACTION P^{31} (n, 2n) P^{30}
WITH NEUTRONS OF 14.8 Mev ENERGY.

B. Mitra, Arun Chatterjee and A.M. Ghose
Nuclear Physics Laboratory, Bose Institute
Calcutta

When phosphorus is bombarded with 14.8 Mev neutrons Al^{28} and P^{30} with close lying half-lives of 2.28 min and 2.55 min are produced by (n,α) and (n,2n) reactions respectively. These activities cannot be separated by β -counting and hence recourse is taken to γ -ray measurements. Al^{28} emits 1.78 Mev photons while annihilation radiation is given out by the positrons from P^{30}. In the present experiment we have measured the two cross-sections using the well-known cross sections of Si^{28} (n,p) Al^{28} and Cu^{63} (n,2n) Cu^{62} reactions. Unlike the experiments of Grimeland and Opsahl-Andersen(1) in this connection, our method involves no uncertain parameters like the photopeak efficiencies of the counting crystals for the two photons, fractional contribution to the annihilation peak by the degenerate photons derived from higher energy γ -rays. The method is based on the fact that $P^{31}(n,\alpha)$ and Si^{28} (n,p) reactions have the same daughter nucleus and Cu^{62} is a pure positron emitter.

In our experimental arrangement three identical cylinders containing Cu, P and Si samples are irradiated on a slowly rotating aluminium ring (fig.1). Rotation ensures that the samples occupy, on an average, the same geometrical disposition relative to the target. The samples are then counted on analyser with the channels set approximately to cover the two photopeaks. It is not necessary to know the location of the peaks very accurately. Let C_1 and C_2 be the corrected saturation count rates observed in the higher and lower energy channel respectively with P. Let C_3 and C_4 be the corresponding rates for Si while C_5 be the rate in the annihilation channel observed with Cu - then, the contribution of degraded photons in the lower channel with

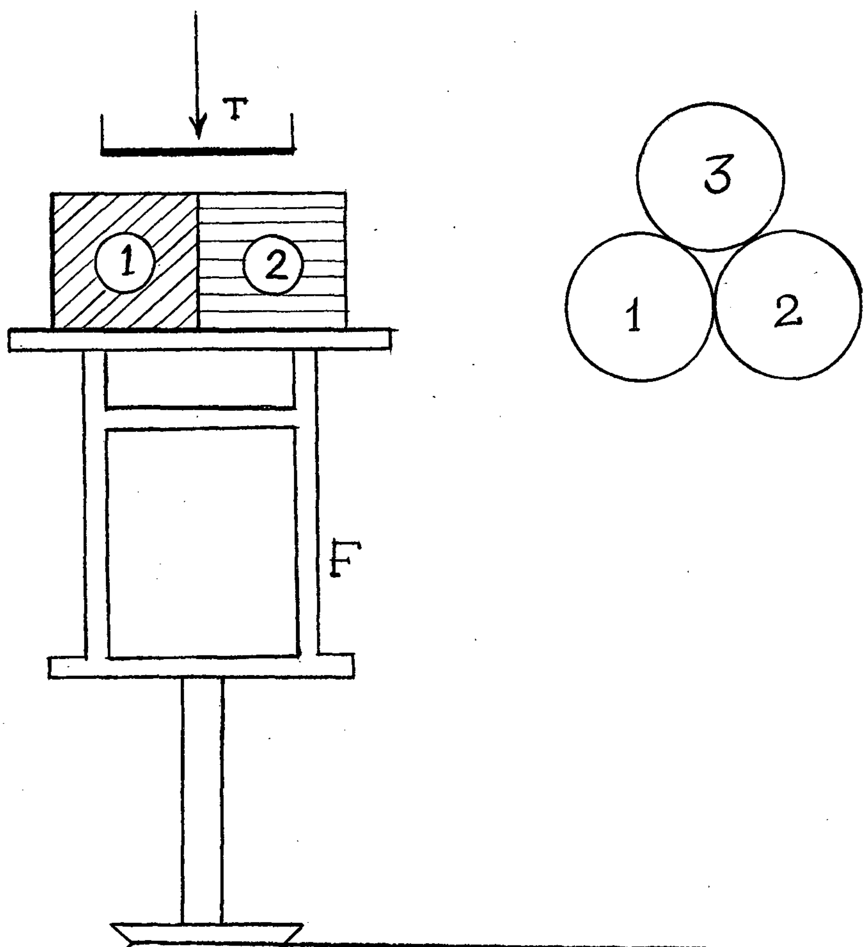
T
1
2
F
R
3
1
2

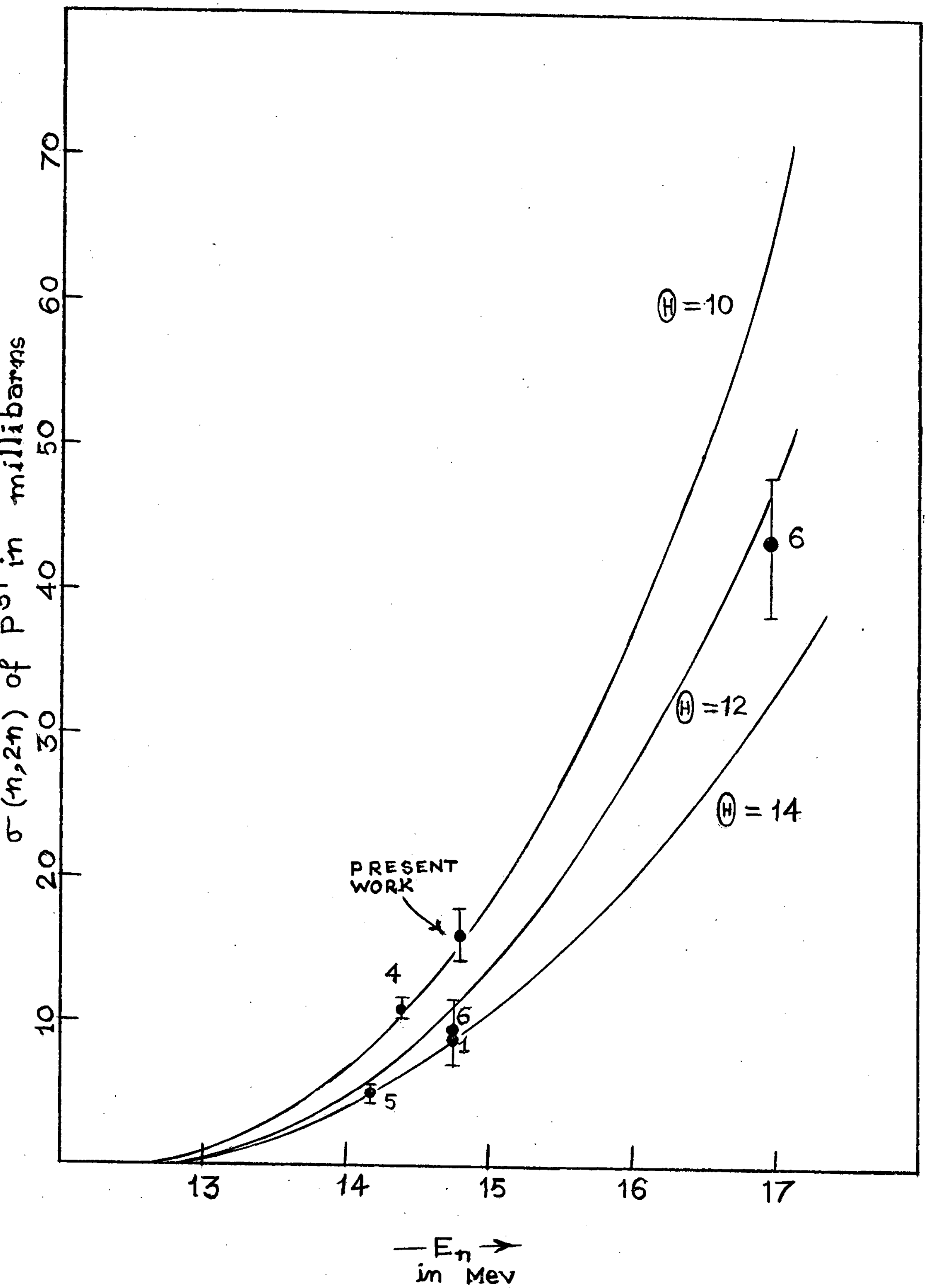
σ (n,2n) of P^{31} in millibarns
70
60
50
40
30
20
10
13
14
15
16
17
Θ = 10
Θ = 12
Θ = 14
PRESENT WORK
4
6
1
5
6
— E_n →
in Mev

P is $\frac{C1}{C3}$ C_4 so that its positron activity is proportional to $(C_2 - \frac{C1}{C3} \cdot C_4)$. Comparing this with C_5, we easily get the value of σ (n, 2n) of P^{31} in terms of σ (n,2n) of Cu^{63} . Similarly σ (n,α) of P^{31} is obtained in terms of σ (n,p) of Si^{28} by comparing C_1 with C_3.

The value of σ (n,α) of P^{31} obtained by us is 109 ± 11 mb which can be compared with the values 146 ± 29 obtained by Paul and Clarke (2) and 98 ± 12 obtained Gabbard and Loomies (3).

The value of σ (n,2n) obtained by various workers in shown in fig. 2. Our values will be seen to agree with those of Rayburn (4). It is proposed to carry out further experiments in this field especially in view of the large dispersion of results of various workers.

REFERENCES

1. Nuclear Physics 51, 302 (1964).
2. Canad. J. Phys. 31, 267 (1953).
3. Bull. Am. Phys. Soc. 3, 206 (1958).
4. Phys. Rev. 122, 168 (1961).
5. Cevolani and Petralia Nuo. Cim. 26, 1328 (1962).
6. Ferguson and Thomson Phys. Rev. 118, 228 (1960).

NEUTRONS ACTIVATION CROSS-SECTION AT 24 KeV II

A.K. Chaubey & M.L. Sehgal
Muslim University, Aligarh

Neutron activation cross-sections at 24 KeV have been measured for the following target nuclei:-
Zn^{68}, Ga^{69}, Ga^{71}, Se^{80}, Br^{79}, Br^{81}, Rh^{103}, Pd^{108}, Pd^{110}, Ag^{109}, In^{113}; Ba^{138}, Pr^{141}, W^{186}, Re^{185}, Re^{187}, Ir^{193}, Pt^{198}; and Pb^{208}. An Sb-Be photoneutron source was used forthe measurement. The theoretical values are obtained using the expression given by R. Booth et al. (2). In general there is a good agreement between the experimental and theoretical values. The results are shown in the attached table and figure. It is found that at the neutron magic numbers σexp. /σtheo. has a high value.

TABLE

Neutron activation cross-sections at 24 KeV, relative to I^{127} whose cross-section (1,2) at this energy was taken equal to 0.82 b.

Target Nucleus X	Halflife of (X +1)	Observed cross-section σ(mb)	$\Delta\sigma$(mb)	Calculated cross-section σ_q(mb)	Earlier cross-section values(mb)
Zn^{68}	13.8 h	5	1	31.4	5.6(1),6.1(12)
Zn^{68}	52 min	22	3		26(2),24(18)
Ga^{69}	21.1 min	50	5	126.4	68(1),140(17)
Ga^{71}	14.2 h	75	10	122	151(18)
Se^{80}	57 min	7	1.5	14.7	
Se^{80}	18 min	6	1		
Br^{79}	4.5 h	80	10		
Br^{79}	18 min	545	45	676	
Br^{81}	36 h	560	75		550(1)
Rh^{103}	4.4 min	55	25		
Rh^{103}	42 sec	455	45	527	
Pd^{108}	4.8 min and 13 h	185	15	530	540(1),290(17)
Pd^{110}	22 min	120	15	1982	> 300(2)
Ag^{109}	24 sec	690	60	647	
In^{113}	72 sec	260	90	1046	
Ba^{138}	84 min	7	1	0.5	11.4(1),8.6(18)
Pr^{141}	19 h	405	55	49	547(1) 170(2)
W^{186}	24 h	155	20	64	249(1),270(2)
Re^{185}	89 h	1765	265	1530	2650(1)
Re^{187}	17 h	875	80	637.5	~970(1)
Ir^{193}	19 h	630	50	1598	
Pt^{198}	30 min	205	30	200	240(2)
Pb^{208}	3.3 h	6.5	1	0.5	

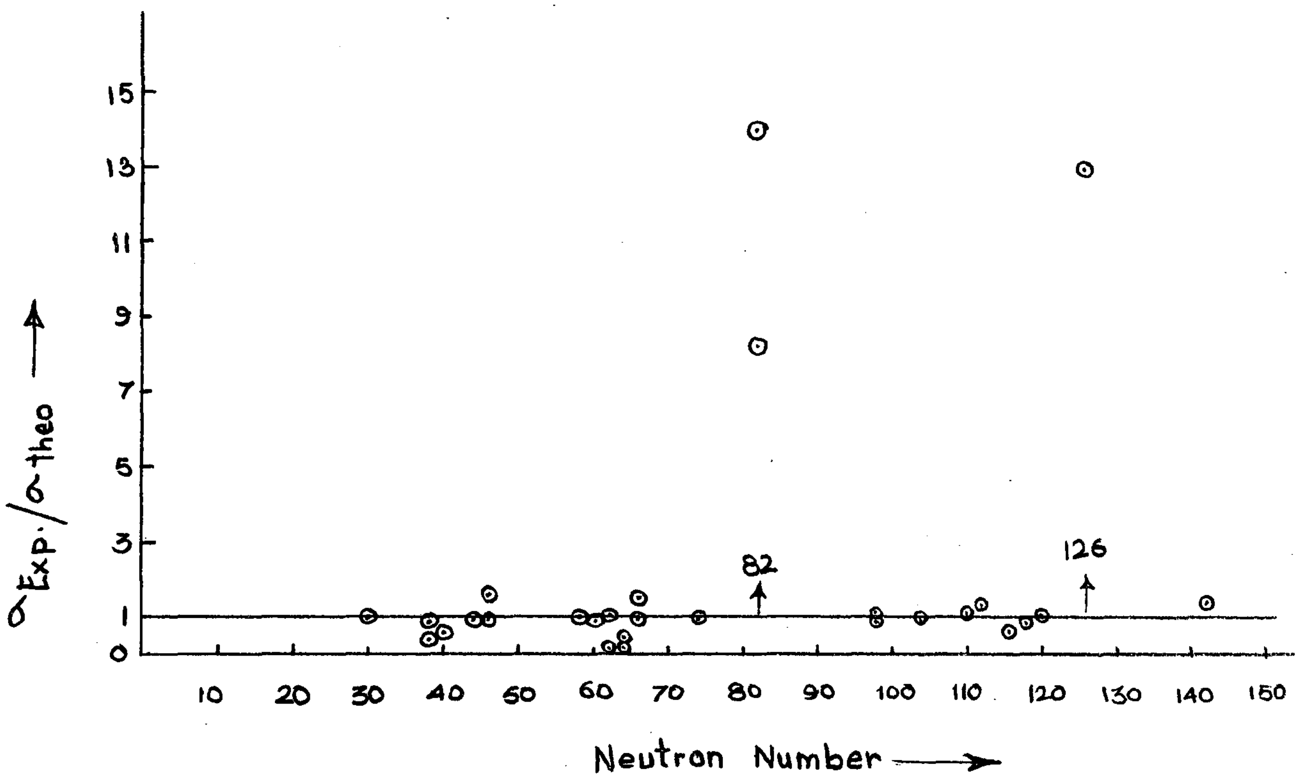

15
13
11
9
7
5
3
1
0
$\sigma_{Exp.}/\sigma_{theo}$
82
126
10
20
30
40
50
60
70
80
90
100
110
120
130
140
150
Neutron Number

REFERENCES

1. R.L. Maclin et al Phys. Rev. 107, 504 (1957).

2. R. Booth et al Phys. Rev. 112, 226 (1958).

3. H.W. Schmitt Nuclear Physics 20, 220 (1960).

4. Burbridge et al. Rev. Mod. Phys. 29, 547 (1957).

5. Hughes, D.J., Pile Neutron Research p.p. 186 and 22.

6. M.L. Sehgal Ind. J. Phys. 31, 630 (1957).

7. Nuclear Data Sheets, National Academy of Science National Research Council Washington, 1960 to 1964.

8. D. Strominger et al. Rev. Mod. Phys. 30, 30 (1958).

9. R.E. Sund et al Nuclear Physics 38, 478 (1962).

10. P.N. Trehan et al Phys. Rev. 126, 266 (1962).

11. Henry W. Brandhorst; Jr et al. Phys. Rev. 125, 1323 (1962).

12. V. Hummel and B. Hamermesh Phys. Rev. 82, 67 (1951).

13. D.J. Hughes and R. Swartz BNL-325, (1958) second ed.

14. J.S. Levin and D.J. Hughes Phys. Rev. 101, 1328 (1956).

15. Harvey, Hughes, Carter and Pilcher Phys. Rev. 99, 10 (1955).

16. Carter, Harvey, Hughes and Pilcher Phys. Rev. 96, 113 (1954).

17. W.S. Lyon et al Phys. Rev. 114, 1619 (1959).

18. Kononov et al J. Nuclear Energy A 11, 46 (1959)

19. Berhard Keisch Phys. Rev. 129, 769, (1963).

DISCUSSIONS

N. Nath : What is the order of the error in you cross-section measurements?

A.K. Chaubey: Errors due to all the factors are near about 10% plus the statistical error depending upon the counting rate in the individual cases.

Comment: It seems the error have been under estimated.

P.N. Trehan: How do you know the neutron energy that is given by the Sb-Be source?

A.K. Chaubey: Sb-Be neutron source is a photoneutron source giving neutron of energy 24 KeV.

LIFE-TIME AND ANGULAR CORRELATION MEASUREMENTS IN THE DECAY OF Cd^{117}

V. R. Pandharipande, K.G. Prasad, R.M. Singru and R.P. Sarma
Tata Institute of Fundamental Research, Bombay-5

The decay scheme of Cd^{117} has been established earlier (1) and is shown in Fig.1. The present study was initiated to study the structure of the levelsin In^{117}.

Angular correlation measurements have been carried out and the results are summarised in table 1. The observed angular correlation has been expressed in the standard form $W(\theta) = 1 + A_2P_2(\cos\theta) + A_4P_4(\cos\theta)$.

TABLE I

Cascade	A_2	A_4
1300-280 KeV	$+ 0.271 \pm 0.013$	$+ 0.026 \pm 0.042$
1050-1070 KeV	$- 0.022 \pm 0.012$	$+ 0.015 \pm 0.038$
540-1410 KeV	$- 0.011 \pm 0.012$	$+ 0.060 \pm 0.038$

The results of the 1300-280 KeV cascade indicated that the spins of the levels at 590 and 1890 KeV are $3/2^-$ and $\frac{1}{2}^+$ respeceively. The parity assignment has been made from the log ft values of the beta transitions to these states. The transitions are nearly pure E1 and M1 respectively.

The spin and parity of 1070 KeV level is $7/2^+$ as obtained from beta gamma and gamma-gamma coincidence measurements. The 2120 KeV level can have spins 9/2 or 11/2. The latter possibility is ruled out by the angular

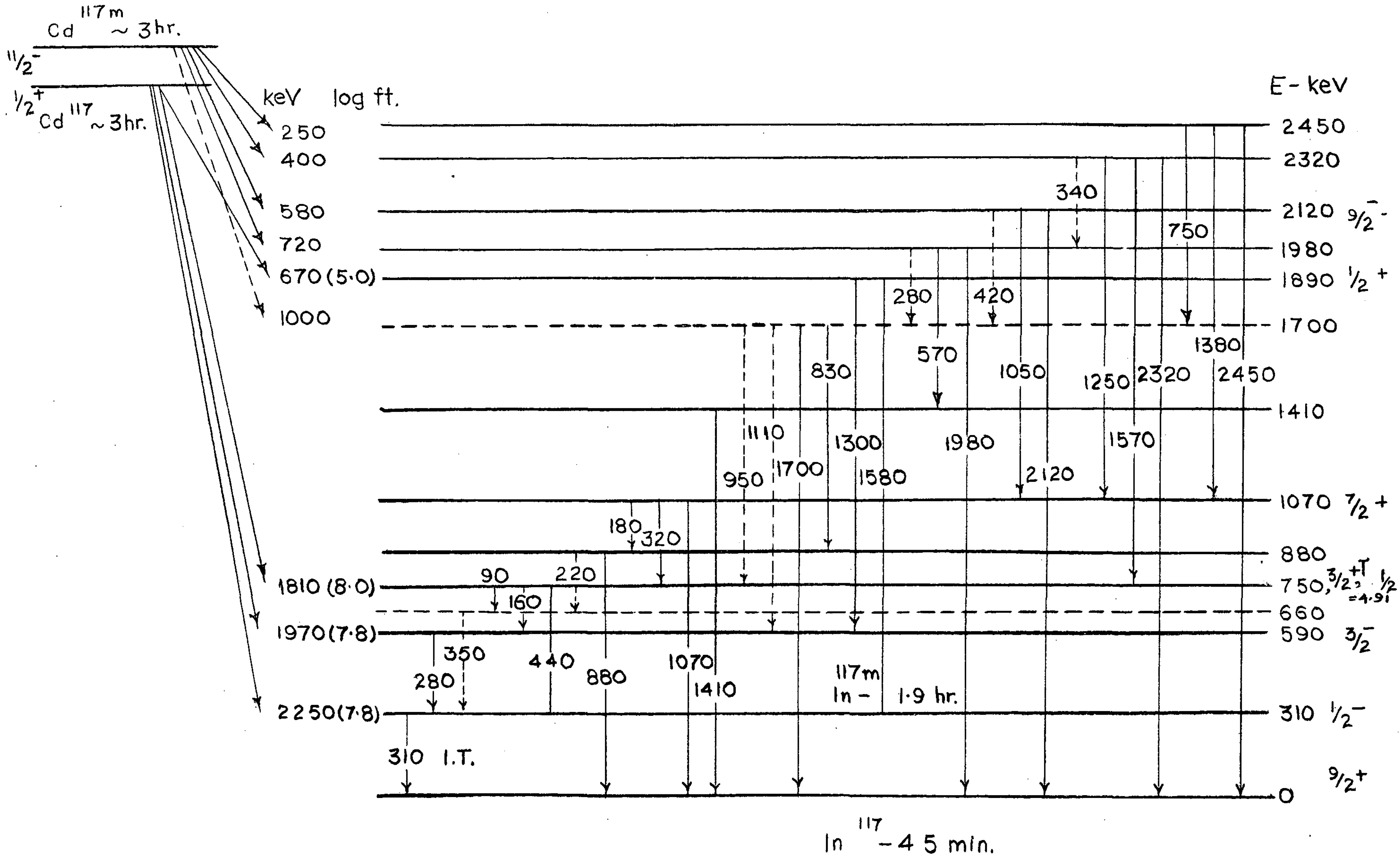

Cd 117m ~ 3hr.
11/2−
1/2+ Cd 117 ~ 3hr.
keV log ft.
250
400
580
720
670 (5·0)
1000
1810 (8·0)
1970 (7·8)
2250 (7·8)
E - keV
2450
2320
2120 9/2−
1980
1890 1/2+
1700
1410
1070 7/2+
880
750, 3/2+, T1/2 = 4·91
660
590 3/2−
310 1/2−
0 9/2+
340
750
280
420
570
830
1050
1250
2320
1380
2450
1110
1300
1980
1570
950
1700
1580
2120
180
320
90
220
160
350
280
440
880
1070
1410
117m In − 1·9 hr.
310 I.T.
In 117 − 45 min.

correlation measurements, provided the 1070 KeV gamma ray is assumed to be an E_2 transition. This assumption is valid if the level at 1070 is due to the coupling of one phonon with the ground state (2). In this way the analysis of 1050 -1070 KeV cascade shows that the most likely spin of 2120 KeV level is 9/2. The multipolarity of 1050 KeV gamma transition cannot be obtained from this measurement alone.

The analysis of the angular correlation of the 560 -1410 KeV cascade has indicated a positive A_4 term. Such a term indicates some M2 mixture in the 560 KeV transition. The possibility of M2 mixture in these transitions(560 and 1050 KeV) indicates a large retardation of El transition such a retardation (3) is also observed in $5^- \rightarrow 4^+$ transition in Sn^{118} (2290 → 2250 KeV) and is of the order of 3×10^4. The 5^- level at 2290 KeV in Sn^{118} is two quasi-particle level with one quasi-particle in $h_{11/2}$ and the other in $S_{\frac{1}{2}}$ orbital. The 4^+ level at ($g_{7/2}$ and $S_{\frac{1}{2}}$). In this transition ($5^- \rightarrow 4^+$) the odd neutron goes from $h_{11/2}$ orbital to $g_{7/2}$ orbital and $\Delta j = 2$, thus retarding the El transition. Hence the present measurements indicate that the high energy levels In^{117} may be due to the breaking of a neutron pair. The errors in the measurements of A_4 are quite large and we propose to improve on these measurements.

The half-life of the 750 KeV level was measured by the standard time to pulse height conversion method. The delayed coincidences were observed between the beta rays of energy 1200 ± 100 KeV and the 440 KeV gamma ray. The observed half-life is 4.91 ± 0.3 ns. A similar level at 820 KeV in the neighbouring In^{115} isotope has a half life of 5.1 ns and there it is indicated to be a $3/2^+$ level. The level at 750 KeV in In^{117} may be of similar nature.

REFERENCES

1. R.P. Sharma, K.P. Gopinathan and S.R. Amtey, Phys. Rev. Vol.134B 730 (1964).

2. V.R. Pandharipande, R.P. Sharma and Girish Chandra, Phys.Rev 136B 346 (1964).

3. Nuclear Data Sheets.

LIFE-TIME AND ANGULAR CORRELATION MEASUREMENTS IN Au^{199}

K.G. Prasad, R.P. Sharma and B.V. Thosar
Tata Institute of Fundamental Research, Bombay -5

The energy levels in odd mass isotopes of Au have been of great interest and various investigations, experimental as well as theoretical, have been carried out in the recent past. The 79th proton in these isotopes moves in the $d_{3/2}$ orbit $(d^3_{3/2})$ and the lowest positive parity excited states according to core excitation model may result from the coupling of the odd nucleon to the 2^+ state of the core, leading to the quadruplet $\frac{1}{2}^+$, $3/2^+$, $5/2^+$ and $7/2^+$. The recent investigations in Au^{197} have supported the presence of such a quadruplet. In the present work the energy levels in Au^{199} have been investigated from the decay of 30 minute Pt^{199}. These energy levels have been reported by us earlier as studied from the beta-gamma and gamma-gamma coincidence measurements. Further work is carried out to investigate the nature of these levels.

The half-life of the first excited state at 75 KeV has been measured to be 1.46 ± 0.6 nano secs. In this measurement the usual T.P.C. method has been utilised by observing the delayed coincidences between the 75 KeV and 715 KeV gamma rays.

The gamma-gamma directional correlation measurements have been carried out by using three detectors and the coincidence counts were collected at two angles simultaneously. The measurements were made at three angles and the coefficients A2 and A4 defined by the equation $W(\theta) = 1 + A_2P_2(\cos\theta) + A_4P_4(\cos\theta)$ have been calculated. For the 475 -320 KeV cascade these coefficients A2 are as follows:

$$A2 = 0.082 \pm .01$$

$$A4 = 0.042 \pm .031$$

In a similar way the 197 — 540 KeV cascade was analysed and the values of A_2 and A_4 are

$$A2 = 0.064 \pm .013$$

$$A4 = -0.051 \pm .04$$

Based on this data we would like to say something about the nature of the energy levels in Au^{199}. These energy levels are shown in the figure.

The ground state of Au^{199} is known to be $3/2^+$ as measured from the atomic beam method. The ground state of Pt^{199} is $5/2^-$ as obtained from the earlier measurements of the energy levels in Pt^{199}. As compared with the neighbouring odd mass isotopes of Au and the observed high log ft value of the beta transition the spin and parity of the first excited state has been put as $\frac{1}{2}^+$. By calculating the reduced E2 transition probability from the observed halflife of such a state in Au^{197} and the E2 + M1 mixing ratio, Braustein and de Shalit have recently explained this state to be the lowest state of the core multiplet. In the present case also this excited state at 75 KeV could be a member of the core multiplet.

The gamma gamma directional correlation analysis of the 475 –320 KeV cascade has indicated a possible spin of 3/2 and 5/2 for the states at 790 and 320 KeV. The other possibilities are ruled out from the observed sign and the finite value of the A_4 term. The analysis of this cascade has further indicated the possibility of some E2 mixture in these transition. Due to the large error in A_4 term the percentage E2 mixture varies in wide range. With the 320 KeV level as $5/2^+$ the observed large intensity of 240 KeV transition compared to 320 KeV can only be explained by assuming another level very close to 320 KeV. In that case when compared with the neighbouring Au^{197} this level

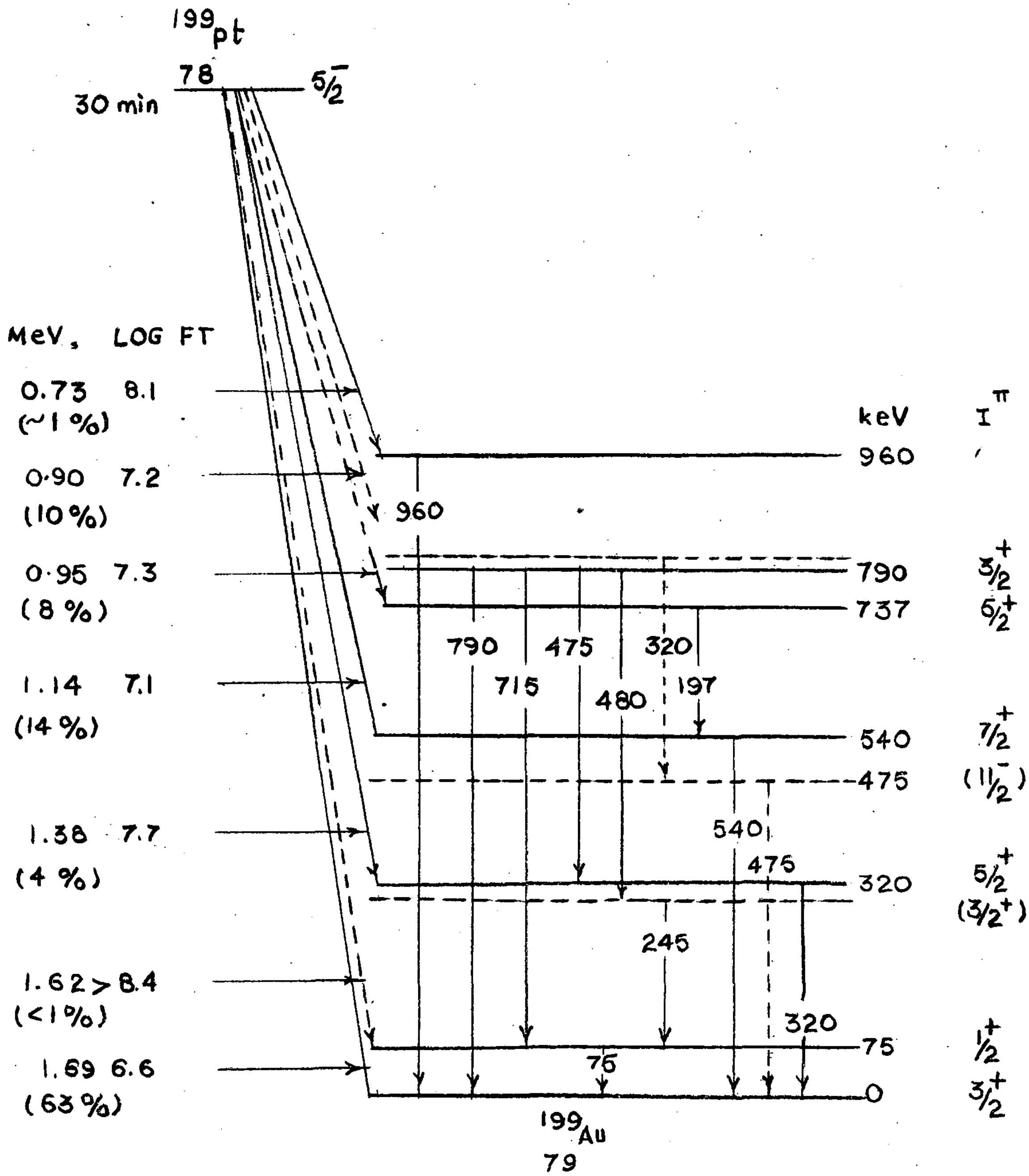
199 Pt
78
5/2−
30 min
MeV, LOG FT
0.73 8.1
(~1 %)
0·90 7.2
(10 %)
0·95 7.3
(8 %)
1.14 7.1
(14 %)
1.38 7.7
(4 %)
1.62 > 8.4
(<1 %)
1.69 6.6
(63 %)
keV
Iπ
960
790
5/2+
737
5/2+
540
7/2+
475
(11/2−)
320
5/2+
(3/2+)
75
1/2+
0
3/2+
960
790
715
475
480
320
197
540
475
245
320
75
199 Au
79

can be $3/2^+$.

From angular correlation measurements the 197-540 KeV cascade can be interpreted as $5/2 \longrightarrow 7/2 \longrightarrow 3/2$ cascade provided the intermediate state at 540 KeV is assumed to be 7/2 in analogy with Au^{197}, where such a state has been observed in Coulomb excitation experiments. On this assumption the 540 KeV is a pure E2 transition while the 197 KeV transition is mostly M1. The analysis indicates a 5 to 7% E2 mixture in this transition. The observed -ve value of the A_4 term and the log ft value rule out the other values of spin for the 737 KeV state. In this way the levels at 75 KeV, 320 KeV and 540 KeV could be the members of the quadruplet formed by coupling of the first phonon with the $d_{3/2}$ ground state. Further work is in progress to say more definitely about these levels.

A MAGNETIC COOLING SET-UP FOR STUDIES WITH ORIENTED NUCLEI

Girish Chandra and V.R. Pandharipande
Tata Institute of Fundamental Research, Bombay-5

By static method appreciable degree of nuclear orientation can be achieved generally in the temperature region of 0.01° k -0.1° k. These temperatures are obtained by adiabatic demagnetisation of a suitable paramagnetic salt. In this report we will describe briefly our apparatus for adiabatic demagnetisation and the preliminary result obtained with the aligned Co^{60} nuclei.

Figure 1 shows the helium cryostat used for magnetic cooling. The paramagnetic salt chrome potassium alum, used as the cooling agent, is suspended in a perspex-stainless steel assembly and enclosed in a copper tube. This tube is suspended from the top of the cryostat by means of a stainless steel tube which also serves as the pumping line. The magnetic susceptibility of the salt is used as the temperature dependent parameter to measure the temperature below 4°k. It is calibrated in 4.2° -1.2° k range using helium vapour pressure thermometry. A set of mutual inductance coils wound over the salt with secondary output connected to a ballistic galvanometer enables us to measure the variation of susceptibility. The copper tube is surrounded by liquid helium which is then surrounded by liquid nitrogen shield. The adiabatic demagnetisation is carried out in an initial magnetic field of about 22 kgauss and a temperature of 1.15°k. The final temperature of 0.011°k is obtained.

Co^{60} nuclei were aligned in a single crystal of cobalt. The cobalt crystal was in a form of a disc of diam. 3 mms. and thickness 0.2 mms with the hexagonal axis parallel to the plane of the disc. At room temperature

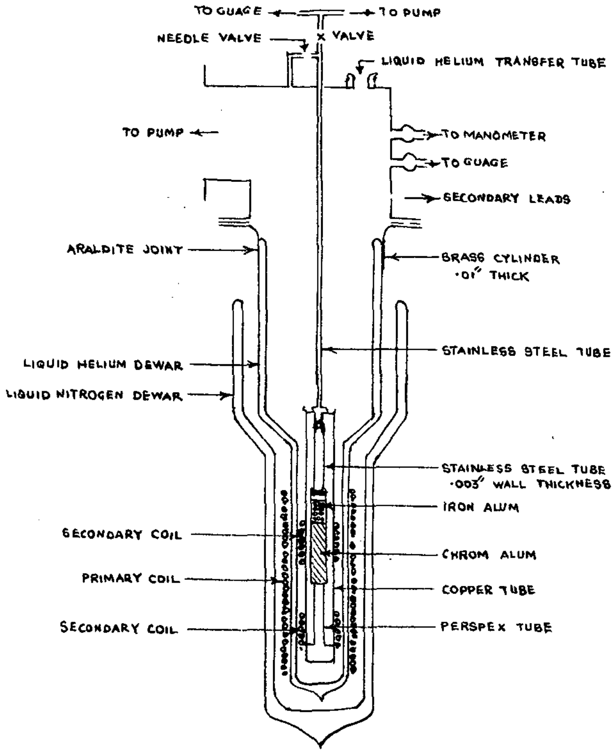
TO GUAGE
TO PUMP
NEEDLE VALVE
VALVE
LIQUID HELIUM TRANSFER TUBE
TO PUMP
TO MANOMETER
TO GUAGE
SECONDARY LEADS
ARALDITE JOINT
BRASS CYLINDER
·01" THICK
STAINLESS STEEL TUBE
LIQUID HELIUM DEWAR
LIQUID NITROGEN DEWAR
STAINLESS STEEL TUBE
·003" WALL THICKNESS
IRON ALUM
SECONDARY COIL
CHROM ALUM
PRIMARY COIL
COPPER TUBE
SECONDARY COIL
PERSPEX TUBE

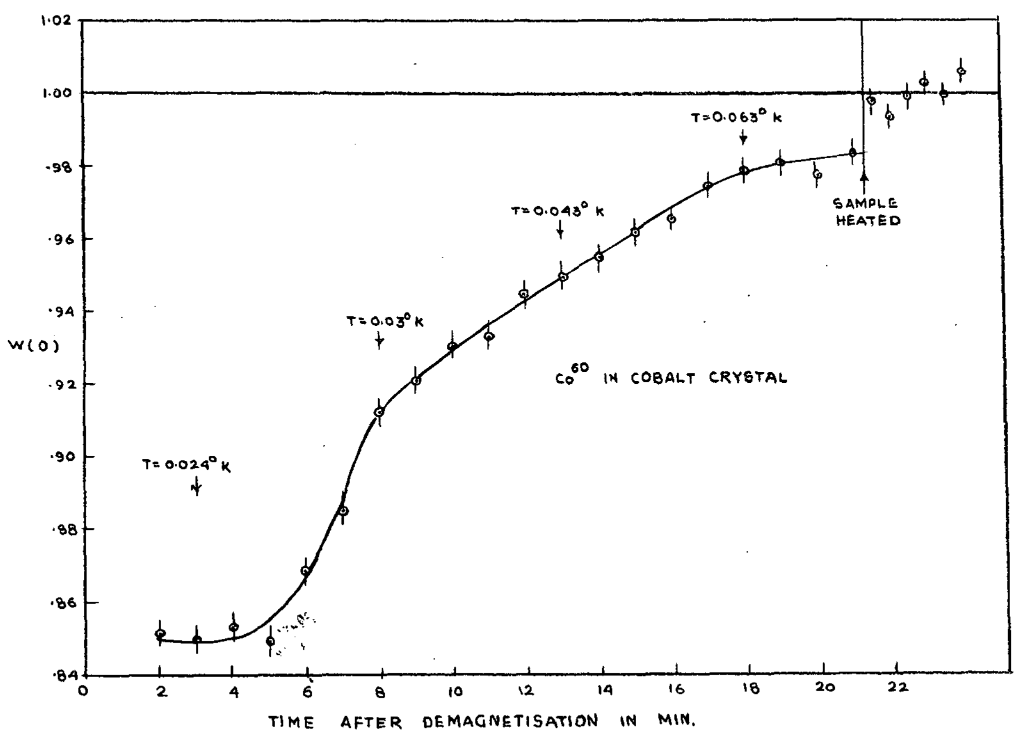
W(0)
1·02
1·00
·98
·96
·94
·92
·90
·88
·86
·84
T=0·024° K
T=0·03° K
T=0·043° K
T=0·063° K
SAMPLE
HEATED
Co60 IN COBALT CRYSTAL
0
2
4
6
8
10
12
14
16
18
20
22
TIME AFTER DEMAGNETISATION IN MIN.

it has hexagonal closed packed structure with the hexagonal axis as the only easy axis of magnetisation with the result that all the magnetic domains are aligned along this axis. Upon cooling the crystal to 0.01°k an appreciable degree of nuclear alignment along the hexagonal axis is obtained. The crystal was irradiated by thermal neutrons in a reactor to obtain Co^{60}, which was then annealed in vacuum at 380°C for about 20 days. The crystal was sandwiched between two cylinders of chrome potassium alum with thin coating of Apiezon B oil on either side of the crystal for thermal contact. After magnetic cooling Co^{60} gamma rays were counted along the orientation axis and perpendicular to the axis. The result is shown in Fig.2. About 15% change in counting rate along the axis is obtained at the lowest temperature. More detailed measurements at three different angles are in progress. It is expected to clarify the large discrepancy between the results of Grace et al (1) and Daniels et al. (2).

Alignment of other nuclei such as Co^{57} and Co^{58} in single crystal of cobalt will be undertaken soon.

REFERENCES

1. M.A. Grace, C.E. Johnson, N. Kurti, R.G. Scurlok and R.T. Taylor, Philos. Mag., 4, 948 (1959).

2. J.M. Daniels and M.A.R. Leblanc, Can. J. Phys., 37, 1321 (1959).

BETA GAMMA DIRECTIONAL CORRELATIONS IN Tm^{170}

W. V. Subba Rao & Swami Jnanananda
Laboratories For Nuclear Research, Andhra University, Waltair

The anisotropy A as a function of energy is measured in the energy region 227.5 KeV - 747 .5 KeV of 883 KeV -84 KeV beta gamma cascade in Tm^{170}. The correlation coefficient (W) is obtained. The analysis is carried out to test the validity of various approximations and to get the values of nuclear matrix parameters following the procedure suggested by Dulaney et al. The absolute values of the matrix elements are also calculated.

DISCUSSIONS

R.M. Steffen: I am afraid that the analysis used here which is based on Kotani's formalism is not good enough for such a largeZ. The exact wave-functions of Rose and Bhalla should be used to extract meaningful results?

W.V. Subba Rao: Dulaney himself has tried this sort of analysis for Tm^{170} to extract the parameters. However, being more refined and I am naturally interested to adopt the wavefunctions given by Rose and Bhalla to conduct further analysis.

R.M. Steffen: What sources have been used? The attenuation of the correlation due to the quadrupole coupling in the 2^+ state should be considered.

W.V. Subba Rao: Liquid source evaporated to dryness on a mylor films is used. The attenuation of the correlation function due to the quadrupole coupling in the 2^+ state is under consideration. But in the present analysis it has not been accounted for.

BETA-GAMMA DIRECTIONAL CORRELATION IN Nd^{147}

V. Sehagiri Rao, And V. Lakshminarayana
The Laboratories for Nuclear Physics
Andhra University, Waltair

The isotope Nd^{147} decays to Pm^{147} through various beta transitions of which the most intense transitions are of end-point energies 790 KeV and 350 KeV feeding respectively the 91 KeV and 531 KeV levels of Pm^{147}. Several investigations were carried out to infer the characteristics of this radiations. In a recent investigation Sharma et al. (1) found that the shape of the beta spectrum with the end point of 350 KeV was statistical while that of the transition with 790 KeV as end point deviated from the statistical shape. Both of these transitions are first forbidden ($5/2^-$ to $5/2^+$). Assuming that $\lambda = 0$ rank tensor matrix elements contribute to the transition and neglecting the contributions of other ranks (λ=1 and 2), they obtained ratios of matrix element parameters from their observed shape factor $C(W) = K(1 - 0.23W)$ or $C(W) = - K(1 + 0.2W - \frac{20}{W})$ for the beta transition feeding the 91 KeV level. They concluded that, on this assumption, the beta-gamma directional correlation should be isotropic. Both of the beta transitions being of the type $5/2^- (\beta) - 5/2^+ (\gamma)$ it is also interesting to study beta-gamma directional correlations from the view-point of obtaining information on the structure of these states. However, the analysis will be complicated owing to the occurance of 6 matrix elements in these $\Delta 1 = 0$ beta transitions. Integral and differential beta-gamma correlations are therefore conducted with these transitions of the type

$$5/2^- (\beta) - 5/2^+ (\gamma) - 7/2^+$$

The experimental arrangement as well as the experimental procedure are similar to those of Subba Rao et al. (2). The isotope is obtained from AEET as Neodymium Chloride in dilute HCl solution with a specific activity of 170 mc/gm. A thin source is prepared by depositing a few drops of on a Mylar film of thickness 600 micrograms/cm^2.

RESULTS

1) <u>350 KeV beta- 531 KeV gamma</u>: The photopeak of the 531 KeV gamma is accepted in a 10% channel and anisotropy is measured with the output of the beta detector in the region of energy 150 KeV to 350 KeV divided into 10 parts in a 10-channel analyzer. The observedanisotropy is quite small and the results could be taken to indicate isotropic distribution. Thus the beta-gamma directional isotropy together with the statistical spectrum shape (1), a log ft value of 7.0 for the transition, a ξ value of 13.3 and Z = 60 can be taken as an indication of the validity of ξ - approximation for this transition.

2) <u>790 KeV beta-91 KeV gamma:</u> The integral correlation experiment has been conducted by accepting betas above 400 KeV in a single channel analyzer and the photopeak of 91 KeV gamma in a 12% window of the gamma channel. After the usual corrections, the beta-gamma correlation function is represented as:

$$W(\theta) = 1 + (0.038 \pm 0.005)\ P_2 \cos\theta + (0.005 \pm 0.008)\ P_4 \cos\theta$$

which shows $A_4 \simeq 0$.

For differential correlation studies the portion of the beta spectrum between 400 and 750 KeV is accepted in a 10-channel analyzer. The corrected values of correlation coefficients had indicated a finite anisotropy ($\approx$ 7%). A plot of the modified correlation coefficient as a function of energy is shown in Fig. 1. It can be seen from the figure

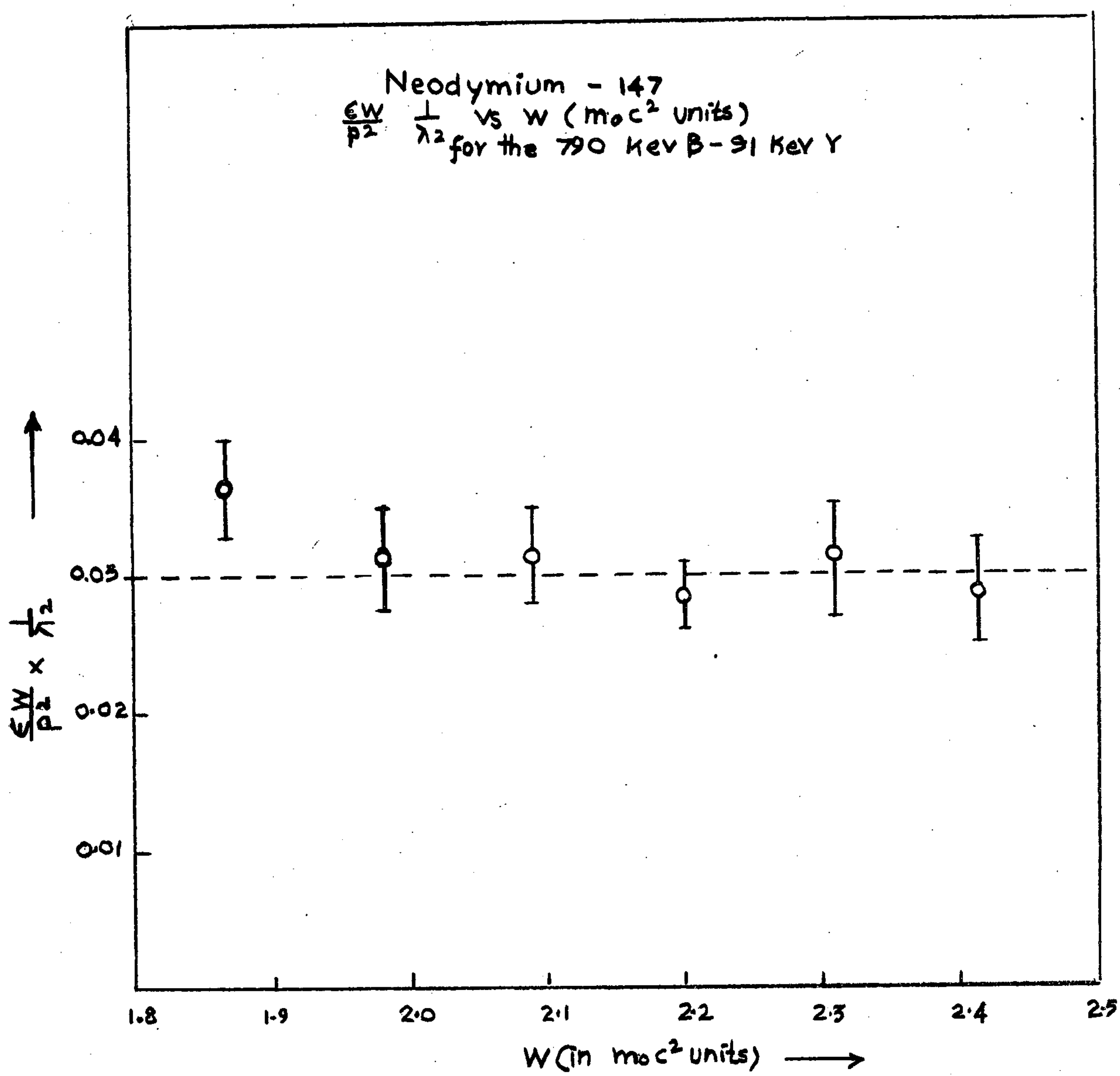
Neodymium - 147
$\frac{\epsilon W}{p^2} \frac{1}{\lambda_2}$ vs W (m_0c^2 units)
for the 790 Kev β - 91 Kev γ
0.04
0.03
0.02
0.01
$\frac{\epsilon W}{p^2} \times \frac{1}{\lambda_2}$
1.8
1.9
2.0
2.1
2.2
2.3
2.4
2.5
W (in m_0c^2 units)

that the modified correlation coefficient is approximately independent of energy. This plot is based on a normalized value of C (W) = 1. (The anisotropy in this case, however, is finite and in fact should be larger than the values observed in as much as no correction for the attenuation due to a life-time of 2 nanoseconds of the 91 KeV state is mode). The anisotropy observed is of the order of $1/\xi$. This fact together with the log ft value, 7.4; ξ in relation to W and Z can be taken to indicate the validity of ξ approximation in this case also. However, the observed deviation of the spectrum shape from statistical nature cannot be reconciled with this conclusion. It may therefore be possible that the contributions of λ = 1 and 2 tensor rank matrix elements be non-zero. However they may not be so large as to justify the applicability of the modified B_{ij} approximation. To show that this is the case the ratios of spectrum shape factors at energies 1.74 and 2.09 and 2.09 and 2.42 are obtained from the experimental shape formula

$$C\ (W) = K\ (1 - 0.23\ W)$$

and the corresponding factors under modified B_{ij} approximation

$$C(W) = V^2 + Y^2 + 1/12 \left[(W_o - W)^2 + \lambda_1 (W^2 - 1) \right]$$

in Kotani's notation (3).

On equating the corresponding ratios the following equations are obtained:

$$0.156V^2 + 156Y^2 + 0.88 = 0 \text{ and } 0.169\ V^2 + 0.169Y^2 + 0.152 = 0.$$

It is therefore not possible to obtain conics in either case and hence no solution can be obtained for V and Y. This case therefore cannot be fitted under any of the extreme cases in which the evaluation of the matrix elements is possible. The only possible way of obtaining information on the matrix elements is to attempt solution on a computer with several observables.

Unfortunately not many observables are available for this transition. Beta-Gamma circular polarization studies have not been made, probably due to the low energies of the gamma transitions. Results on the orientation experiment are however available. Attempts are being made to write equations for a computer programme utilising the available data.

REFERENCES

1. R.P. Sharma, S.H. Devare and B. Saraf, Phys. Rev., 125, 2071 (1962).
2. W.V. Subba Rao and Swami Jnanananda, Nuclear Physics Symposium Calcutta (1965).
3. T. Kotani, Physics. Rev., 114, 795 (1959).

GAMMA-GAMMA DIRECTIONAL CORRELATION IN Te^{123}

S.L. Gupta, M. M. Bajaj and N.K. Saha
Department of Physics and Astrophysics
University of Delhi
Delhi

INTRODUCTION

The long lived (104 days) Te^{123m} decays to the ground state in a simple two step 89KeV - 159 KeV gamma-gamma cascade. Earlier investigations(1-10) reveal an M4 character of the 89 KeV transition and a predominantly M1 for the 159 KeV with a small E2 admixture. Though there is a general agreement on the principal features of both the transitions, some discrepancy still exists about the E2 transition lifetime of the 159 KeV radiation. The reason is that the E2/M1 ratio obtained from the direct measurement of τ (E2) by Coulomb excitation (7) differs markedly from that obtained from the electron gamma correlation (8) and the L subshell ratios (11).

We considered it therefore necessary to make an independent measurement of the E2/M1 ratio by carrying out gamma-gamma directional correlation of the 89 KeV- 159 KeV cascade, which has not been attempted so far, perhaps due to the high internal conversion of the 89 KeV transition.

EXPERIMENTAL PROCEDURE AND MEASUREMENTS

All measurements were carried out with a conventional slow-fast coincidence arrangement with an effective resolving time of $\sim$ 30 ns. Activity was produced by the pile bombardment of enriched Te^{122} (94.8%) at ORNL.

The gamma-ray spectrum of Te^{123} is shown in Fig. 1. and the spectrum in coincidence with the 159 KeV photopeak is shown in Fig. 2. The

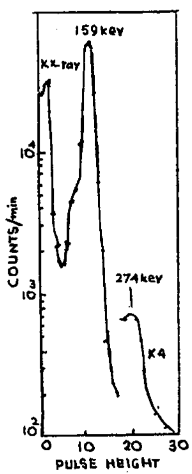

Fig. 1.

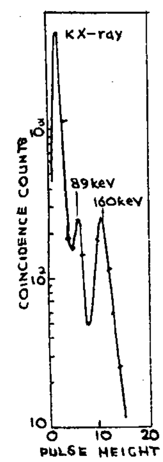

Fig. 2

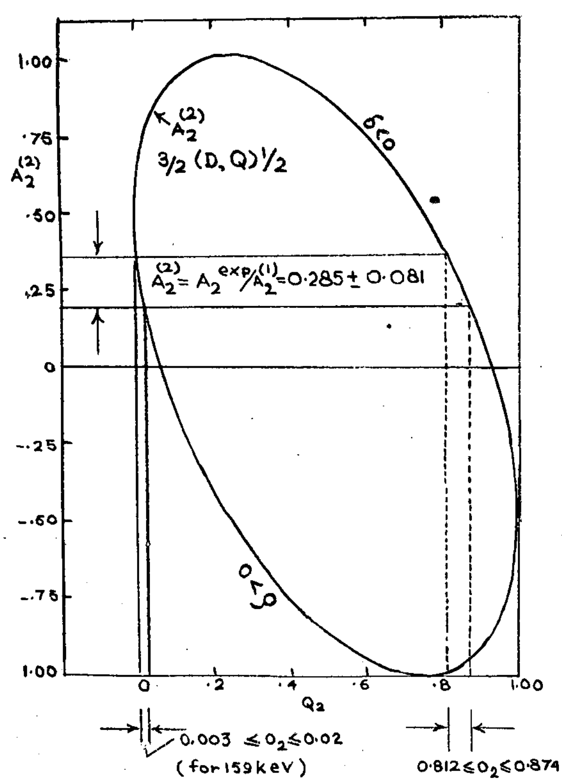

fig. 3

coincidence spectrum clearly establishes the existence of the 89 KeV gamma line, despite its very weak intensity ($\sim$0.1% of the 159 KeV gamma transition). The unknown peak at 160 KeV due to some slight impurity contributes $\sim$4% to the 89 KeV- 159 KeV cascade. The interference is found to be angle dependent and is corrected for.

RESULTS

After allowing for the 4% interference, the solid angle corrected angular correlation function for the 89 KeV- 159 KeV cascade was found to be

$$W(\theta) = 1 - (0.088 \pm 0.025)\, P_2(\cos\theta), \qquad (1)$$

whereas A_2 (theo.) = -0.154 for a pure 11/2(M4) 3/2(M1)1/2 cascade. Analysis of eq. (1) in terms of 11/2(M4) 3/2(D,Q) 1/2 spin sequence (fig.3) results in the M1 multipolarity for the 159 KeV transition with a $Q_2 = 0.011 \pm 0.008$.

DISCUSSION

For the $d_{3/2} \rightarrow s_{\frac{1}{2}}$ neutron transition in Te^{123}, the τ (E2) values and the $\tau(E2)_{s.p}/\tau(E2)_{exp.}$ enhancement factors calculated from different independent measurements (7,8,11) and also from the present investigations are summarised in Table I.

TABLE I

Summary of the results obtained for the 159 KeV transition

Method	E2/M1 $= \delta^2$	$\tau_{exp}(M1)/\tau_{s.p}(M1)$ M1 retardation	$\tau(E_2)_{Exp.}$ x 10^{-9} sec	$\tau(E_2)_{s.p}/\tau(E_2)_{exp.}$ = E2 enhancement
(K $\bar{e}$) (γ) (θ)	(8) 0.013 ± 0.001	41	25.34	8.9
Present work (γ)(γ) (θ)	0.011 ± 0.008	41	29.89	7.2
$L_1/L_{2,3}$ ratios	(11) 0.0067 ± 0.0011	41	48.87	4.5
Coulomb excitation	(7) $\sim$0.0037	41	87.20	2.5

It is clear that the E2 speed is practically the same from the electron-gamma and gamma-gamma correlation measurements, and quite different from Coulomb excitation. The attenuation of the A_2 coefficient in correlation measurements is, however, not possible in view of the short halflife (0.19ns) of the 159 KeV excited state. In the light of this difficulty it would be worthwhile to remeasure Coulomb excitation data to check up the degree of E2 enhancement of the 159 KeV transition. Some E2 enhancement of the $d_{3/2} \rightarrow s_{\frac{1}{2}}$ transition is expected on the ground of polarisation of the proton closed shell by the odd neutron-interaction. A similar mechanism is known to exist in the deserved enhancement of E2 transition in the low lying excited states of Pl^{207}.

As regards M1 retardation, there is no ambiguity at all and all the four methods yield identical results.

REFERENCES

1. S.D. Drell, Phys. Rev 75, 132 (1949).
2. R.D. Hill, Phys. Rev. 76,333(1949).
3. R.Katz, R.D. Hill, M. Goldhaber, Phys. Rev. 78, 9 1950).
4. F.K. McGowan, (a) Phys. Rev. 85, 142 (1952);(b)Phys.Rev. 93, 163 (1954).
5. J.W. Mihelich, Phys. Rev. 87, 646 (1952).
6. R.L. Graham, R.E. Bell, Can.J. Phys. 31, 377 (1963).
7. L.W. Fagg, Phys. Rev. 100, 1299 (1955).
8. N. Goldberg and S. Frankel, Phys. Rev. 100, 1350 (1955).
9. N. Goldberg, Bull. Am. Phys. Soc. 1, No.4 204 R7. (1956).
10. M. Schmorak, A.C. Li, and A. Schwarzschild, Phys. Rev. 130, 727 (1963).
11. Y.Y. Chu, P.C. Kistner, A.C. Li, S. Monaro and M.L. Perlman, Physics. Rev. 133, B1361 (1964).

GAMMA-GAMMA DIRECTIONAL CORRELATIONS IN Dy^{160}

S. L. Gupta and N.K. Saha
Department of Physics and Astrophysics
University of Delhi
Delhi

INTRODUCTION

The level structure of Dy^{160} following the beta-decay of Tb^{160} has been investigated by many authors (1-9) and seems to be well established. There are however, some uncertainties which still appear to exist for example in regard to the angular correlation of the relatively weak 215 KeV -960 KeV cascade which has been only recently investigated by Michaelis (8), and the multipole character of the strong 877 KeV transition. The first is rendered difficult by two interfering $\gamma-\gamma$ cascades. The angular correlation measurements in the case of three cascades, namely 215KeV- 960 KeV,298 KeV-964 KeV and 298 KeV - 877 KeV were therefore considered necessary in order to re-examine the results of other authors(2,6,7,8). Particular care has been taken in the present work to estimate the Compton contribution of the latter two cascades to the former as best as possible.

All measurements were carried out using a conventional fast-slow coincidence circuit with an effective resolving time of 30 ns. The gamma-ray spectrum is shown in fig.1 and the high energy coincidence spectra of 215 KeV and 298 KeV in gate are shown in figs. 2(a) and (b). These spectra were used to find out the true pulse height distribution in order to interprete the angular correlation data.

RESULTS

The solid angle corrected correlation function for the cascade 215 KeV-960 KeV was found to be

$$W(\theta) = 1 + (0.44 \pm 0.012)\, P_2(\cos\theta) + (0.003 \pm 0.020)\, P_4(\cos\theta) \qquad (1)$$

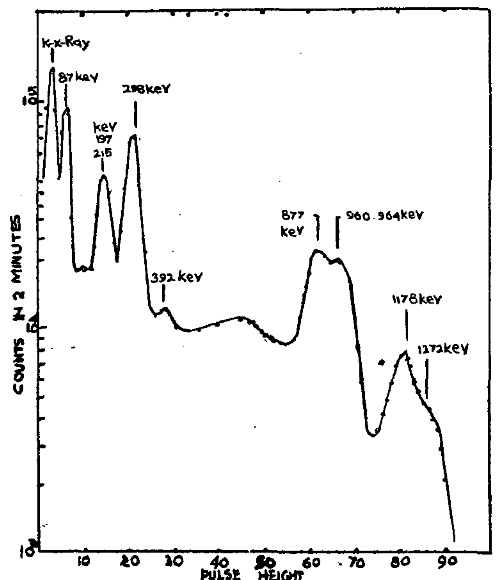

FIG1

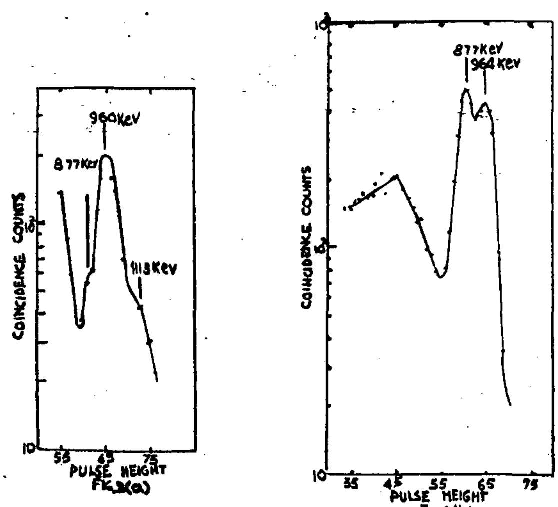

FIG.2(a)

FIG.2(b)

This has still to be corrected for $\sim$ 24% Compton contribution from the 298 KeV - 964 KeV cascade and $\sim$3% from the 298 KeV -877 KeV cascade as can be computed from the singles and the coincidence spectra. The interfering coincidences follow anisotropic distribution of their respective cascades and are corrected for. An isotropic interference of (25$\pm$ 5)% suggested by Michaelis (8) due to pile-up effects* seems to be absent in our case.

The angular correlation function thus corrected anisotropically becomes

$$W'(\theta) = 1 - (0.01 \pm 0.02)\ P_2\ (\cos\theta) \tag{2}$$

The change in the sign of A_2 with a relatively large error is quite obvious in the light of the large percentage, of interfering coincidences mainly from the 298 KeV - 964 KeV cascade which shows strong positive anisotropy ($\sim$ 40%). This interference becomes all the more important as the 215 KeV - 960 KeV cascade is relatively weak in comparison with its neighbouring cascades.

Analysis of eq. (2) in terms of a 2 (D,Q) 3 (D,Q) 2 spin sequence for the 215 KeV- 960 KeV cascade was done graphically. With $Q_1 = 0$ for 215 KeV transition (taking pure E1) the analysis gives a quadrupole content of $Q_2 = 0.05$ or $Q_2 = 0.995 \pm 0.005$, and with $Q_1 \leqslant 0.015$ (from ICC data), it gives $Q_2 \leqslant 0.04$ or $Q_2 = 0.991 \pm 0.006$. The lower value of $Q_2 \leqslant 0.05$ is ruled out on the basis of other supplementary data (4,5,8). The 960 KeV transition, therefore, turns out to be almost pure E2 with a maximum M1 admixture of $\leqslant 0.9\%$. This result is also supported by A_2 (theoretical) $= -0.042$ for a pure 2(E1) 3(E2) 2 cascade against the A_2 (experimental) $= -0.01 \pm 0.02$, though within the large experimental error.

---

* W. Michaelis - Private communication.

The true angular correlation functions for the cascades 298 KeV 964 KeV and 298 KeV - 877 KeV, after taking into account their mutual interference of (14 $\pm$ 5)% become

$$W(\theta) = 1 + (0.245 \pm 0.043)\ P_2\ (\cos\theta) + 0.014 \pm 0.067)\ P_4(\cos\theta) \qquad (3)$$

$$W(\theta) = 1 - (0.124 \pm 0.022)\ P_2\ (\mathrm{cls}\ \theta) + (0.14 \pm 0.022)\ P_4(\cos\theta) \qquad (4)$$

Eq. (3) when analysed in terms of 2(D,Q) 2(Q)0 spin sequence for the 298 KeV - 964 KeV cascade shows that 298 KeV transition is predominantly E1 with a maximum of 0.5% of M2. The graphical analysis of eq.(4) in terms of 2(D,Q) 2 (D.Q) 2 spin sequence for the 298 KeV-877 KeV cascade results in the E2 multipolarity of the 877 KeV transition having M1 admixture of only (4.5 $\pm$ 4.2%). These conclusions are in excellent agreement with the results of other authors (3-6,8).

DISCUSSIONS

A close agreement between α_K (expt.) (4,5) and α_K(E2) $_{\mathrm{theo.}}$ for the 960 KeV transition does not permit any M1 or M2 admixture within the accuracy of the measurements. If however, there is any small M1 admixture in the 960 KeV transition, as ($\bar{e} - \gamma$) coincidence and direct γ -ray intensity measurements (1,3,4,5,8,9) seem to suggest, it will be very difficult to determine it precisely from the angular correlation measurements in presence of the large interference from the strong neighbouring cascades.

REFERENCES

1. O. Nathan, Nuclear Physics, 4, 125 (1957).

2. S. Ofer, Nuclear Physics. 5, 331 (1958).

3. G. Backstrom, J. Lindskog, O. Bergman, E. Bashandy and A Backlin, Arkiv Fysik 15, (1959).

4. G.T. Ewan, R.L. Graham and J.S. Geiger, Nuclear. Phys. 22, 610 (1961).

   Proc. Int. Conf. on Nuclear Structure 603 (1960).

5. M.A. Clark, Can. J. Physics 38, 262 (1960).

6. R.G. Arns, R.E. Sund and M.L. Weidenbeck, Nuclear Physics 11, 411 (1959).

7. M.V. Klimentovskaya and G. Chandra, JETP (SSSR) 38, 290 (1960).

8. W. Michaelis, Nuclear Physics 44, 78 (1963).

9. E. P. Grigore'v, A.V. Zolotavin and B. Kratsik, Izv. Akad. Nauk. SSSR, Ser. Fiz. 23, 191 (1959).

DISCUSSIONS

E. Kondaiah: What is the error in α_k^{E2} exp. ? If the error is $\pm$ 10% , it ties up with the probability of 10% M1 mixture in E2 for the 960 KeV γ - ray. In that case it is not purely E2.

S.L. Gupta: Large errors in relative intensity measurements and α_K expt. may be taken either way in the interpretation of the 960 KeV multipolarity.

STRIPPING REACTION STUDIES ON THALLIUM ISOTOPES

Paresh Mukherjee

Saha Institute of Nuclear Physics
Calcutta

(d,p) and (d,t) reactions studies are made with isotopically enriched Tl^{205} (99%) and Tl^{203} (92.6%) oxide targets, using the 15 MeV deuteron beam of the University of Pittsburgh Cyclotron. Excitation spectra, up to about 5 MeV, are obtained for the Tl^{206}, Tl^{204} and Tl^{202} nuclei. From the (d,p) and (d, t) cross section the ground state wave function of Tl^{205} is found to be 74% $(S\frac{1}{3}-)_p$ — 1 $(P\frac{1}{2})_n^{-2}$. Experimental level schemes of Tl^{206}, Tl^{204} and Tl^{202p} are compared with the shell model predictions, and evidences for considerable configuration mixing are obtained

STUDY OF Cl^{37} (p,n) Ar^{37} REACTION MECHANISM

K.V.K. Iyengar, S.K. Gupta, B.Lal and E.Kondaiah
Tata Institute of Fundamental Research, Bombay-5

INTRODUCTION

(p, n) reactions in light, intermediate weight and heavy nuclei have been studied by several investigators (1,2,3,4,5,6) with a view to find out the mechanism responsible for the interaction. The angular and energy distribution of neutron emitted from light nuclei are characteristic of direct interaction whereas those emitted from intermediate and heavy nuclei show essentially compound nucleus features. Very little information exists on the interaction mechanism responsible for (p, n) reactions in nuclei in the mass region A = 20 to 40. It was for this reason the study of the angular distribution of neutrons to ground state of Ar^{37} in Cl^{37} (p,n) Ar^{37} reaction was undertaken.

EXPERIMENTAL RESULTS AND CONCLUSIONS

The excitation function for the production of the 1.42 MeV gamma rays in the $Cl^{37}(p,n'\gamma)Ar^{37*}$ was obtained in the proton energy region 3.2 to 4.8 MeV at intervals of every 0.1 MeV. A KCl target of about 150 KeV thick target was used for the measurement and a NaI 2" x 2" crystal mounted on a R.C.A. 6810 was used for detection of gammas. The resolution of the gamma detector was 9% for Cs^{137} gamma rays.

The 1.42 MeV gamma ray yield has been compared in Fig.1 with the yield of neutrons to 1.42 MeV level obtained by Barnard et al.

The yield of the 1.42 MeV gamma ray shows two broad peaks instead of a smooth variation suggesting of levels in certain regions of

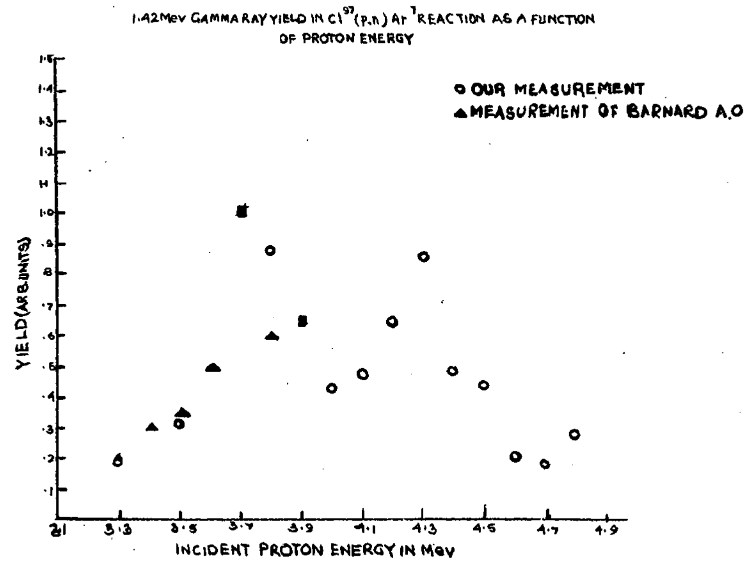
1.42Mev GAMMA RAY YIELD IN Cl37(p,n) Ar37 REACTION AS A FUNCTION OF PROTON ENERGY
OUR MEASUREMENT
MEASUREMENT OF BARNARD A.O
YIELD (ARB.UNITS)
INCIDENT PROTON ENERGY IN Mev

Fig. 1.

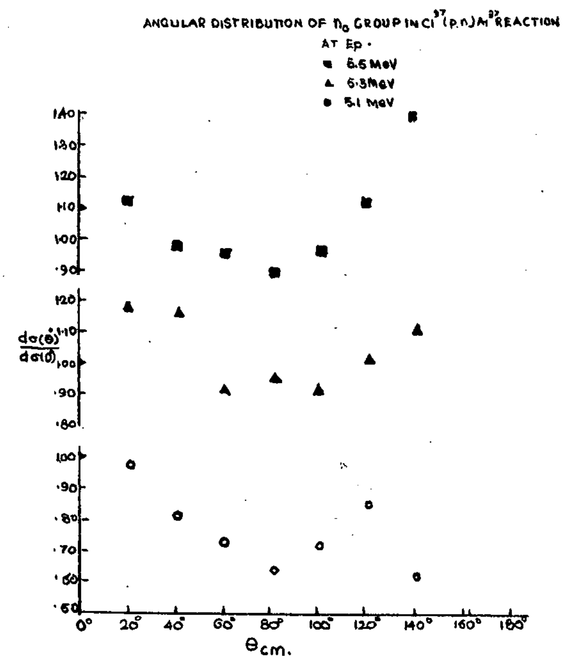
ANGULAR DISTRIBUTION OF n0 GROUP IN Cl37(p,n)Ar37 REACTION
AT Ep -
5.5 MeV
5.3 MeV
5.1 MeV
dσ(θ)/dω(θ)
θcm.

Fig. 2.

excitation of the compound nucleus.

The angular distributions of the neutron group to the ground state of Ar^{37} were studied using a stilbene crystal mounted on an RCA 6810A type photomultiplier. Pulse shape discrimination was employed in order to reject gamma pulses and linear discrimination to limite measurements to neutron group leading to the ground state. NaCl targets of thickness 150 KeV at 5 MeV proton energy evaporated on to tantalum backings were used as the chlorine targets. Neutrons are primarily due only to $Cl^{37}(p,n)Ar^{37}$ reaction as the Q value for $Na^{23}(p,n)\ Mg^{23}$ is -4.84 MeV and $Cl^{35}(p,n)Ar^{35}$ is - 6.76 MeV whereas $Cl^{37}(p,n)Ar^{37}$ is-1.598 MeV. The measured intensity of recoil protons were corrected for the variation of recoil proton pulse height with neutron energy as a function of the (p,n) reaction angle and also for the variation of efficiency of the stilbene detector with neutron energy. The corrected intensity at each angle was the normalized with respect to monitor counts. A thin plastic scintillator of about 2 mms.thickness and 2.5 cms diameter mounted on an RCA 6342A was used for monitoring neutrons. The measured angular distributions at the three proton energies 5.1, 5.3 and 5.5 MeV are presented in Fig.2.

The angular distributions were least square fitted to a Legendre Polynomial series consisting of both odd and even order as they were asymmetric around 90°. in the c.m and the χ^2 test was employed to determine the number of terms in the series required to give the best fit to the measured distributions. It is necessary to mention that the values of χ^2 obtained for the best fit are not equal to the allowed degrees of freedom. The best agreement is obtained at $E_p = 5.3$ MeV.

$E_p = 5.1$ MeV

$$W(\theta) = 1 + (0.270 \pm 0.067)\, P_1(x)$$
$$- (0.131 \pm 0.128)\, P_2(x) + (0.538 \pm 0.170)\, P_3(x)$$
$$- (0.367 \pm 0.185)\, P_4(x) + (0.151 \pm 0.115)\, P_5(x)$$

$E_p = 5.3$ MeV

$$W(\theta) = 1 + (0.182 \pm 0.020)\, P_1(x)$$
$$- (0.052 \pm 0.028)\, P_2(x) + (0.339 \pm 0.035)\, P_3(x)$$
$$- (0.346 \pm 0.034)\, P_4(x) + (0.248 \pm 0.033)\, P_5(x)$$
$$- (0.324 \pm 0.022)\, P_6(x)$$

$E_p = 5.5$ MeV

$$W(\theta) = 1 + (0.222 \pm 0.025)\, P_1(x) + (0.304 \pm 0.041)\, P_2(x)$$
$$- (0.096 \pm 0.049)\, P_3(x)$$

where $x = \cos\theta$ and θ is the (p,n) reaction angle.

The large values of the odd order coefficients in the series required to give the best fit to the data indicate the excitation of mixed parity states. They further suggest the non-validity of the statistical assumption for the Ar^{38} compound nucleus at the excitation of $\sim$16 MeV reached in the present experiment. The appearance of higher order coefficients in the series indicate that some type of direct interaction may also be contributing to the measured reaction yield. The 1.42 MeV γ - ray excitation function also seems to question the continuium assumption for the compound nucleus, Ar^{38} in the excitation region covered.

REFERENCES

1. P. Dagley, W. Haeberli, J.X. Saladin and R.R. Borchers, Proc. Int. Conf. on Nuclear Structure (Kingston) 359, (1960) edited by Bromley and Vogt.

2. Hissatake, J. Phys. Soc. Japan 15, 741 (1960).

3. R.D. Albert, S.D. Bloom and N.K. Glendenning, Phys. Rev. 122, 862 (1961).

4. T.W. Bonner and R.L. Barshall, Nucl. Phys. 20, 395 (1960).

5. C.H. Holbrow and H.H. Barnard, G.S. Mani and P.D. Forsyth, Nucl. 42, 264 (1963).

6. R.D. Albert, J.D. Anderson and C. Wong, Phys. Rev. 120, 2149 (1960).

7. A.C.L. Barnard, G.S. Mani and P.D. Forsyth, Nucl. Phys. 28, 464 (1961).

8. G.S. Mani, A.C.L. Barnard, T.A. Tombrellow and D.A.A.S.N. Rao, Nucl. Physics. 28, 456 (1961).

THE (He^3,α) REACTION ON C^{13}

V.K. Deshpande, I.I.T. Kanpur
and
H.W. Fulbright, University of Rochester

The (He^3,α) reaction on C^{13} has been studied previously (1,2) for bombarding energies below 4.5 MeV. In a plane wave analysis of this data, Owen, et. al. (3) attributed the large backward peaks, observed in the angular distributions, to the presence of heavy particle stripping in addition to the presence of the normal pick up process. In the present work, data are obtained at higher energies upto 10.3 MeV. Good fits to the angular distributions are obtained in terms of the pickup process alone, in a treatment, in which distortions of plane wave are taken into account.

EXPERIMENT

The variable energy cyclotron of the University of Rochester was used to obtain the beam. The carbon target was 100μg.thick and it contained about equal amounts of C^{12} and C^{13}. Surface barrier silicon counters were used to detect the reaction products. Angular distributions of alpha particles, leading to the two lowest states of C^{12} were obtained at 8.82, 9.44 and 10.30 MeV. Data were analysed at the Oak Ridge National Laboratory, using the DWBA programme 'Julie' (4,5) written for the IBM7090 computer.

DATA AND ANALYSIS

The optical potential used for the analysis was a Saxon - Wood well, for both real and imaginary parts. The optical parameters obtained by Alford, et.al (6) in the analysis of $O^{16}(He^3,\alpha)$ reaction, in the same energy range, were used in the present analysis. These are shown

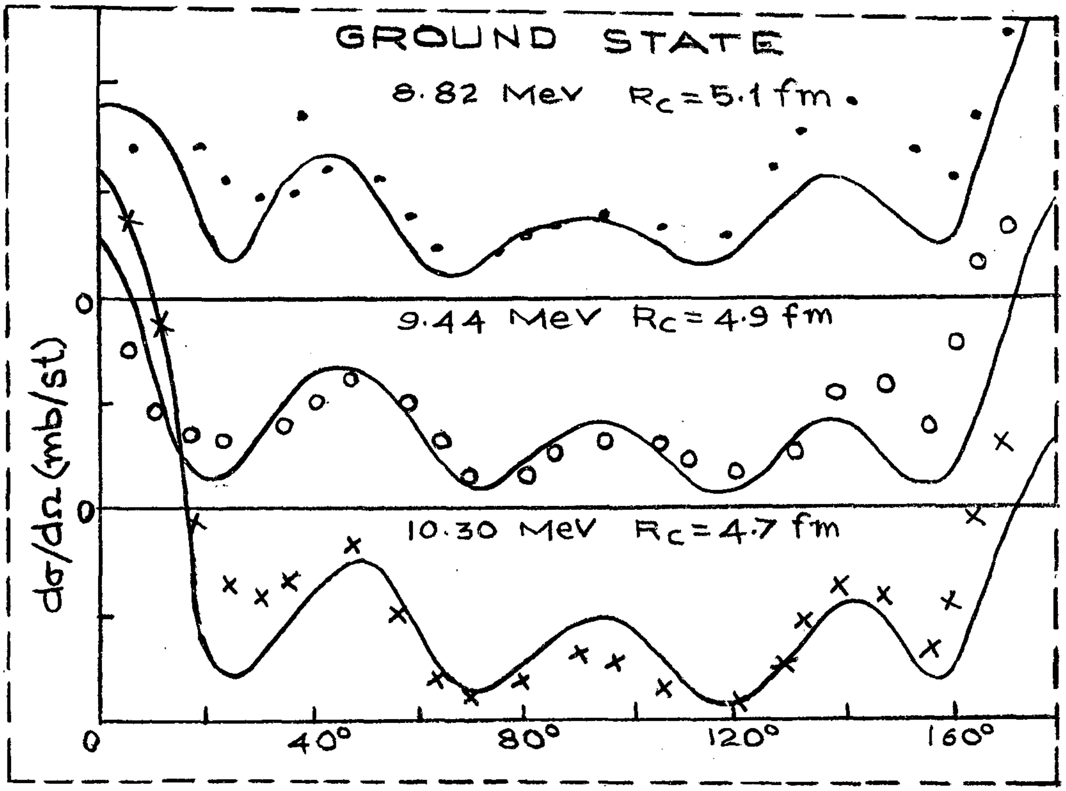
GROUND STATE
8.82 MeV Rc=5.1 fm
9.44 MeV Rc=4.9 fm
10.30 MeV Rc=4.7 fm
dσ/dΩ (mb/st)
0
0
0
40°
80°
120°
160°

FIG. 1.

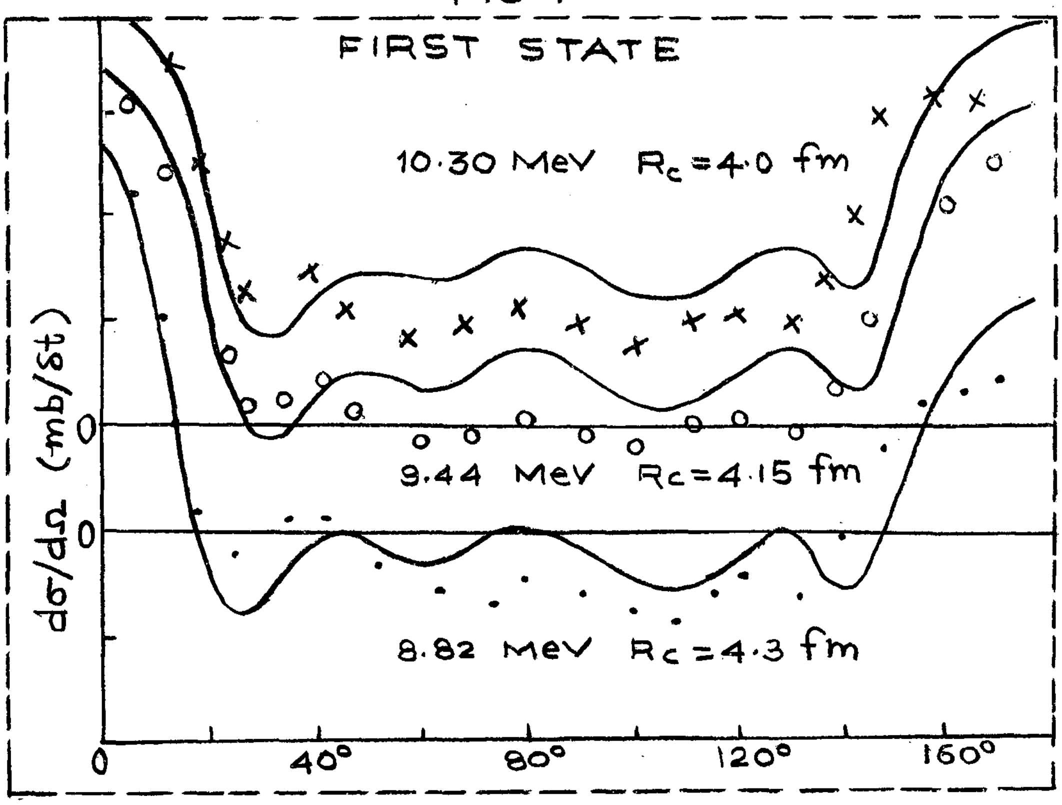
FIRST STATE
10.30 MeV Rc=4.0 fm
9.44 MeV Rc=4.15 fm
8.82 MeV Rc=4.3 fm
dσ/dΩ (mb/st)
0
0
0
40°
80°
120°
160°

FIG. 2.

in Table I. No fits could be obtained without a cut-off radius Rc. This single parameter was used as the adjustable variable of the problem.

The Ground state, $1/2^-$ 0^+ transition, involves the pick up of a $p_{1/2}$ neutron. The angular distributions and the computed fits for this case are shown in Fig.1. A slight variation in the cut-off radius with energy reproduces the observed variation in the intensity of the forward peak. Strong backward peaks are produced by the pick up mechanism alone when the plane wave approximation is dropped.

The reaction leading to the first excited state involves a $1/2^- \longrightarrow 2^+$ transition in which a $p_{3/2}$ neutron is picked up. The angular distributions and the DWBA fits obtained with the same optical parameters as those for the ground state are shown in fig.2. With the variation in only one parameter R_c, DWBA curves are found, which fairly well reproduce the general features of these angular distributions.

The Oak Ridge programme computes the transition matrix element in the zero range approximation. The absolute cross section σ in terms of the programme output σout is given by

$$\sigma = (C^2S)_{TARGET} \times (C^2S)_{PROJECTILE} \times D_o^2 \times \sigma_{OUT}$$

where C is the appropriate isopin Clebsch - Gordon coefficient, S is the spectroscopic factor and D_o is the "effective" strength of the Zero range interaction, between He^3 and the picked neutron. If the n- He^3 well is actually assumed to be of zero range, D_o is equal to $2.38 \times 10^3 \times \sqrt{B/\mu}$ where B and μ are the binding energy and the reduced mass of the neutron. Using this value of D_o and with the maximum possible values of the spectroscopic factors, the computed cross section is found to be smaller than the measured cross section by a factor of ten.

In view of the uncertainty in the strength of the effective zero range interaction, analysis was made on the basis of the ratio σ (I excited state) / σ (ground state). This ratio is independent of D_o and the spectroscopic factor of the projectile. Using the experimental values of total cross sections, we obtain a value of 1.29 for the ratio $(S^*/S)_{target}$. Calculations of Macfarlane and French (7) lead to a lower limit of 1.2 for this ratio. Their plane wave analysis of the available (p,d) and (d,t) data on C^{13} gave values less than 1. The present value of 1.29 therefore perhaps represents some improvement.

TABLE I

OPTICAL PARAMETERS

	V	W	r_o	r_c	a
IN	105	21	1.52	1.3	0.65
OUT	110	5	2.4	1.3	0.68

REFERENCES

1. H.D. Holmgren, Phys. Rev. 106 (1957) 100

2. H.D. Holmgren, E.H. Gear, R.L. Johnston and E.A. Wolicki, Phys. Rev. 106 (1957) 102.

3. G.E. Owen, L. Madansky and S. Edwards, Phys. Rev. 113 (1959) 1575

4. R.H. Bassel, R.M. Drisko and G.R. Satchler, "The Distorted-Wave Theory of Direct Nuclear Reactions", ORNL -3240.

5. G.R. Satchler, Nuclear Physics 55 (1964) 1 and private communication.

6. W.P. Alford, L. Blau and D. Cline, Private communication.

7. M.H. Macfarlane and J.B. French, Rev. Mod. Phys. 32(1960) 567.

DISCUSSIONS

S.M. Bharathi : What is the error in your measurements?.

V.K. Deshpande: The relative error was about 3%, the absolute error perhaps about 10 to 15% mainly due to uncertainty in the target thickness.

P.N. Mukherjee: Have you measured the elastic angular distribution for He^3 on C^{13}?

V.K. Deshpande: No. C^{13} targets free from C^{12} are not presently available. The parameters used are for He^3 scattering on C^{12}. This work was done by Alford et.al. at Rochester.

M.K. Mehta : You have bombarding energy from 8 to 11 MeV. What sort of resolution you need, and did the excitation curve show any variation with energy?

(b) **What was the** excitation used in selecting the energy for the angular distribution measurements?

V.K. Deshpande: The target thickness was about 100μg., the beam energy spread about 50 KeV. The energies at which angular distributions were obtained were chosen arbitrarity.

M.L. Chatterjee: You have made the cut-off approximation at 4fm. What is the upper limit of radius you have used in this radial integral?

V.K. Deshpande : 20 fm.

A STUDY OF NUCLEAR REACTIONS RESULTING FROM PROTON BOMBARDMENT OF Al^{27}

Joseph John, S.S. Kerekatte, M.K. Mehta
Nuclear Physics Division
Atomic Energy Establishment Trombay

Proton bombardment of Al^{27} with a bombarding energy above 4 MeV would amount to an excitation energy of above 15 MeV in the Al^{27} nucleus. Generally, it is expected that at energies as high as this, the level density would be so high as to make the statistical model of compound muclear reactions valid. In such a case the excitation curves would exhibit a smooth nature. At the other extreme, if the excitation energy is low enough, one would be exciting only one or a few levels at a time, and the excitation curves would exhibit the familiar phenomenon of resonances. During the last five years, a phenomena called the Ericson fluctuations has been ascertained which is exhibited by excitation curves, taken with high resolution in the so called 'Statistical' region.

The Al^{27} $(p,p'\gamma)$ experiments performed at this laboratory showed ' resonances' in the excitation curves, and the present experiment was undertaken to investigate the nature of these resonances.

Thin self supporting targets of Al^{27} were prepared by evaporating aluminium on to glass slides and by floating the aluminium film off the glass slides in water. The target thickness was measured to be 3 KeV for about 2 MeV protons. This measurement was done by observing the shift in the Li^{7} (p,n) Be^{7} threshold when the protons passed through the aluminium target before hitting the lithium target.

These targets were mounted in a cylindrical chamber designed to take solid state counters. The excitation curves were obtained by using two solid state counters simultaneously, the outputs from which were fed into a TMC 400 channel analyser, after suitable amplification. The elastically scattered protons from Al^{27}, O^{16}, C^{12} as well as the α_0, P_1, P_2, and P_3 groups from the reactions $Al^{27}(p,\alpha_0)Mg^{24}$, $Al^{27}(p,p_1)Al^{27*}$ $(p,p_2)Al^{27*}$ and $Al^{27}(p,p_3)Al^{27*}$, respectively, could be easily identified in the resulting particle spectra.

Excitation curves were evaluated for the P_0, α_0 and P_3 groups at 90° in the Lab. and the P_0 and α_0 groups at 150° in the lab, for a bombarding energy range of 4 to 5.5 MeV. The resulting curves are shown in fig. 1. The energy step was about 5 KeV. All the curves show a relatively sharp structure. In many cases, a "resonance" appears in all the channels and at both the angles. There are a number of qualitative Criteria which can be applied to determine whether these "resonances" are real resonance effects and do represent Γ/D which is small($\Gamma \sim$ 20-50 KeV, $D \sim$ 200 KeV) or they are the fluctuations which Ericson describes.

First, there is the energy correlation between various channels and angles, which should be absent for fluctuations and present for resonances. In the present work the energy correlations do exist for many 'resonances'.

If these are resonance effects, then angular distributions meassured on prominent resonances could be analysed in terms of the (J,π) values of one or more neighbouring levels in the compound nucleus, which could contribute to a single resonance. Although the actual calculations for such an analysis are quite cumbersome, they could be done with a fast digital computer. With this aim in mind, six angular distributions were measured at the six prominent resonances marked 'A' in fig.1. These angular

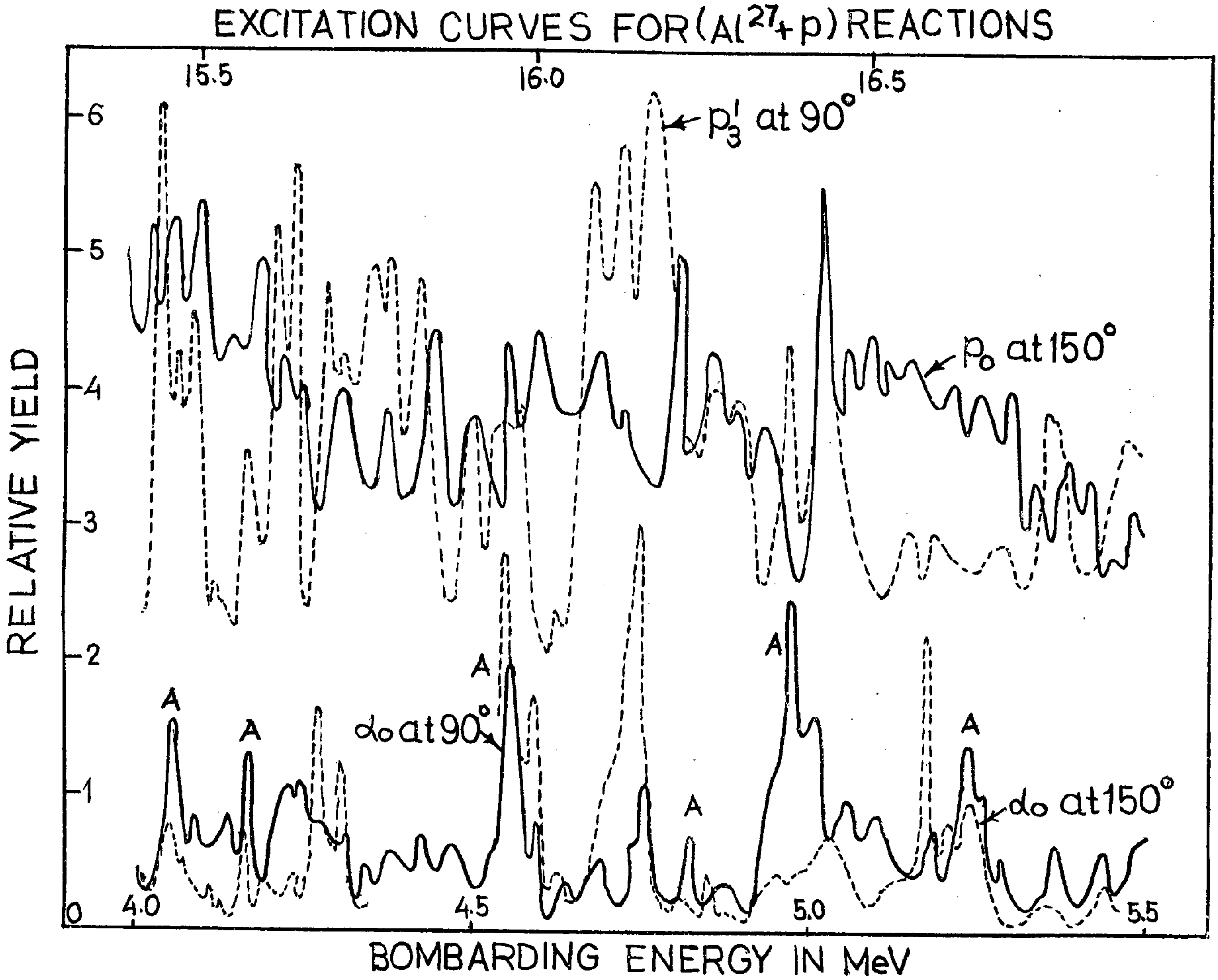
EXCITATION CURVES FOR(Al27+p) REACTIONS
15.5
16.0
16.5
6
5
4
3
2
1
0
RELATIVE YIELD
p'3 at 90°
Po at 150°
A
A
A
A
A
A
αo at 90°
αo at 150°
4.0
4.5
5.0
5.5
BOMBARDING ENERGY IN MeV

FIG·1

$Al^{27}(p,\alpha_0)$ ANGULAR DISTRIBUTIONS

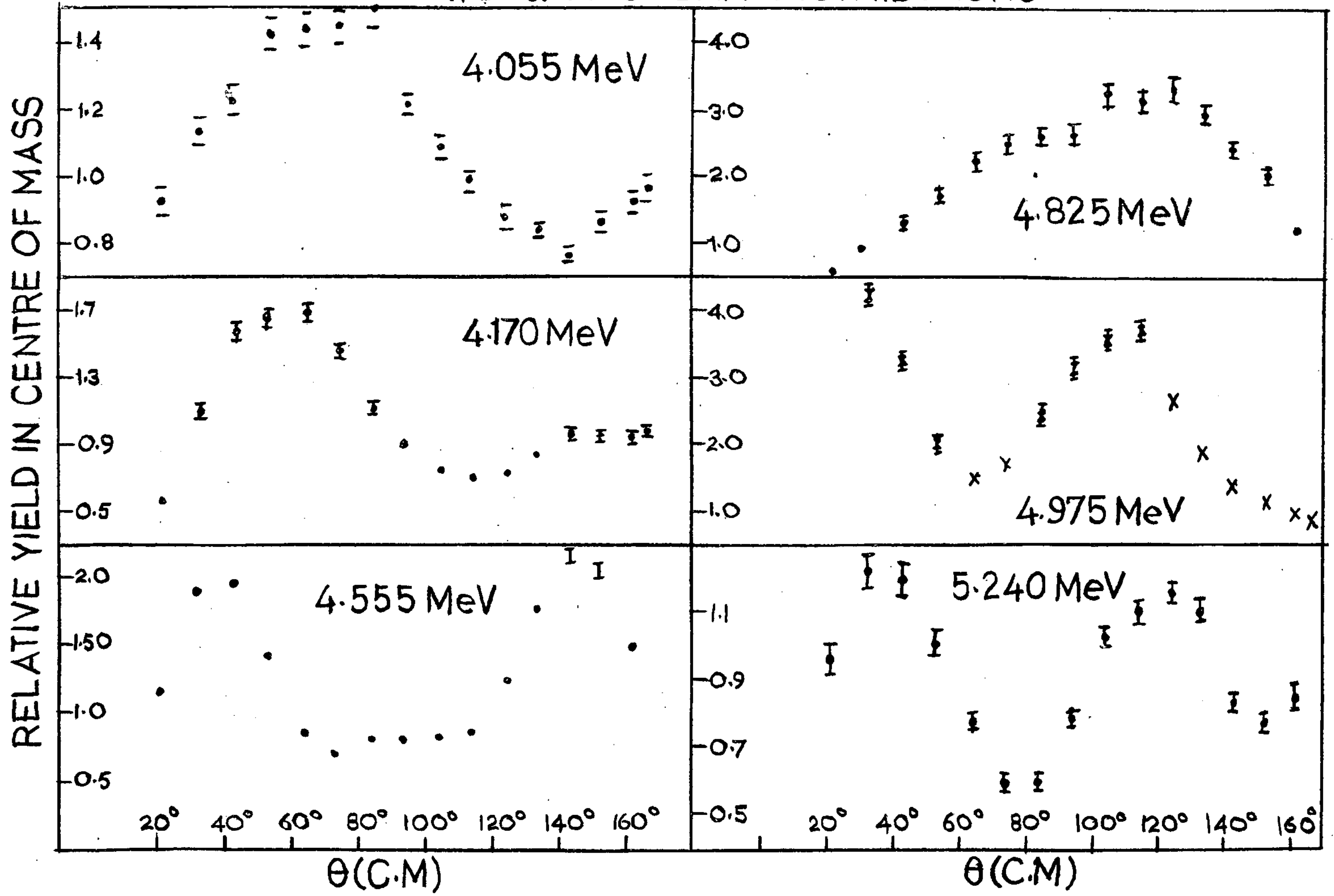

FIG·2

distributions are shown in fig. 2. The lack of symmetry about 90°, in general may imply levels of opposite parity, if these are resonances.

A proper fluctuation analysis for the excitation curves and a resonance analysis of the angular distributions have to be done before any definite conclusions can be reached, but qualitatively speaking it is possible that the data represents the "resonance" region as against the "fluctuation" region of excitation in the compound nucleus Si^{28}.

STUDY OF F^{19} (α, n) Na^{22} REACTION USING A 4 π NEUTRON COUNTER

K.K. Sekharan, M.K. Mehta and A.S. Divatia
Nuclear Physics Division
Atomic Energy Establishment Trombay

INTRODUCTION

Measurement of absolute cross sections of (α ,n) and (α, n) reactions yields valuable information. For example, the properties of the compound nucleus are studied by analysing the energy dependence of these cross sections. To interpret the reaction mechanism it is necessary to know the total reaction cros section and below the coulomb barrier the (α, n) and (p, n) cross sections form a large fraction of the total reaction cross section.

Using a 4 π counter (1) for absolute reaction cross section measurement has the advantage that the yield curve will be characteristic of the resonance levels in the compound nucleus. The levels in the residual nucleus will not contribute significantly to the resonances in the yield curve. This method was used for studying the F^{19} (α, n) Na^{22} reaction.

DESCRIPTION OF APPARATUS

Accelerated alpha particles were obtained from the 5.5 Mev Van de Graaff Accelerator at Trombay. The targets were made of spectroscopically pure CaF_2 evaporated on a thick tantalum backing. The targets were about 10 KeV thick for 3 MeV alpha particles.

A sketch of the 4 π Neutron counter is shown in Fig. 1. It consists of twelve enriched $B^{10}F_3$ counters (1" diameter x 18" long) embedded in a paraffin block 2'x2'x2' in dimensions. The counter is shielded by a 1/2" thick layer of boric powder and 80 mil thick cadmium layer to prevent scattered neutrons reaching the B^{10} F_3 counters. Six counters are mounted

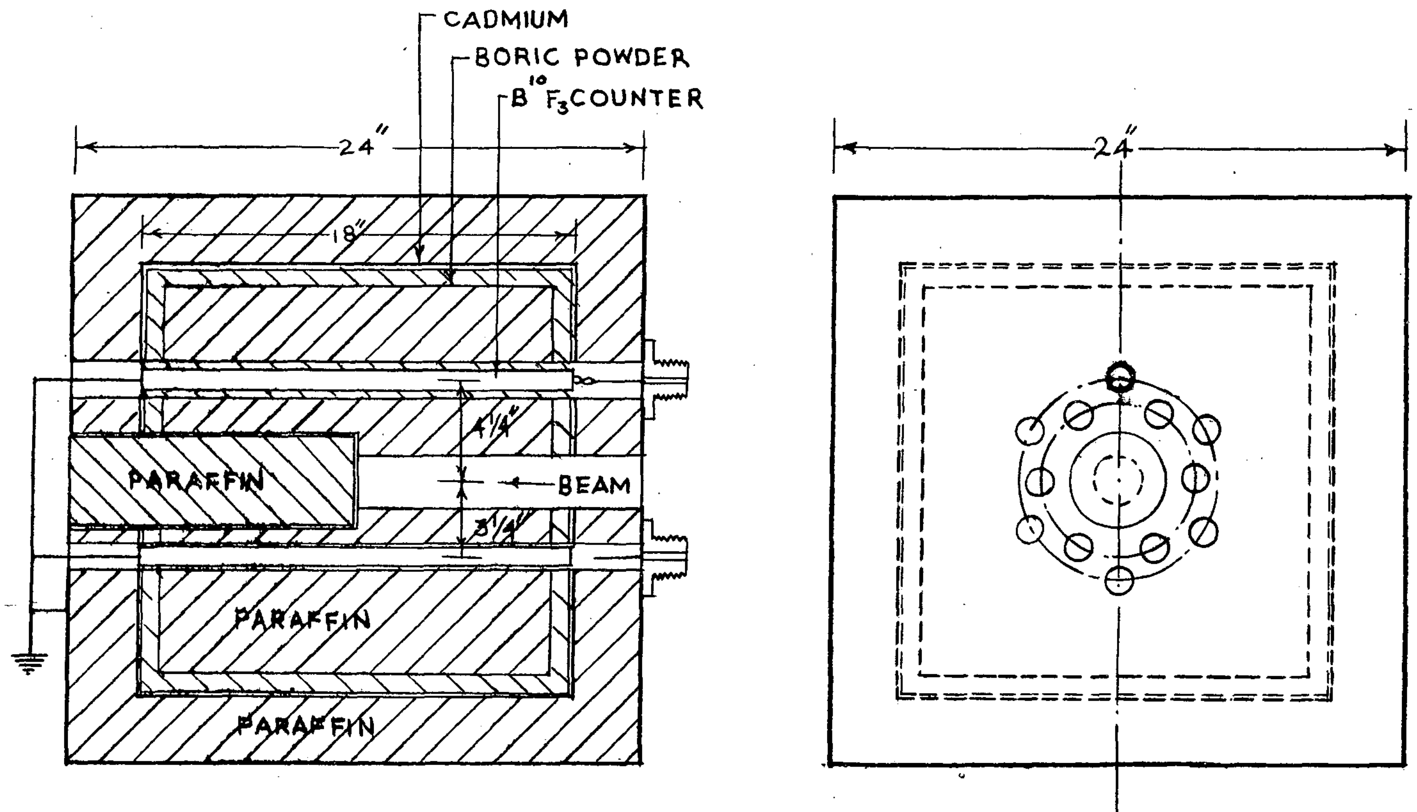

4π NEUTRON COUNTER

FIG. 1

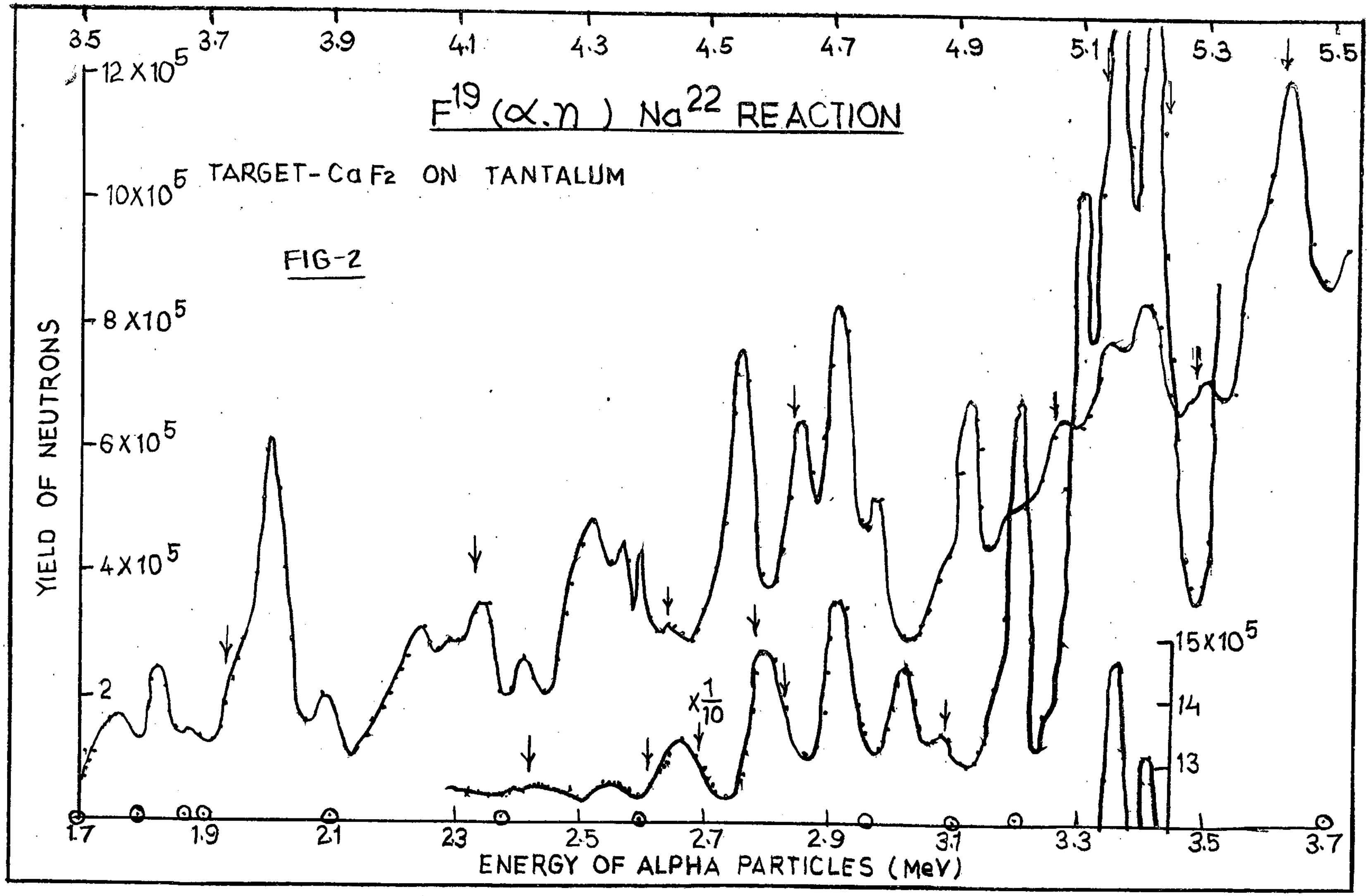

F^{19} (α, n) Na^{22} REACTION
TARGET - CaF_2 ON TANTALUM
FIG-2
YIELD OF NEUTRONS
12 X 10^5
10X10^5
8 X10^5
6X10^5
4X10^5
2
3.5
3.7
3.9
4.1
4.3
4.5
4.7
4.9
5.1
5.3
5.5
X$\frac{1}{10}$
15X10^5
14
13
1.7
1.9
2.1
2.3
2.5
2.7
2.9
3.1
3.3
3.5
3.7
ENERGY OF ALPHA PARTICLES (MeV)

201

symmetrically in a circle of $3\frac{1}{4}''$ radius and the other six in a circle of $4\frac{1}{4}''$ radius. The inner counters are connected in parallel to a conventional electronic set up and the outer counters to another identical set up and counts recorded separately.

EXPERIMENT

The excitation function of this reaction has been measured from 2.4 to 5.5 MeV and is shown in Fig. 2. Readings were taken in steps of 6 KeV in low energy region and 10 KeV in high energy region. The threshold for this reaction is about 2.36 MeV. The yield of neutrons at threshold is low and hence it was masked by the back ground neutrons from the carbon contamination on the target. Separate investigations have been made to establish that the background is due to the $C^{13}(\alpha, n)\,O^{16}$ reaction neutrons. Arrows in Fig. 2 show the positions of peaks from this reaction.

The $F^{19}(\alpha, n)\,Na^{22}$ reaction has been studied by Williamson (2) et.al. up to 3.5 MeV using a modified long counter. There is a general agreement in spacing and peaks in the two data. The fact that different types of counters were used limits the scope for complete similarity in the two sets of curves. Data has just been obtained for the determination of target thickness and absolute efficiency of the counter. The $F^{19}(\alpha, n)\,Na^{22}$ yield is being analysed to correlate it with the levels in Na^{23}.

REFERENCES

1. J.B. Marion et.al., Nucl. Instr. & Methods 8, 297 (1960).

2. R.M. Williamson et.al., Phys. Rev. 117, 1325 (1960).

A STUDY OF THE LEVELS OF Ti^{44}

M.G. Betigeri and N. Sarma
Nuclear Physics Division
Atomic Energy Establishment Trombay.

INTRODUCTION

Investigations of the nuclide Ti^{44} by nuclear reaction methods is not easy because Ti^{44} is very inaccessible. The only possible reactions that may be used are:

$Ca^{40} (\alpha, \gamma) Ti^{44}$	Q = 5.235
$Ca^{42} (He^3, n) Ti^{44}$	Q = 5.979
$Ca^{43} (He^3, 2n) Ti^{44}$	Q = -19.5
$Ca^{46} (p, t) Ti^{44}$	Q = -14.12

With presently available facilities only the first two are feasible.

We report our progress in the investigation of Ti^{44} using the reaction $Ca^{40} (\alpha, \alpha) Ca^{40}$. This method gives us the excited states of the nucleus from about 8.5 MeV to 10 MeV. The second phase of our program would be to study the gamma de-excitation of the nucleus.

APPARATUS

The scattering chamber has been described in a published paper (1). Five ORTEC surface barrier detectors of depletion depth 500 to 300 microns were mounted 15 cms away from the target. One detector was used by the accelerator operations crew to monitor the beam on target and so adjust focussing conditions. The signals from the detectors were fed through low noise preamplifier-amplifier systems to the inputs of a TMC-400 channel analyser. It was therefore possible to record spectra from four detectors simultaneously. Correction for dead time of the analyser was made in the usual manner.

The targets used were natural calcium oxide evaporated on to thin self supporting carbon films. It was estimated that the thickness of the carbon was about 40 micrograms/cm^2. It was not found necessary to use separated Ca^{40} isotope because the solid state detector is able to resolve the elastic scattered peaks from the different calcium isotopes.

The targets were found very stable and could suffer continuous bombardment of more than 1 micrompere without rupture.

RESULTS

Spectra from the detectors printed out by the analyser were plotted. Fig. 1 shows a typical spectrum. The area under the Ca^{40} peak was then measured. Similar measurements were made at intervals of 10 KeV from 3.5 MeV to 5.5 MeV. After correction for dead time, an excitation function for the elastic scattering of alpha from Ca^{40} was computed (fig.2). The results are still being analysed and the excitation function at three angles should be measured before long.

The resonance behaviour of the excitation curve indicates that analysis of this data must obviously be carried out in terms of compound nucleus theory. We use the theory of Blatt and Beidenharn (2) for the analysis. However, their final expression is for a single isolated resonance only. Here several closely spaced resonances are found, and multilevel theory involving several resonance is required. We therefore use the ability of the CDC - 3600 to tackle complex numbers and write

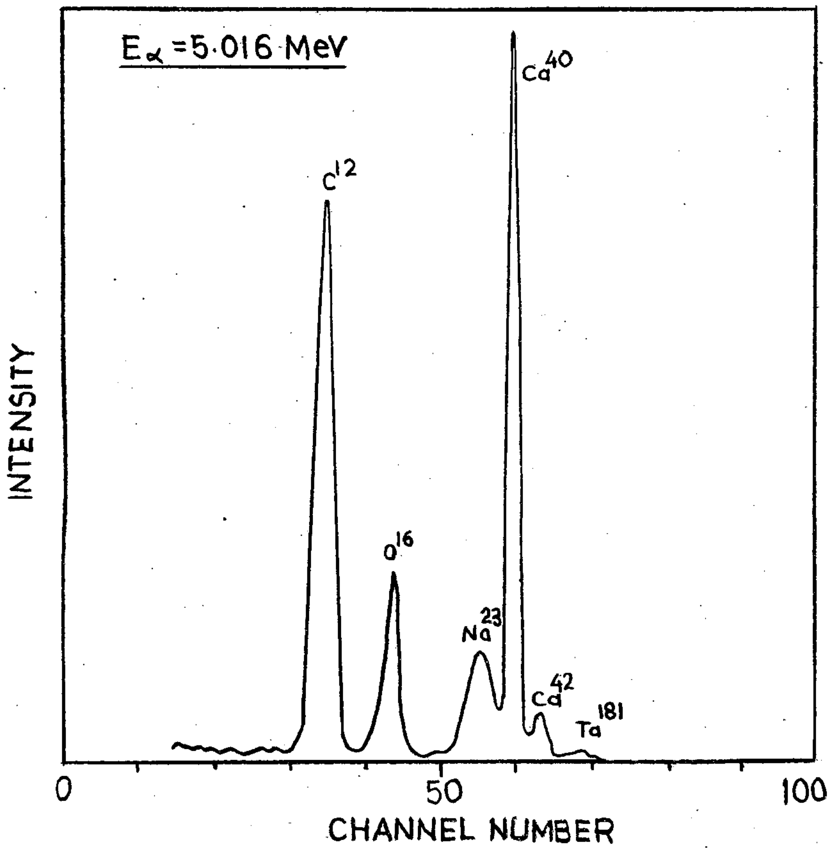

FIG.1. SPECTRUM OF ALPHA PARTICLES SCATTERED FROM TARGET (90°)

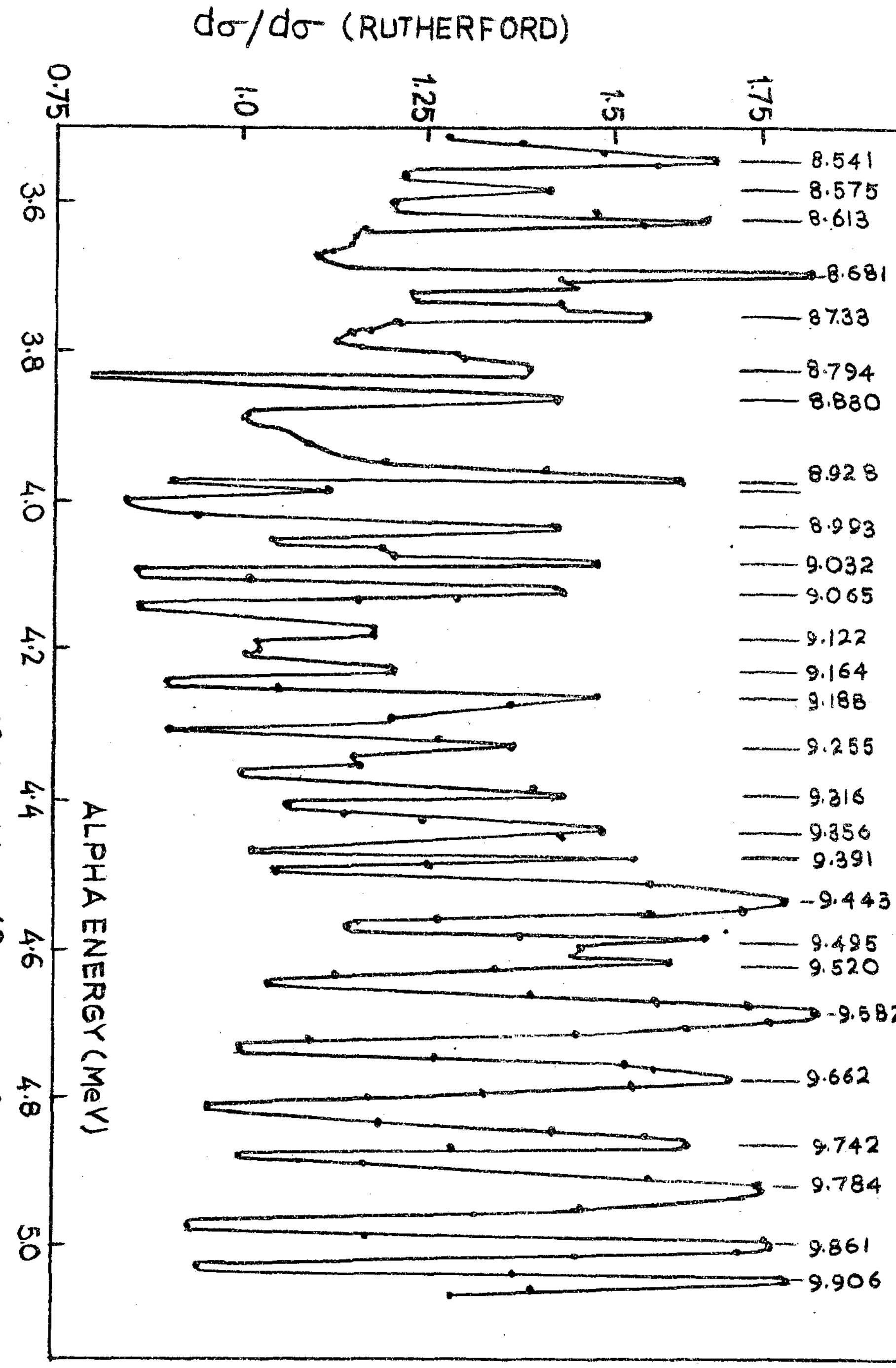

EXCITATION FUNCTION $Ca^{40}(\alpha,\alpha)Ca^{40}$ AT θ 90°

$$f_c(\theta) = -Z \operatorname{cosec}^2(\theta/2)\exp[2i(\sigma_0 - \eta \ln \sin(\theta/2))]$$

$$f_{cH}(\theta) = i\lambda\pi^{1/2}\sum_{\ell'=0}^{\infty}(2\ell'+1)^{1/2}\exp[(2i\sigma_\ell) - \exp(2i\xi_\ell)]\, Y_{\ell'}^{0}(\theta,\phi)$$

$$f_R(\theta) = \sum_{\substack{SS'M_SM_S'J \\ M\ell\ell'\mu'}} i^{\ell-\ell'}\pi^{1/2}(2\ell+1)^{1/2}(\ell s 0 M_S|\ell SJM)(\ell' S'\mu' m_S'|\ell S'JM)\left(\delta_{\alpha\alpha'}\delta_{SS'}\delta_{\ell\ell'} - S^J_{\alpha S\ell,\alpha' S'\ell'}\right) Y_{\ell'}^{\mu'}(\theta,\phi)$$

where

$\ell\ell'$ = incoming and outgoing orbital angular momentum

$Z = \dfrac{Z_\alpha Z_X e^2}{2Mv^2}$, $\eta = \dfrac{Z_\alpha Z_X e^2}{\hbar v}$

σ_0, σ_ℓ = Coulomb phase shifts

ξ_ℓ = hard sphere scattering phase shifts

There may be several terms for the type $f_R(\theta)$ depending on the number of interfering resonances in the energy range fed into the computor. We are now writing a search program forthe computer where in the selected energy range which contains for example, two reasonances, the computer selects two J, π values out of the range J = 0 to 4 which if used in the dispersion theory give best fit to the results. These two values are printed out along with the best fit curve for comparison. This spin search program is being debugged and we hope to be able to label the spins and parities of the most of the levels in the compoun nucleus Ti^{44} very soon. The values of E_o and Γ for each resonance has to be fed into the computor. This is done at present by direct measurements on the excitation function into a series of Breit-wigner curves.

REFERENCES

1. N.Sarma, C.K. Kumar and K.S. Jayaraman
Nuclear Physcis, 44, 205, 1963.

2. J,M. Blatt and L.C. Beidenharn
Rev. Mod. Phys, 24, 258, 1952.

DISCUSSION

M.K. Mehta.

Comment: Looking at the amount of structure in your excitation curve, you might have to use quite a few levels for your Briet-Wigner analysis, and the reronance scattering matrix would become quite complicated. I suggest that instead of this a phase shift analysis technique would be less difficult as this is a zero channel spin case. We found this type analysis worked very well for $O^{16}(\alpha,\alpha)O^{16}$ work that we did at Florida State University.

LIFETIMES OF EXCITED STATES IN Cu^{63} , Cu^{65} , Ni^{62} AND Fe^{56} BY DOPPLER SHIFT ATTENUATION MEASUREMENTS@

M.A. Eswaran**
Nuclear Physics Division, Atomic Energy Establishment Trombay

and

H.E.Gove*, A.E.Litherland and C. Broude
Chalk River Nuclear Laboratories, Chalk River, Ontario, Canada

The lifetimes of the first three excited states in Cu^{63} and Cu^{65} and the first excited states in Ni^{62} and Fe^{56} have been measured by the Doppler shift attenuation method; the states were Coulomb excited using a beam of oxygen ions from a tandem accelerator. The mean lifetimes of the 0.668, 0.961 and 1.327 MeV states in Cu^{63} were found to be $3.3^{+0.5}_{-0.4}$, $9.6^{+0.9}_{-0.8}$ and $8.3^{+0.9}_{-0.8}$ in units of 10^{-13} second. Those of the 0.770, 1.114 and 1.482 MeV states in Cu^{65} were found to be $1.3^{+0.3}_{-0.3}$, $5.3^{+0.5}_{-0.4}$ and $7.6^{+1.1}_{-1.0}$ in units of 10^{-13} second. For the 1.172 MeV state in Ni^{62} and 0.845 MeV state in Fe^{56} the mean lifetime values obtained were $2.26^{+0.19}_{-0.16}$ and $11.3^{+4.0}_{-2.4}$ in units of 10^{-12} second. The results for the levels in the copper isotopes are compared with the predictions of the core excitation model.

@ To be published in 'Nuclear Physics' (in press)

** Work perofrmed during the author's IAEA fellowship at the Chalk River Nuclear Laboratories, Chalk River, Ontario, Canada.

* Present Address: University of Rochester, Rochester, N.Y., U.S.A.

DISCUSSIONS

N.K. Saha : What is the accuracy of the lifetime measurement by the Doppler shift method you use?

M.A. Eswaran: About 10%. At also depends on the relation between the attenuation values observed and the slowing down times involved.

N.K. Saha: I wonder if the large size crystal as used, is not an inconvenience in respect of accuracy.

M.A. Eswaran: No. Half angle of the cone of detection of gamma rays is about 20°. As you observe in the slides the gamma ray peaks were not very much broad.

ENERGY LEVELS OF Ag^{111}

V.R. Pandharipande, R.M. Singru and R.P. Sharma
Tata Institute of Fundamental Research, Bombay - 5

The decay of 22-min Pd^{111} and 5.5 -hr Pd^{111m} has been studied earlier by McGinnis(1), W. Pratt et al (2) and S.F. Eccles(3). However, no detailed coincidence work was carried out on the decay of Pd^{111} and Pd^{111m}. The present study was initiated to establish the energy levels of Ag^{111} from the decay of Pd^{111} and Pd^{111m} and then to compare them with the neighbouring isotopes. This work has been carried out by employing gamma-gamma and beta-gamma coincidence techniques with scintillation phosphors.

Enriched (91.4%) sample of Pd^{110} obtained from ORNL was irradiated in Apsara Reactor, Trombay. For the study of the decay of 22-min ground state of Pd^{111} the sample was irradiated for 20 minutes and then chemically purified for any contamination of Ag^{110} and Na^{24}. In a similar way the 5.5-hr isomer of Pd^{111} was studied by irradiating the samples for 10 hrs and then chemically purifying them.

The gamma spectra of both the activities were recorded with a 3" x 3" NaI (Tl) crystal and a 512-channel analyser and the observations were extended over several half lives. The singles gamma spectra of 5.5 hr. activity was analysed in the usual way by using standard line shapes and the intensities of various gamma rays as normalised to a value of 100 for the intensity of 630 KeV gamma ray are given in Table I.

The gamma-gamma coincidence measurements were carried out with two scintillation spectrometers consisting of 3" x 3" NaI(Tl) crystals mounted on Dumont 6363 photomultiplier tubes. The coincidence arrangement was the

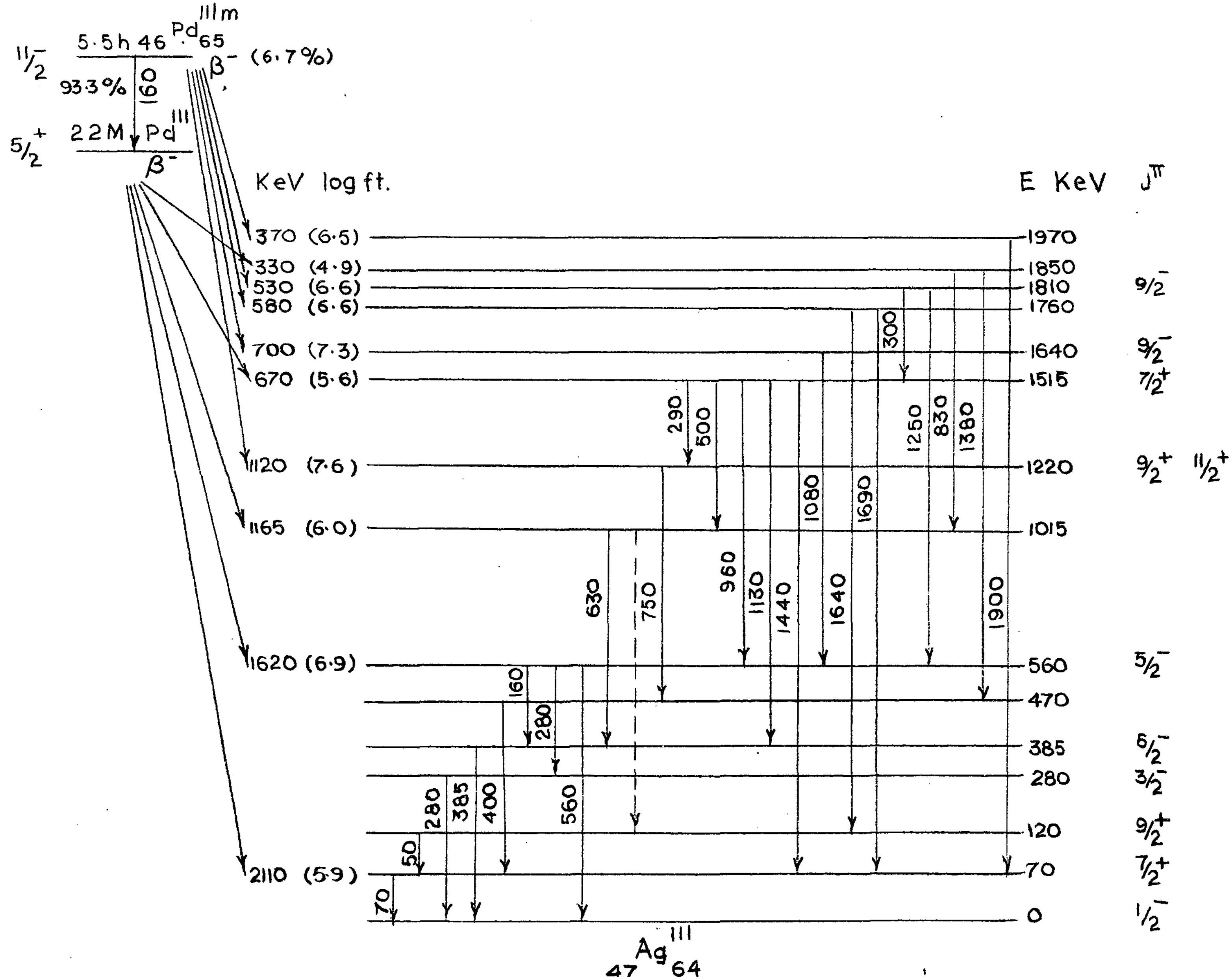
11/2−
5.5h 46 Pd 111m 65
β− (6.7%)
93.3%
160
5/2+
22M Pd 111
β−
KeV log ft.
370 (6.5)
330 (4.9)
530 (6.6)
580 (6.6)
700 (7.3)
670 (5.6)
1120 (7.6)
1165 (6.0)
1620 (6.9)
2110 (5.9)
E KeV
Jπ
1970
1850
1810
1760
1640
1515
1220
1015
560
470
385
280
120
70
0
9/2−
9/2−
7/2+
9/2+ 11/2+
5/2−
5/2−
3/2−
9/2+
7/2+
1/2−
290
500
300
1250
830
1380
1080
1690
630
750
960
1130
1440
1640
1900
160
280
280
385
400
560
50
70
47 Ag 111 64

Fig. 1.

usual fast-slow type with a resolving time $2\tau = 0.12 \mu sec$. All the coincidence spectra were recorded on a 512 channel analyser. The results of all the gamma-gamma coincidences are summarised in Table II.

The beta spectrum of Pd^{111} and Pd^{111m} as studied on a scintillation spectrometer using anthracene crystal ($\frac{1}{2}$" thick) showed the highest beta energy in both the cases extending upto 2110 KeV. The end points of different beta groups feeding the different energy levels were determined from the beta-gamma coincidence measurements and their intensities were calculated from the gamma ray intensities. The relative intensities of the beta transitions to the various energy levels and their log ft values are given in Table III.

The energy levels of Ag^{111} which are fed in the decay of Pd^{111} and Pd^{111m} and which are consistent with the present data are given in Fig.1. The Pd^{111m} decays (93.5%) to the ground state (Pd^{111}) by the emission of 160 KeV isomeric gamma-transition and remaining by beta emission to different excited states of Ag^{111}. From the systematics in the odd-mass Pd isotopes the spin and parity of the isomeric state of Pd^{111} appears to be $11/2^-$ while that of the ground state is $5/2^+$. The spin and parity assignments to first four low excited states of Ag^{111} at 70, 120, 290 and 385 KeV have been made from the systematics of such levels in odd-mass silver isotopes. The levels at 560, 1640 and 1810 KeV are assigned as $5/2^-$, $9/2^-$ and $9/2^-$ respectively. This assignment is based on the fact that the levels at 1810 and 1640 KeV are populated by the beta decay of $11/2^-$ isomeric state of Pd^{111} and on the assumption that the gamma transitions from these levels could be at the most quadrupole in character.

A detailed discussion of the decay scheme and spin assignments would be found elsewhere(4).

REFERENCES

1. C.L. McGinnis, Phys. Rev. 87, 202 (1952).
2. W.W. Pratt and R.G. Cochran, Phys. Rev. 118, 1313 (1960).
3. S.F. Eccles, Physica, 28, 251 (1962).
4. V.R. Pandharipande R.M. Singru and R.P. Sharma, Physics. Rev. (To be published).

TABLE I

E (KeV)	Intensity	E (KeV)	Intensity
160 ± 5	620	830 ± 10	10.3
280 ± 10	71.1	900 ± 20	8.9
295 ± 10		960 ± 20	11.5
385 ± 10	177.3	1080 ± 15	18.1
400 ± 10		1130 ± 15	17.2
450 ± 15	36.4	1250 ± 15	15.9
500 ± 10	32.2	1380 ± 15	8.8
560 ± 10	67.6	1440 ± 15	5.0
630 ± 10	100	1640 ± 20	22.6
750 ± 15	39	1690 ± 20	11.1
		1900 ± 20	8.6

TABLE II

Gamma -Gamma Coincidence Data

Gamma ray in gate, KeV	Gamma rays in coincidence, KeV
1630	50
1380	400
1250	160, 290, 385, 560
1100	160, 290, 385, 560
960	160, 290, 385, 560
830	385, 630
750	160, 300, 400, 560, 630
630	290, 385, 500, 630, 820, 1080, 1250
560	290, 385, 630, 960, 1080, 1250
510	290, 385, 630, 510.

Intensities of beta transitions calculated from gamma intensities and their log ft values.

TABLE III

(i) 5.5 hour activity

E (KeV)	Daughter level (KeV)	Intensity	log ft.
370	1970	0.5%	6.5
530	1810	1.9%	6.6
580	1760	1.8%	6.6
700	1640	1.0%	7.3
1120	1220	1.5%	7.6

(ii) 22-minute activity

E (KeV)	Daughter level (KeV)	Intensity	log ft.
330	1850	1.0%	4.9
670	1515	3.0%	5.6
1165	1015	3.1%	6.0
1620	560	1.7%	6.9
2110	70	84.5%	5.9

THE LEVELS OF I^{131}

S.H. Devare, R.M.Singru and H. G. Devare
Tata Institute of Fundamental Research, Bombay - 5

The levels of I^{131} are fed in the decay of Te^{131} and Te^{131m}. The decay energy of the 30 -hr Te^{131m} is quite large being $\sim$ 2.5 MeV and levels upto 2.3 MeV are excited. The levels fed in the decay of Te^{131} will not be considered here as a detailed account of this decay scheme is already published(1).

Measurements and analysis of the gamma spectrum, gamma-gamma and beta-gamma coincidences were done in the usual manner and a fairly good idea of the level scheme was obtained. In order to get a more detailed knowledge about the energy and multipolarity of the gamma-rays, conversion electron spectra were studied in a high resolution double focussing spectrometer. The source was electroplated on Mylar backing made conducting with a thin coating of gold vacuum-evaporated on it. The resolution used was 0.4%. The following conversion lines were observed: K, L-81, K,L-102, K,L-149, K-201, K-241, K-335, K-775, and K-854 KeV. The K/L ratio for the 149 KeV transition was used to determine the E2/M1 mixing and hence the theoretical value of α_K. Using this value of α_K, and the relative gamma-ray intensities as found from the analysis of the gamma-spectrum, the conversion coefficients for the other transitions were calculated. The multipolarities of the various transitions were determined on the basis of these values of α_K and K/L ratio wherever available. These results are summarized in table I. It can be seen from this that the 775 KeV transition is mainly E2, the M1 admixture being $\leqslant$ 30%. This assignment to the 775 KeV transition is in disagreement with the E1 assignment made by the Russian group (2) on the basis of the very low value of α_K observed by them.

TABLE I

E (KeV)	α_K (Exptl)	α_K Theoretical E_1	E_2	M_1	K/L (Expl)	K/L Theoretical M_1	E_2	Multipole Assignment
81	1.6 ± 0.3(0)	3.2(−1)	2.5(0)	1.6(0)	9.6 ± 2	7.6	1.8	M_1
102	7.0 ±1.0(−1)	1.6(−1)	1.1(0)	6.2(−1)	9.6 ± 2	7.6	2.7	M_1
149	2.05±0.07(−1)	5.3(−2)	3.2(−1)	2.0(−1)	6.7	7.6	4.0	M_1 + 15% E_2
200	3.0 ± 0.5(−2)	2.4(−2)	1.3(−1)	9.3(−2)	−	−	−	E_1
241	2.1 ± 0.5(−2)	1.5(−2)	6.6(−2)	5.6(−2)	−	−	−	E_1
335	3.4 ± 0.6(−2)	6.2(−3)	2.3(−2)	2.4(−2)	−	−	−	M_1,E_2
452	1.0 ±0.25(−2)	3.0(−3)	9.0(−3)	1.1(−3)	−	−	−	M_1,E_2
775	2.2 ± 0.4(−3)	8.0(−4)	2.3(−3)	3.1(−3)	−	−	−	E_2, $\lesssim$ 30% M_1
854	1.9 ± 0.5(−3)	7.0(−4)	1.8(−3)	2.5(−3)	−	−	−	E_2, M_1

It was interesting to see if any of the levels has a meausrable lifetime. This was done by scanning the gamma-spectrum on a multichannel analyzer in delayed coincidence with very low energy beta rays. The delayed discriminator bias was adjusted to cut off prompt coincidences completely even in the region of 50 KeV. This delayed coincidence spectrum showed peaks at 200, 240, 775, 805, 850 and a very weak peak at 1050 KeV. This combined with the results of the gamma-gamma coincidence measurements led to the conclusion that the 1829 KeV level in I^{131} has a measurable life time. The decay of this level was observed on the multichannel analyzer by taking delayed coincidences between 100-200 and 100-240 KeV gamma rays and also between beta and 775 KeV gamma rays using the usual tehnique of time to pulse height conversion. The result is shown in Fig. 1 which also shows the prompt curve obtained with a Na^{22} source selecting the same energies

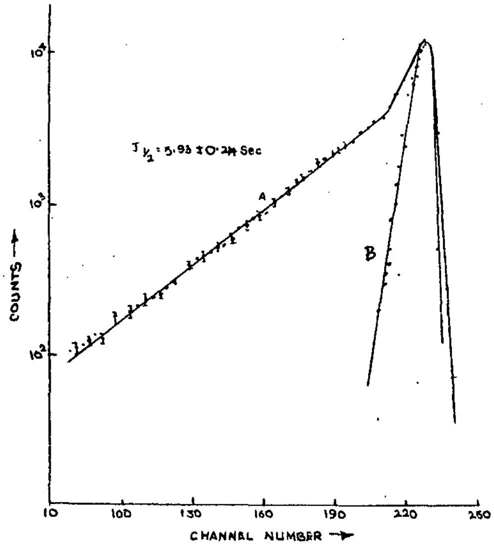

COUNTS
CHANNEL NUMBER
A
B

Fig. 1

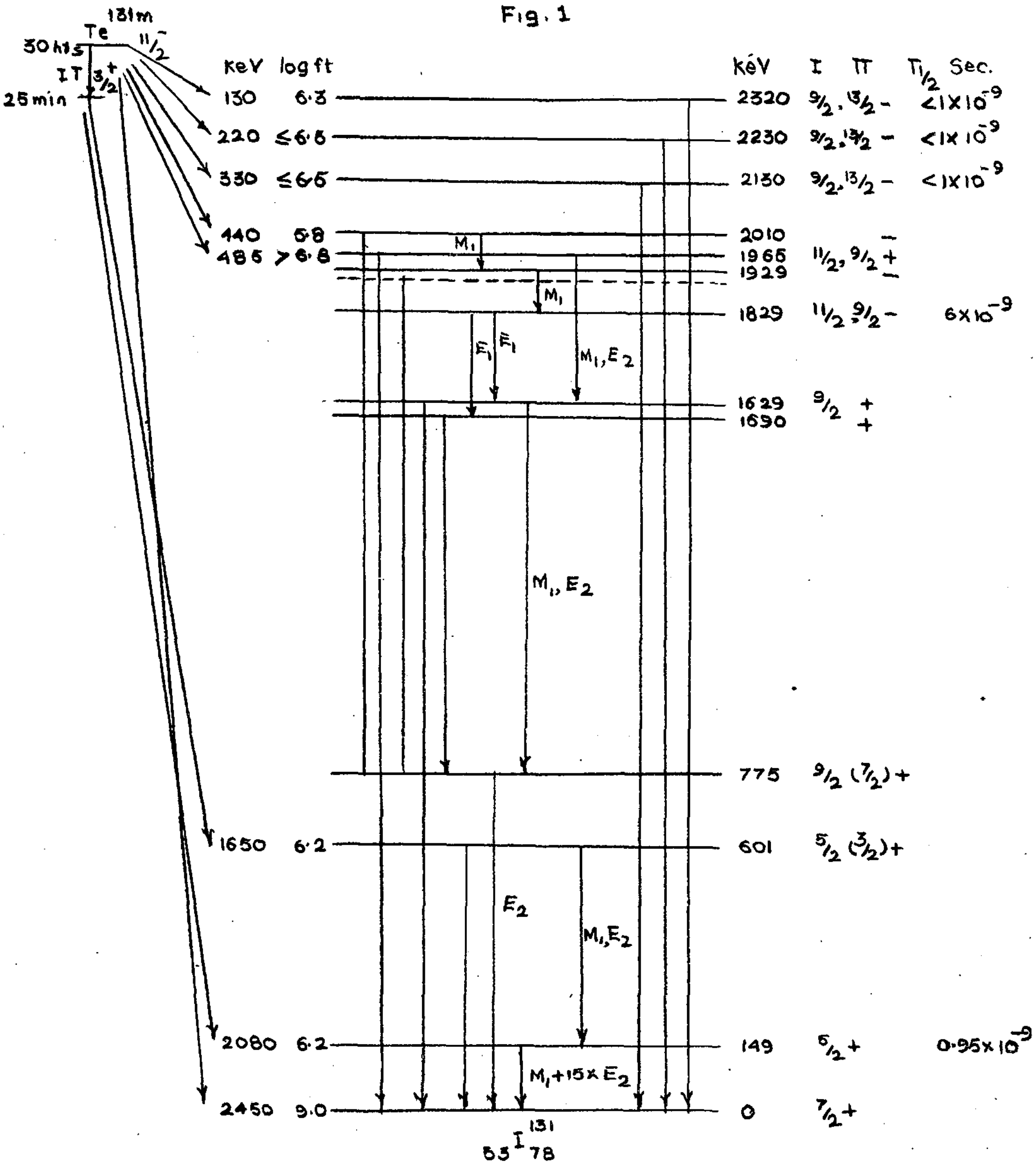

Te 131m
30 hrs
IT
25 min
KeV log ft
130 6.3
220 ≤6.5
330 ≤6.5
440 6.8
485 >6.8
1650 6.2
2080 6.2
2450 9.0
KeV I π T½ Sec.
2320
2230
2130
2010
1965
1929
1829
1629
1690
775
601
149
0

Fig. 2.

as in the case of Te^{131m}. The observed half-life corresponding to the slope is 6 n sec.

Gamma-gamma directional correlation measurements were also carried out for some intense cascades. The results of these measurements are given in Table II. The measurements were made at seven angles and the method of

TABLE II

Results of Gamma-gamma Directional correlation Measurements in I^{131}

Cascade	A_2	A_4
452 -149 KeV	+ 0.063 ± 0.009	+ 0.008 ± 0.013
854 -775 KeV	+ 0.0043± 0.0076	- 0.031 ± 0.010
335 -854 KeV	- 0.18 ± 0.007	+ 0.004 ± 0.012
200 -854 KeV	+ 0.075 ± 0.009	- 0.017 ± 0.014

least squares was used for fitting the data. It can be seen that the775- 854 KeV cascade gives an almost isotropic directional correlation and the A_4 term is relatively larger and negative. Analysis shows that the 775 KeV transition is almost purely E2 which supports the internal conversion coefficient measurement. The A_4 value in the case of 854 -200 KeV cascade seems to be above the error though 200 KeV transition is expected to be E1 in nature from its conversion coefficient. However, one cannot attach much importance to this as the error in A_4 itself is quite large. Better statistics will be able to tell more definitely about the A_4 term. In any case the conversion coefficient measuresuments will not allow more than 5% M2 contribution in the 200 KeV transition.

The decay scheme is shown in Fig.2. The highest energy levels mainly decay to the ground. The log ft values of the beta transitions indicate that these levels are of negative parity. The spin assignments of $5/2^+$ or $3/2^+$ for the 590 KeV, $9/2^+$ to the 1629 KeV levels are made from gamma-gamma directional correlation measurements. The level at 1829 KeV which has a lifetime of 6 ns can have spin $11/2^-$ or $9/2^-$. The exact assignment would be possible only after deciding about the magnitude of the A_4 term. The present results favour the assignment $11/2^-$. The negative parity of these levels may arise due to two reasons viz., the proton going in h 11/2 orbital or the coupling of the particle motion to the octupole vibrations of the core. The second seems unlikely in the case of the 1829 KeV level as it has no transition to the ground state. The configuration of this state could be g $7/2^2$ h 11/2. The other positive parity levels may have considerable admixture of d 5/2 in which case the transitions from the 1829 KeV level to these other levels would be forbidden and so retarded. This may explain the observed half life of this level. Further work to establish this more definitely is in progress.

REFERENCES

1. S.H. Devare, P.N. Tandon and H.G. Devare, Phys. Rev. 131, 1750 (1963).

2. A. Badercu, O.M. Kalinkina, K.P. Mitrofenov, A.A. Sorokin, N.V. Forafonton and V.S. Shpinel, JETP 13, 65 (1961).

ON THE STRUCTURE OF 1.86 AND 3.22 MeV STATES OF Sr^{88}

S. Shastry
Saha Institute of Nuclear Physics, Calcutta

INTRODUCTION

In a recent experiment (1)a 3.22 MeV level of Sr^{88} was found in the decay of Y^{88}. Calculating the E2-M1 mixing (2) from the given a_2 and a_4 coefficients there we get $\delta = 1.13 \pm 0.42$; where δ^2 is the ratio of the reduced matrix elements (3) of E2 and M1 transitions.

POSSIBLE CONFIGURATIONS AND SPECTROSCOPIC CALCULATIONS

In the present work the effect of neutrons was not considered and only proton excitation was considered. The possible proton configurations for the $J = 2^+$ state are $2p^{-1}_{3/2}\ 2p_{1/2}$ and $1f^{-1}_{5/2}\ 2p_{1/2}$. The unperturbed energies for these configurations were found from the experimental data on Rb^{87} and Y^{89}.

The hole-particle to particle-particle matrix element is given by, (we are not considering isotopic spin formalism).

$$\langle j_1^{-1} j_2 J | V | j_3^{-1} j_4 J \rangle = (-1)^{j_1+j_2-j_3-j_4} \sum_{J_1} \sqrt{\frac{[J_1]}{[J]}}\, U(j_1 j_2 j_4 j_3, J J_1)$$
$$\times \left[\langle j_3 j_2 J_1 | V | j_1 j_4 J_1 \rangle - (-1)^{j_1+j_4-J_1} \langle j_3 j_2 J_1 | V | j_4 j_1 J_1 \rangle \right]$$

where the first and second terms inside the brackets on the right hand side are direct and exchange terms, and $U(j_1 j_2 j_4 j_3, JJ_1)$ is the Jahn's U coefficients. The symbol $[J]$ is an abbreviation for $(2J + 1)$.

Four types of interaction wer investigated.

1. $-\frac{1}{2}(1+P_X) V_0\, e^{-r^2/2\sigma^2}$
2. $-\frac{1}{2}(1+P_X) V_0\, e^{-r/a}/r/a$
3. $(-0.1\, Q^S + \tau Q^T)\, V_0\, e^{-r^2/2\sigma^2}$ and
4. $(-0.6\, Q^S + \tau Q^T)\, V_0\, e^{-r/a}/r/a$

Here Px is the space exchange operator, Q^S and Q^T are the projection operators which select the singlet and triplet parts of the two-particle wave functions respectively, and τ is the Rosenfeld exchange mixture. In all the above four interactions V_o was kept at 45 MeV and the range of the Yukawa shape was kept at 1.4 fm. For the Gaussian potential three values of λ was tried as given in ref. (4) viz. λ = 0.5; 0.75 and 1.0, but it was found that the interaction (3) with V_o = 45 MeV, λ =1 and τ = 0.375 gave the best agreement with the experiment and the wave functions were calculated with the energy obtained from this which was used in finding various transitions.

The normalised wave function are thus given by

$$\psi_{1.86} = 0.911 | 1f_{5/2}^{-1}\, 2p_{1/2} \rangle + 0.412 | 2p_{3/2}^{-1}\, 2p_{1/2} \rangle$$

$$\psi_{3.22} = -0.412 | 1f_{5/2}^{-1}\, 2p_{1/2} \rangle + 0.911 | 2p_{3/2}^{-1}\, 2p_{1/2} \rangle$$

CALCULATION OF TRANSITION PROBABILITIES

The transition probability per sec for gamma rays of a given multipolarity L is given by

$$T(L) = \frac{8\pi (L+1)}{L[(2L+1)!!]^2} \frac{1}{\hbar} \left(\frac{\Delta E}{\hbar c} \right)^{2L+1} B(L\sigma)$$

where ΔE is the transition energy and $B(L\sigma)$ is the reduced transition probability and is given by

$$B(L\sigma) = \frac{1}{2J_i+1} | \langle J_i \| M^L_\sigma \| J_f \rangle |^2$$

in which J_i and J_f are the initial and final spins and M^L_σ is the multipole operator to be defined below for M1 and E2 transitions.

The second quantized form for the E2 transition operator is given by

$$E^2_M = e \sum_{\alpha\beta} \langle \alpha | r^2 Y^2_M | \beta \rangle \eta^+_\alpha \eta_\beta$$

where the operators η^+_α and η_β are the creation operators for particle and holes respectively, and $\alpha\, \beta$ stand for the jj coupling single particle states.

The operator of M1 transition is given by

$$M_1 = \sqrt{\frac{3}{4\pi}} \left(\frac{e\hbar}{2m_p c} \right) [\mu_p \sigma_z + l_z]$$

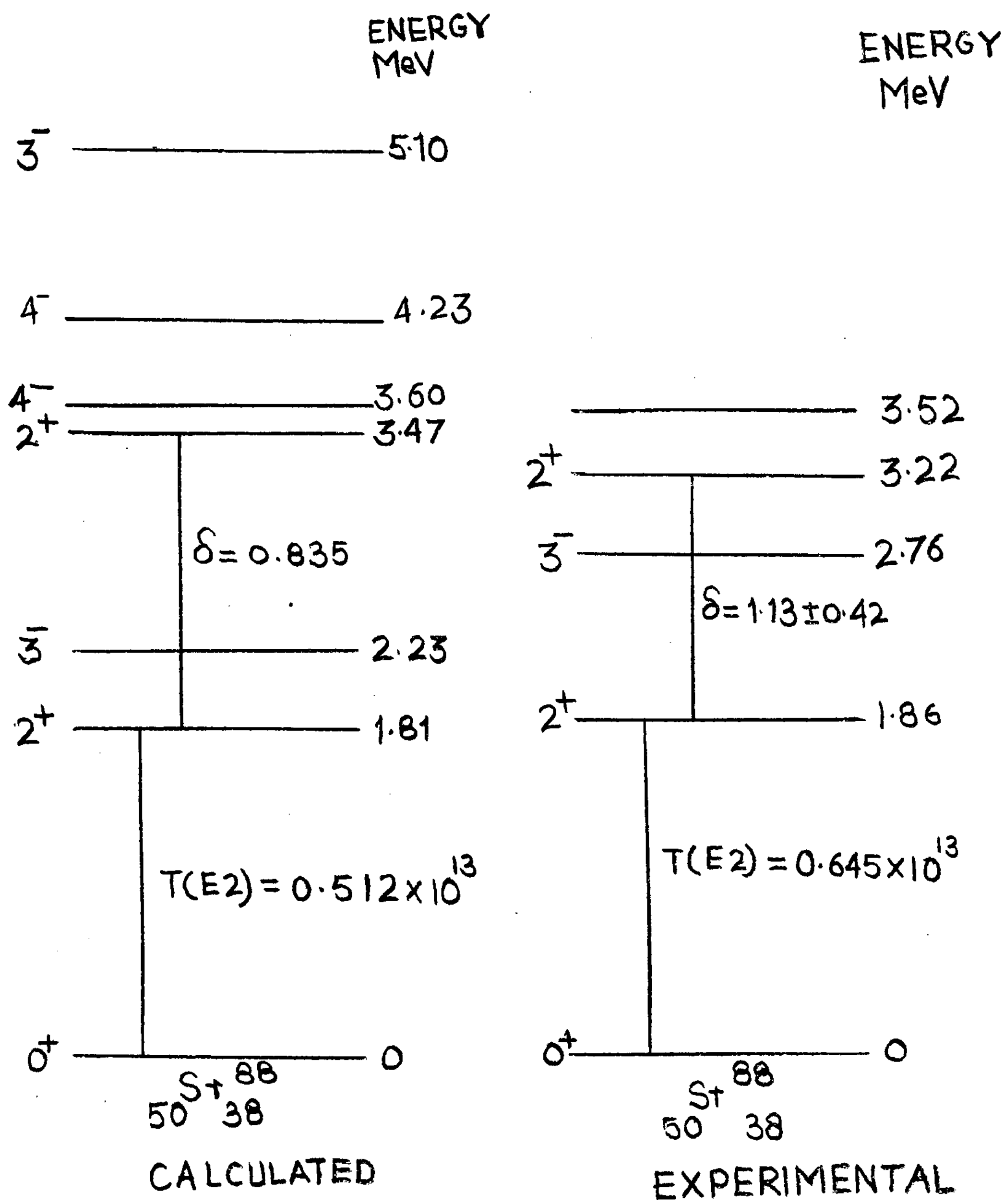
ENERGY MeV
ENERGY MeV
3⁻ 5.10
4⁻ 4.23
4⁻ 3.60
2⁺ 3.47
δ = 0.835
3⁻ 2.23
2⁺ 1.81
T(E2) = 0.512×10^13
0⁺ 0
$_{50}Sr^{88}_{38}$
CALCULATED
3.52
2⁺ 3.22
3⁻ 2.76
δ = 1.13±0.42
2⁺ 1.86
T(E2) = 0.645×10^13
0⁺ 0
$_{50}Sr^{88}_{38}$
EXPERIMENTAL

Fig. 1.

In the above calculations harmonic oscillator wave functions were used with harmonic oscillator well parameter adjusted to 2.08 fermi to fit the r.m.s. radius of Sr^{88} . The results are shown in Tables I and II.

TABLE I

Interaction	V_o (MeV)	Range	τ	E1 in MeV	E2 in MeV	E1 Exp in MeV	E2 Exp
$-\frac{1}{2} V_0 (1+P_x) e^{-r/a} / r/a$	45	1.4 fm		2.88	3.71		
$-\frac{1}{2} V_0 (1+P_x) e^{-r^2/2\sigma^2}$	45	2.08		2.65	4.38		
$(-0.6 Q^S + \tau Q^T) V_0 e^{-r^2/2\sigma^2}$	45	2.08	0.375	1.81	3.47	1.86	3.22
$(-0.6 Q^S + \tau Q^T) V_0 e^{-r/a} / r/a$	45	1.4 fm	0.375	2.63	3.96		

Finally with the interaction $(-0.6\ Q^S + \tau Q^T)\ V_o\ e^{-r^2/2\sigma^2}$ with V_o = 45 MeV and τ = 0.375 we have the following results

TABLE II

3.22 to 1.86 (2^+ 2^+) mixing $\delta = \sqrt{\frac{E2}{M1}}$	T(E2) from 2^+ to ground state 0^+
Calculated = 0.835	Calculated = 0.512×10^{13}
Measured = 1.13 ± 0.42	Experimental(5)= 0.645×10^{13}

It is worth mentioning that for the 2.76 MeV 3^- state of Sr^{88} with configuration $2p_{3/2}^{-1}$ $1g_{9/2}$ and $1f_{5/2}^{-1}$ $1g_{9/2}$ the calculated energy gave good agreement with the experiment giving 2.23 and 5.13 MeV but the E1 transition between 3^- to 2^+ state cannot be explained with these configurations for 3^- state as operator for E1 transition vanishes between these configurations for 3^- and configurations for 2^+. The calculated and experimental level scheme is shown in Fig. 1. A much more elaborate calculation to explain this 3^- state with all the 14 possible configurations (only one hole - one particle configuration) is in progress. The calculation was done on CDC 3600 belonging to Tata Institute of Fundamental Research Bombay.

REFERENCES

1. S. Shastry and R. Bhattacharyya, Nuclerar Physics, Vol. 55 (1964) 397 - 400.
2. R.G. Arns and M.L. Wiedenbeck, University of Michigan, Ann Arbor, Michigan.
3. L.C. Bidenharn and M.E. Rose, Revs. Modern Phys. 25, 729 (1953).
4. B.F. Baymen, A.S. Reiner and R.K. Sheline, Phys. Rev. 115, 1627 (1959).
5. S. Ofer and A. Schwarzschild, Physical Rev. Letters, Vol. 3, 384 (1959).

INCOHERENT SCATTERING OF GAMMA RAYS BY K-SHELL ELECTRONS

A. Ramalinga Reddi, V. Lakshminarayana and Swami Jnanananda
Laboratories for Nuclear Research, Andhra University, Waltair.

Incoherent scattering of gamma-rays is one of the major processes of interaction in the gamma-ray energy domain 0.1 to 5 MeV. The cross-section for this process is predicted with high accuracy by Klein-Nishina formula in the case of scattering by free and stationary electrons. On the other hand, accurate formula for estimation of scattering cross-sections by bound electrons are not available. The usual method of description is, in these cases, to use the incoherent scattering function $S(q,z)$ to multiply the free electron cross-section in order to obtain the bound electron scattering cross-section. The theoretical estimates(1) of $S(q,z)$ make use of unphysical atomic charge distributions. A few experimental studies have been made to obtain information on the K-sehll electron binding effects on incoherent scattering. All these studies (2-5) have been made with Cs^{137} gamma-rays, employing gamma-K-X-ray coincidence technique. The effect of electron binding averaged over all electrons is studied by Sood et.a. (6) at angles of scattering between 4° and 15°. The present investigation is an attempt to obtain information on the K-shell electron binding effects of gamma-rays with energy 320 KeV, employing the conventional coincidence technique.

The experimental arrangement is similar to that of Sujkowski and Nagel (3) and the experimental procedure and analysis is similar to that of Motz and Missoni (4). A Cr^{51} source of 5.5 curies is employed with scatterers of Pb, (14.85 mg/cm.^{2}), Ta (9.32 mg/cm^2), and Sm(54.14 mg/cm^2). The source-holder is a 2 ft. x 2 ft. steel cylinder filled with lead containing an axial hole of 1" diameter in which the source is adjusted to be at 6" from the edge on the scatterer side. Two NaI (Tl) crystals of dimensions $1\frac{3}{4}$" X 2" and $1\frac{1}{2}$" X $\frac{1}{4}$" are used with DuMont 6292 Photomultipliers for gamma and X-ray detection respectively. A conventional slow-fast coincidence arrangement with an effective resolving time of 60ns.is used. The differential K-electron incoherent scattering cross-section is obtained from the formula

$$\frac{d\sigma_K(\theta)}{d\Omega} = \frac{N_c}{N_0 \epsilon_{\gamma K} \omega_{\gamma K} \epsilon_x \omega_x \epsilon_c d \nu_K \nu_{abs}(x) \nu_{abs}(\gamma_K)}$$

where N_c is the coincidence count rate, N_o is the number of gamma rays incident on the target per unit time, $\epsilon_{\gamma K}$ is the efficiency of the gamma detector for detection of the scattered gamma rays into the solid angle $\omega_{\gamma K}$, ϵ_x is the efficiency of the X-ray detector for the detection of K-X-rays incident on the crystal in the solid angle ω_x, ϵ_c is the coincidence **efficiency,** d is the thickness of the target expressed as the number of K electrons per unit area, ν_K is the fluorescente yield of the target, $\nu_{abs}(x)$ is the fraction of K-X-rays reaching the detector without being absorbed by the target and $\nu_{abs}(\gamma_K)$ is the corresponding factor for the gamma case.

It is usually difficult to obtain N_o with sufficient accuracy. As such, it is eliminated by conducting an auxiliary experiment in which a free electron scattering cross-section $\frac{d\sigma_F}{d\Omega}$ (in aluminium) at the same angle is determined under identical geometry. Since the free electron scattering cross-section in aluminium is believed to be accurate within 1%, it is employed to eliminate N_o. Thus

$$\frac{d\sigma_K}{d\sigma_F} = \left(\frac{N_c}{N_F}\right) \left(\frac{1}{\omega_x \epsilon_x \epsilon_c \nu_K}\right) \left(\frac{\epsilon_\gamma}{\epsilon_{\gamma K}}\right) \left(\frac{\nu_{abs}(\gamma)}{\nu_{abs}(\gamma_K)}\right) \frac{1}{\nu_{abs}(x)} \frac{d_{Al}}{d} \frac{A}{A_l} \left(\frac{13}{2}\right)$$

where N_F is the number of gamma-rays scattered by free electrons in aluminium of thickness d_{Al} expressed in mg/cm^2. The factors $\left(\frac{\epsilon_\gamma}{\epsilon_{\gamma_K}}\right)$ and $\left[\frac{\nu_{abs}(\gamma)}{\nu_{abs.}(\gamma K)}\right]$

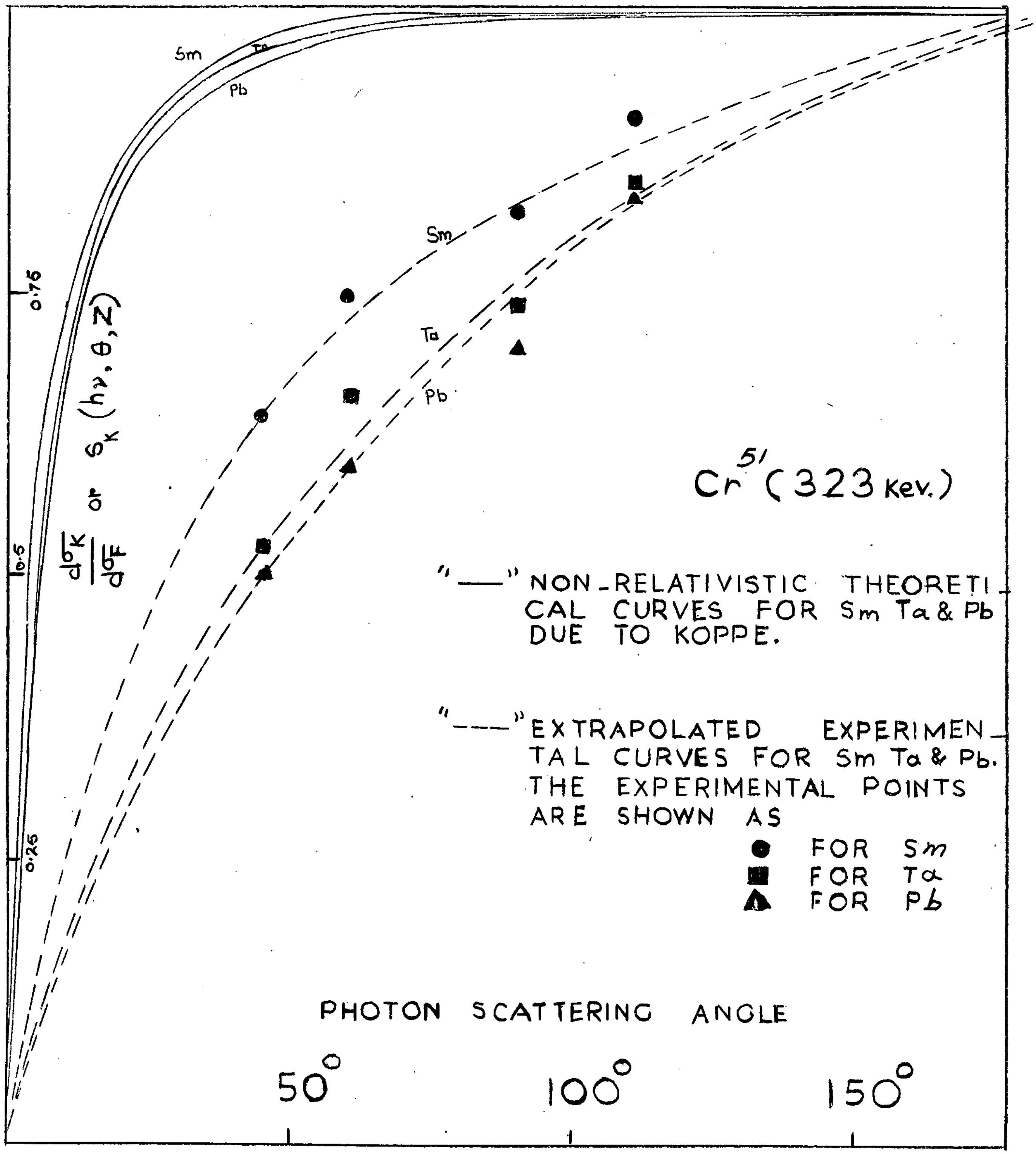

FIG. 1. VALUES OF S_K AS A FUNCTION OF THE ANGLE OF SCATTERING

are difficult to estimate but the error in assuming them to be approximately unity is quite small. A and A_{Al} are the atomic weights of the target and aluminium respectively. The factor (13/2) takes into account the fraction of bound electrons in aluminium.

As pointed out in the earlier measurements (4), the accuracy of this investigation is limited by the accuracy of estimation of N_c after correcting for chance and spurious coincidence events. In the present investigation, chance coincidence counts are estimated from the signals count rates and the known resolving time. Spurious coincidences are minimised by adopting the following measures:

1) Using sufficiently thin targets.
2) Using lead anti-scatter cones on the detectors to restrict their field of view to the target.
3) Reducing stray materials alround.

The remanant spurious coincidences are estimated by measuring the coincidences replacing the target by an aluminium scatterer containing equal number of electrons.

The experiment is conducted at 45°, 60°, 90° and 110°. In each case, a minimum of 250 true coincidence counts are obtained and $d\sigma_K/d\sigma_F$ is evaluated. The experimental values of the ratio for the 3 elements are shown in Fig.1. which also contains the theoretical curve S(q,z) based on Koppe's interpolation method (7). The interpolation was made between two modes of atomic charge distribution Thomas-Fermi and Koppe for large q and small q respectively. It can be seen from the figure that the general trend of decrease of S as θ decreases is supported. However, the actual values of S are much smaller in the experiment. It may be accounted by the fact that whereas the computation refers to the average effect of all electrons in an atom, the experimental values are for K-electrons which are the most rightly bound.

Z-dependence of differential scattering cross-section is analysed using a formula of the type $\frac{d\sigma_K}{d\Omega} = K Z^n$ at each angle and the constants K and n are evaluated from the experimental values of $(d\sigma_K/d\Omega)$ by least squares fitting. The values of the exponent 'n' are negative varying from-1.03 to 0.127 as the photon scattering angle is varied from 45° to 110°. K-N theory predicts n =1 for all angles of scattering.

REFERENCES

1. G.W. Grodstein, N.B.S., Circular No. 583 (1957).
2. D. Brini, E. Fuschini, N.T. Grimeline, and D.S.R. Murty Nuovo Cimento 16, 727 (1960).
3. Z. Sujkowski and B. Nagel, Arkiv Fysik, 20, 323 (1961).
4. J.W. Motz and G. Missoni, Phys. Rev., 124, 1458 (1961).
5. J. Varma, and A.Eswaran, Phys. Rev. 127, 1197 (1962).
6. B. Sood, M.Singh and S. Anand, Nuclear Physics Symposium, 1964 p.300.
7. H.Koppe, Z. Physik, 124, 658 (1947).

DISCUSSIONS

J.Varma: The scattered γ-ray spectrum has been unambigously shown to be a continuum and unless this fact is taken into consideration the cross-section measurements can be very wrong.

V. Lakshmi Narayana : The experimental conditions are the same as those of Varma and Eswaran. The spectrum is integrally biased above 150 KeV and thus not likely to yield a considerable error.

J.Varma: The previous results of Mott et al and others gave a value of to be larger than 1 beyond experimental or statistical errors and the small observed crosssectioncan be explained if the precaution mentiond in (1) are not taken into consideration. One should measure the cross-section σ_K for scattered photon energies from zero to the maximum

V.Lakshminarayana: Mott and Misson's results are at an energy of 662 KeV and the present experimental results are for 320 KeV gamma rays. Hence those conclusions may not be expected to hold in the present case.

Ghose: You have used a strong source. How have you taken the effect of degenerate photons which inevitably occur in such sources?

V. Lakshminarayana: The effect is not taken into account.But it is not likely to introduce considerable error.

COMPTON SCATTERING OF LOW ENERGY GAMMA RAYS

P. V. Ramana Rao, J. Rama Rao and V. Lakshminarayana
Laboratories for Nuclear Physics, Andhra University
Waltair

A few experimental investigations on the incoherent scattering of photons by bound electrons are reported in literature (1,2,3). All these investigators studied scattering of 662 KeV gamma rays by the K-shell electrons in various elements, using the "scattered gamma-KX -ray coincidence technique". The results Brini et.al. were at large variance with those of other investigators. Recently, Ramalinga Reddy (4) extended similar investigations down to 320 KeV. His experimental results at this energy were found to disagree with theoretical predictions.

The present investigation is an attempt to obtain data on the incoherent scattering process at still lower photon energies. However, at such low photon energies, the experimental problems involved in the coincidence technique used by the previous investigators are severe due to the non-availability of intense sources and the inadiquate resolution of the various scattered events with scintillation spectrometer. On the other hand, It is fairly easy to determine the total cross -sections with good statistical accuracy. The integral incoherent scattering cross-sections can then be obtained by subtracting from the total cross-section the theoretical sum of photo-electric and coherent scattering cross-sections. However, such a procedure is justifiable only when subtracted contributions are estimated accurately. This situation obtains for the interaction of low energy photons with low and medium z elements. Recent experimental and theoretical investigations on the photo-electric interaction (5) have established procedures for the estimation of photo-electric cross-sections. Similarly, theoretical (6) and experimental (7) studies on coherent scattering of gamma rays have clearly established the validity of the form factor formalism for the evaluation of coherent scattering cross-sections of low energy gamma-rays in light elements. The present method enables a comparison of the bound electron and free electron scattering cross-sections integrated over all directions, of scattering and summed over all the electrons, and the results indicate the trends of the influence of electron binding as a function of atomic number and photon energy.

EXPERIMENTAL DETAILS

The total atomic cross-sections are determined in a good geometry arrangement. A scintillation spectrometer assembled with a DuMont 6292 photo-multiplier and $\frac{3}{4}$" x $\frac{3}{4}$" NaI (Tl) crystal is used as the detector. The isotopes Hg^{203}, Ce^{141}, Os^{191} and Gd^{153} are used to provide gamma rays of energies 280, 145, 129 and 100 KeV respectively, in sealed radiographic capsules having active pellet dimensions 4 mm x 4mm. All but Ce^{141} are of 10 mc. strength. The initial strength of Ce^{141}, however, is 20 mc and it is allowed to decay through one half life to eliminate the contaminant activity Ce^{143}. The scattering materials are C, Al, Cu and Cd. The total atomic cross-sections are determined with a statistical accuracy within 1%. The K -shell photo-electric cross-sections for the elements and energies of the present investigation are computed using the analytical expressions provided by Nagel (8) and the values are accurate to within 2%. The cross-sections for coherent scattering (Rayleigh type) are computed under the form-factor approximation and the results are not likely to involve an error exceeding 3%. The theoretical sum of photoelectric cross-section, $_a\tau$, and coherent cross-section, σ coherent, is subtracted from the experimentally determined total atomic cross-section $_a\mu$ to extract the integral bound electron incoherent scattering cross-section σ_b.

For a comparison with σ_b , the integral free electron incoherent scattering cross-sections σ_f are calculated using the well-known Klein Nishina formula. The ratio (σ_b/σ_f)Experimental, thus formed, is a measure of the influence of electron binding. The values of incoherent scattering function S calculated on the basis of Thomas-Fermi (9) atomic charge distribution and compiled by Grodstein (10) and Nelms (11) are used in the theoretical evaluation of σ_b to compute the ratio $(\sigma_b/\sigma_f)_{\text{Theor.}}$ The overall error involved in the procedure is estimated to be about 3%.

RESULTS AND DISCUSSION

The experimental and theoretical ratios of (σ_b/σ_f) are given in table 1 in which the percentage deviations ($\Delta\%$)are also furnished. The ratio (σ_b/σ_f) enables a quantitative estimation of the electron binding effects. The deviation of this ratio from unity is a simple measure of the diminution of the cross-section due to binding effects and hence of the severity of the binding effects. It can be seen from Table 1 that $(\sigma_b/\sigma_f)_{\text{Exptl}}$ and $(\sigma_b/\sigma_f)_{\text{Theor}}$ show a progressive decrease with increasing atomic number and decreasing energy in conformity with the expected trends of variation in these directions. An examination of percentage deviations ($\Delta\%$)between the two ratios reveals that there is agreement between theory and experiment whenever the diminution due to binding effects does not exceed about 10%. Beyond this limit, the deviation shows a proportionate increase with the magnitude of diminution due to binding effects. It can thus concluded that the Thomas-Fermi atomic charge distribution underestimates the severity of binding effects.

REFERENCES

1. D. Brini, E. Fuschini, N.T. Grimelini and D.S.R.Murty, Nuovo Cimento 16, 727 (1960).

2. Z. Sujkowski, and B. Nagel, Ark. Fys., 20, 323 (1961).

3. J.W. Motz, and G. Missoni, Phys. Rev., 124, 1458 (1961).

4. A. Ramalinga Reddy, Ph.D. Thesis: Studies on the Incoherent Scattering of Gamma rays by K-shell Electrons, Andhra University (1964).

5. K. Parthasaradhi, Ph.D. Thesis: Studies on Absolute Photoelectric Cross-sections, Andhra University (1963).

6. G.E. Brown, R.E. Peierls, and J.B. Woodward, Proc. Roy. Soc. (London) 227A, 51 (1954); G.E. Brown, and J.B. Woodward, Proc. Roy. Soc. (London) 227A, 59, (1954).

7. V.A. Narasimha Murty, D.Sc. Thesis: Studies on The Elastic Scattering of Gamma Rays, Andhra University (1963).

8. C.H. Nagel, Ark. Fys., 18, 1 (1960).

9. L.H. Thomas, Proc. Cambridge Phil.Soc., 23, 542 (1926).

10. G.W. Grodstein, National Bureau of Standards Circular 583 (1957).

11. A.T. Nelms, National Bureau of Standards Circular 542 (1953).

DISCUSSION

Ghose: What is the percentage error in your determination of σ_b ? For lower energy photons, the errors in theoretical values (due to larger photoelectric and coherent scattering) is bound to be large and hence your method is not applicable with any accuracy.

P.V. Ramana Rao: The error in the determination of σ_b differs with energy and element. The subtraction technique may not be feasible at very low photon energies but this contention does not apply at the energies we have employed for our investigation.

TABLE I

Energy (KeV)	Element	C	Al	Cu	Cd
280	Ex	0.98 ± 0.01	0.97 ± 0.01	0.93 ± 0.01	0.90 ± 0.02
	Th	0.98 ± 0.03	0.97 ± 0.03	0.95 ± 0.03	0.92 ± 0.03
	Δ%	0.0 ± 3.2	0.0 ± 3.2	2.0 ± 3.2	2.2 ± 4.0
145	Ex	0.96 ± 0.01	0.94 ± 0.01	0.88 ± 0.02	0.68 ± 0.08
	Th	0.96 ± 0.03	0.95 ± 0.03	0.93 ± 0.03	0.88 ± 0.03
	Δ%	0.0 ± 3.2	1.0 ± 3.2	4.4 ± 4.0	22. ± 10.
129	Ex	0.93 ± 0.01	0.90 ± 0.01	0.78 ± 0.03	0.59 ± 0.10
	Th	0.96 ± 0.03	0.94 ± 0.03	0.91 ± 0.03	0.87 ± 0.03
	Δ%	3.0 ± 3.2	4.4 ± 3.6	14.4 ± 4.6	31. ± 11.
100	Ex	0.91 ± 0.01	0.84 ± 0.01	0.65 ± 0.04	0.34 ± 0.25
	Th	0.95 ± 0.03	0.93 ± 0.03	0.89 ± 0.03	0.34 ± 0.03
	Δ%	4.0 ± 3.2	10.0 ± 3.6	26.6 ± 5.5	62.5 ± 31.

STUDIES ON THE LEVEL WIDTHS OF SOME 2^+ STATES

P.S. Raju, A. Durga Prasad, and Swami Jnanananda
The Laboratories for Nuclear Research
Andhra University, Waltair

INTRODUCTION

The resonance scattering of γ-rays which is analogous to the familiar resonance fluorescence in atomic physics, is under investigation for measuring the level widths of 2^+ states of Ti-46, Co-56 and Ir-192, belonging to even-even group. These isotopes are chosen since they satisfy the resonance conditions, although they lie in different regions.

The scattering cross-section of γ-photons of energy E_γ may be expressed (1) as

$$\sigma(E_\gamma) = \sigma_0 \frac{1}{1 - \left(\frac{E_\gamma - E_\pi}{\Gamma/2}\right)^2} \qquad (1)$$

σ_0 being equal to $2\pi\lambda\!\!\!^{-2}\left(\frac{2J+1}{2I+1}\right)$, where E_γ and $\lambda\!\!\!^{-}$ are the energy and wave length of γ-quanta, E_π is the energy by virtue of which scattering is observed, Γ the natural width and J the spin of the excited state and I the spin of the nuclear ground state.

The term $(E_\gamma - E_\pi)$ occuring in the denominator of eq. 1 represents the energy loss due to recoil (2). The value of Γ for Ti-46 is theoretically computed (3) and found to be 3.802×10^{-5} ev. A substitution of the values for energy loss and Γ in eq (1) gives the value of the cross-section which is of the order of 10^{-30} cm^2. The cross-section, as can be seen, is difficult to measure being appreciably small. The measurement of the cross-section of this order especially associated with a large Compton background, is difficult unless some method is employed for compensation of recoil loss.

In this method it is assumed that the energy loss sustained during the transition from the 2^+ level to the ground state is compensated by the recoil energy supplied by the γ-photon from 4^+ to 2^+ state as shown in Fig. 1. On the basis of this assumption the resonance scattering of 892 KeV - component from Ti-46 has been expermentally observed.

METHOD

If the recoil arising out of the electron and neutrino emissions in the β-decay under investigation, be ignored, and the nuclei which are assumed at rest emit γ-quanta give a cascade of the form shown in Fig. 1, then the energies $E^{o}_{\gamma_1}$ and $E^{o}_{\gamma_2}$ are related by the expression

$$\cos\phi_o = - E^{0}_{\gamma_1} / E^{0}_{\gamma_2} \tag{2}$$

ϕ_o being the angle subtended between the directions of radiations at maximum resonance scattering. The terms E_{γ_1} and E_{γ_2} occuring in the level diagram are the energies of the Gamma components of the nuclei in motion. In the case of Ti-46 the value of $\phi_o = 142°5'_o$. This method requires that the energy $E^{o}_{\gamma_2}$ be greater than $E^{o}_{\gamma_1}$ and that the angle ϕ_o be such that the relation between $E^{o}_{\gamma_1}$ and $E^{o}_{\gamma_2}$ is satisfied.

The source giving rise to the two components under investigation is in a state of thermal agitation. The γ-component from this agitated source is incident upon the target giving rise to a corresponding thermal agitation to the nuclei of the target so that the average effective resonance scattering cross-section is of the form

$$\sigma = \sigma_o \Psi(\xi, x) \tag{3}$$

where $\Psi(\xi, x)$ is of the form (4) given by $\xi = \Gamma/\Delta$ and $x = E_\gamma - E_n / \Gamma/2$ where Δ is the Doppler shift given by

$$\Delta = E_{\gamma_1} \sqrt{\frac{2k(T_1 + T_2)}{MC^2}} \tag{4}$$

T_1 and T_2 being the absolute temperatures of the source and the target respectively and k the Boltzman's constant. In the present investigation both the source and the target are at the temperature of the air-conditioned chamber.

If the Doppler shift is much greater than level width $(\Delta \gg \Gamma)$ then the scattering cross-section has the form

$$\sigma = \sigma_0 \sqrt{\frac{\pi}{2}} \frac{\Gamma}{D} \exp.\left[-\left(\frac{E_{\gamma_1} - E_{\pi}}{\Delta^2}\right)^2\right] \quad (5)$$

The angle ϕ is the function of energy $E^0_{\gamma_1}$ so that

$$E_{\gamma_1} = E^0_{\gamma_1} \psi$$

where

$$\psi = E^0_{\gamma_1} \left[1 + E^0_{\gamma_1}/Mc^2\right] \quad (6)$$

The resulting resonance energy E_{π} is related to $E^0_{\gamma_1}$ by the expression

$$E_{\pi} = E^0_{\gamma_1} \left(1 + \frac{E^0_{\gamma_1}}{Mc^2}\right) \quad (7)$$

Now the resonance scattering depends on ϕ and can be expressed as:

$$\sigma = \sigma_0 \frac{\sqrt{\pi}}{2} \frac{\Gamma}{D} \exp\left[-\frac{(E^0_{\gamma_1})^2}{\Delta^2}\left\{\frac{E^0_{\gamma_2} \cos\phi}{Mc^2} - \frac{E^0_{\gamma_1}}{Mc^2}\right\}^2\right] \quad (8)$$

If $E^0_{\gamma_2} > E^0_{\gamma_1}$ and the angle is the same as that given by (2), the resonance scattering cross-section is a maximum given by

$$\sigma_{max.} = \sigma_0 \frac{\sqrt{\pi}}{2} \frac{\Gamma}{\Delta} \quad (9)$$

If the deviation from compensation angle $\phi_1 = \phi - \phi_0$ be small, the expression (8) takes the form as

$$\sigma = \sigma_{max} \exp.\left[-\phi_1^2/\Delta\phi^2\right] \quad (10)$$

where $\Delta\phi$ is the angular line width, given by

$$\Delta\phi = \frac{\Delta}{E^0_{\gamma_1}} \cdot \frac{Mc^2}{\sqrt{(E^0_{\gamma_2})^2 - (E^0_{\gamma_1})^2}} \quad (11)$$

In the case of Ti-46 under investigation $\Delta\phi = 0.09833$. Employing the approximation for Γ already mentioned the maximum cross-section may be derived as

$$\sigma_{max\,(\text{Theoretical})} = 0.3757 \times 10^{-24} \text{ cm}^2$$

APPARATUS.

A slow fast triple coincidence spectrometer is construted and employed in conjuction with correlation unit, with a view to study experimentally the resonance scattering phenomena and to determine the cross section of the isotopes mentioned in order to test the validity of the theoretically computed values of the cross section and level width.

The Sc-46 source is obtained in the form of ScCl dissolved in dilute Hcl. This solution iscarefully introduced in a perspex tube of thin walls, 4 mm in diameter and 10 mm in length. This source is fixed at the centre of a circular plate the edge of which being graduated into degrees. The two channels and the source are fixed at the centre of the plate, so that the arms of the channels can be rotated to any desired angle and can be fixed in that position. This assembly is mounted on a fixed table of light material in order to maintain a stationary position even if the sources are changed, when required. The NaI (Tl) scintillator- Photomultiplier (Dumont 6292) assembly and the source are so arranged that the solid angles subtended at the source by the surface of the windows of the photomultipliers are of the same magnitude. The areas of the wave front of the collimated beam incident is identical with those of the windows. This arrangement eliminates back scattering. With this arrangement the angles of rotation are varied from 90° to 180°.

The pulses from each one of the scintillator-photomultiplier assembly are fed through a fast amplifier to the fast coincidence unit of resolving time 18 x 10^{-9} sec. The pulses from the dynides are transmitted through amplifiers, through single channel analysers, to a triple coincidence unit with a resolving time of 10^{-6} sec, the pulses from which are recorded.

The gamma photons pass through the titanium powder housed in thecollimator the output from which is put in coincidence with a direct photon from the other channel. With this arrangement a beam of gamma photons with an energy of 892 KeV is selected into the channel where Ti is lodged while the direct beam passing through the other channel is of 1118 KeV energy. With the fulfillment of the condition for compensation an increased attenuation of the incident gamma photons is observed on account of resonance scattering. A purely absorbing material such as Al is incapable of producing any resonance scattering. In this arrangement the column of Ti - 46 powder is 1.25 cms. The length of aluminium with which observations of absorption are made, is so chosen that thesingles counts in either case is identical.

RESULTS AND DISCUSSION

Let the coincidence rate from Ti- 46 scatterer be N_{Ti} and that with Al scatterer be N_{Al} and the scattering angle be ϕ. The ratio $A \simeq N_{Ti}/N_{Al}$ as a function of ϕ is plotted as shown in fig.2. The average coincidence rate is 8 min $^{-1}$. From the plot it can be seen that the minimum of the curve represents maximum attenuation due to resonance scattering.

Setting the target in the fixed position the ration of the true to total coincidence is carefully measured using a delay coincidence method and the value N_{true}/N_{Total} is found to be 0.74 ± 0.01. With the results so obtained calculations of the resonance scattering cross-section are made akin to the method carried out by a previous worker (5), with the exception of the modification employed to match the size and form of the solid angle employed. In the present case, apertures and the scintillators, being circular the expression for the resonance scattering cross-section averaged over the appropriate solid angle can be written as,

$$\bar{\sigma}_{Ti\gamma} = \left[\frac{\Omega_1 \Omega_2}{W_1 W_2} \exp. \left\{ - \frac{\phi_1^2}{\Delta\phi_1^2} \right\} \right] \sigma_{max.} \quad \text{-- (12)}$$

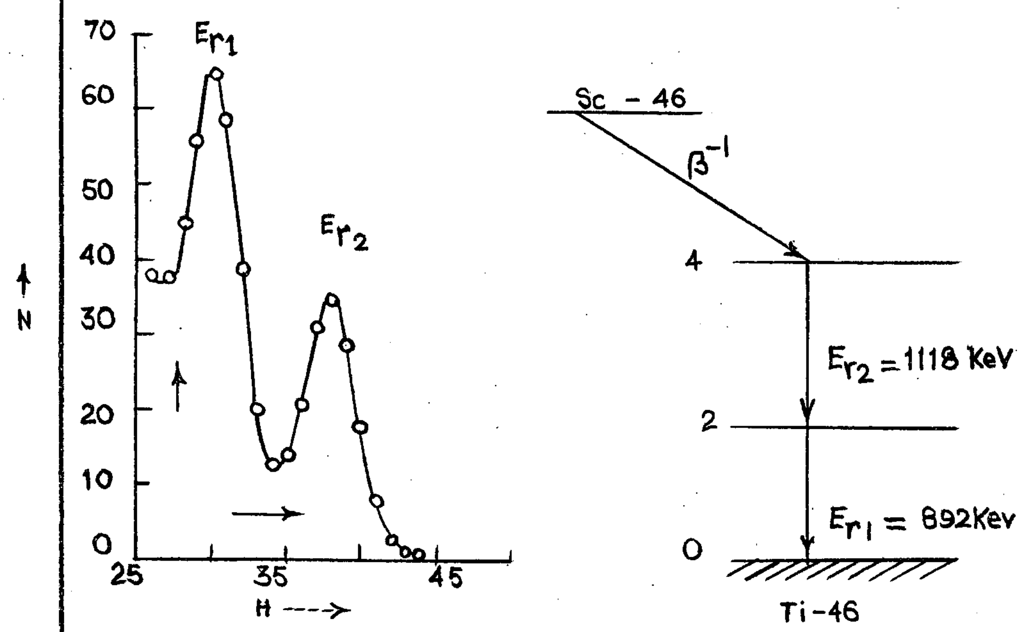

Fig. 1 DECAY SCHEME

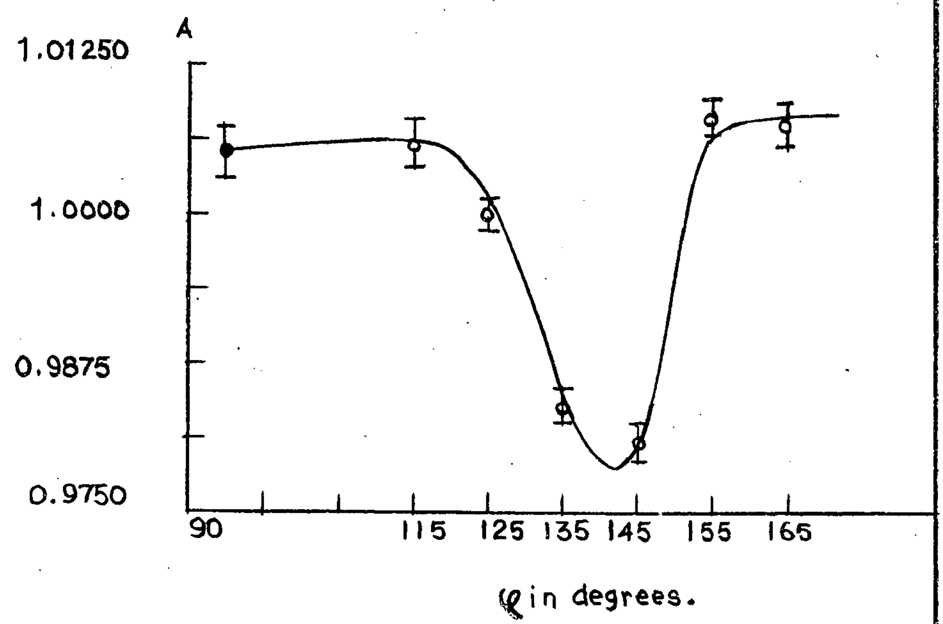

Fig 2 TRANSMISSION CURVE.

Ω_1 and Ω_2 (6) being the solid angles subtended by the slits of the collimators and W1 and W2 being the angles subtended by the detectors at the same central point of the source.

For a second order of smallness of ϕ_1 , which is occurring in the Eq. 12., can be expressed as

$$\phi_1 = 2\Omega_1 + \Omega_2^2 \cot\phi_0 + \frac{\Omega_2^2}{\sin\phi_0} \tag{13}$$

In the present case $\Omega_1 = \Omega_2$ = 0.02344 and W1 and W2 are equal to 0.02251. Substituting the values of W1 and W2 and Ω_1, Ω_2 in eqs. 13 and 12 and assuming that the angle subtended by the apparatus is greater than the angular line width $\Delta\phi$, the cross-section is obtained as

$$\sigma_{max} = 0.347 \pm 0.05 \text{ brans.}$$

Now recalling theoretically computed value which is equal to 0.3757 barns it can be seen that the present experimental value does verify and confirmthe validity of the theory.

The assumption employed for the derivation of the expression for the angle ϕ given by Eq. 2 may not be strictly true. Consequently it is required that the value of σ_{max} is to be employed with caution in deducing the width Γ of 892 KeV level (2^+state) of Ti-46. These assumptions involve that the recoil during beta decay is absent and the recoil motion of the nucleusafter emitting 1118 KeV gamma photon is regligible, which however cannot be deemed to be strictly true. The observation of the resonance effect is effective in as much as some nuclei are apt to lose their recoil energy after beta decay within the lifetime of the 2nd excited state (2.01MeV level), for which the recoil volicity is small and that no change of direction of motion is present during the lifetime of the 2^+ state in them.

On the basis of the conditions mentioned, the maximum cross-section fixes the level width at a lower limit for the 2^+ state of Ti-46 as 0.304×10^{-4} ev. This work with Co-56 and Ir-192 is in progress.

REFERENCES

1. K.G. Malmfors, Beta and Gamma-ray spectrometry, North-Holland Publication.
2. E. Pollard and D. Alburger, Phys. Rev. 74, 926 (1948).
3. V.F. Weisskopf, Physics. Rev. 83, 1073 (1951).
4. H.A. Bethe, Nuclear. Physics. (1950).
5. N.A. Burgov and Yu.V. Terekhov, J. Nucl. Energy, 11, 1958 Vol. 7 pp. 247 - 254.
6. A.H. Snell, Nuclear Instruments Vol.1. (1962).

DISCUSSIONS

R.M. Steffen: How does your value compare with the lifetime measurement done by delayed coincidences?

P.S. Raju: The measurement is in agreement with the lifetime measurement done by delayed coincidences.

E. Kondaiah: Is the source in the form of a solid or liquid?

P.S. Raju: The source is in liquid form — dissolved in dilute HCl.

J. Varma : Have you taken into consideration the angular spread of your detector?

P.S. Raju : Yes, we have taken into consideration the angular spread of our detector.

DECAY OF Hf^{183} AND NUCLEAR LEVELS OF Ta^{183}

H. Bakhru and S. K. Mukherjee
Saha Institute of Nuclear Physics, Calcutta

The first known report for the production of Hf^{183} nuclide was made by Gatti and Flegenheimer (1). They observed a half-life of 64 ± 3 min and assigned this to Hf^{183}. By means of Feather plot, they obtained a maximum beta energy of 1.4 MeV.

Hf^{183} was produced by irradiating natural W of spectroscopic purity having a natural abundance of 28.64% for W^{186} by means of DT neutron from Cockcroft-Walton accelerator. Radiochemical separation of Hf fraction was made. For identification and checking W isotopes enriched in W^{186} (98%) were employed. The possible known hafnium activities through (n,α) reactions on the different isotopes are Hf^{183} (64 min), Hf^{181} (46 days), Hf^{180} (5.5hr) and Hf^{179} (19 Sec). By suitably adjusting the irradiating time, it was possible to keep the contributions from all Hf-isotopes other than the desired Hf^{183} to a minimum.

EXPERIMENTAL RESULTS

Half-life Measurements:

The previous assignment of 64 ± 3 min activity to Hf^{183} by Flegenheimer was confirmed by observing a 64 ± 1 min activity in irradiation of enriched W^{186}. Fig.1 presents the half-life determined by following the gross beta-decay with a low background counter with a chemically separated source. Three half-lives of 64 min (Hf^{183}), 5.5 hrs (Hf^{180m}) and 91 days are observed. For identification and cross check for the 91 days activity a sample of tungsten enriched in W^{186} to 98% was bombarded and the decay

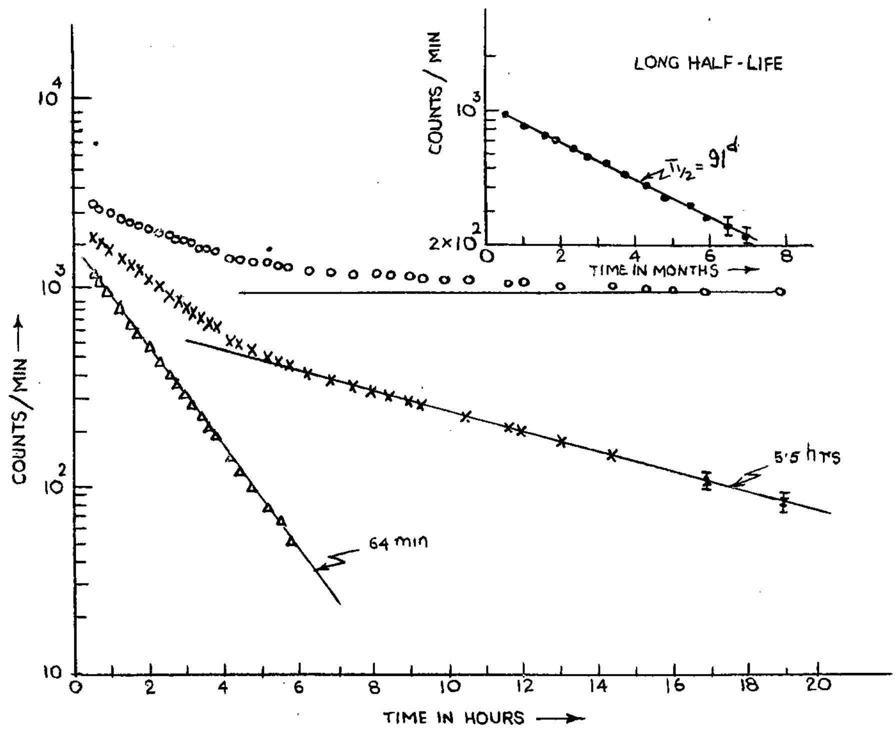

LONG HALF-LIFE
COUNTS / MIN
TIME IN MONTHS
$T_{1/2} = 91^d$
COUNTS/MIN
TIME IN HOURS
5.5 hrs
64 min

Fig. 1

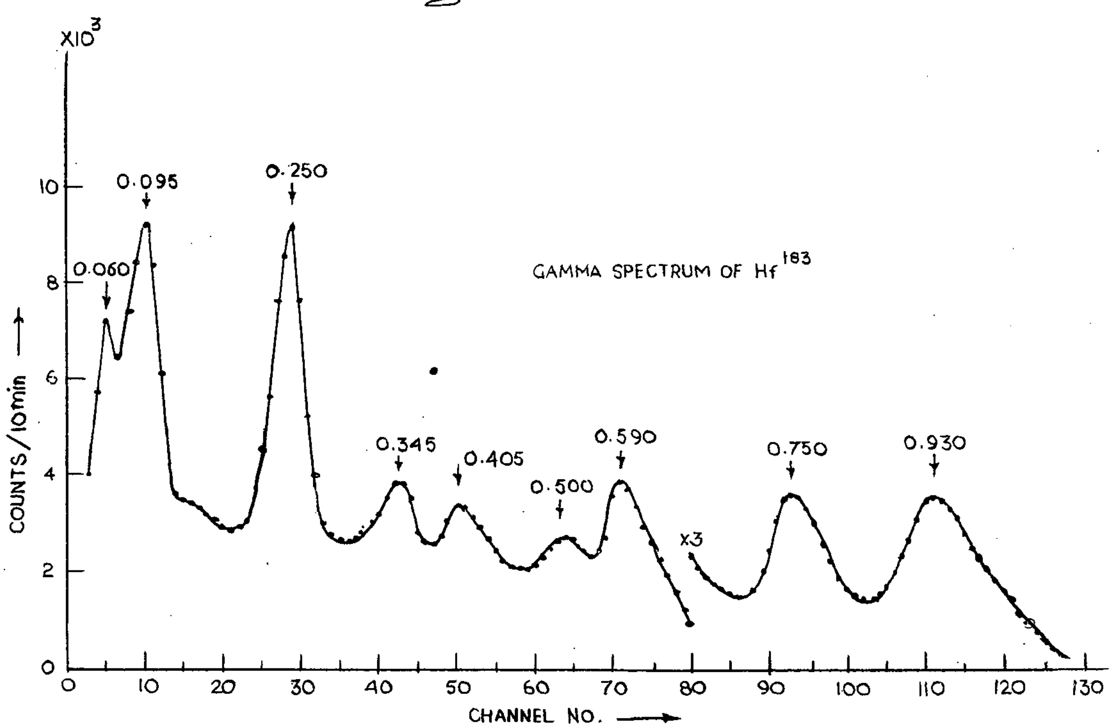

X10³
GAMMA SPECTRUM OF Hf¹⁸³
0.060
0.095
0.250
0.345
0.405
0.500
0.590
0.750
0.930
X3
COUNTS/10min
CHANNEL NO.

Fig. 2

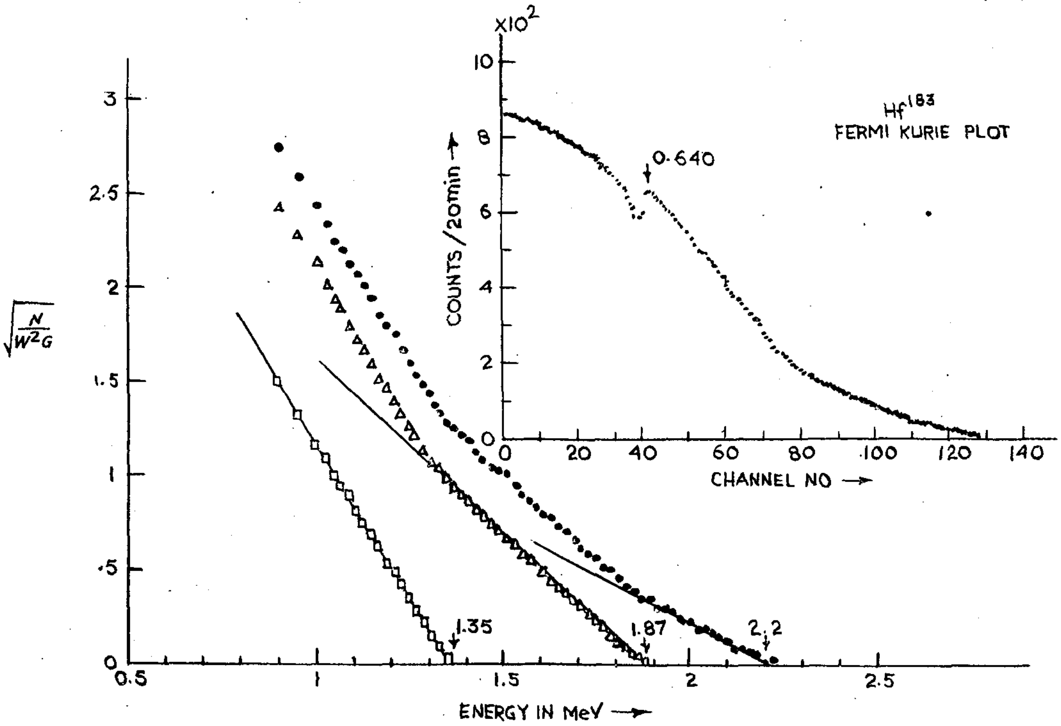

Fig. 3.

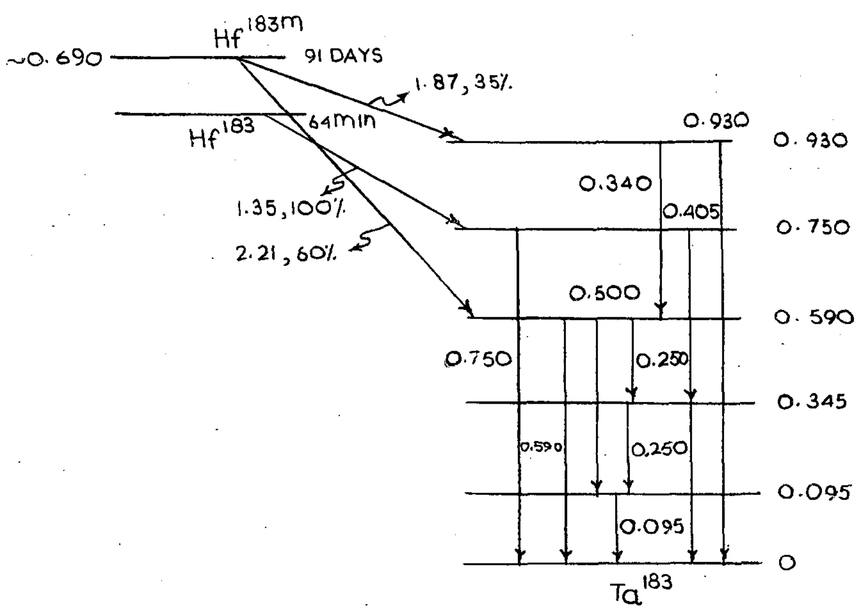

PROPOSED DECAY SCHEME OF Hf^{183}

Fig. 4.

of resulting products gave both the above half-lives.

GAMMA-RAY MEASUREMENTS

A gamma ray spectrum of Hf^{183} was taken with the 10.2 cm x 10.2 cm NaI (Tl) counter with chemically separated Hf-fraction (Fig. 2). The gamma-rays which decay with a half-life of 64 min are observed to have the energies 95 KeV, 250 KeV, 345 KeV, 405 KeV and 750 KeV. The 750 KeV photopeak was found to be a cross over peak. Another spectrum was taken after 48 hrs after the shorter lived activity had decayed out. A number of longer lived activities were identified and followed upto 8 months. The gamma rays which decay with a half-life of 91 days are 95, 250, 340, 500, 590, and 930 KeV.

BETA MEASUREMENTS

The Fermi-Kurie plot of beta spectrum exhibits threebeta groups of energy 2.21, 1.87 and 1.35 MeV (Fig. 3). Another spectrum was obtained by subtracting one spectrum taken at the 3rd hour from the end of bombardment from another taken at 15th min. This procedure eliminated any contamination from all longer lived activities due to other isotopes except 64 min Hf^{183}. From the Fermi-Kurie plot of the above subtracted spectrum, an end point energy of 1.35 MeV was obtained. An electron conversion peak at 640 KeV was observed in the first beta spectrum which decays with 91 days half-life.

COINCIDENCE RESULTS

For gamma-gamma coincidence, two 2" x2" NaI (Tl) crystals coupled to 6810A tubes were used. For beta-gamma coincidence assembly a 2" x $\frac{1}{2}$" Anthracene crystal and 2" x 2" NaI (Tl) crystals were used. The results are shown in Table 1. These experiments are done with 91 days activity.

TABLE I

Gamma-Gamma coincidence		Beta-Gamma coincidence	
Gamma energy selected in (KeV)	Coincident Gamma Energy in (KeV)	Gamma Energy selected in (KeV)	Coincident Beta energy (MeV)
95	250, 340, 500	95	2.21, 1.87
250	95, 250, 340	250	2.21, 1.87
340	95, 250, 340 500, 590	930	1.87

Beta-gamma coincidence experiments with 64 min Hf^{183} activity showed that when gated with 340 KeV gamma, all the three beta groups are observed, and when gated with 750 KeV gamma a single beta group with end point energy of 1.35 MeV is observed.

Based on above results, a decay scheme of Hf^{183} shown in Fig.4 is proposed.

REFERENCES

1. O.O. Gatti and J. Flagenheimer, Z. Naturforsch. 11A 679 (1956).

2. Nuclear data sheets, National Research Council Washington, D.C.

DISCUSSIONS

C.V.K. Baba: The levels of Dy^{162} are known from the decay of Ho^{162}. There the log ft values found one low. Do you also find low log ft values in the Tb^{162} decay?

H. Bakhru: Yes, the log ft values are found to be low.

Kondaiah: How muchmaterial did you use in your experiments?

H.Bakhru: 10 to 15 gms.

THE ISOTOPE Tb^{162} AND ITS DECAY CHARACTERISTICS

H. Bakhru and S. K. Mukherjee
Saha Institute of Nuclear Physics, Calcutta

In 1951, Butement (1) reported for the first time the existence of an isotope having a half-life of 14 min which he assigned to Tb^{162} or Tb^{163}. Willie and Fink (2) next reported an activity decaying with a half-life of 7 min and assigned this to Tb^{163}. But a subsequent report by Takahashi et al (3) in 1062 assigned to Tb^{163} an activity of 6.5 hr. Recently inserted data in Nuclear data sheets (4) showed the half-life of 7 min and 2 hr assigned to Tb^{162}.

In order to identify the Tb^{162} activity, we have produced this activity by (n,α) reaction on Ho^{165} (100% abundance) and also by (n, p) reaction on Dy^{162} (25.5 % natural abundance). The other possible reactions with Ho^{165} (specpure sample) through (n, 2n, (n, p) and (n,α) being well known it was easier to identify Tb^{162} obtained through (n,α) reaction. This was verified by bombarding natural specpure Dy having Dy^{162} (25.5% abundance) and also samples having Dy^{162} enriched to 98%. Tb^{162} thus obtained through (n,p) reaction became relatively easy to identify.

HALF-LIFE MEASUREMENT

The half-life was measured by the following different ways.

(a) Samples produced by $Ho^{165}(n,\alpha)\ Tb^{162}$ reaction and activities measured by G.M. Counter. Even with samples irradiated for 10 min, the 39 min activity due to (n, 2n) products almost masked the 7.5 min activity of Tb^{162}.

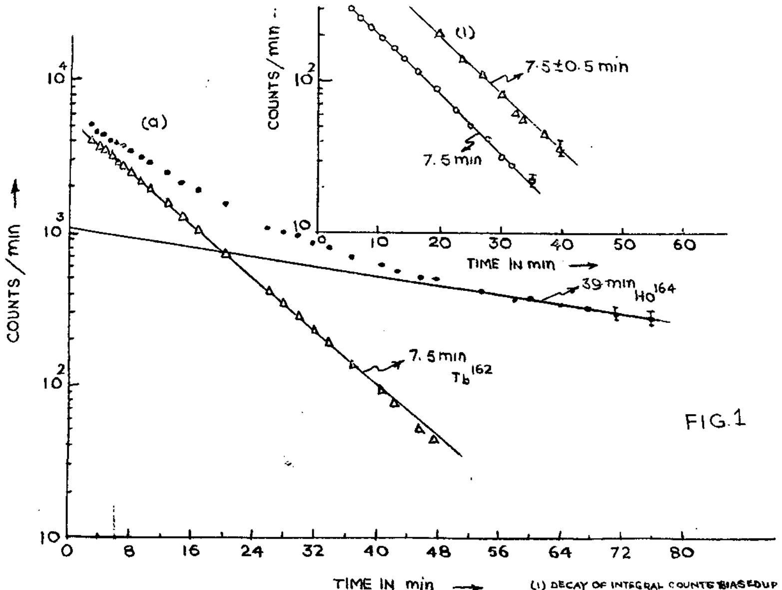

FIG.1

(a) DECAY OF 81 KeV GAMMA $Ho^{165}(n,\alpha)Tb^{162}$

(b) (1) DECAY OF INTEGRAL COUNTS BIASED UP TO 200 KeV BY A LEAD ABSORBER

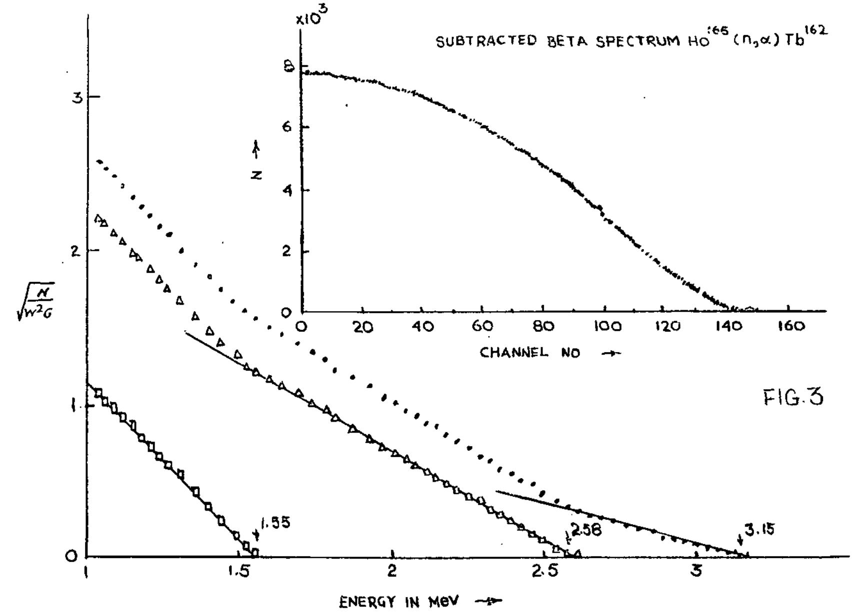

FIG.3

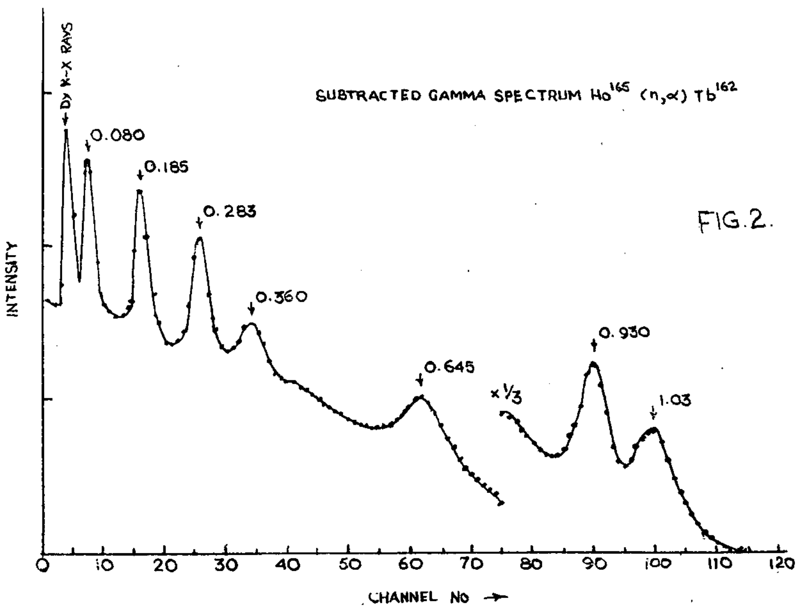

FIG.2.

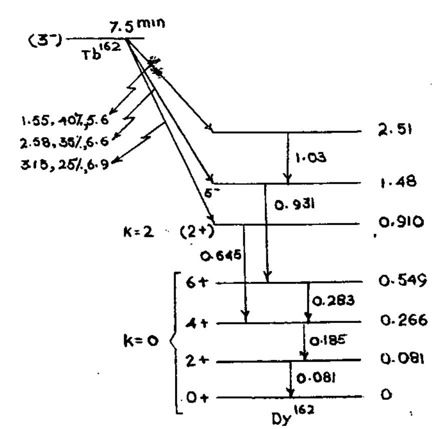

PROPOSED DECAY SCHEME OF Tb^{162}

FIG.4.

(b) Samples produced as above and decay of 81 KeV gamma ray was measured by gamma spectrometer (Fig. 1.a)

(c) The same sample was also measured by cutting off all gamma rays below 200 KeV by inserting a lead absorber (Fig. B.i)

(d) Sample produced by Dy^{162} (n,p) Tb^{162} reaction and decay of 0.283 MeV gamma ray followed (Fig. B.ii). The result of all the above measurements gave a half-life of 7.5 $\pm$ 0.5 min.

BETA SPECTRUM MEASUREMENT

The Fermi-Kurie plot of the beta groups having an end point energy of 3.15 MeV (25%), 2.58 MeV (35%) and 1.55 MeV (40%). All the longer lived activities were subtracted and results are presented in Fig. 2.

GAMMA-RAY MEASUREMENTS

Gamma spectrum was taken with a 4" x 4" NaI (Tl) crystal together with 512 channel analyser. The gamma rays decaying with a half-life of 7.5 min are picked out as 81, 185, 283, 645, 931 and 1030 KeV. Fig. 3.

COINCIDENCE MEASUREMENTS

The results are shown in Table I.

TABLE I

Beta-gamma coincidences		Gamma-gamma coincidences	
Gamma ray in Gate (KeV)	Coincident end point energy (MeV)	Gamma ray in Gate (KeV)	Coincident Gamma rays (KeV)
81	3.15, 2.58, 1.55	81	185,283,645, 931, 1030
185	3.15, 2.58 1.55	185	81, 283, 645, 931, 1030
283	2.58, 1.55	283	81, 185, 931, 1030
645	3.15	645	81, 185
931	2.58, 1.55		
1030	1.55		

Based on above results a decay scheme of Tb^{162} as shown in Fig. 4 is proposed and following conclusions are drawn.

1) Half-life of 7.5 $\pm$ 0.5 min should be attributed to isotope Tb^{162}. Tb^{162} decays by three beta groups having the end point energies of 3.15, 2.58 and 1.55 MeV.

2) The ground state of Tb^{159}, Tb^{161} and Tb^{163} all have a configuration of 3/2 +(5). From the Nilsson diagrams a 3/2 + 411 state is expected for large deformations. This proton state seems insensitive for variation of the number of neutrons. Spin values 3/2 and 5/2 are deduced from experiments for odd-A nuclei with 93, 95, or 97 neutrons. These values agree with the states $3/2^-$ [521] , $5/2^-$ [532] and $5/2^+$ [413] expected on the basis of the Nilsson diagrams for nuclei with an odd number of neutrons of

about 97. A 3^- ground state of Tb^{162} is obtained by coupling of the $3/2^+$ 411 proton state with the $3/2^-$ 521 neutron state. This is in accordance with coupling rules of Gallagher and Moszkowski (6) in odd nuclei.

REFERENCES

1. F.D.S. Butement, Proc. Phys. Soc. (London) 64A 395 (1951).
2. R.G. Wille and R.W. Fink, Phys. Rev. 118, 242 (1960).
3. K. Takahashi, J. Phys. Soc. (Japan) 17, 1229 (1962).
4. Nuclear Data Sheets National Academy of Sciences, Washington, D.C., (1964).
5. J.M. Baker and B. Bleaney, Proc. Phys. Soc. 68A 257 (1955).
6. C.G. Gallagher and S.A. Moszkowski, Phys. Rev. 111, 1282 (1958).

"GAMMA RAY ANGULAR CORRELATION STUDIES IN NUCLEAR REACTIONS"

M.A. Easwaran
Nuclear Physics Division
Atomic Energy Establishment Trombay

INTRODUCTION

Gamma ray angular correlation experiments play an important role in the study of low-lying states in nuclei. In this talk I shall be describing the gamma-ray angular correlation experiments which are applicable for the study of states in nuclei excited in nuclear reactions. We shall particularly consider the recent methods and procedures developed for the measurement and analysis of these correlation experiments since these methods are independent of any assumption regarding reaction mechanisms. These procedures were developed by Litherland and Ferguson (1).

Before going to the details of these methods let us consider the limitations of simpler type of gamma-ray angular distribution experiment. The interpretation of the simplest angular distribution namely the angular distribution of an outgoing gamma radiation with respect to the bombarding beam is usually attended by ambiguity. This is due to the fact that such a simple experiment does not provide very much information. More specially in a typical experiment when multipolarity of the gamma ray is limited to quadrupole the angular distribution can be represented by the formula,

$$W(\theta) = a_0 P_0(\cos\theta) + a_2 P_2(\cos\theta) + a_4 P_4(\cos\theta) \quad (1)$$

where $W(\theta)$ is the intensity of the radiation at the angle θ relative to the incident beam and the a_k are the coefficients of the corresponding legendre polynomials $P_k(\cos\theta)$. It happens very often that the angular distribution coefficients are a function of several unquantized parameters for example, channel spin mixtures and orbital angular momentum mixtures for the incoming particles and a multipole mixture for the outgoing gamma-ray. Hence, it may be possible to adjust the parameters to fit the measured a_2/a_0 and a_4/a_0 for several choices of the spin of the state. In such a case the spin could not be determined from the measurements.

It has been pointed out by Ferguson (2) that substantially more information can be obtained from a triple correlation such as the reaction (p,γ,γ). Assuming the axis of quantization to be defined by the incoming particle beam, the intensity of the two gamma rays in coincidence will be a function of the polar angles θ_1 and θ_2 for each radiation and the relative azimuthal angle φ between them. In this case the intensity is given by the series.

$$W(\theta_1, \theta_2, \varphi) = \sum_{KMN} a^N_{KM} \quad X^N_{KM} \quad (\theta_1, \theta_2, \varphi) \qquad (2)$$

where the functions $X^N_{KM}(\theta_1\, \theta_2\, \varphi)$

have angular dependence in the form,

$$P^N_K(\cos\theta_1) \quad P^N_M(\cos\theta_2) \quad \cos N\varphi$$

K and M are limited by the multipolarities of the two gamma rays and are even, if the nuclear states have sharp spin and parity and N is positive or zero, may be even or odd and does not exceed the smaller of K and M; corresponding to quadrupole radiations K and M are restricted to maximum value of 4 and in these cases the series (2) has 19 terms. For a sufficiently varied set of points the angle functions of series (2) are linearly independent, so that the coefficients a^N_{KM} can all be determined. It may be seen that the amount of available information (i.e.) the number of measurable parameters generously exceeds the number of unknowns comprising the channel spins and orbital and multipole mixing ratios. These considerations are applicable when all the states concerned have definite spins and parities. This will be

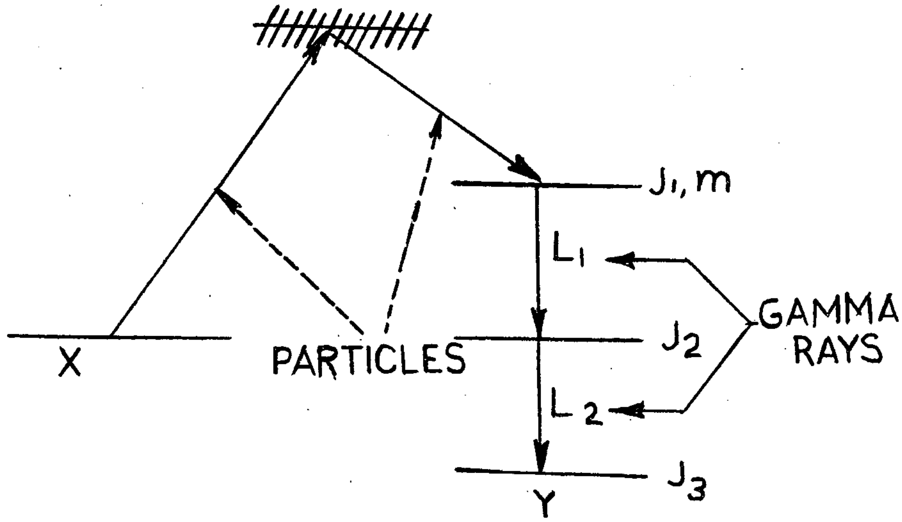
J1, m
L1
GAMMA
RAYS
J2
X
PARTICLES
L2
J3
Y

Fig. 1

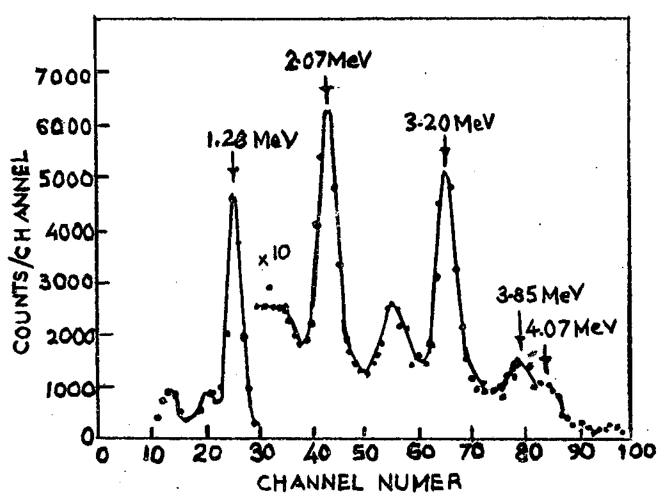
2.07MeV
3.20MeV
1.28 MeV
x10
3.85 MeV
4.07MeV
COUNTS/CHANNEL
7000
6000
5000
4000
3000
2000
1000
0
0 10 20 30 40 50 60 70 80 90 100
CHANNEL NUMER

Fig. 3.

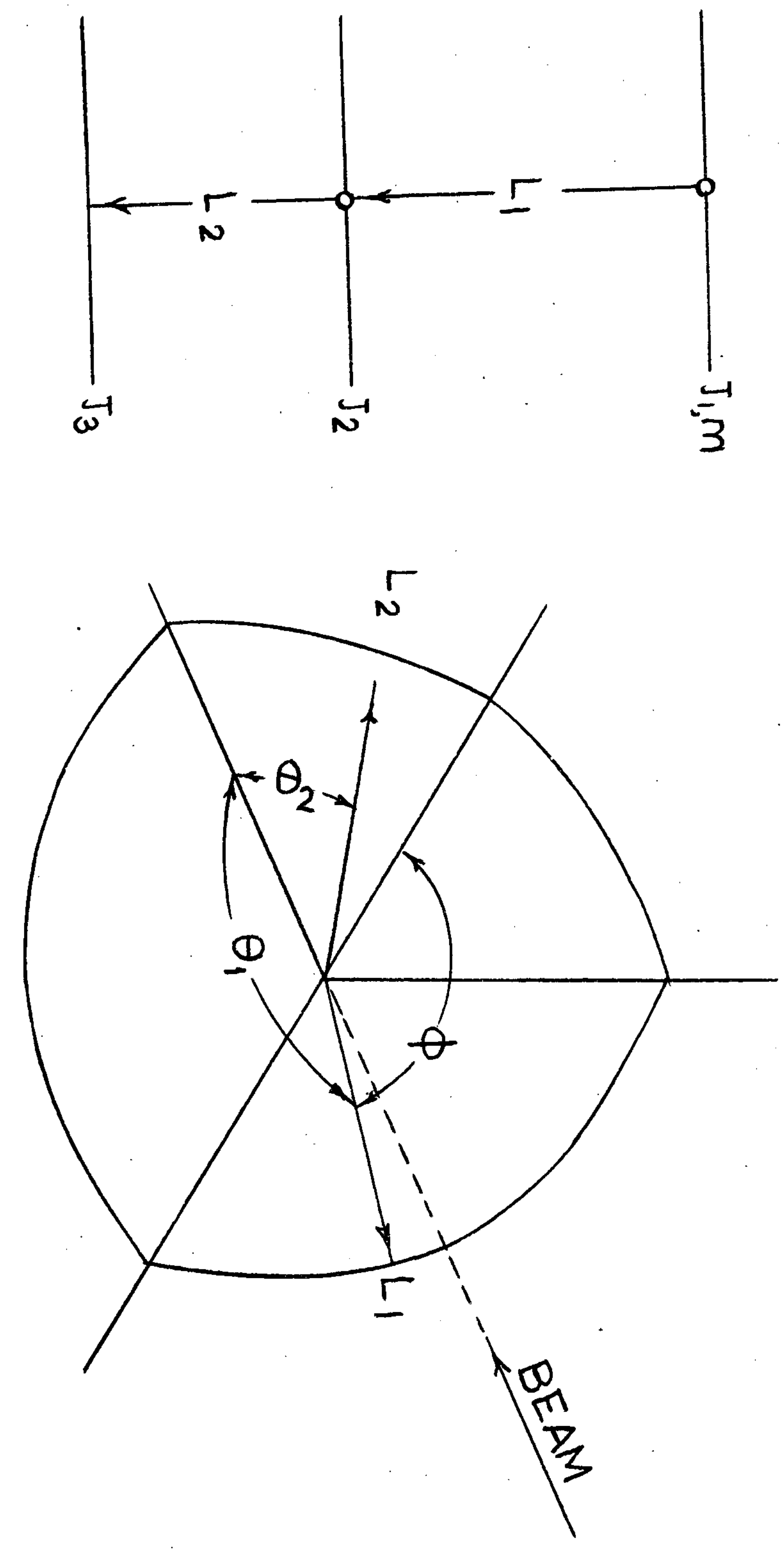

Fig.2.

the case only if the incident particle is captured in a sharp well isolated resonance. Very often the reaction may not be proceeding through a well isolated resonance, the compound state formed by the capture of a particle of several MeV energy will be too complex due to the excitation of several overlapping levels. Or in cases like deuteron bombardment the reaction may be dominated by direct interaction type of behaviour for which compound state has no definite spin. To enable the interpretation of gamma-ray angular correlations in such cases to derive the properties of the states in the residual nucleus, the present procedures have been developed. The essential feature of these methods is to consider a state of sharp spin and parity in the residual nucleus prepared in a way such that there are certain strong limitations on the population of magnetic substates. The subsequent decay of this state can then be treated as if it were aligned.

METHOD I

Let us consider a reaction $X(h_1, h_2)Y^*$ the process of which is illustrated in fig. 1. J_1, J_2, J_3 are the spins of the states in the residual nucleus Y and L_1 and L_2 are the multipolarities of the gamma radiations from the decay of the states. 'm' refers to magnetic substate of state J_1. The cross hatching on the compound state indicates that it need not have sharp spin and parity.

The state of spin J_1, which is formed in the nuclear reaction as the final one involving the capture of an unpolarized particle incident along the Z-axis followed by emission of one or more unobserved radiations in cascade is symmetric about the beam axis. The state is then aligned. Since the state considered has definite parity and if no polarization is present in the incident particles and target, there is symmetry between the population of the positive and negative magnetic substates (i.e.) P (m) = P(-m) where P(m) refers to the population of magnetic substate 'm'. In this experiment the outgoing particle in the reaction are not observed and coincidence correlation of the two cascade gamma rays from the decay of the state J_1, are measured. In such a case, Litherland and Ferguson(1) have pointed out that angular correlations of the radiations from the well defined state J_1 can be described independently of the complexity of the compound nucleus and its formation since there is an unobserved radiation from the compound nucleus to the sharp state. The parameters determining the angular correlations are the magnetic substate populations P(m) of state J_1 and the multipole ratios of the succeeding radiations. The number of independent magnetic substate population parameters required to describe the state of spin J_1, is $J_1 + 1$ or $J_1 + 1/2$ depending on whether J_1 is integral on half integral. The angular correlations of subsequent gamma rays from this state are homogeneous in these parameters so that one parameter can be indentified as a normalization factor which need not be measured. The essential number of parameters is consequently J_1 or $J_1 - 1/2$. If the state decays with the emission of two gamma rays in cascade then two more unquantized parameters comprising the multipole mixing ratios of the transitions must be expected. As an example, the correlation between two cascade gamma rays from a state of spin 4 will entail 6 parameters. As we have seen before, the measurement of such a triple correlation can yield 18 parameters so that ample information for the determination of the unknowns is generally available.

The correlation function $W(\theta_1, \theta_2, \varphi)$ in terms of the population parameters and the multipole mixing ratios is given by Litherland and Ferguson(1) and quoted in reference (3). The general geometrical form of the function is quoted here in the following equation.

$$W(\theta_1, \theta_2, \varphi) = \sum_{\substack{m \\ L_1 L_1' L_2 L_2'}} P(m)\, \delta_1^{p_1} \delta_2^{p_2} \sum_{KMN} C_{KM}^{N} (J_1\ J_2\ J_3\ L_1\ L_2\ L_3\ m)\, Q_K Q_M X_{KM}^{N}(\theta_1 \theta_2 \varphi) \tag{3}$$

The angular dependence of the functions X_{KM}^{N} $(\theta_1, \theta_2, \varphi)$ and the restrictions on the values of K, M and N are the same described with regard to equation(2). δ_1 and δ_2 are the quadrupole to dipole amplitude mixing ratio for the first and second radiations. The exponents p_1 and p_2 take on the values 1 and 2 depending on L_1, L_1' and L_2, L_2' (for pure dipole radiation p = 0 for mixed dipole quadrupole p = 1 and for pure quadrupole p = 2) Q_K and Q_M are the correlation attenuation factors (4) introduced for taking the finite solid angle of the gamma ray detectors into account. The coefficients C_{KM}^{N} involve the vector coupling and Racah coefficients and 9-j symbol. Most convenient tabulation of the C_{KM}^{N} coefficients are given in reference (3). Till todate in the experiments done, the second radiation is a pure one and only the first radiation involves a multipole mixing ratio. Hence for further discussions here we will omit the term δ_2.

Not much use has been made of the general triple correlation measurements upto date but limited information have been derived by employing specific geometries of arrangements of counters (i.e) by keeping two of the angles θ_1, θ_2, and φ fixed and varying the third. For example Broude and Gove (5) have made an extensive series of triple correlation measurements for the study of levels in even-even nuclei from Ne^{20} to S^{32} by exciting the levels by inelastic scattering of protons. By carrying out the analysis by the population parameter method they have assigned spins to 14 levels.

We shall now consider the analysis of data to derive information regarding the spins of the levels and multipole mixtures. If θ_1, or θ_2 is chosen to be $\pi/2$ then the terms with odd N will vanish in the expansion since associated Legendre polynomial $P_K^N(\cos\pi/2)$ or $P_M^N(\cos\frac{\pi}{2})$ will vanish unless both indicies are even or odd. Since K and M are even only terms with even N will be present for this choice of angles, consequently the total number of terms in the expansion will be reduced to 15. All associated Legendre polynomials with both indicies even can be expanded in terms of Legendre polynomials and hence in such geometries the data can be analysed in terms of Legendre polynomials. Further the whole analysis can proceed in two stages(i.e.) first a least square fitting procedure is done on the data points to get the coefficients corresponding to various Legendre polynomials and these coefficients are then treated as data for another least square fitting procedure to get the values of the unknowns P(m) and δ values for different choices of spins J_1, J_2, J_3. However since there are definite advantages in carrying out the analysis in a single stage (i.e.) to get the unknown P(m) values directly from the data points we shall now consider this method of analysis in detail.

In this method series in equation (3) is used in fitting the data. Direct linear least squares fitting procedure is carried out using the data points $W(\theta_1, \theta_2, \varphi)$ where P(m) values are the unknowns for specific choice of J_1, J_2, J_3 and δ_1. Using the multipole mixing parameter $\tau = \tan\delta_1$

least squares fitting is carried out taking τ in steps of 5° or 10° from − 90° to + 90°. This procedure is repeated for different choices of spin combinations of the levels and by locating the minimum in the χ^2

(the weighted sum of the squares of the deviations of the measured points) the spin values and δ_1 value are determined.

APPLICATION OF METHOD I

As an application of this method I shall now describe an experiment carried out by Broude and Eswaran (6) for the study of levels in Ne^{22} excited by the reaction F^{19} (α, p) Ne^{22}. The first three excited states in Ne^{22} are at 1.277, 3.343 and 4.473 MeV and coincidence gamma ray angular correlations of the cascade decays from the second and third excited states through the first excited state have been measured. 6.5 MeV alpha beam from the Chalk River tandem accelerator is used to bombard a target of approximately 700μg/cm^2 Barium Fluoride evaporated on gold backing. The target was mounted in a target chamber located at the centre of an angular correlation table. Three 5 in. dia. x 6 in. thick NaI (Tl) detectors were, mounted on the angular correlation table at a distance of 6¼ in. from the target. One gamma ray detector could be rotated both in altitude and in azimuth with respect to the beam and was used to measure gamma ray intensities over the edges of the octant shown in fig.2. A second detector could be rotated only in horizontal plane. Third detector is not movable. These will be referred to as the movable, fixed and monitor detectors respectively.

In the correlation measurements three spectra were recorded at each angle. In the terminology of fig.2. the spectra are (1) gamma rays in the movable detector in coincidence with L_2 in the fixed detector (2) gamma rays in the fixed detector in coincidence with L_2 in the movable detector (3) gamma rays in the monitor detector in coincidence with L_2 in the fixed detector. The bombarding energy was chosen to allow simultaneous measurement of the correlations from the 3.34 and 4.47 MeV states. Fig. 3

shows a typical spectrum from the movable detector in coincidence with the fixed detector. Gamma rays from the group of close states around 5.3 MeV in Ne^{22} are also seen but the levels are too close for useful analysis.

The first two of the spectra described above give simultaneous measurement of independent points of the correlation function. The third spectrum is used as a monitor. The three spectra were accumulated in part of a 900 channel multidimensional analyser used in conjunction with two fast coincidence circuits two 100 channel pulse height analysers and digital stabilizers(7). The details of these electronicsystem can be found in (6). An added convenience for rapid data reduction was the use of a PDP -1 computer with direct access to the multichannel analysers, allowing rapid transfer of data to the computer memory and subsequent evaluation of peak and background areas for estimates of gamma ray relative intensities.

The correlation measurements were made in two sets; the movable detector was set at angles in the octant spaced by 15° (with one point missed because the movable counter is obstructed by the monitor counter) with the fixed detector being at 90° to the beam and then 65° to the beam. The 17 points in each set were measured in random order. Each measurement gives two independent points on the correlation function of each level when the gamma ray intensities in the movable and fixed detector spectra are normalized to the corresponding gamma ray intensity in the monitor spectrum. This gives four sets of 17 measurements each for each of the two levels, these sets or geometries are internally normalized by the use of monitor counter. The four geometries are as follows:

1) L_1 detected in fixed detector at 90° to the beam

2) L_2 detected in fixed detector at 90° to the beam

3) L_1 detected in fixed detector at 65° to the beam

4) L_2 detected in fixed detector at 65° to the beam

The common points among the geometries are expressed in the following identities:

$$W_1\,(65°,\ 180°) = W_4\,(90°,\ 180°) \quad \& \quad W_2\,(65°,\ 180°) = W_3\,(90°, 180°)$$
$$W_1\,(65°,\ 270°) = W_4\,(90°,\ 90°) \quad \quad W_2\,(65°,\ 90°) = W_3\,(90°,\ 90°)$$

where in the notation $W_i\ (\theta,\ \varphi)$, i refers to the geometry, θ refers to the movable detector elevation angle and φ the azimuthal angle. The common points between geometries 1 and 2 include the complete arc for which θ is 90°. Using the above common points the intergeometry normalization is carried out. Hence complete set of 68 normalized data points with weights are available for each of the two levels. These sets of data points were analysed by least squares fitting procedure using a computer program written by Dr. A.J. Ferguson. The data points are fitted directly from equation (3) with the magnetic substate populations as parameters. In these measurements the second radiation L_2 is a transition from spin 2 first excited state to spin 0 ground state and hence it is a pure quadrupole. The least squares fitting is performed for a fixed spin value for J_1 and a fixed multipole mixing ratio δ_1 for the primary radiation. The fit is repeated over the range of S_1 appropriate to the spin value for spin choices of 0 to 4 for J_1. The result of this fitting is a series of χ^2 values versus multipole mixing ratio for each spin value.

In figs. 4 and 5 are shown the normalized angular correlation measurements from the 3.34 and 4.47 MeV state in Ne^{22}. In figs. 6 and 7 are shown the plots of χ^2 verus τ (= $\tan^{-1} \delta_1$) for spins 0 to 4 for each of the two correlations. The fits have been made at equal intervals in τ

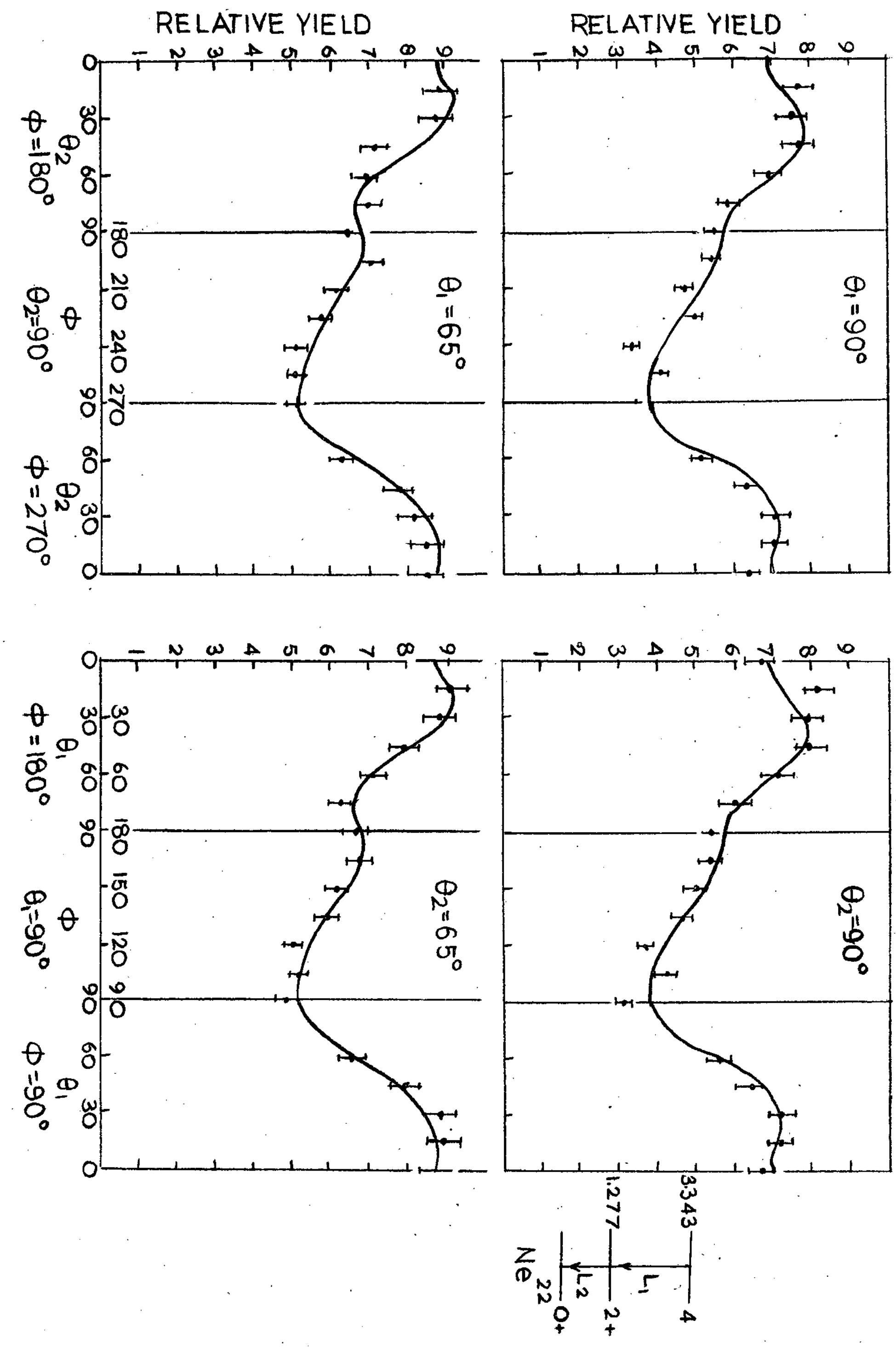
RELATIVE YIELD
$\theta_1 = 90°$
$\theta_2 = 90°$
$\theta_1 = 65°$
$\theta_2 = 65°$
θ_2
$\Phi = 180°$
$\theta_2 = 90°$
$\Phi = 270°$
θ_1
$\Phi = 180°$
$\theta_1 = 90°$
$\Phi = 90°$
Φ
3.343
1.277
4
2+
0+
L_1
L_2
Ne^{22}

Fig. 4.

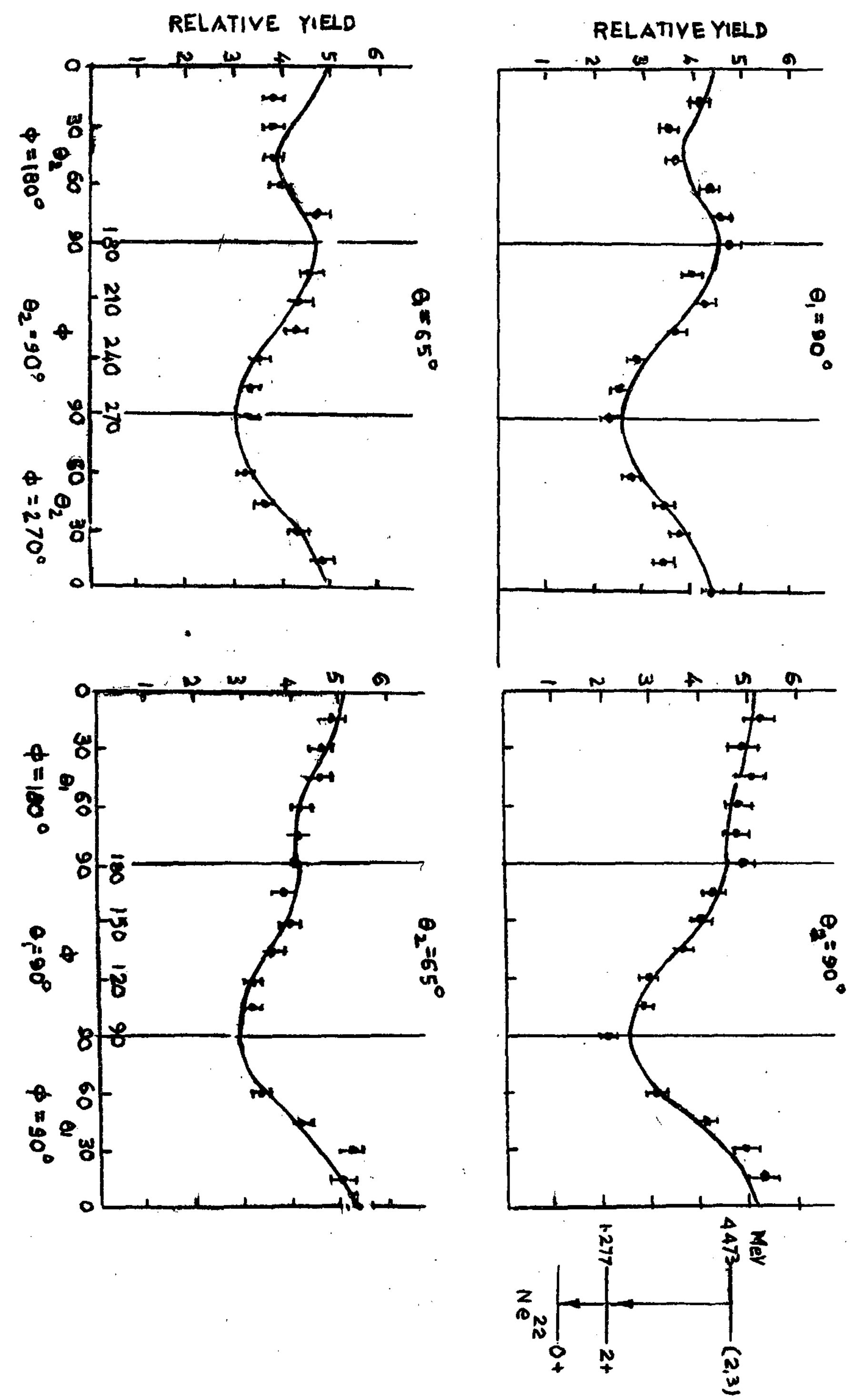
RELATIVE YIELD
RELATIVE YIELD
$\theta_1 = 90°$
$\theta_2 = 90°$
$\theta_1 = 65°$
$\theta_2 = 65°$
$\Phi = 180°$
$\theta_2 = 90°$
$\Phi = 270°$
$\Phi = 180°$
$\theta_1 = 90°$
$\Phi = 90°$
MeV
4.473
1.277
(2,3)
2+
0+
Ne^{22}

FIG: 5

with extra fits in the regions of χ^2 minima. Levels of statistical significance in χ^2 are drawn to show that the fits are consistent with the statistical accuracy of the measurements. The points plotted as crosses represent fits which have some negative populations but as none of these are statistically significant they need not be investigated further.

It can be concluded from χ^2 minima in these plots, that the spin assignment to the 3.34 MeV state is 4. An ambiguous assigment of 2 or 3 can be made to the 4.47 MeV state. The quadrupole to dipole amptitude ratio δ_1 for spin 2 fit is -0.11 and for spin 3 fit, δ_1 = 1.07. The solid curves in figs. 4 and 5 are the theorëtical fits for spin 4 and spin 2 respectively. The full parameters for the fits are given in table I.

TABLE I

Normalized (P (0) =1) population parameters P(m) and multipole mixing ratio δ_1 for the least squares fits to the correlations.

Level energy MeV	Spin	P(1)	P(2)	P(3)	P(4)	δ_1
3.34	4	1.27	0.63	0.025	0.086	
4.47	2	0.54	0.25			-0.11 ± 0.03
	3	1.19	0.90	0.30		-1.07 ± 0.10

METHOD II

Now I shall mention the basic features of the second method in which the angular correlation of gamma ray is measured in coincidence with the outgoing particle in the nuclear reaction the particle being detected at zero or 180° with respect to the beam in a small counter. This method has been developed and discussed in detail by Litherland and Ferguson (1).

Let us consider a reaction $X(h_1, h_2)\ Y^*$ the process of which is illustrated in fig. 8. 'a' is the spin of the target nucleus and δ_1 and δ_2 are the spins of incoming and outgoing particles in the reaction. 'c' is the spin of the excited state Y^* of the residual nucleus and this state decays by gamma emission of multipolarity L to the state of spin 'd'. 'γ' refers to the magnetic substate of state of spin 'c'. The outgoing particles P_2 are detected in a small counter at 0° or 180° with respect to the beam and the angular distribution of the subsequent de-excitation gamma ray is measured in coincidence with the detected particles.

If a state is formed by the absorption on of an unpolarized particle in the direction of the quantization axis followed by the emission of a second particle which is detected along the same axis, then the magnetic substates which can be populated do not exceed the sum of the spins of the target nucleus and the incident and emergent particles. This arises basically from the fact that orbital momenta contained in plane waves in the direction of the quantization axis have only zero projections on this axis. The system clearly has axial symmetry. Further since the state has definite parity the population of the positive and negative magnetic substates will be equal.

Hence according to these considerations the magnetic substate γ of the state of spin 'c' is limited by a, δ_1 and δ_2 (i.e.)

$$= a + \delta_1 + \delta_2 \qquad (4)$$

This conclusion is independent of the presence of interfering compound state spins b or the interfering orbital angular momenta of the incoming and outgoing particles.

The angular distribution of the gamma ray emitted from the state is

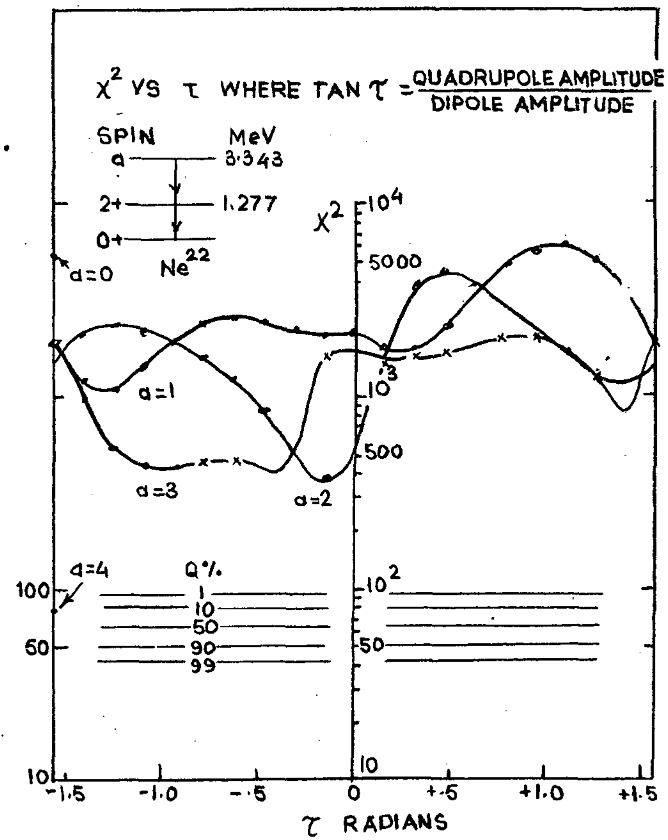

Fig 6.

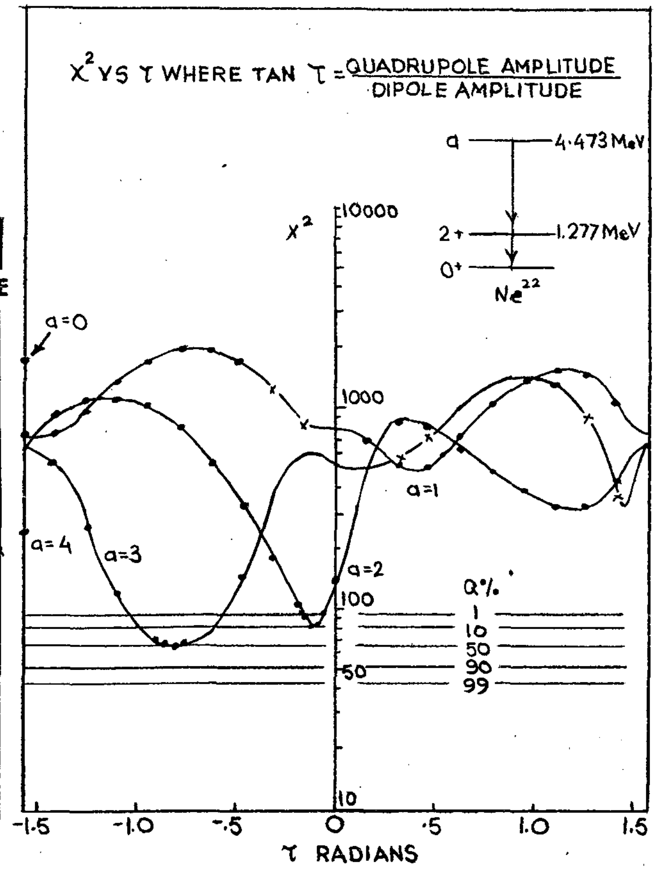

Fig. 7.

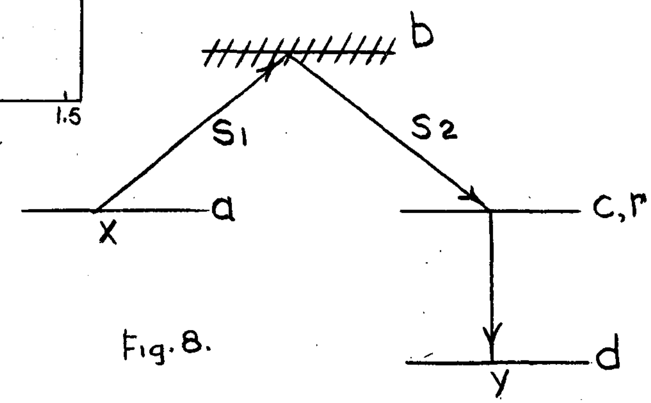

Fig. 8.

then governed by the population parameters P (γ) and the multipole mixing ratio of the gamma radiation. The distribution will be of the form given in equation (1) and the information obtainable will in general be the ratios a_2/a_0 and a_4/a_0. Thus if no more than two arbitrary parameters describe the distribution then the amount of information will be just sufficient or in favourable cases, more than sufficient to determine them.

The angular distribution function of the gamma ray in terms of the magnetic substate population parameters is given as

$$W(\theta) = \sum_{\gamma k p} (-1)^{f} P(\gamma)\, \delta^{p}\, (c\,\gamma\, c\, -\gamma / k\, o)\, Z_1 (L c L' c, d k)\, Q_k P_k(\cos\theta) \qquad (5)$$

where δ is the quadrupole to dipole amptitude mixing ratio and Q_k is the attenuation factor due to the finite solid angle of the gamma detector. Z_1 is the coefficient tabulated by Sharp et al (8) and $f = d + \gamma + L + L' + k/2$

If $a + s_1 + s_2 \leqslant 0$ Or $\frac{1}{2}$ then there is only one population parameter in the distribution function which can be treated as normalization constant and hence only unknown is δ for a specific choice of spins c and d. If $a + s_1 + s_2 \leqslant 3/2$ or 1 then one unknown ratio $P(3/2)/P(1/2)$ or $P(1)/P(0)$ will occur in the function in addition to the unknown value of δ. Since this is a double correlation measurement giving only two parameters a_2/a_0 and a_4/a_0 this method is of limited applicability. But very often there will be more than one gamma ray from the decay of a state and hence the measurements of angular correlation of all these gamma rays in coincidence with the particle group feeding the state will provide additional information.

APPLICATION OF METHOD II

This method has been usefully employed in the study (9) of the low lying levels of Ne^{20} excited by the reaction $C^{12}(C^{12}, \alpha)\, Ne^{20}$. The

C^{12} ion beam from the tandem accelerator was well collimated by a pair of gold apertures 1/8 inch in diameter 1 meter apart and the alpha particle counter which was a silicon p-n junction detector was placed at zero degree to the incident beam. The incident beam is stoped in the target backing. The alpha particle detector was substending a cone of half angle 5° at the target. Gamma rays were detected in a 5 inch dia x 6 inch thick NaI (Tl) crystal situated with its front face at $6\frac{1}{4}$ inch from the target spot. This counter can be rotated over a suitable range of angles. One more NaI (Tl) gamma counter was kept at fixed position to be used as a monitor. A coincidence pulse height analyser was used so that gamma ray pulse spectra from each counter could be recorded in coincidence with the various alpha particle groups leading to different excited states in the residual nucleus Ne^{20}. Such spectra are recorded for various angular positions of the movable counter rotating it in the horizontal plane about the vertical axis passing through the target. The spectra recorded in the fixed gamma counter in coincidence with alpha particle groups serve as the monitor.

Some examples of the results are shown in figs.9 and 10. Fig. 9 shows the result for the first excited level in Ne^{20} and Fig. 10 shows the results for the cascade gamma rays from the second excited level. The first and second excited states at 1.63 and 4.25 MeV are known to have spins of 2 and 4 from measurements by Broude and Gove (5) with the $Ne^{20}(p,p'\gamma)Ne^{20}$ reaction. In the reaction $C^{12}(C^{12},\alpha)Ne^{20}$ the incident target and outgoing particles are having spin zero and hence in this case only the magnetic substate zero can be populated in the excited state in Ne^{20} since the alpha particles are detected at zero degree to the beam. However due to the finite size of the alpha particle counter magnetic substate 1 will also be

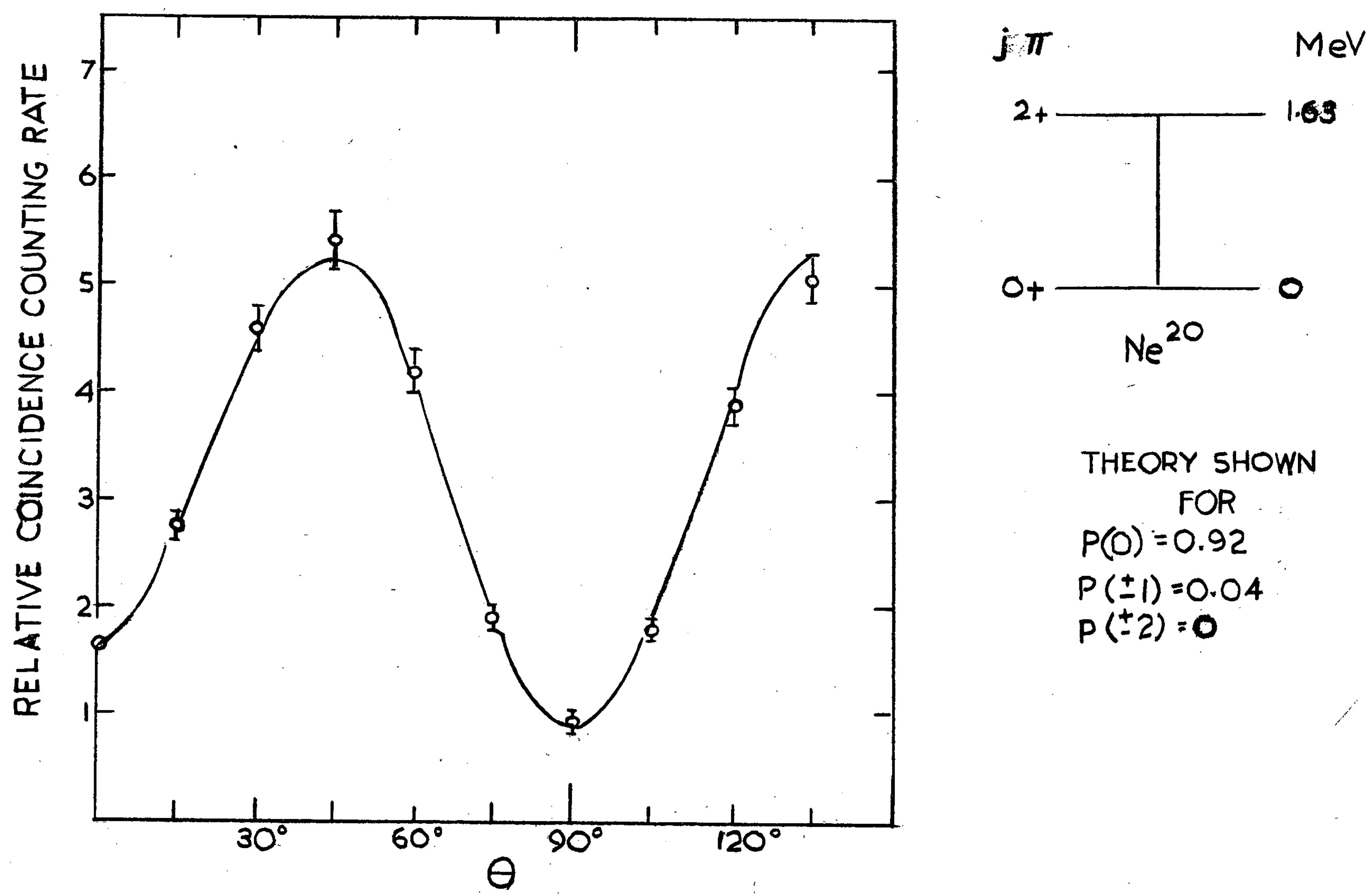

RELATIVE COINCIDENCE COUNTING RATE
7
6
5
4
3
2
1
30°
60°
90°
120°
Θ
jπ
MeV
2+
1.63
0+
0
Ne20
THEORY SHOWN
FOR
P(0) = 0.92
P(±1) = 0.04
P(±2) = 0

Fig. 9.

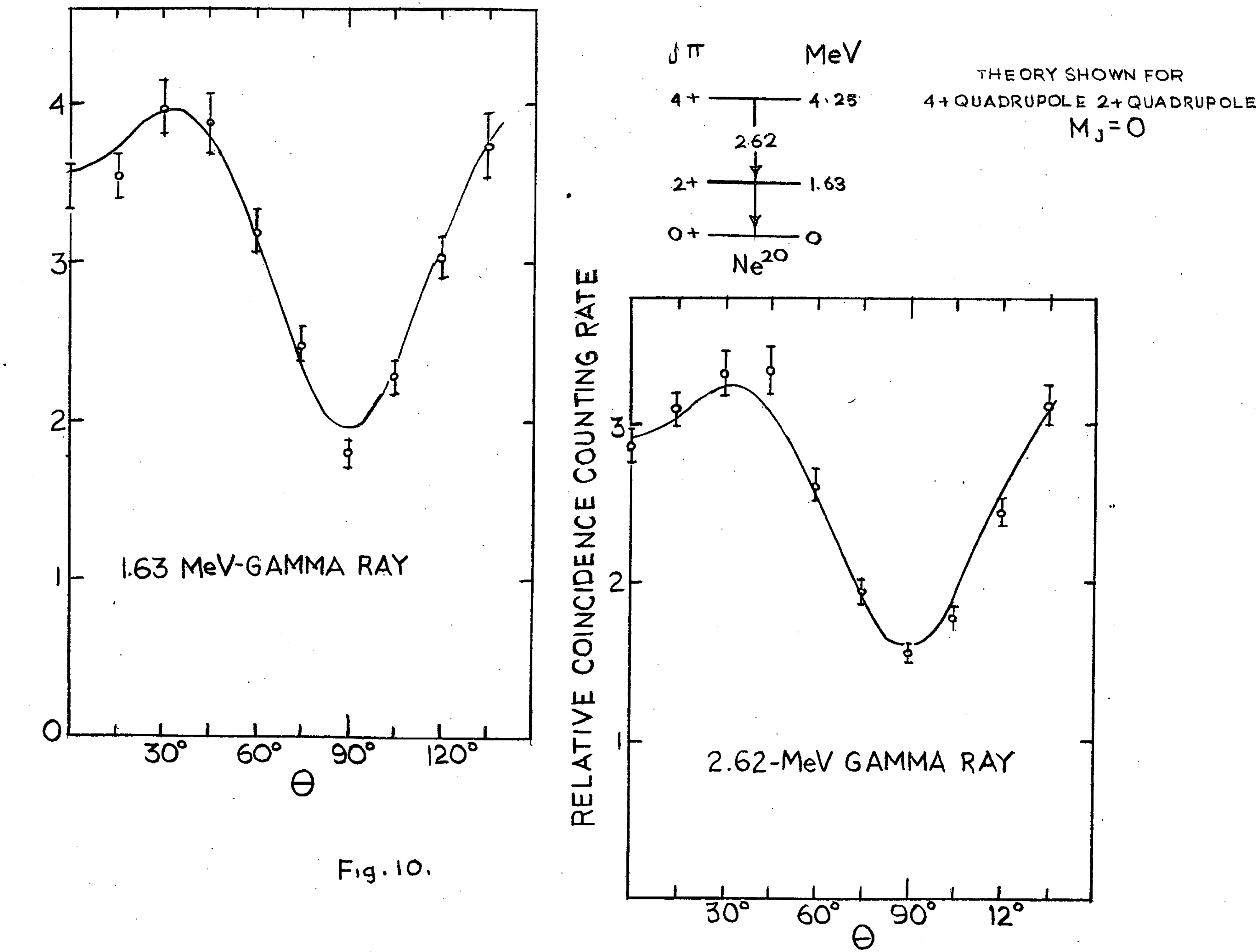
4
3
2
1
0
30°
60°
90°
120°
Θ
1.63 MeV-GAMMA RAY
Jπ
MeV
4+
4.25
2.62
2+
1.63
0+
0
Ne20
THEORY SHOWN FOR
4+ QUADRUPOLE 2+ QUADRUPOLE
Mj = 0
RELATIVE COINCIDENCE COUNTING RATE
3
2
1
30°
60°
90°
12°
Θ
2.62-MeV GAMMA RAY

Fig. 10.

populated to a small extent depending on the orbital angular momenta of the outgoing alpha particles (1) Fig. 9 shows the fit of the angular correlation data of 1.63 MeV gamma ray in terms of magnetic substate populations. It is seen from the results of the fit that $P(\pm 1) \ll P(0)$ and that $P(\pm 2)$ is negligible. In this case there are two measured ratios a_2/a_0 and a_4/a_0 so that population ratios can all be uniquely determined. The radiation pattern in this case is very nearly the pure $\Delta M = 0$ quadrupole pattern attenuated by the finite size of the gamma ray counter.

Fig. 10 shows the angular correlation of both the 1.63 and 2.62 MeV cascade gamma rays each in coincidence with the alpha particle group feeding the 4.25 MeV second excited state. Solid curves through the points are for spin sequence 4, 2, 0 for the second and first excited states and ground states, both the gamma rays being pure quadrupole. In this case there are two experimentally determined ratios a_2/a_0 and a_4/a_0 for each gamma ray and only one unknown ratio taking into account the finite size of the particle counter. The ratio $P(\pm 1)/P(0)$ was found to be less than 10%. It was shown that it was not possible to fit other spins to the experimental data.

CONCLUSIONS

It is observed that the method I which is a triple correlation measurement has considerable advantage over method II since it can provide a possible total of 18 measurable ratios if both gamma rays contain a quadrupole component. However method II has the advantage of providing a comparatively simple gamma ray spectra since these are recorded in coincidence with the particle group feeding a particular excited state. This discussion naturally leads to a combination of both methods I and II. In this case a particle detector of large solid angle should be used at zero degree to the beam placed in axially symmetrical position with respect to the incident beam. Then the analysis proceure of method I can be used but this being a triple coincidence observation, will suffer from a low counting rate. However in reactions like deuteron stripping where the outgoing particles are strongly peaked forward relatively large fraction of outgoing particles can be detected in the axially symmetrical particle counter and hence a combination of methods I and II may be practical. It should also be noted that the full exploitation of the triple correlation measurements (method I) require the use of an electronic computer while the analysis of data in method II is relatively easy.

REFERENCES

1. Litherland A.E. and Ferguson A.J. Can. J.Phys. 39, 788 (1961).
2. Ferguson A.J. and Rutlege A.R. Atomic Energy of Canada Report,AECL -420.
3. Smith P.B. Nuclear Reactions Vol. II North Holland Publishing Co. Ed. by Endt & Smith p. 248.
4. Rose M.E. Phys. Rev. 91, 610 (1953).
5. Broude C and Gove H.E. Ann.Phys. (N.Y) 23, 71 (1963).
6. Broude C and Eswaran M.A. Can. J. Phys. 42, 1300 (1964).
7. Ladd J.A. and Kennedy J.M. Atomic Energy of Canada Report, CREL - 1063.
8. Sharp W.T. Kennedy J.M., Sears B.J. and Hoyle M.G. Atomic Energy Canada Report 97, CRT -556.
9. Litherland, Broude, Eswaran, Evans and Gove (1963)(unpublished).

ON THE HALF LIFE MEASUREMENT OF THE 273 KEV LEVEL OF Au^{196}

B. Sethi and S. K. Mukherjee
Saha Institute of Nuclear Physics, Calcutta.

The decay scheme of Au^{196m}, with the omission of a few very weak transitions recently reported by Wapstra(1), is shown in Fig. 1. The orders of half lives of the 85 KeV and the 273 Kev levels have been reported to be 0.5μ s and 1 ns respectively, by Wapstra. The present paper deals with the measurement of the half life of the 273 KeV level with the help of a fast slow coincidence circuit.

APPARATUS

The block diagram of the apparatus used is shown in Fig.2. Gamma-rays were detected in 1" x1" NaI (Tl) phosphors mounted on 6810A photomultiplier tubes. Fast pulses were taken from the anodes. After one stage of limiting and amplification, they were fed into the start and stop channels of the model TH-300 time pulse height converter. Slow pulses were taken from the 12th dynode. They were inverted, to meet the input requirements of the linear amplifiers. Required energies were selected in single channel pulse height analysers. Triple coincidence was taken between the outputs of the two slow channels and a part of the output of thetime to pulse height converter. A fixed delay of 2-5μ sec was introduced in the third branch in order to compensate for the delays introduced by the amplifiers and pulse height analysers in the other two branches. A resolving time of 2μ sec was employed in the triple coincidence. The output of the time to pulse height converter was gated with the tiple coincidence output and analysed by means of 512 channel pulse height analyser. Width of the linear gate was adjusted to 3μsec.

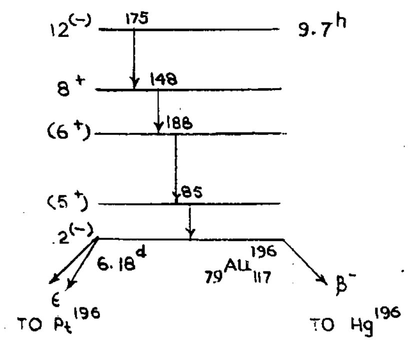

DECAY SCHEME OF THE 9.7 HOUR Au^{196} ISOMER.

Fig. 1

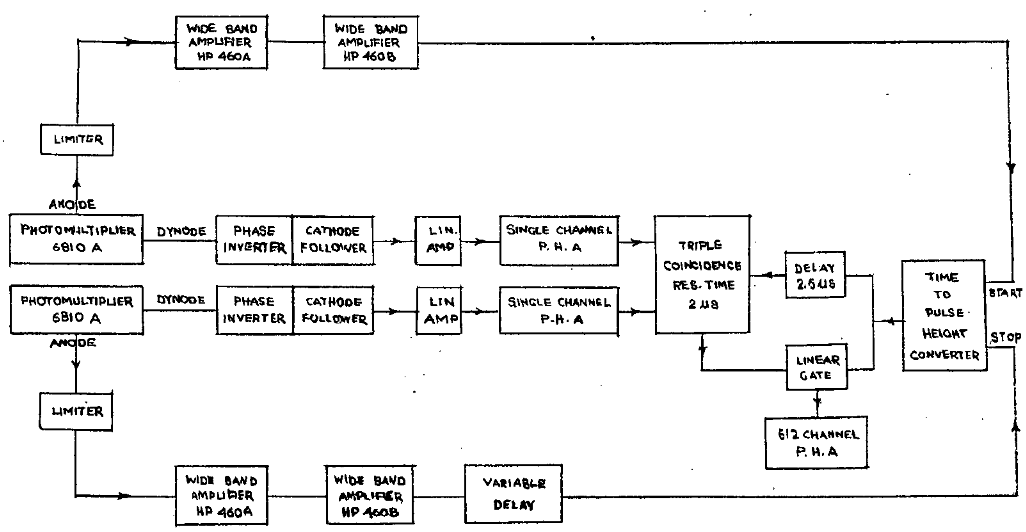

BLOCK DIAGRAM OF THE FAST SLOW COINCIDENCE CIRCUIT

Fig. 2

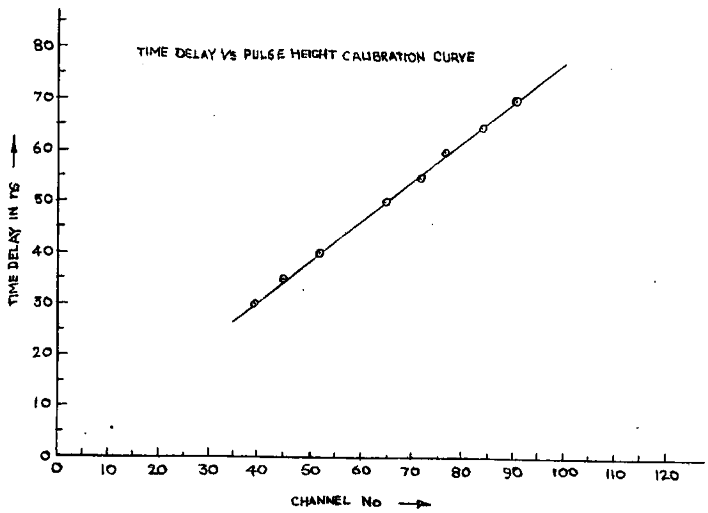
TIME DELAY Vs PULSE HEIGHT CALIBRATION CURVE
TIME DELAY IN nS
CHANNEL No

Fig. 3.

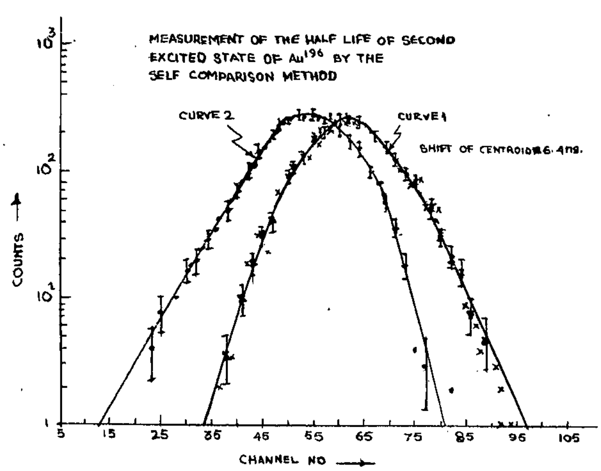
MEASUREMENT OF THE HALF LIFE OF SECOND
EXCITED STATE OF Au196 BY THE
SELF COMPARISON METHOD
CURVE 2
CURVE 1
SHIFT OF CENTROID
COUNTS
CHANNEL NO

Fig. 4.

TIME CALIBRATION

In order to calibrate the channels of the multichannel analyser with respect to time, a variable delay was introduced in one of the fast branches. Calibration was done by measuring the shift in the prompt resolution curve, when a known time delay was introduced in one branch. Fig. 3 shows the calibration curve. Prompt coincidence resolution curve obtained by using the 510 MeV annihilation gammas of Na^{22}. Slope of the curve was 0.75 ns.

SOURCE PREPARATION AND MEASUREMENTS

Source was produced by bombarding a foil of spectroscopically pure gold by 14 MeV neutrons. Au^{196m} was produced as a result of (n, 2n) reaction on Au^{197}. The foil was placed between the counters after 1 hr bombardment with a flux of 10^{10} neutrons/ sec. Gammas of 188 KeV and 148 KeV were selected in the start and stop channels respectively and counts were accumulated in the multichannel analyser. After that the start and stop gammas were interchanged and once again the data was accumulated under similar conditions. Curves of Fig. (4) show the results thus obtained. There is a shift of centroid to the left by an amount 6.4 ± 1.5 ns. Next a prompt coincidence resolution curve was obtained, keeping the same channel settings and using Na^{22} source. On repeating the above procedure in this case, a new prompt curve was obtained. It was found that there is no observable shift in the centroid of the prompt curve. Therefore, the shift observed in the case of Au^{196} is equal to 2τ, where τ is the mean life of the level under question. This gives

$$T_{\frac{1}{2}} = 2.2 \pm 0.5 \text{ ns}$$

REFERENCE

1. Wapstra, A.H., Priv. Comm., Nuclear Data Sheets, Dec. 1962.

DECAY OF Nb^{98}

S.C. Gujarathi and S.K. Mukherjee
Saha Institute of Nuclear Physics, Calcutta

Nb^{98} was first reported by Boyd (1) who assigned a 30 min activity to Nb^{98} obtained presumably through Mo^{100} (d,α) Nb^{98} reaction. Pappas and Thomassen observed a half-life of 26 min for Nb^{98}, whereas Troutner measuring the fission yields of Nb isotopes assigned a 51 $\pm$ 3 min activity to Nb^{98}. The decay scheme of this isotope is not yet establised (2).

The present investigation was undertaken to determine the half-life of Nb^{98} more precisely, to measure its beta and gamma energies and to obtain some information about the nature of its decay. It is a part of our programme of studying short lived isotopes by 14 MeV neutron induced reactions.

HALF-LIFE MEASUREMENTS

For the determination of half-life, enriched Mo^{98} (97%) was bombarded by 14 MeV neutrons. The study under G.M. Counter gave composite half-life, as shown in the Fig. 1. The long half-life of 67 hrs is due Mo^{100} (n,2n) Mo^{99} reaction since enriched sample contained 1% of Mo^{100} and the 74 min is due to Mo^{98} (n, d) Nb^{97} reaction. The study under G.M. Counter gave the half-life of 51 min. in confirmation with previous report and also indicated the presence of shorter half-life. So the sample was bombarded for short time and immediately studied under low background counter which gave the half-life of 1.6 min.

GAMMA - RAY MEASUREMENTS

For the study of γ -spectrum enriched Mo^{98} was bombarded with 14 MeV neutrons and the gamma ray spectrum was taken with 2"x 2" NaI(Tl) spectrometer

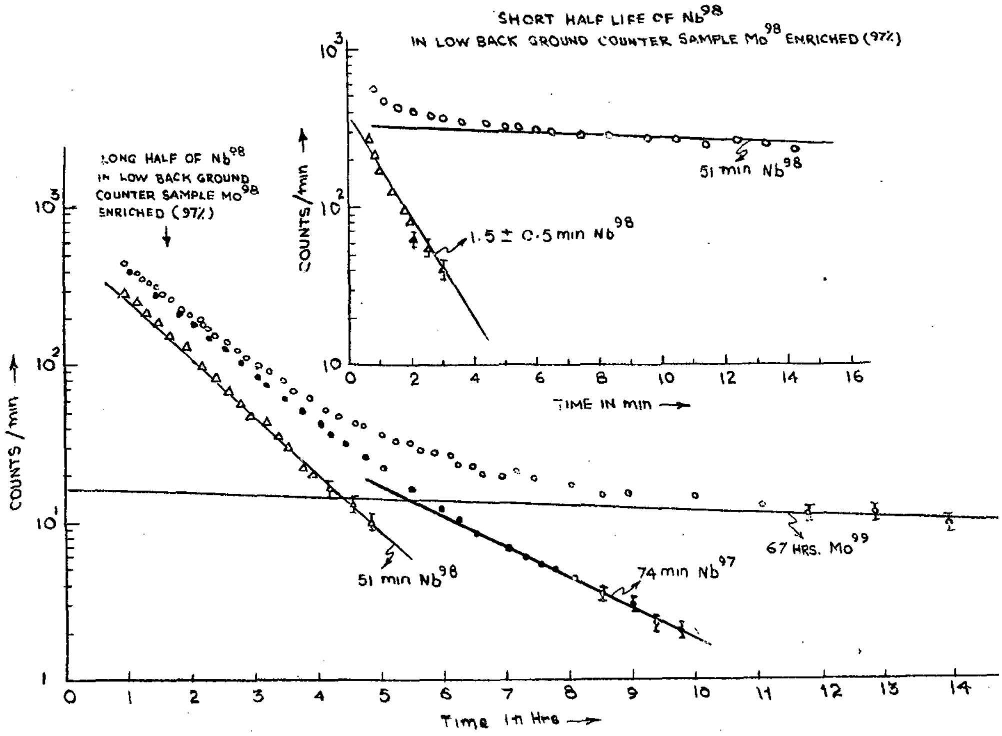
SHORT HALF LIFE OF Nb^{98}
IN LOW BACK GROUND COUNTER SAMPLE Mo^{98} ENRICHED (97%)
COUNTS/min
TIME IN min
51 min Nb^{98}
1.5 ± 0.5 min Nb^{98}
LONG HALF OF Nb^{98}
IN LOW BACK GROUND
COUNTER SAMPLE Mo^{98}
ENRICHED (97%)
COUNTS / min
Time in Hrs
51 min Nb^{98}
74 min Nb^{97}
67 HRS. Mo^{99}

Fig 1.

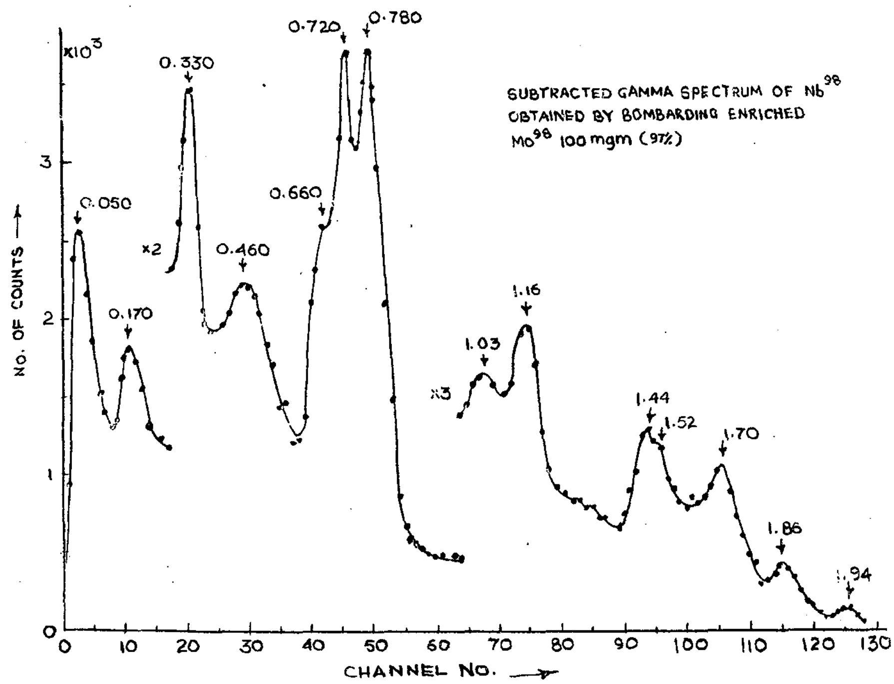
SUBTRACTED GAMMA SPECTRUM OF Nb^{98}
OBTAINED BY BOMBARDING ENRICHED
Mo^{98} 100 mgm (97%)
NO. OF COUNTS
x10^3
CHANNEL NO.
0.050
0.170
0.330
0.460
0.660
0.720
0.780
1.03
1.16
1.44
1.52
1.70
1.86
1.94
x2
x3

Fig 2.

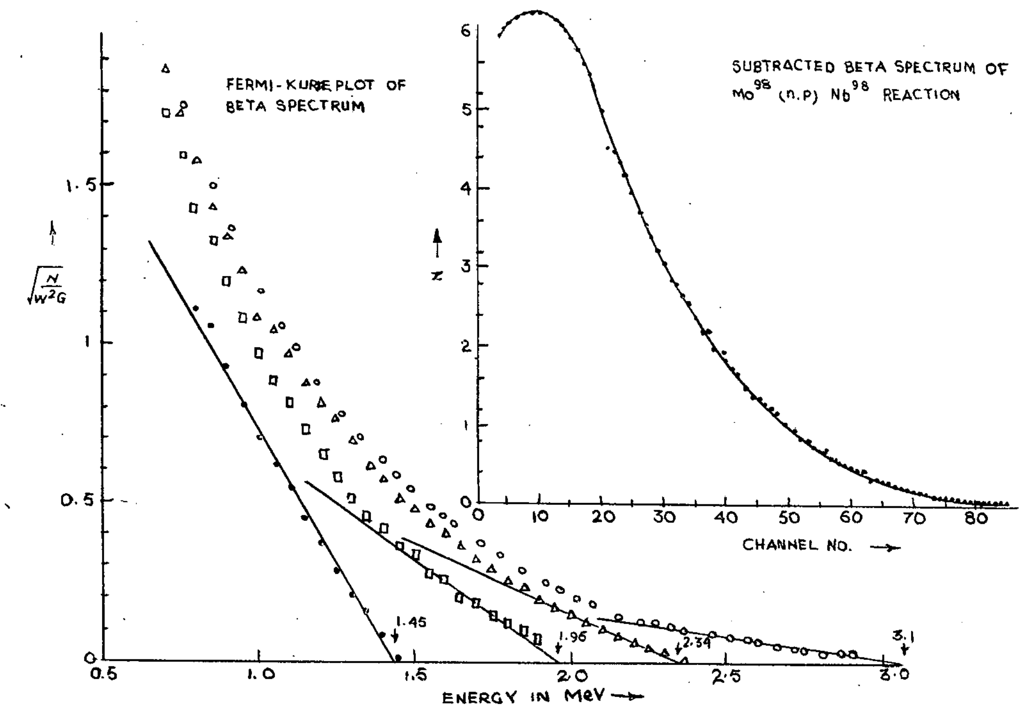
FERMI-KURIE PLOT OF BETA SPECTRUM
SUBTRACTED BETA SPECTRUM OF Mo^{98} (n.p) Nb^{98} REACTION
CHANNEL NO.
ENERGY IN MeV
1.45
1.95
2.39
3.1

Fig. 3.

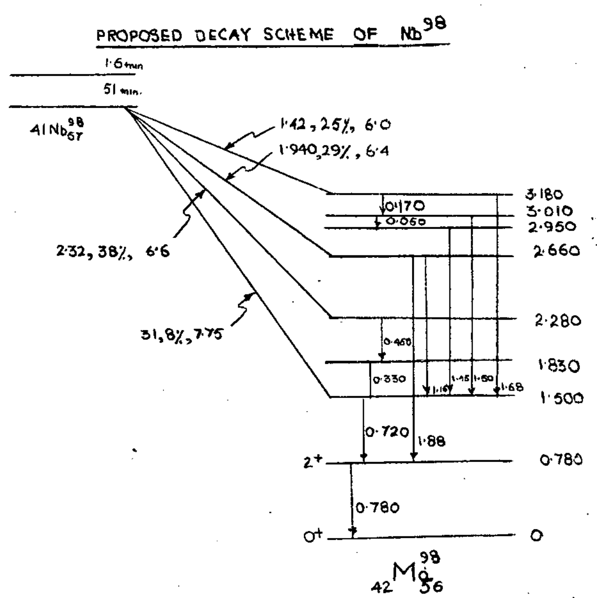
PROPOSED DECAY SCHEME OF Nb^{98}
1·6 min
51 min.
$_{41}Nb^{98}_{57}$
1·42, 2.5%, 6·0
1·940, 29%, 6·4
2·32, 38%, 6·6
31, 8%, 7·75
3·180
3·010
2·950
2·660
2·280
1·830
1·500
0·780
0
0·170
0·060
0·450
0·330
0·720
1·88
0·780
2^+
0^+
$_{42}Mo^{98}_{56}$

Fig. 4.

and 512 channel analyser. Fig. 2 shows the γ - spectrum obtained after subtracting longer activities. In the spectrum all the gamma rays are due to the Nb^{98} activity produced by the Mo^{98} (n,p) Nb^{98} reaction except the two, namely 650 KeV and 1030 KeV which are due to Mo^{98}(n,d) Nb^{97} reaction. The half-life measurements of these gamma-rays in single channel analyser supported our assignments.

Gamma spectrum was also obtained from chemically separated Nb activity. For this Ammonium Molybdate of specpure quality was bombarded with 14 MeV neutrons and Nb activity was separated by standard chemical procedure. The activities obtained by this method were mainly of Nb^{100} (11.5 min), Nb^{98} (51 min), Nb^{97} (74 min) and Nb^{96} (23 hrs). So for the first hour after chemical separation, data were taken to get the information about Nb^{100}. After subtracting the longer and shorter activities we could get the information about Nb^{98}.

BETA-RAY MEASUREMENTS

For β - ray measurements the enriched as well as chemically separated samples were used along with anthracene β -spectrometer and 512 channel analyser. Fig. 3 shows the β -spectrum and Fermi-Kurie plot. Four β -groups obtained were also confirmed in coincidence experiments.

COINCIDENCE MEASUREMENTS

Number of γ-γ and β-β coincidence experiments were performed. The results are summarised in the table.

Based on thse observations a decay scheme is proposed as shown in Fig. 4.

REFERENCES

1. G.E. Boyd, Oak Ridge National Laboratory Report ORNL -229 (1949).

2. Nuclear Data Sheets, National Research Council Washington, D.C.

TABLE

Long Half-Life = 51 min

Short Half-Life+ 1.6 min

E_γ (KeV)	In coincidence with
50 $\pm$ 5	170,720, 780, 1450
170 $\pm$ 5	50,720, 780, 1450, 1520
330 $\pm$ 5	450, 720, 780
450 $\pm$ 10	330, 720, 780
720 $\pm$ 5	50, 170, 330, 450, 780, 1160, 1450, 1520, 1680
780 $\pm$ 5	50, 170, 330, 450, 720, 1160, 1450, 1520, 1680, 1880
1160 $\pm$ 5	720, 780
1450 $\pm$ 10 1520 $\pm$ 10	50, 170, 720, 780
1680 $\pm$ 10	720, 780
1880 $\pm$ 10	780
1940 $\pm$ 10	

$E_{\beta\ max}$ (MeV)	Percentage Intensity	Log ft Values
3.10 $\pm$ 0.1	8	7.75
2.32 $\pm$ 0.1	38	6.6
1.940 $\pm$ 0.05	29	6.4
1.420 $\pm$ 0.1	25	6.0

E_γ (KeV) in Gate	Coincidence End Point Energy $E_{\beta\ max}$ (MeV)
170	1.420
330	2.320
460	2.320
720, 780	1.420, 1.940, 2.32, 3.1
1160	1.940

THE DECAY OF Ba^{133}

P.C. Mangal and S.P.Sud

Department of Physics, Panjab University, Chandigarh-3

The "sum coincidence" technique of A.H. Hoogenboom (1) has so far been mostly used for the study of cascading gamma rays whose total energy is $\geq$ 1 MeV. In the present work the applicability of this technique has been tried out in the lower energy region. As the decay of Ba^{133} involves a maximum energy of 438 KeV, this nucleus has been selected for study using above technique.

The electron capture decay of 7.2 years Ba^{133} to Cs^{133} has been investigated by a number of workers using scintillation and magnetic spectrometer techniques, but considerable disagreement exists about certain aspects of the decay scheme. The most recent decay scheme put forward by Yin and Wiedenbeck (2) is shown in fig.1. The excited levels at 82,162, 384 and 438 KeV have been well established and are shown in the decay scheme along with the main transitions. A disagreement among the various authors exists about the existence of the 222 KeV γ -ray. Also disagreement exists about the spin assignment of the 162 KeV level. Further the intensities of almost all the gamma rays have not yet been well established and a considerable disagreement exists among various authors (3-7) on this point.

The main reason for the above disagreement lies in the fact that when coincidence measurements are made, it is not possible to avoid contributions due to unwanted gamma rays e.g. if we study coincidences between 356 KeV and the rest of the gamma rays we cannot avoid contribution from 384 KeV gamma ray which lies, to some extent, in the window of the single channel analyser, set for the 356 KeV gamma-ray. To overcome these difficulties we have made use of the Hoogenboom technique for the study of this nucleus.

The block diagram of a modified coincidence spectrometer used in the present investigation is shown in fig. 2. The source mounted on a perspex strip was placed in between the two 2" dia x 2" thick NaI(Tl) crystals mounted on RCA 6342 photomultipliers. The resolution of the fast coincidence circuit was about 0.2 μ secs and that of the slow coincidence circuit was about 4 μ secs. The rest of the set up was of the usual type. Fig. 3 shows the sum coincidence spectrum observed on gating the sum channel at 438 KeV. From the figur it is clear that (54+384), (82 + 356) and (126 + 276) KeV are the main cascades arising from the 438 KeV level. There are three additional spurious peaks observed at 116, 307 and 400 KeV. The spurious peaks at 116 and 307 KeV can be explained to be due to the summing (8) of 31 KeV Cs^{133} X-ray, 82 KeV gamma-ray and compton of 356 KeV. The peak at 400 KeV may be due to the summing of 31 KeV Cs^{133} X-ray and the higher energy and of 384 KeV gamma ray.

To check the validity of the above argument for spurious peaks we placed about 15 mil thick copper absorber in front of both the crystals. This thickness of copper was sufficient to absorb 31 KeV X-ray of Cs^{133}. The sum coincidence spectrum with this absorber is shown in fig.4. It is clear from the spectrum that no spurious peaks are coming up now.

The relative intensity of 54 KeV and 276 KeV gamma rays have been obtained from the present measurements. Taking the intensity of 356 KeV gamma ray to be 100% the relative intensity of 54 KeV gamma ray comes out to be 5 $\pm$ 1 and that of 276 to be 13 $\pm$ 2. The intensity of 276 KeV gamma ray has been calculated by using N80/N162 to be 3.5, given by Stewart and Lu (5). These intensities have been corrected for absorption in the copper

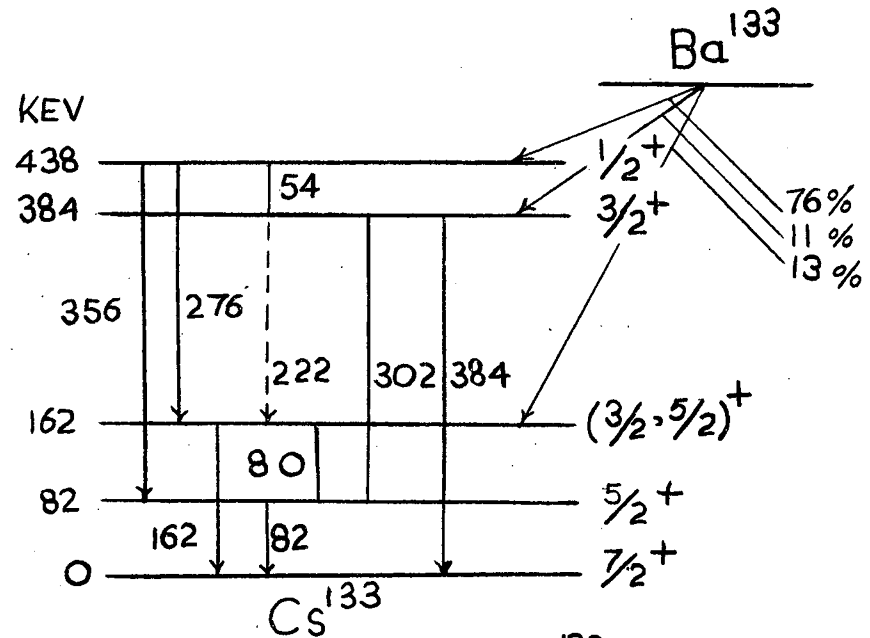

FIG. 1 DECAY SCHEME OF Ba^{133}

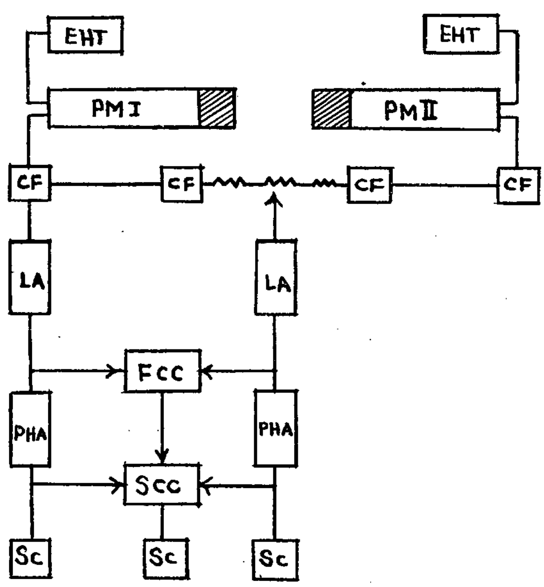

FIG. 2 BLOCK DIAGRAM

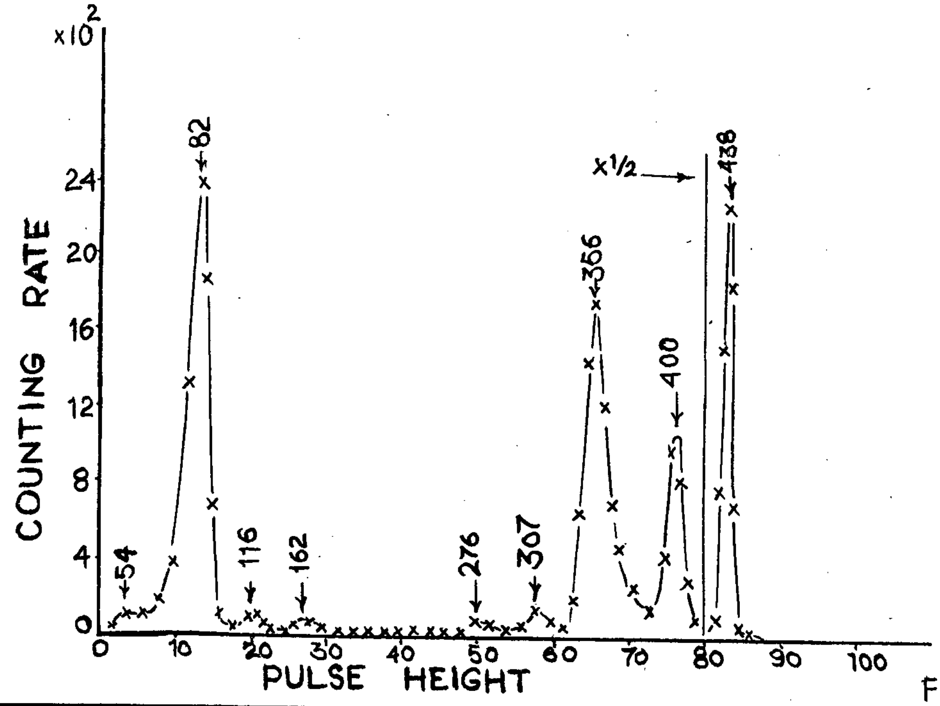
COUNTING RATE
x10^2
0
4
8
12
16
20
24
54
82
116
162
276
307
356
400
438
x1/2
0
10
20
30
40
50
60
70
80
90
100
PULSE HEIGHT

FIG. 3.

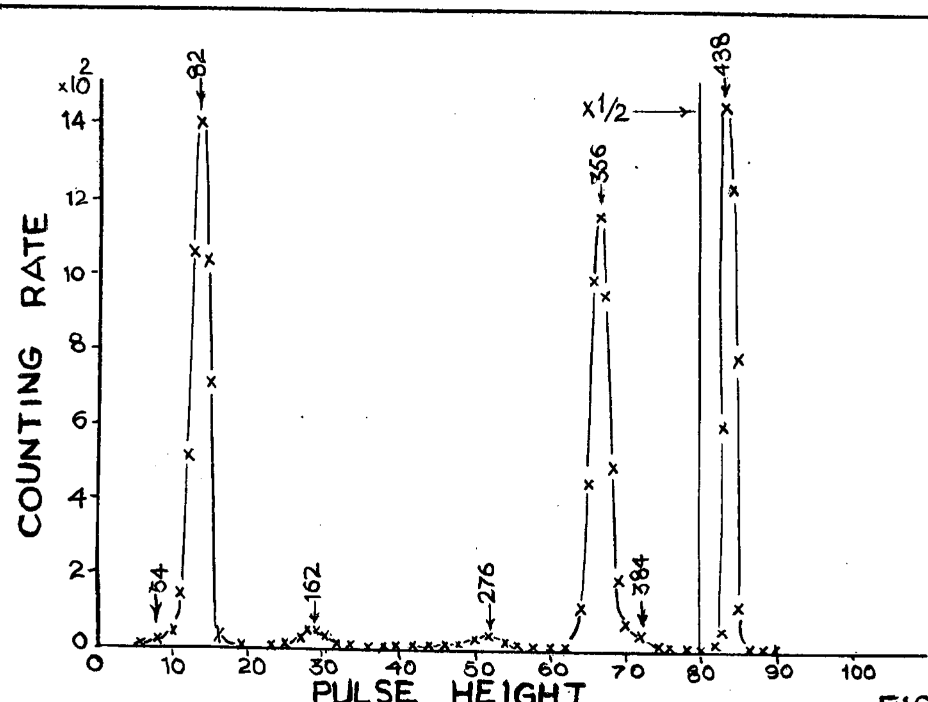
COUNTING RATE
x10^2
0
2
4
6
8
10
12
14
54
82
162
276
356
384
438
x1/2
0
10
20
30
40
50
60
70
80
90
100
PULSE HEIGHT

FIG. 4.

absorber.

The two peaks at 162 and 276 KeV are clearly separated out and angular correlation experiments for these two gamma rays are planned. This will help us in deciding about the spin assignement of 162 KeV level.

REFERENCES

1. A.M. Hoogenboom, Nucl. Instr. and Methods 3, 57 (1958).

2. L.I. Yin, and M.L. Wiedenbeck Nucl. Phys. 54, 86 (1964).

3. B. Crasemann J.G. Pengra and I.E. Lindstrom Phys. Rev. 108, 1500 (1957).

4. R.K Gupta, S.Jha, M.C. Joshi, and B.K. Madan.; Nuovo Cimento 8, 48 (1958).

5. M.G. Stewart and D.C. Lu.; Phys. Rev. 117, 1044 (1960).

6. M.K. Ramaswamy, Skeel and P.S. Jastram.; Nuclear Physics 16, 619 (1960), Nuclear Physics 19, 299 (1960).

7. K.C. Mann, and R.P. Chaturvedi ; Cand. J. Phys. 41, 932 (1963).

8. S.O. Schrilier, and B.G. Hogg., Nuclear Instr. and Method 26, 141 (1964).

DISCUSSIONS

P. Jagam: What is the Linear Adder circuit used?

P.C. Mangal : We used an ordinary resistance adding net work.

NUCLEAR STRUCTURE EFFECTS IN THE DECAY OF Ce^{141}

S.M. Brahmavar
Physics Department, Panjab University, Chandigarh-3
and
A.S. Venkatesha Murthy
Department of Physics, Indian Institute of Technology, Madras -36

INTRODUCTION

The details of the nuclear structure effect can be obtained from the analysis of the so-called ℓ -forbidden M1 transitions. These ℓ -forbidden ($\Delta\ell = 2$) magnetic dipole (M1) transitions are strongly retarded when compared to the (allowed) single particle M1 transition rates. Church and Weneser (1) have suggested that the internal convession process should be sensitive to nuclear structure through a contribution due to the penetration of the atomic electrons into the nucleus. The structure effects should be especially large for the ℓ -forbidden magnetic dipole (M1) transitions. Identification of these effects requires precise knowledge of the conversion co-efficient. Based on this theory many attempts have been made previously to account for nuclear structure effects. Of these the significant are of Gerholm et al (2), Pattersson et al (3), Grabewski et al (4) and Ramaswamy (5). Very recently Herrlander and Graham (6) have obtained additional evidence for nuclear structure effects.

Thus, it is intended here to analyse the ℓ -forbidden (M1) transition in the decay of Ce^{141}. This transition takes place between $g7/2 \rightarrow d5/2$ and is strongly retarded with a retardation factor of about 330, Here it seems worth while to analyse this transition for nuclear structure effects.

DATA ANALYSIS AND RESULTS

In recent years there have been many measurements of the K-shell conversion coefficient of 142 KeV transition in P^{141}. Now it has been definitely established as a M1 transition. The K-shell conversion coefficient has been measured by Rao (7) taking into account every possible error.

The value of α_K according to him is (0.38 $\pm$ 0.04). Also the mixing-ratio for this transition has been measured rather accurately by Haag et al (8). Their value for ϵ (E2/M1) is (0.066 $\pm$ 0.022).

The total K-conversion coefficient for a mixed M1- E2 transition can be written in the usual notation as

$$\alpha_K = \frac{1}{1+\delta^2}\left[\beta(M_1) + \delta^2\alpha(E_2)\right] \tag{1}$$

from which we obtain,

$$\beta(M_1) = \alpha_K(1+\delta^2) - \delta^2\alpha(E_2) \tag{2}$$

substituting for α_K δ and taking the theoretical value of $\alpha(E_2)$ = 0.32 (assuming that α(E2) (9) is not influenced by nuclear structure), we get

$$\beta(M1) = 0.380 \pm 0.004$$

The effects on internal conversion due to peneration depend on the details of the nuclear structure. For M1 transitions Church and Weneser (1) write,

$$\lambda = \frac{m_e}{m_\gamma} \tag{3}$$

where me is that part of the matrix element due to the peneration of the electron into the nucleus and m_γ is the matrix element for M1 gamma emission. In terms of λ, the corrected M1 conversion coefficient is given approximately by

$$B(\lambda) \sim \beta(1)\left[1-(\lambda-1)C(Z,k)\right]^2 \tag{4}$$

Where λ = 1 means that the currents are confined to the nuclear surface (Sliv's assumption) $C(Z,k)$ can be determined from the corrected table of Church and Weneser.

For the 142 KeV transition in Pr^{141} the experimental value of B(λ) = (0.380 $\pm$ 0.004), the value of B (1) (10) is 0.42*, and for Z = 55 and K = 0.27, C(Z,k) = 0.0117. Putting al these values in eq(4), we obtain,

$$\lambda = +6.1 \pm 1.1$$

This result shows that the penetration matrix element is about 6 times as large as the gamma matrix element. Church and Weneser evaluated λ for Δl =2,M1 transitions for odd- Z nuclei using empirical gamma matrix elements and using single particle wave functions to evaluate m_e. They found values of λ falling between 5 and 10, for Z ~55. The value of 6.1 ± 1.1 for λ in Pr^{141} (Z=59) is in this region.

REFERENCES

1. E.L. Church and J. Weneser, Physics. Rev. 104, 1382 (1956).
2. T.R. Gerholm, B.G. Pattersson, B. Van Nooigen and Z. Grabowski, Nuclear Physics 24, 177 (1961).
3. B.G. Pattersson, T. R. Gerholm, Z. Grabowski and B.Van Nooijen, Nuclear Physics 24, 196 (1961).
4. Z. Grabowski, B.G. Pattersson, T.R. Gerholm and J.E. Thun, Nuclear Physics 24, 251 (1961).
5. M.K. Ramaswamy, Phys. Rev. 119, 2021 (1960).
6. C.J. Harrlander and R.L. Graham, Nuclear Physics 58, 544 (1964).
7. G.N. Rao, Nuovo cimento 30, 501 (1963).
8. J.N. Haag, D.A. Shivley and D.H. Temyoleton, Physics. Rev. 129, 1601 (1963).
9. M.E. Rose, in Beta- and Gamma-Ray Spectroscopy (North -Holland publishing company, Amsterdam, (1955).
10. M.E. Rose, Internal conversion coefficient (North-Holland publishing company, Amsterdam, 1958).

---

* Attention is drawn to the fact that different values are quoted for the theoretical value of α_k(M1) by various workers. The value used in the present investigation is re-evaluated by careful extrapolation of the necessary graphs.

DISCUSSION

N.K. Saha : I hope you are aware that Geiger and others pointed out in 1963 and afterwards that the previous prediction of Nuclear structure effect was erroneous and arose due to a mistake of sign in the calculation.
Are the present investigation of your paper inspite of the above?

S.M. Brahmwar: Yes I am aware of the comment and the present investigations are inspite of the above remark.

ANOMALIES IN INTERNAL CONVERSION COEFFICIENTS OF E2 TRANSITIONS IN EVEN-EVEN NUCLEI

S.M. Brahmavar and M.K. Ramaswamy
Karnatak University, Dharwar.

A survey and analysis of $4^+ \longrightarrow 2^+$, $6^+ \longrightarrow 4^+$, $0^+ \longrightarrow 2^+$, $8^+ \longrightarrow 6^+$ E2 transitions bring to light certain anomalies in internal conversion coefficients of these transitions. The smooth variation of $\left[\frac{\alpha_k(\mathrm{expt})}{\alpha_k(\mathrm{theo})}\right]$ with mass number A and collective parameter $C_k = N/Z$ indicate the possibility of internal conversion coefficients depending on the deformation of the nucleus.

ASSOCIATED PARTICLE METHOD FOR THE D (d,n) He^3 REACTION

A. S. Divatia
Nuclear Physics Division
Atomic Energy Establishment Trombay

and
D.L.Bernard, B.E. Bonner, G.C. Philips and C. Poppelbaum
Department of Physics, Rice University, Houston Texas

INTRODUCTION

Interactions between nucleons or nucleon clusters can be studied well by investigating few nucleon systems, generally implying systems with A $\leq$ 5 n +D is such a system, and a detailed study of n +D elastic and inelastic scattering should yield information about n -n and n - p interactions. With this objective, a study of the neutrondeuteron scattering was undertaken, for $E_n \lesssim$ 11 MeV, using the Tandem Van de Graaff Accelerator for producing the neutrons. Time of flight techniques were used for detecting the scattered neutrons. Neutron-deuteron elastic scattering was studied and a search was made for the neutrons coming from the three-body break up reaction, n + D $\longrightarrow$ n + p.

Since we are faced with problems of low yield and high background in searching for the break up neutrons, choice of the neutron source and the method of observation are quite important. The possibilities of the D (d,n) He^3 reaction as a neutron source, using the associated particle in coincidence, were therefore fully investigated.

ASSOCIATED PARTICLE IN THE D (d,n) He^3 REACTION

From kinematical considerations, we can examine the possibilities of detecting the He^3 particles at various angles and energies. Elastic scattering [the D (d , d) D reaction] and the D (d,p) T reaction are two

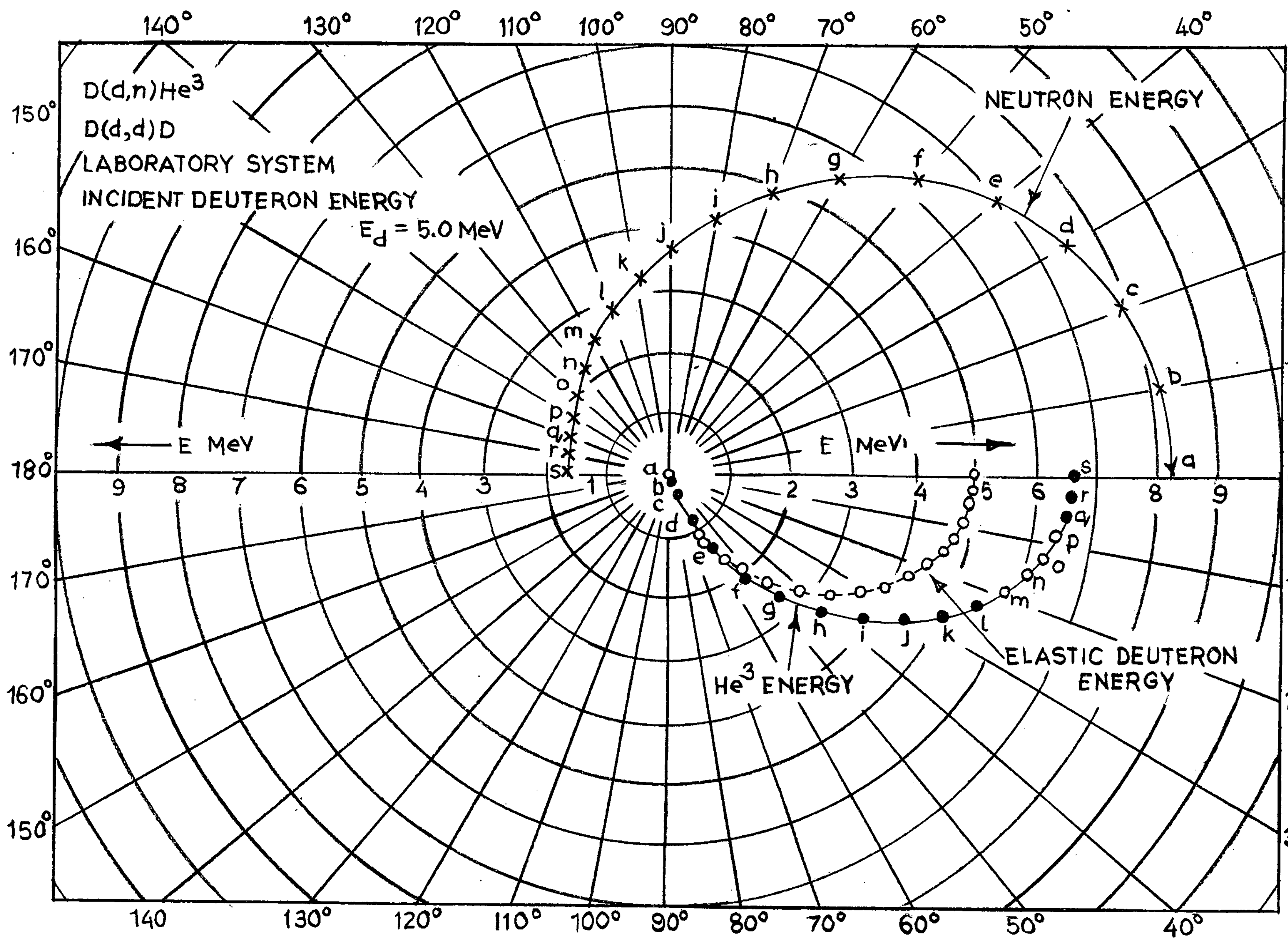
D(d,n)He3
D(d,d)D
LABORATORY SYSTEM
INCIDENT DEUTERON ENERGY
Ed = 5.0 MeV
NEUTRON ENERGY
He3 ENERGY
ELASTIC DEUTERON ENERGY
E MeV
E MeV

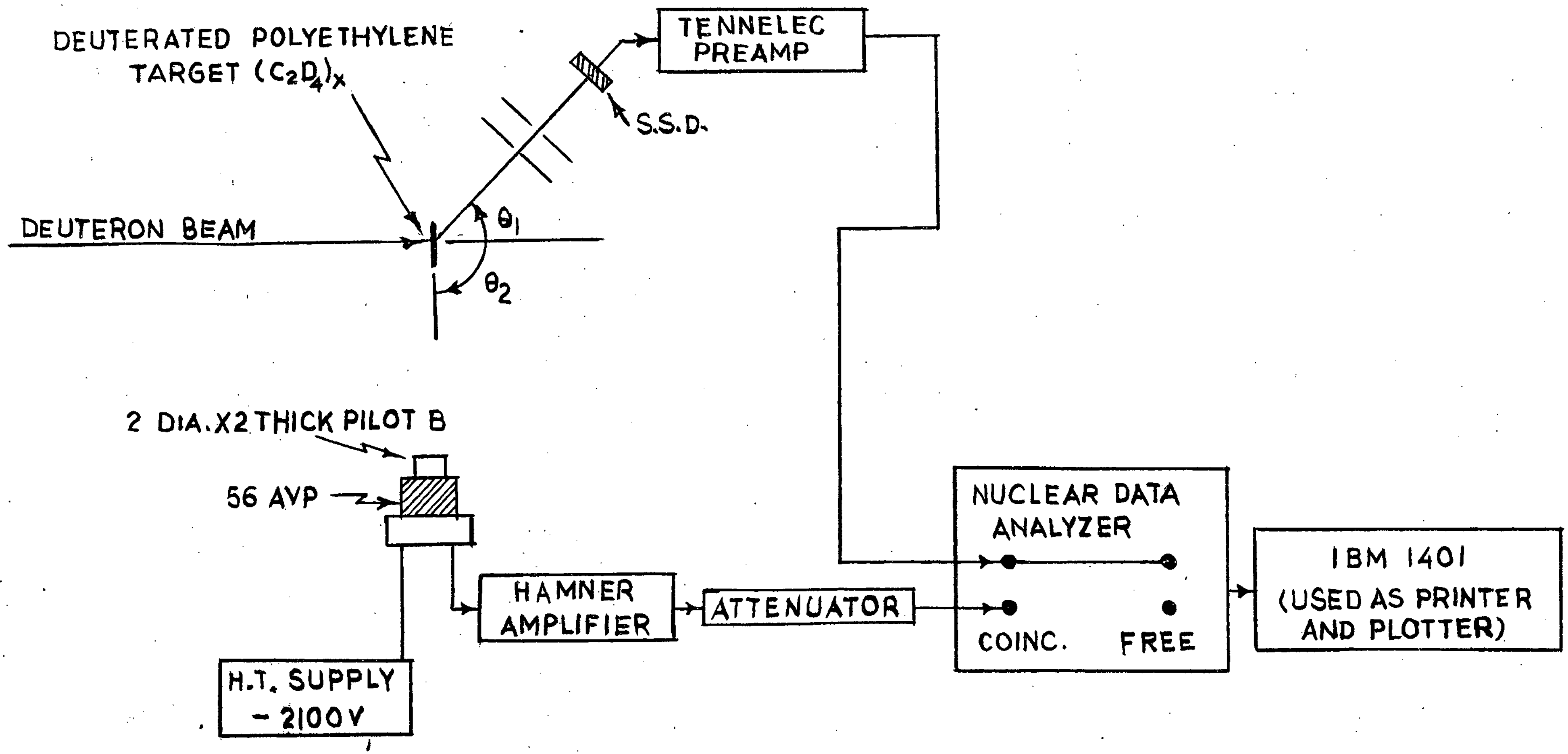

DEUTERATED POLYETHYLENE TARGET $(C_2D_4)_x$
TENNELEC PREAMP
S.S.D.
DEUTERON BEAM
θ_1
θ_2
2 DIA. X 2 THICK PILOT B
56 AVP
H.T. SUPPLY
− 2100 V
HAMNER AMPLIFIER
ATTENUATOR
NUCLEAR DATA ANALYZER
COINC.
FREE
IBM 1401
(USED AS PRINTER AND PLOTTER)

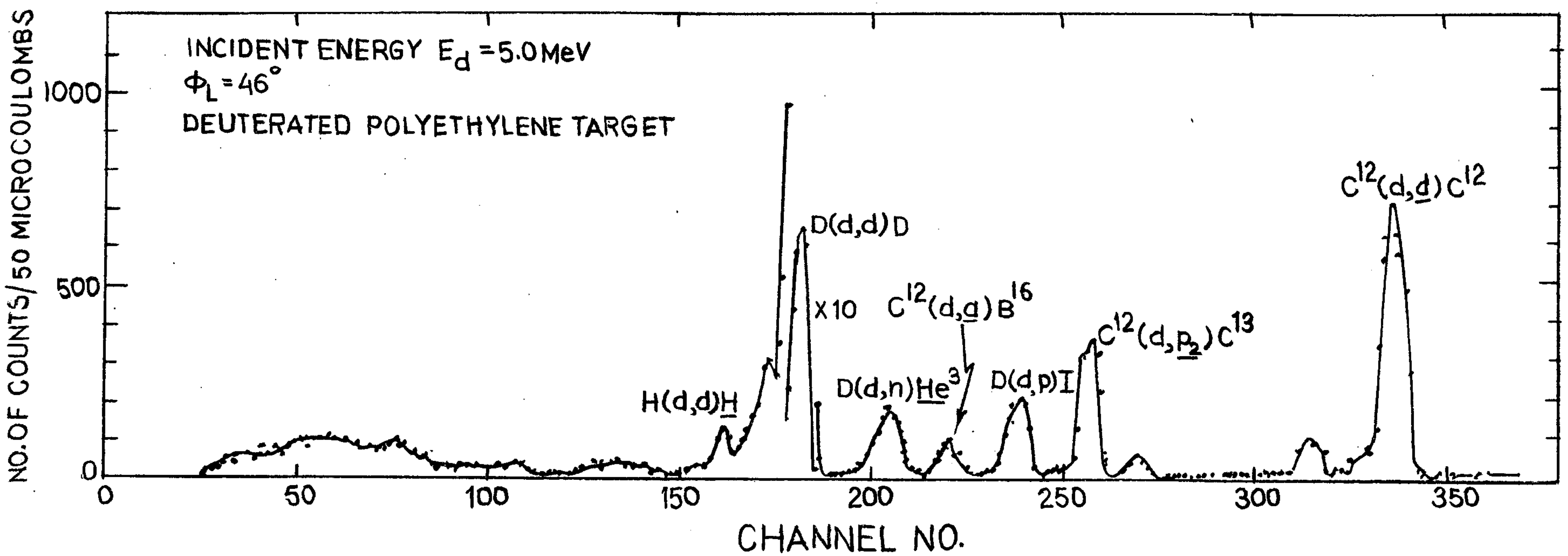
INCIDENT ENERGY E_d =5.0 MeV
Φ_L=46°
DEUTERATED POLYETHYLENE TARGET
NO. OF COUNTS/50 MICROCOULOMBS
CHANNEL NO.
H(d,d)H
D(d,d)D
X10
C^{12}(d,α)B^{16}
D(d,n)He^3
D(d,p)T
C^{12}(d,p_2)C^{13}
C^{12}(d,d)C^{12}
0
500
1000
0
50
100
150
200
250
300
350

completing processes. Figure 1 illustrates a radial plot of neutron energies, He^3 energies, and the energies of the elastically scattered deuterons for incident deuteron energy Ed = 5.0 MeV. From this and other available data we conclude:

1. At suitable angles of observation, sufficiently energetic He^3 particles, well resolved from the elastically scattered deuterons and the tritons from the D(d,p)T reaction are available for detection.

2. Neutron energies in the range 4-11 MeV are available.

3. Available differential cross section for neutron production is limited to about 10 mb/steradian.

4. A coincidence condition with the He^3 particles should improve the signal to noise ratio.

5. By counting the associated He^3 particles with 100% efficiency, using a semi-conductor detector, an absolute measure of the efficiency of a neutron counter can be obtained.

6. For $E_d \gg 7$ MeV, a second neutron group is produced in the d +d reaction; a coincidence with the associated He^3 particle should eliminate interference from this group.

RESULTS

A typical charged particle spectrum obtained at an incident deuteron energy E_d = 5.0 MeV and a laboratory angle φ_L = 46 degrees, using deuterated polyethylene target, is shown in Fig. 2. The He^3 peak is well resolved from the neighbouring peaks. Results with other targets such as Ti - D, Zr-D, and D_2 gas, were not equally satisfactory; more work is necessary before these targets can be used.

Absolute efficiency measurements of a neutron counter, Pilot B plastic scintillator, 4.45 cm dia x 5. 10 cm long, mounted on a 56 AVP Photomultiplier, are given in Table 1. The experimental arrangement is shown in Fig.3.

TABLE I

Energy of Deuteron E_d MeV	Lab. Angle for Neutron θ_L	Lab. Angle for Particle φ_L	Neutron Energy E_n MeV	He^3 Energy E_{He^3} MeV	Measured Absolute Efficiency %
3.0	100°	31°	2.83	3.43	22.8
3.0	65°	50°	4.27	2.01	14.5
4.0	50°	54.3°	5.60	1.67	6.3

AN ANALYTICAL METHOD OF ANALYSING GAMMA-RAY PULSE HEIGHT SPECTRA*

P. Subrahmanyam and P. Ammiraju
Tata Institute of Fundamental Research
Bombay

An analytical method for the conversion of count rate distribution due to gamma-rays to the true incident photon spectrum by means of a "sensitivity matrix" has been discussed. The method of determining the sensitivity matrix by using radioactive gamma ray sources, and its correctness regarding intensity and energy reproduction for various gamma-ray spectra is described. Finally the limitations of the method are discussed.

---

* Details of this are under publication in Nucl. Inst. and Methods (in press)

A SIMPLE NON-INTERUPTING METHOD OF MEASURING PULSED ELECTRON BEAM CURRENT IN LOW ENERGY ELECTRON LINAC *

P. Subrahmanyam and P. Ammiraju
Tata Institute of Fundamental Research
Bombay

A simple method of continuous monitoring of the absolute pulsed electron beam current in low energy electron LINAC using a brass monitor as a Faraday cage inside the scattering chamber of the accelerator is described. The advantage of this monitor with respect to the scattering chamber is discussed.

---

* Details of this are under publication in Nucl. Inst. and Methods (In Press).

A MATRIX METHOD FOR RESOLUTION AND BACKSCATTERING CORRECTIONS IN SCINTILLATION BETA-SPECTROMETRY

by

P. Sen and A. P. Patro
Saha Institute of Nuclear Physics, Calcutta

Scintillation counters have been widely used for beta spectrometry. The main corrections required are for resolution and backscattering. Resolution correction gives a correction in end energy and backscattering correction removes the up-turn in the Kurie plot in the low energy region. The up-turn usually starts at an energy equal to half the end energy and the correction is important if more than one beta-group is involved and if intensities of the different groups have to be determined. A method for resolution correction has been given by Palmer and Laslett(1). Freedman et al (2) give a method for correcting bacscattering as well as resolution.

If A_{n1}, A_{n2}, A_{n3} ... are the fractions of the number M of monoenergetic electrons of energy E_n recorded in the pulse height analyzer in channels 1,2 3 ..respectively, then

$$M = A_{n1} M + A_{n2} M + A_{n3} M + \dots$$

In case of continuous spectrum the numbers M_1, M_2, M_3 ... of a true spectrum having energies E_1, E_2, E_3 ... respectively, while being recorded in the pulse height analyzer gives the numbers M_1', M_2', M_3' ... in different channels of the pulse height analyzer because of resolution and backscattering. The true and the observed spectrums are related by:

$$\begin{bmatrix} M_1' \\ M_2' \\ M_3' \\ \cdot \\ \cdot \\ \cdot \end{bmatrix} = \begin{bmatrix} A_{11} & A_{12} & A_{13} & \cdot & \cdot \\ A_{21} & A_{22} & A_{23} & \cdot & \cdot \\ A_{31} & A_{32} & A_{33} & \cdot & \cdot \\ \cdot & \cdot & \cdot & \cdot & \cdot \\ \cdot & \cdot & \cdot & \cdot & \cdot \\ \cdot & \cdot & \cdot & \cdot & \cdot \end{bmatrix} \begin{bmatrix} M_1 \\ M_2 \\ M_3 \\ \cdot \\ \cdot \\ \cdot \end{bmatrix}$$

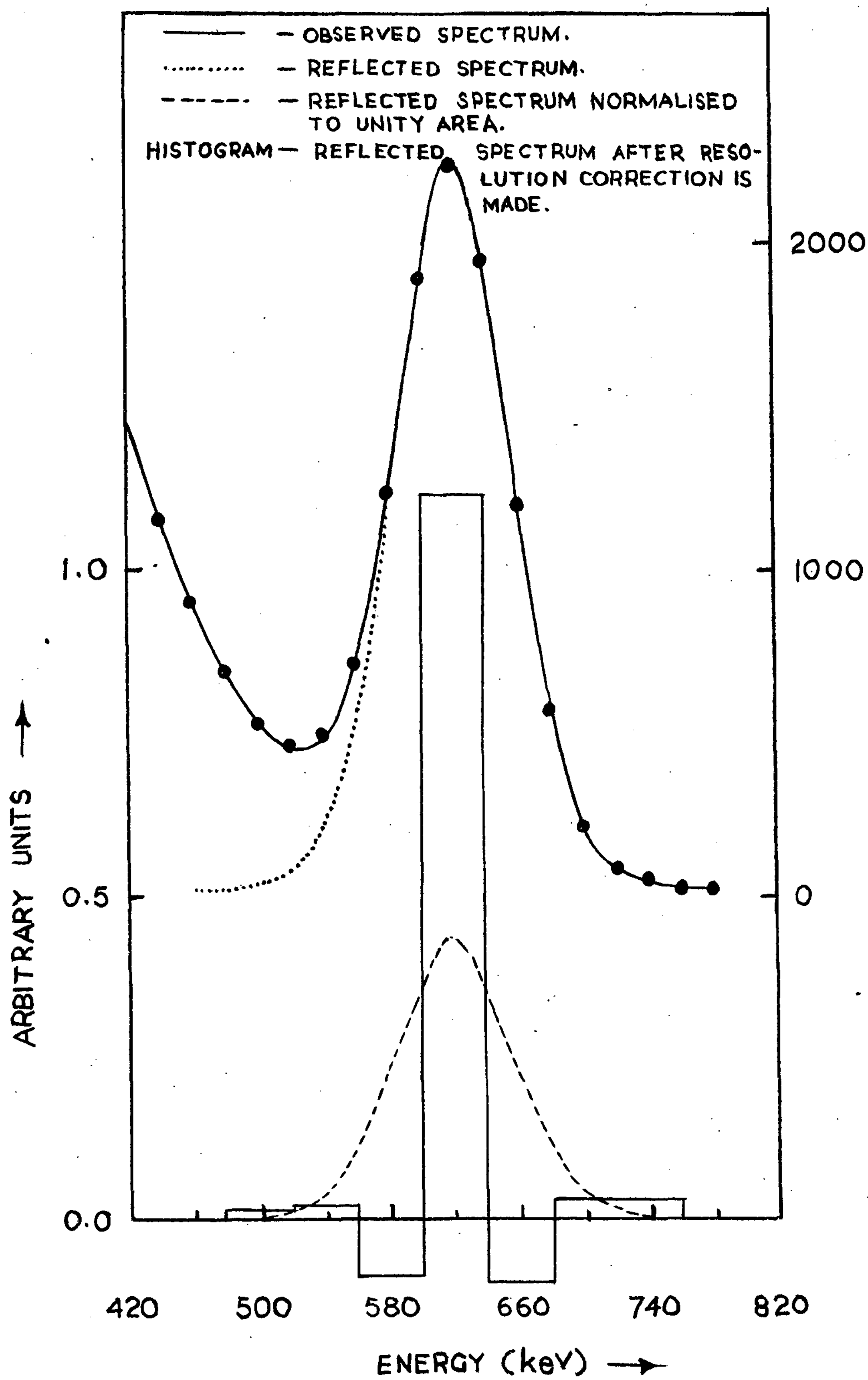

— OBSERVED SPECTRUM.
— REFLECTED SPECTRUM.
— REFLECTED SPECTRUM NORMALISED TO UNITY AREA.
HISTOGRAM — REFLECTED SPECTRUM AFTER RESOLUTION CORRECTION IS MADE.
2000
1000
0
COUNTS
1.0
0.5
0.0
ARBITRARY UNITS
420
500
580
660
740
820
ENERGY (keV)

FIG.1

or shortly $M' = AM$ and $M = A^{-1}M'$

The matrix A was constructed assuming no backscattering and the scintillator response of the monoenergetic electrons to be Gaussian. The variation of resolution with energy has also been assumed to obey a $E^{-\frac{1}{2}}$ law. In the matrix A (neglecting backscattering) there are diagonal elements and few off diagonal elements. Four forward matrices have been prepared assuming resolutions 13%, 13.5% , 14% and 15% for 620 KeV electrons. The inverse matrices have been obtained by inversion in an Electronic Computer. Fig.1 shows the observed spectrum and the corrected spectrum for 620 KeV conversion electrons of Cs^{137}. The matrix method was applied to continuous gamma- ray spectrum by Kockum and Starfelt (3). The errors involved in the matrix method have been discussed by Rand (4).

A triple coincidence arrangement was set up for determining positron spectrum avoiding backscattering by requiring the positrons to annihilate in the crystal and detecting the annihilation gammas in two NaI (Tl) crystals. Na^{22} positron spectrum was taken and resolution correction was applied using the appropriate inverse matrix. As expected the corrections gave a shift in the end energy only.

If the response function of the monoenergetic electrons for different energies is known, then, it will be possible to prepare matrices including backscattering. There are controversial views on this point. Freedman et al and Bosch and Urstein (5) observe a flat tail along with the gaussian peak, the tail to peak ratio remaining constant. Bertolini et al (6) observe a similar response function with the tail to peak ratio decreasing with increasing energy. Persson (7) observes a slope in the tail. It is possible that all these controversies are due to geometry and scattering materials around the source and detector. The proper way to incorporate it is to study in our geometry. Preliminary measurements for a few energies were made and the results are in agreement with that of Bertolini et al, though the ratios (tail to peak) are higher. This is due to the fact the measurements were made in air. Response functions are required before matrices including backscattering can be constructed. The work is being continued.

REFERENCES

1. J.P. Palmer and L.J. Laslett, U.S.A.E.C. Bulletin ISC - 174 (1950).
2. M.S. Freedman, T.B. Novey, F.T. Porter and F. Wagner Jr., Rev. Sci. Instr. 27, (1956), 716.
3. J. Kockum and N. Starfelt, Nucl. Instr. and Meth. 4, (1959), 171.
4. R.E. Rand, Nucl. Instr. and Meth. 17, (1962) 65.
5. H.E. Bosch and T. Urstein, Nucl. Instr. and Meth. 24, (1963), 109.
6. G. Bertolini, F. Cappelani and A. Rota, Nucl. Instr. and Meth. 9, (1960) 107.
7. B. Persson, Nucl. Instr. and Meth. 27, (1964) 1.

DEVELOPMENT OF A SURFACE IONIZATION TYPE ION SOURCE
AND ITS USE IN THE DETERMINATION OF IONIZATION POTENTIAL

S.D. Dey
Saha Institute of Nuclear Physics, Calcutta

INTRODUCTION

The formation of ions +ve or −ve when evaporation of atoms or molecules take place from a heated filament is known as Surface Ionization. When +ve ions are formed, the ratio of the number of emitted ions to neutral atoms is given by the Saha-Langmuir equation,

$$\frac{n^+}{n_a} = g^+/g_a \, e^{(\phi - I)/kT} \tag{1}$$

where g^+ and g_a are the statistical wts. of the emitted ions and neutral atoms. ϕ is the work function of the filament material and I is the ionization potential of the evaporating atom.

Equation (1) can be rewritten in the form

$$\frac{n^+}{n} = \left(G_e \, e^{(I-\phi)/kT} + 1\right)^{-1} \tag{2}$$

where $G_e = g^+/g_a$ and n is the sum of n_+ and n_a. In case when $(I - \phi)$ is greater than kT, unity appearing in equation (2) can be neglected and it reduces to

$$n^+/n = G_e \, e^{(\phi - I)/kT} \tag{3}$$

OR

$$i^+ = n A e^{(\phi - I)/kT} \tag{4}$$

A being some constant and i^+ is the +ve ion current.

Equation (4) may be utilized in the determination of ionization potential. From the equation it is evident that if n is maintained constant, the plot of log i^+ vs $\frac{5040}{T}$ will give a st. line and the negative slope of the curve will give $(I - \phi)$, if ϕ and G_e are assumed to be constant over the temp. range, if the range is small.

The work function ϕ_{eff} determined from the slope of the Richardson plot

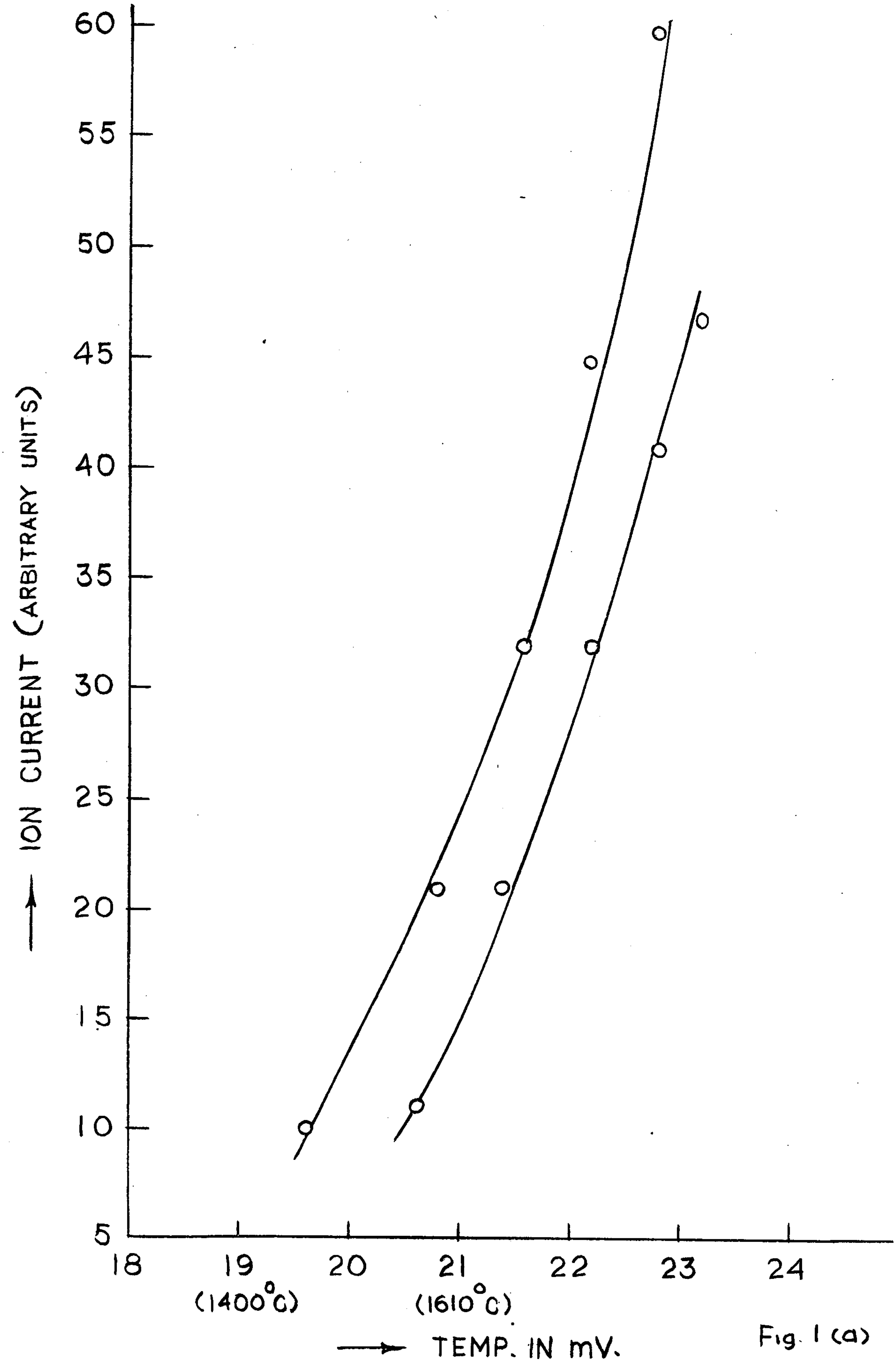
60
55
50
45
40
35
30
25
20
15
10
5
ION CURRENT (ARBITRARY UNITS)
18
19
(1400°C)
20
21
(1610°C)
22
23
24
TEMP. IN mV.
Fig. 1 (a)

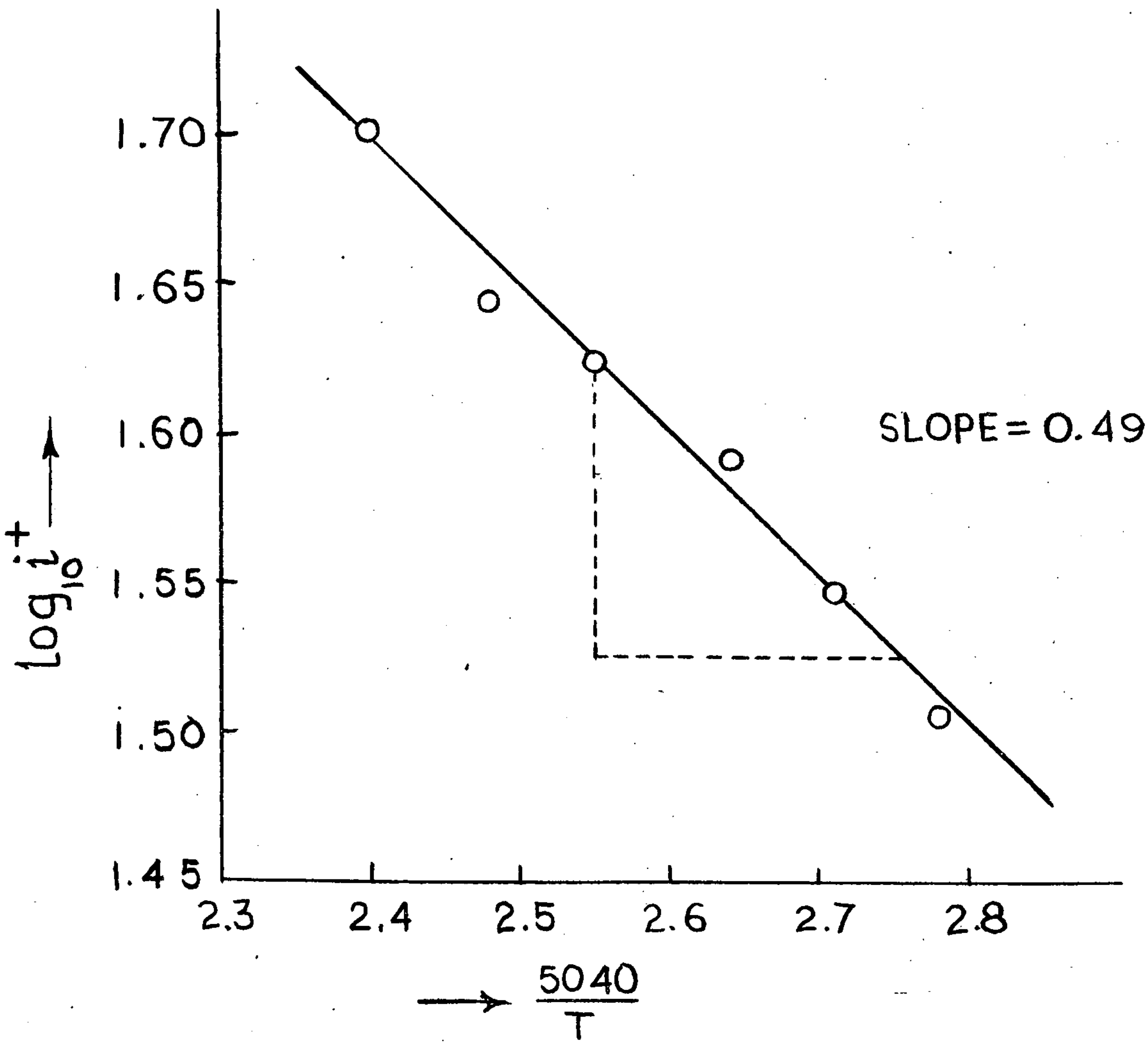

1.70
1.65
1.60
1.55
1.50
1.45
2.3
2.4
2.5
2.6
2.7
2.8
SLOPE = 0.49
$\log_{10} i^{+}$
$\frac{5040}{T}$

Fig. 1 (b)

of electron current vs.temp. differs from the thermionic work function ϕ because of the polycrystalline nature of the filament. The slope of the curve log i^+ vs $\frac{5040}{T}$ will actually give (I- $\phi_{eff.}$); ϕ_{eff} being known, I can be calculated.

GENERAL SET UP

The source and the detector are fitted at the two ends of a 2' x 4" copper cylinder. It is evacuated to a pressure of better than 10^{-5} mm. of Hg, a thermocouple gauge and a Penning gauge being used to measure the vacuum.

THE ION SOURCE SIDE

The three filament ion source after Inghram and Chupka (1) is developed here. The three filaments, each of diameter 12 mil., are mounted on copper rods and these rods pass through special type of kovar seals. The side filaments are used as evaporators whereas the central filament is used as the ionizer. The three-filament ion source has the advantage that the ionization and evaporation processes are separated and as such the ionizing filament can be raised to any high temperature without the element being evaporated. The filaments are heated by transformers, the primaries of which are controlled by variacs. A tungsten-tantalum couple (2)is spot welded at the centre of the central filament to measure its temperature.

Slits are mounted on ergan rods which inturn are screwed in the flange. Altogether three slits are used to accelerate and focus the electron and ion beams. The last wide slit is placed infront of the collector to supress secondary electrons emitted from it when is it bombarded by ions or electrons. The first two slits are of width 1 mm.each and the thrid one is of width 2 mm.

THE DETECTOR SIDE

The ion current is measured by astandard electrometer circuit (3). The 959 pentode tube used as the electrometer tube is placed within the vacuum system along with the highmeg resistances connected between the supressor grid and the cathod of the valve via a steatite type switch. This considerably increases the sensitivity of the electrometer because the grid-current is minimised in this arrangement. The supressor grid of the tube is connected to the faraday cage. The faraday cage is insulated from a metal rod, which controls the movement of the cage from outside the vacuum system, by an insulator. The rod passes through a ring seal fitted at the centre of a5" diameter brass flange. In the same flange the electrometer tube is mounted whose connecting terminals are brought out through knovar seals. Also fitted in the flange is the steatite type switch by means of a ring seal.

RESULTS AND DISCUSSION

The ionization potential of lithium has been measured with the equipment described. Future programme includes measurement of ionization potential of rare-earth elements. The side filaments of the ion source are coated with lithium sulphate. The constancy of n in equation(4) is achieved by maintaining the current through the side filament constant.

The three filaments of the ion source are raised to a common potential of + 1210 volts. The first slit, starting from the filament, is maintained at 1200 volts. This one acts as the ion extractor slit. The second slit is at grounded potential and the third at $-1\frac{1}{2}$ volts with respect to the ground is used as the secondary electron supressor. The collector is connected to the grid of the electrometer.

Two curves are drawn, ion current vs. temperature of the ionizing filament, one for no current passing through the side filament and the other for a definite amount of current passing through it. Suitable temperature points are chosen from the curves and the difference of ion current readings are noted. A curve is drawn with these values of ion current and temperature. The method takes into account the influence of heat radiation from the central filament on the magnitude of n and also eliminates the photocurrent to a considerable degree. The procedure is repeated for different evaporation rates in different temperature ranges. Thus a set of curves, log $i^+ \sim \frac{5040}{T}$, are obtained. From the slopes of these $(I-\phi_{eff})$ is obtained. The values obtained are given in the table below:

TABLE I

Temp. range	Observation	Mean value of $(I-\phi_{eff})$	Reference
$1700^\circ K - 2200^\circ K$	The plot of log $i^+ \sim \frac{5040}{T}$ approximates to a st. line.	0.49 e.v.	Figs.1(a) and 1 (b).

To determine ϕ_{eff}, electron current is measured at different temperatures. For electron current measurements, the three filaments of the ion source are raised to a common potential of -3.5 kV. The first slit is maintained at 15 volts -ve with respect to the filaments to supress secondary electrons emitted from the slit due to primary electrons striking it. This is necessary, otherwise the secondary electrons may form a part of the primary beam. The second slit is maintained at -10 volts and the theird one at $-1\frac{1}{2}$ volts. The collector is connected to the ground through a meter. From the Richardson plot in the tem.range $1400^\circ K$ - 1800°K the avarage value of ϕ_{eff} turns out to be 4.87 e.v. The value of ϕ_{eff} above 1800°K could not be measured owing to technical difficulties.

Substituting this value of ϕ_{eff} in the table, the value of I turns out to be 5.36 e.v. The actual value will be slightly different because ϕ_{eff} is not accurately known in the tem.range 1700°K-2200°K the optical spectroscopic value of I is 5.40 e.v.

The value of the ionization potential determined by this method is not as accurate as that obtained from optical spectroscopy. This method is particularly useful where optical analysis is difficult e.g. rare-earths. In this connection it may be mentioned that Ionov and other (4,5) have determined that ionization potentials of Pr, Tb, Ce, Er and particularly Nd by the method of surface ionization. Ionization potential of Nd has been determined from series limit by Hassan (6) and the value obtained agrees with the value obtained by Ionov and others.

REFERENCES

1. Inghram, M.G. and Chupka, W.A., William, A.-Rev. Sci. Instr. 24, 518 (1953).

2. Morgan, F.H. and Danforth, W.E.- Jour. Appl. Phys. 21, 112 (1950).

3. Elmore and Sands- Electronics- McGraw-Hill Book Co. p. 189.

4. N.I. Ionov and M.A. Mittsev-Soviet Phys. JETP, 11, 972 (1960).

5. N.I. Ionov and M.A. Mittsev-Soviet Phys. JETP, 13, 518 (1961).

6. Hassan, G.E.M.A. - Physica, Oct. 1963, Deel 29, NO. 10, pp. 1119-1127.

PHOTOELECTRIC CROSS SECTION OF GAMMA RAYS FOR HEAVY ATOMS

A. M. Ghose
Nuclear Physics Laboratory, Bose Institute Calcutta.

A new method has been developed for the measurement of atomic photoelectric cross sections for high Z atoms. The method is based on the possibility of separation of scattering from true absorption by the measurement of photon transmission through spherical shells of absorbers. In a separate paper theoretical calculations have been presented to consider the effects of multiple scattering as the thickness of the shell is gradually increased (1). It has been shown that the absorption in the shell can be approximated by an effective cross section which can be expanded in a polynomial in the thickness of the shell:

$$\sigma(t) = \sigma_a \quad (1 + at + bt^2 + \ldots) \tag{1}$$

where σ_a is the absorption (essentially photoelectric) cross-section while σ (t) is the effective cross-section at a thickness t of the absorber; a, b etc. are constants independent of t.

Validity of eq. (1) supposes the use of a constant spectral sensitivity photon counter (2) which forms an essential part of our equipment. Using such a counter and a rotation arrangement for averaging out photon intensities, photoelectric cross-sections for lead and mercury have been measured for Co^{60} photons. The results are shown in Table I. It has been found that the experimental results obtained by different workers for Co^{60} γ-rays show mutual agreement, if the ratios of K-shell to total photoabsorption are assumed to have the values given by Hultberg (3). However, our measurements of lead for Cs^{137} photons indicate that these ratios are not

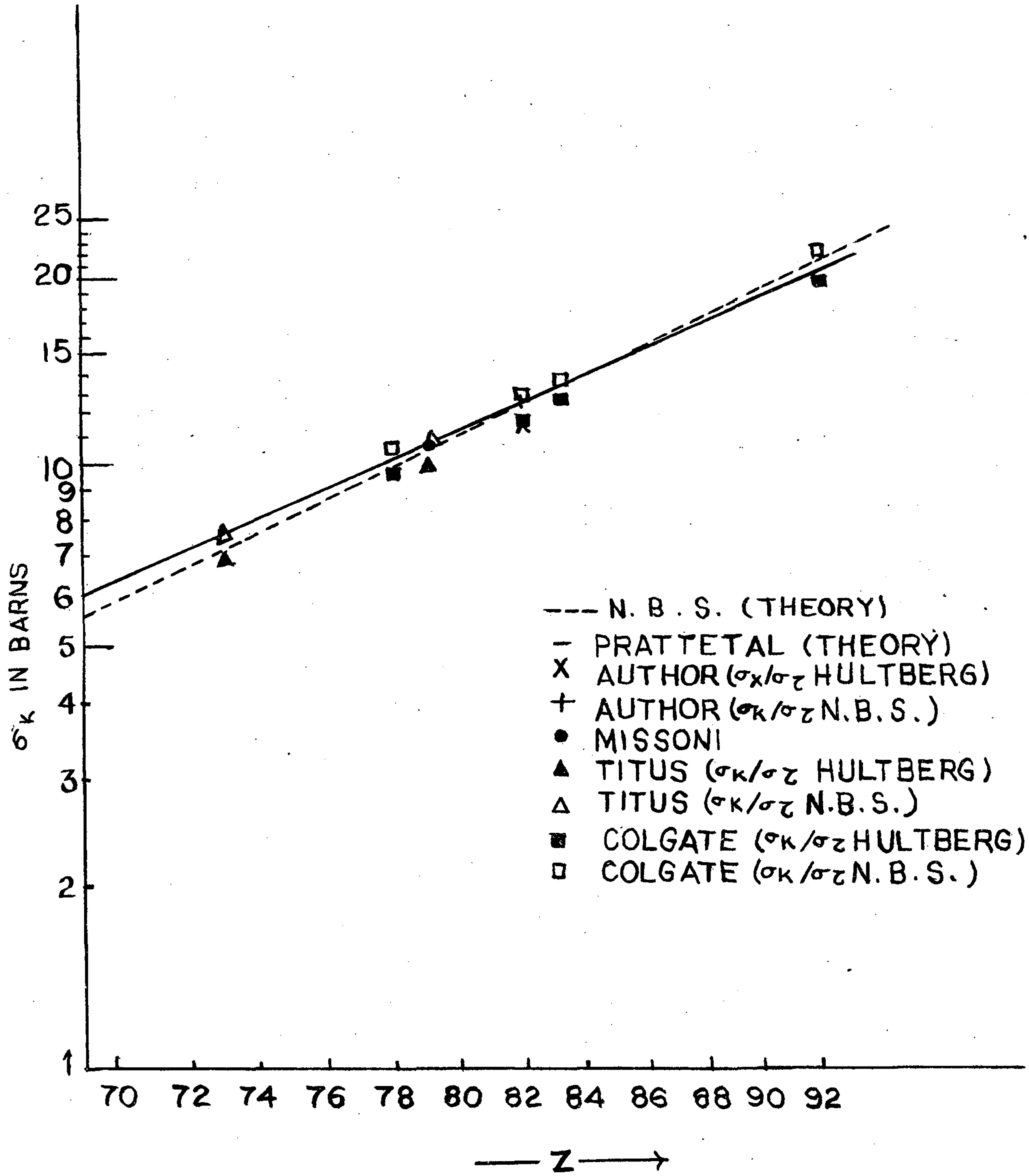

σ_K IN BARNS
25
20
15
10
9
8
7
6
5
4
3
2
1
70 72 74 76 78 80 82 84 86 88 90 92
Z
--- N. B. S. (THEORY)
— PRATTETAL (THEORY)
X AUTHOR (σ_X/σ_τ HULTBERG)
+ AUTHOR (σ_K/σ_τ N.B.S.)
● MISSONI
▲ TITUS (σ_K/σ_τ HULTBERG)
△ TITUS (σ_K/σ_τ N.B.S.)
■ COLGATE (σ_K/σ_τ HULTBERG)
□ COLGATE (σ_K/σ_τ N.B.S.)

FIG.1

Probably applicable in this energy range. In fig. 1 we have shown the results obtained by different workers in this field. Contrary to what is expected on general theoretical grounds, the values given in the NBS table by Grodstein (7) restores agreement between theory, experiments performed directly on σ_K and experiments on σ_a by different methods.

A detailed paper giving various sources of error in this type of experiment and their reduction will be published shortly.

REFERENCES

1. A.M. Ghose (In Press)
2. A.M. Ghose Nuclear Instruments and Methods (In Press)
3. S. Hultberg Ark. Fys. 15, 307 (1959).
4. E. Bleeker, P. Goudsmit and C de Vries Nucl. Phys. 29, 452 (1962).
5. S. Colgate Phys. Rev. 87, 592 (1952).
6. R. Pratt, R. Levee, R. Pexton and W. Aron. Phys. Rev. 134, A 898 (1964).
7. G. Grodstein NBS Circular No. 583 (1957).
8. G. Missoni Quoted in Ref. 6.
9. W. Titus Phys. Rev. 115, 351 (1959).

<u>TABLE I</u>

Photoelectric Cross Sections of Heavy Elements for Co^{60} Photons

Experimenter	Energy of Photons MeV	Element studied	Barns/atom σ_a	Barns/atom σ_k	Theoretical σ_K (barns/atom) Pratt 6 et.al	NBS 7
Hultberg (3) (1959)	1.173	U	-	7.2±0.50	6.32	6.9
	1.332	U	-	5.4±0.30	4.93	5.5
Bleeker(4) et.al(1962)	1.332	Pb	-	3.24±0.13	2.99	3.24
Colgate(5) (1952)	1.332	Pt	2.61±0.07	2.10±0.06	2.31	2.53
	1.332	Pb	3.39±0.07	2.71±0.06	2.99	3.24
	1.332	Bi	3.53±0.07	2.82±0.06	3.20	3.45
	1.332	U	5.45±0.09	4.36±0.09	4.93	5.45
Author	1.173 1.332	Hg (Hgo Powder)	4.01±0.25	3.23±0.20	3.04	3.39
	-d0-	Pb (Pbo Powder)	4.48±0.20	3.58±0.16	3.41	3.66
	-d0-	Pb (foil)	4.38±0.20	3.50±0.16	3.41	3.66

MEASUREMENT OF ABSOLUTE DIFFRENTIAL COLLISION CROSS SECTION OF Co^{60} IN COMPTON EFFECT

A. M. Ghose
Nuclear Physics Laboratory, Bose Institute
Calcutta

Absolute values of the differential collision cross sections of Co^{60} photons (1.17 and 1.33 MeV) in Compton effect have been measured in the angular range of 13° to 140°, in two steps. First the relative values of the cross sections have been determined by using the experimental arrangement described below. Collimated photon beams emerge out of a source placed on a goniometer table. The photons scattered through an angle by the cylindrical copper scatters pass through a fixed system of lead slits and are detected by a uniform spectral sensitivity photon counter developed by the author (1). It can be shown that the present type of experimental arrangement can only yield relative values of the cross-sections.

Corrections have to be made for multiple scattering and absorption in the scatters. This has been done by measuring the relative cross-sections as a function of the radius r of the scatterer. Extrapolation to zero thickness by a polyomial of low degree(first or second) then sufficies to correct for these effects. Corrections have also been made for self-absorption in the source and for small variation of the detector sensitivity with angle. Fig. 1 shows the experimental results along with their theoretically predicted values. The data unequivocally rule out the distribution formula of Breit, Gordon and Dirac in favour of the Klein-Nishina formula.

The relative measurements have been converted to their absolute values by a partial integral type measurement in which the total cross section for

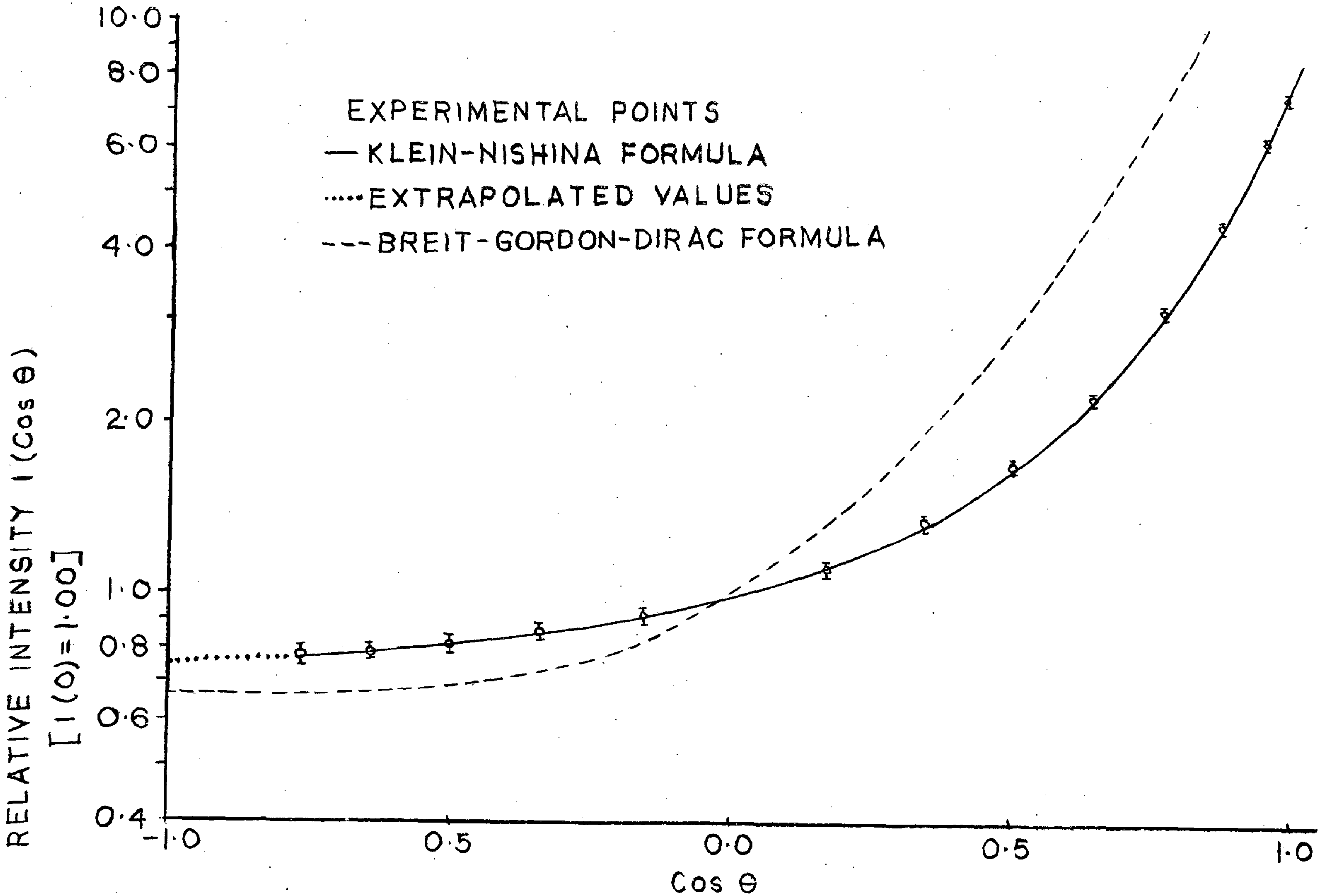
EXPERIMENTAL POINTS
— KLEIN-NISHINA FORMULA
····· EXTRAPOLATED VALUES
--- BREIT-GORDON-DIRAC FORMULA
RELATIVE INTENSITY I (Cos θ)
[I (0) = 1·00]
10·0
8·0
6·0
4·0
2·0
1·0
0·8
0·6
0·4
-1·0
0·5
0·0
0·5
1·0
Cos θ

FIG.1

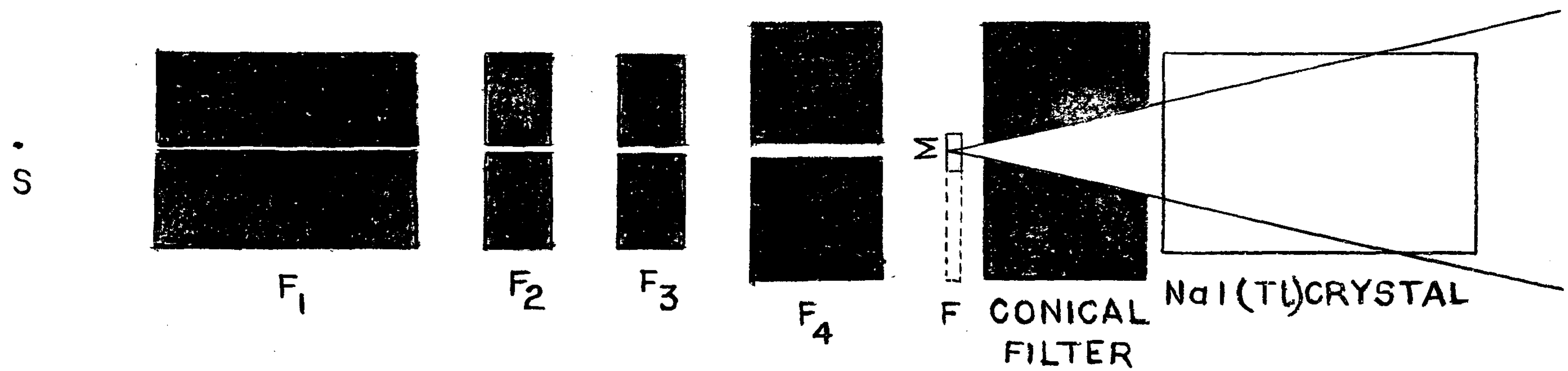

FIG. 2

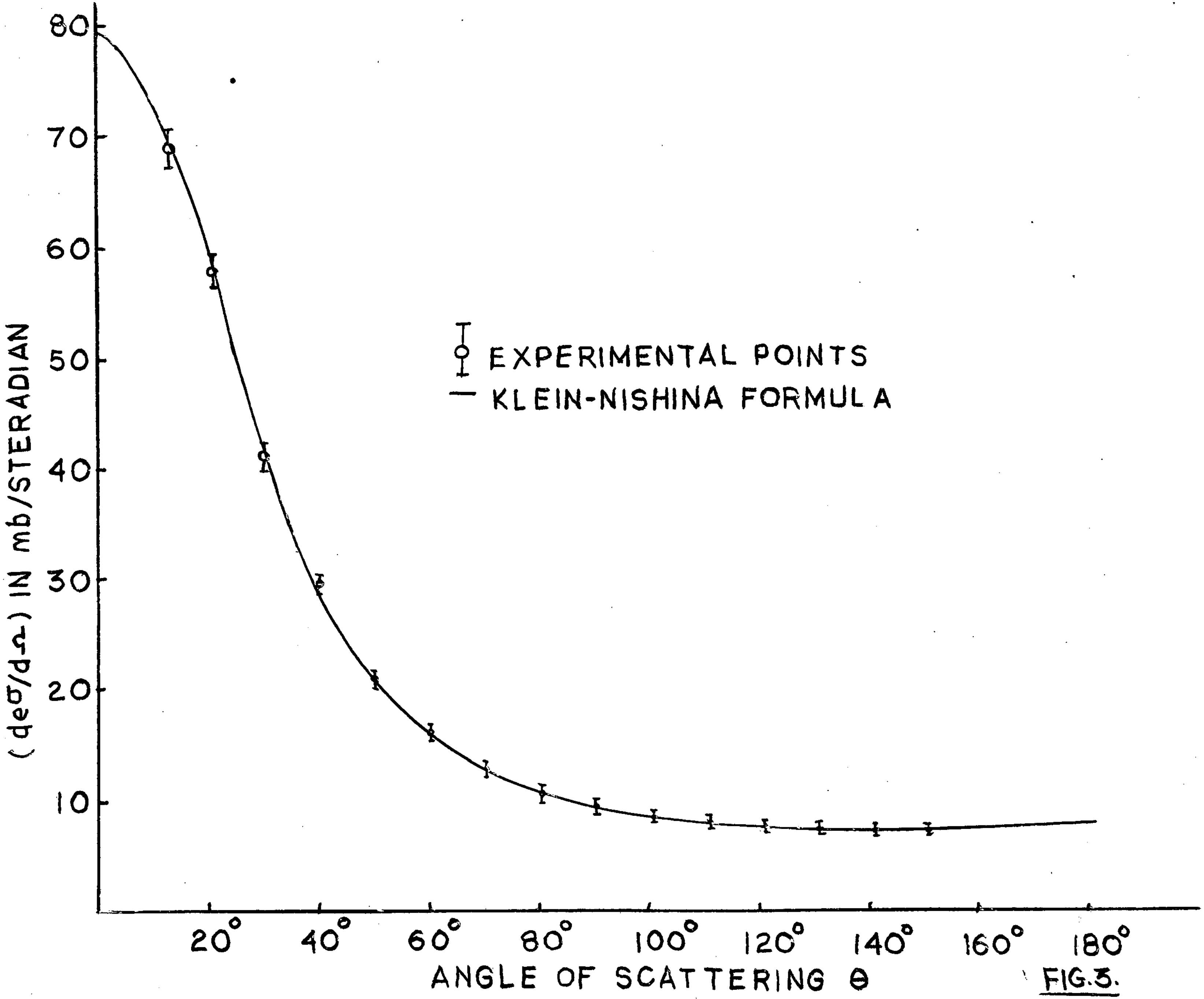

80
70
60
50
40
30
20
10
EXPERIMENTAL POINTS
KLEIN-NISHINA FORMULA
(deσ/dΩ) IN mb/STERADIAN
20° 40° 60° 80° 100° 120° 140° 160° 180°
ANGLE OF SCATTERING θ

FIG.3.

angles 13° to 180° have been measured (Fig.2). A narrow pencil of photons emitted by the sources is selected by a system of filters F_1, F_2, F_3 and F_4, the mean effective angle of the conical umbral beam incident on the scatter being fraction of a degree. The final conical filter selects the value of the minimum angle (13°) through which photons must be scattered before they are removed from the exit channel. The separation of the crystal and the filter has been adjusted in such a manner that the path lengths of the scattered photons is as close as possible to that of the undeviated photons. For the interpretation of these measurements experimental data has been extrapolaed to 180°. This has negligible effect on the over-all accuracy of this experiment. Fig. 4 shows the experimental absolute cross sections and their Klein- Nishina counterpart. The r.m.s. deviation between the experimental and Klein- Nishina values was found to be 1.5% which is well within the mean probable error spread (3.5%) of the experimental points themselves.

REFERENCE

1. A.M. Ghose, Nuclear Instruments and Methods (In Press).

CONFIGURATION MIXING EFFECTS IN SHELL MODEL NUCLEI

Raj K. Gupta *
Physics Department, Panjab University, Chandigarh - 3

In all shell model calculations it is invariably assumed that only low-lying configurations with energies 'nearly degenerate' with the ground state configuration need be mixed to obtain the low-lying levels. This approximation received its justification from the works of Brueckner and others(1). According to this theory, the higher two-particle excitations are all included in the R-matrix by definition. In practice, however, one has to define the 'near degeneracy' quite arbitarily. Banerjee and Dutta Roy (2) considered all the configurations within 1.95 MeV to be nearly degenerate with the ground state configuration for the calculations of the energy levels of Ca^{42} using R-matrix. (1.95 MeV is the single particle energy from Ca^{41} data). Waghmare (3) defined the near degeneracy as $\sim$ 2.5 MeV for his calculations of energy levels of O^{18} and Zr^{92} using a two-body potential (V-matrix). In the light of these definitions for 'near degeneracy' we noticed from the experimental data on single-particle (or single-hole) nuclei that all the shell model nuclei other than ones in 1p shell will have at least their single-excitation configuration degenerate with the ground state configuration. For 1p-shell the single particle excitation energy is even as large as 5 MeV and this makes the ground state as pure configuration.

The calculations for 1p-shell nuclei have generally been carried out based on the Ls-coupling or Intermediate coupling models. It was even remarked (4) that it was not likely that conventional shell model calculations will be made for cases like mass 14 nuclei. However recently True(5) has reported the calculations of the energy levels in N^{14} using a central

TABLE-1

λ	1.0	0.8	0.5	0.3
$-V_S$	13.0	21.3	74.6	350.9

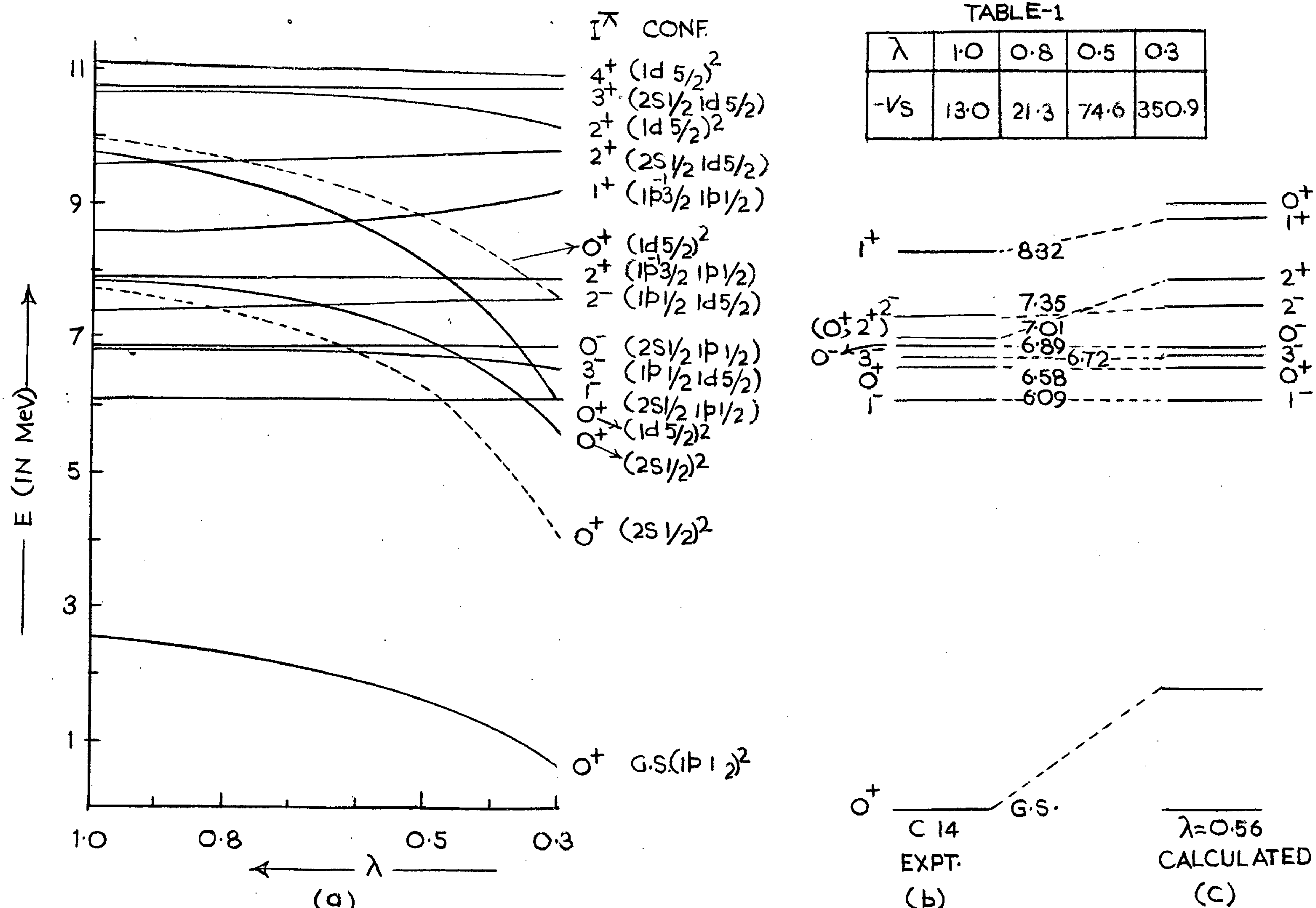

FIG. 1

two-body interaction of the Gaussian type. Here we report the results of our similar calculations for C^{14}. It may be mentioned that whereas several authors(6) had made jj -coupling model calculations for specific problems, involving only odd-parity states of C^{14}, no detailed shell model calculations for this nucleus are available so far. Here we evaluate the central two-body interaction matrix elements by the method of relative coordinates developed by Moshinsky (7) and others (8). A potential well of the Gaussian type has been taken.

Considering C^{12} as the core the ground state of C^{14} is given by the two particles (neutrons) configuration $(1p_{1/2})^2_{0^+}$. The excitation of one or both of these particles would give rise to excited configurations $(1p_{\frac{1}{2}}\ 2S_{\frac{1}{2}})1^-$, 0^-, $(1p_{\frac{1}{2}}\ 1d_{5/2})\ 3^-, 2^-$, $(2S_{\frac{1}{2}})^2_0$ + and $(1d_{5/2})^2_{0^+}$, $2^+, 4^+$ (leaving $1d_{3/2}$ as compared to $1d_{5/2}$ as it is $\sim$ 5 MeV above $1d_{5/2}$). The core, if considered to be soft, also gives rise to the core-excited configuration $(1p^{-1}_{3/2}\ {}^1p_{1/2})1^+2^+$ The relative energy for such hole-particle configurations can directly be calculated (9) from particle-particle configurations. The single particle energies are taken from the experimental data on C^{13}. The calculated level spectrum is shown in fig 1 (a) as a function of the range parameter λ, defined as $\lambda = \frac{r_0}{r_l}$, r_0 being the range of the Gaussian potential and r_l that of nucleon wavefunction, for singlet forces (singlet even + singlet odd). The calculations for other types of the exchange mixtures have also been made and this mixture appears to give most favourable results. The potential strength V_S, calculated from $(1p_{1/2}\ 2S_{1/2})1^-0^-$ doublet, for different values of λ is shown in table 1; given as inset in fig. 1 itself. Since the first excited state $2s_{\frac{1}{2}}$ of C^{13} is at 3.09 MeV the ground state of C^{14} has been taken to be pure in the spirit of the definitions of 'near degeneracy' mentioned above, and only the configuration mixing of other two 0^+ states given by the configurations $(2s_{1/2})^2$ and $(1d_{5/2})^2$ has been allowed. This is shown by dotted lines in fig 1 (a).

First we discuss the relative position of the ground state. As observed by Sood and Waghmare (6) in their study of $p_{\frac{1}{2}}$ doublets, we have to assume, in addition to the above interaction, a pairing force operating only in the $(1p_{\frac{1}{2}})^2\ 0^+$ ground state of C^{14} and depressing it by about 2 MeV. Waghmare and Majumdar (10) have recently calculated this level including the correlations in the ground state in the Random Phase Approximation and the BCS type pairing energy and have obtained satisfactory agreement with the ground state energy. In view of their contributions to the ground state energy we have normalised our calculated energy levels with respect to the 6.09 MeV, 1^- state.

Next we consider the choice of a suitable value of λ, the only free parameter in our calculations, that will lead to the best fit with the experimental data. From the figure it is clear that the energies of the negative parity states vary very little with the variation of λ, and thus cannot provide any criterion for choosing any particular value for the same. However, the variation in the energy of the 0^+ states, is quite marked and we notice that the position of first excited 0^+ level with respect to 1^- level does not leave much freedom, and points to a value $\lambda \approx 0.56$, giving the best fit. The results for this value of λ are shown separately in Fig. 1. (c), and the over all agreement with the experimental results, shown in Fig. 1(b), is very satisfactory. This agreement allows us to make the following configuration assignments to the various energy levels observed in C^{14}.

The odd parity states are given by the two $p_{\frac{1}{2}}$ doublets, in agreement with earlier qualitative considerations. The 0^+, 6.58 MeV level is characterised to be $(2S_{\frac{1}{2}})^2$ with admixtures from $(1d_{5/2})^2$. The 1^+, 8.32 MeV level can be assigned the hole-particle configuration $(1p_{3/2}^{-1}\,1p_{1/2})$ as this is the only one giving 1^+ state. There remains the level 7.01 MeV whose spin-parity has been observed to be $(0^+, 2^+)$. The calculations do not show any other level below 2^- state. However, there is a 2^+ state, due to $(1p_{3/2}^{-1}\,1p_{1/2})$ configuration lying very close to 2^- state. The 2^+ states are also given by the particle-particle configurations $(2S_{1/2}\,1d_{5/2})$ and $(1d_{5/2})^2$. If the configuration interaction between these three 2^+ states be considered, the hole-particle 2^+ state would be depressed in the right direction and could possibly be compared with the observed 7.01 MeV level. Warburton and Pinkston (4) have compared this 7.01 MeV level with the 2^+, 9.16 MeV analog in N^{14}. Further if we consider the O^{16} as the core for C^{14}, the 7.01 MeV state could be identified as 0^+ state due to the O^{16} - core excitation configuration $(1p_{3/2})^{-2}$. But, this state is formed by the C^{12} (t,p) C^{14} double stripping and it is unlikely that such configuration would be strongly formed by such reactions (11). Further, an intermediate coupling calculation due to Wilmore (12) suggests that the lowest 0^+ state of C^{14} arising from such a configuration would have an excitation energy of at least 12 MeV. Thus the character of the character of the 7.01 MeV state as 2^+ due to C^{12} core-excitation configuration $(1p_{3/2}^{-1}\,1p_{1/2})$ seems to be appropriate.

Hence we conclude that C^{14} can be justifiably treated on the jj-coupling model with C^{12} as the core and configuration mixing among the excited states in the spirit of Brueckner theory.

REFERENCES

1. See for example, R.J. Eden, Nuclear Reactions Vol. 1 (Edited by P.M. Endt and M. Demeur; North Holland Publishing Co.; Amsterdam 1959 p.l.
2. M.K. Banerjee and B.Dutta Roy, Ann. Phys.; 7, 484 (1959).
3. Y.R. Waghmare, Phys. Rev. 134, B 1185 (1964).
4. E.K. Warburton and W.T. Pinkston, Phys. Rev. 118, 733 (1960).
5. W.W. True, Phys. Rev. 130, 1530 (1963).
6. I. Unna and I.Talmi, Phys. Rev. 112, 452 (1958); E.K. Warburton, H.J. Rose and E.N. Hatch, Phys. Rev. 114, 214 (1959) ; P.C. Sood and Y.R. Waghmare, Nucl. Phys. 46, 181 (1963) ; F.C. Barber, Phys. Rev. 122, 572 (1961).
7. M. Moshinsky, Nucl. Phys. 13, 104 (1959).
8. R.D. Lawson and M.G. Mayer, Phys. Rev. 117, 174 (1960); A. Arima and T.Terasewa, Prog. Theo. Phys. 23, 115 (1960); A.N. Mitra and S.P. Pandya, Nucl. Phys. 20, 456 (1960).
9. S. P. Pandya, Phys. Rev. 103, 956(1956).
10. Y.R. Waghmare and C.K. Majumdar - to be published.
11. A.A. Jaffe, F. De S. Barros, P.D. Forsyth, J. Muto, I.J. Taylor and S. Ramavataram, Proc. Phys. Soc. (London) 76, 914 (1960).
12. Wilmore, Private Communication to Jaffe et.al. (Ref: 11).

---

* The Author now states "unfortunately some mistake has been noticed in the calculations which changes some of the results presented herein. However the conclusions remain the same"

ROTATIONAL BANDS IN Kr^{82}

P. K. Bindal, Raj K. Gupta and P.C. Sood
Physics Department, Panjab University, Chandigarh-3

The existence of the large quadrupole moments and the greatly enhanced E2 transistion probabilities over the single particle estimates in several nuclei led to the recognition of the collective effects in such nuclei more than a decade ago. The study of low-lying levels by Coulomb excitation process (1,2) provided very striking evidence in favour of such an interpretation. Certain characteristic regularities with respect to energy spacings in even-even nuclei far from closed shells could accurately be represented as belonging to rotational spectra. Such a rotational spectra has since long been noted to be absent in the region $40 < A < 150$. On the other hand, Coulomb excitation experiments (2) had established that essentially all even-even transitions in medium weight non-magic nuclei (roughly from Ti to Te) are from 10 to 30 times faster than single particle transitions and must therefore involve some degree of collective participation. Recently (3) it has been shown that certain nuclei in this region possess deformed shapes and show rotational spectra. In the present note we shall show from simple considerations how the energy levels in Kr^{82} may constiture rotational bands. The analysis is based on the earlier studies of Gupta and Sood (3).

The reduced transition probabilities for a single particle transition of E2 type, given by

$$B(E2)_{S.P.} = 3 \times 10^{-5} A^{4/3} e^2 \times 10^{-48} Cm^4$$

is $1.07 \times 10^{-2} e^2 \times 10^{-48} Cm^4$ for $A = 82$. The experimental value (4) of $0.18 \times 10^{-48} e^2 Cm^4$ from Coulomb excitation of first 2^+ excited state shows an enhancement of about 17 times over the single particle estimate. The reduced transition probability due to Coulomb excitation of first excited state is related to the intrinsic quadrupole moment by the relation

$$B\,(E2) = 5/16\pi \; e^2 \, Q_o^{\,2}$$

which in turn is related to the deformation parameter by

$$Q_o = \frac{3}{\sqrt{5\pi}} \; Z \, R_o^{\,2} \, \beta \, (\,1 = 0.16\beta + \quad .....)$$

Taking the experimental value of B (E2), the intrinsic quadrupole moment is calculated to be $Q_o = 1.35$ barn and the deformation parameter $\beta \simeq 0.18$. This value of β is comparable with the values for other deformed nuclei with well-developed rotational spectra.

The energy levels in the rotational bands are given by the formula

$$E\,(I) = E_o + AI\,(I + 1) - BI^2\,(\,I + 1)^2 \; + ...$$

where A is related to the moment of inertia $\mathcal{J}$ of the deformed nuclei ($= \hbar^2/2\mathcal{J}$) and B is the rotation-vibration coupling constant. The rotational constants A and B for Kr^{82}, calculated by using the experimental (5) energies of the first 2^+ (777 KeV) and 4^+ (1821 KeV) excited states, are 146 KeV and 2.75 KeV respectively. These values of A and B for Kr^{82}, when compared with the known cases of deformed nuclei, fit quite nicely in the general picture. This is clearly shown in table I.

Having obtained the rotational constants A and B from the observed $0^+ - 2^+ - 4^+$ sequence, we use them to obtain the energy separations in the excited bands. The 2^+ level at 1475 KeV may be treated as band-head for K = 2, γ-band. The resulting rotational spectrum is shown in Fig. 1. (1.b) to be compared with the experimental level scheme (5) given in Fig. (1 a). The agreement for the 3^+ 2 (I^π K) level is very good. The 4^+ 2 level is predicted at 2519 KeV. This may correspond to an

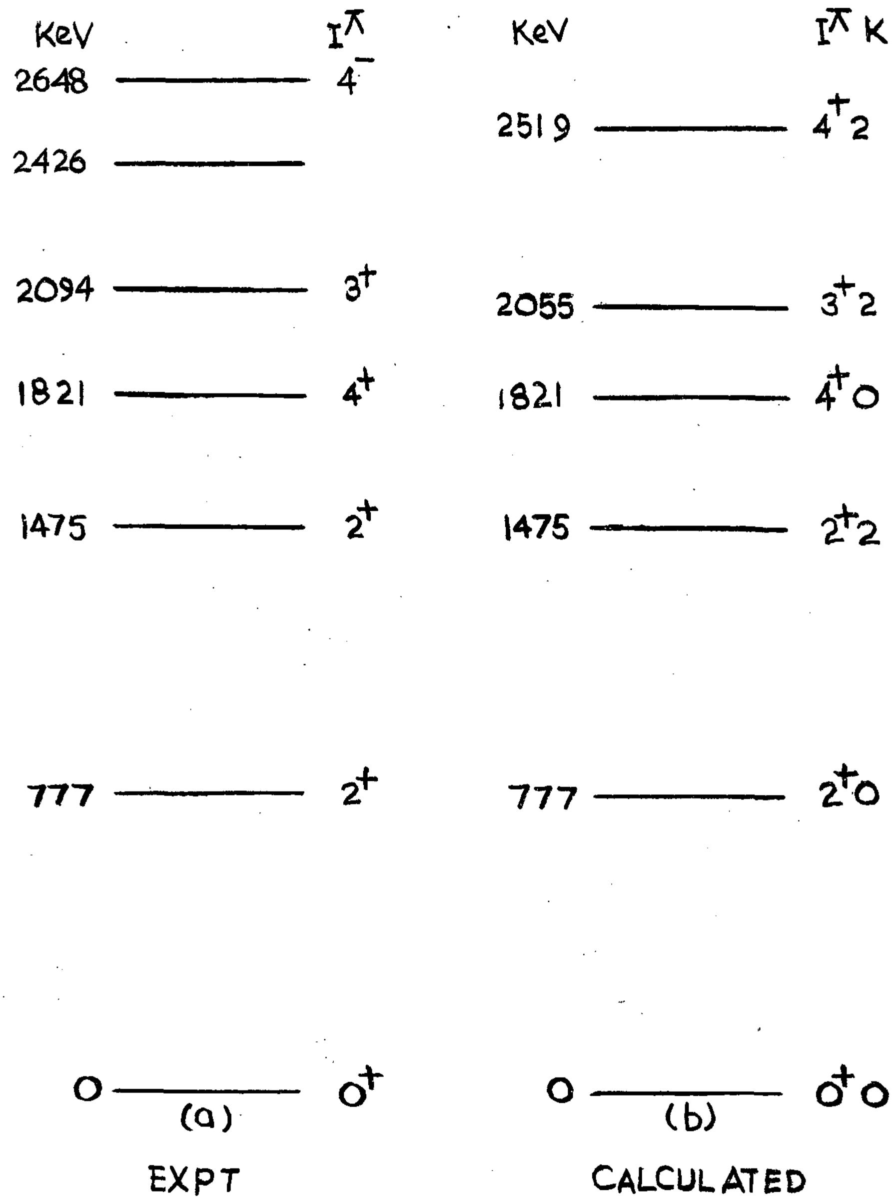
KeV
I^π
2648
4^-
2426
2094
3^+
1821
4^+
1475
2^+
777
2^+
0
0^+
(a)
EXPT
KeV
I^π K
2519
4^+2
2055
3^+2
1821
4^+0
1475
2^+2
777
2^+0
0
0^+0
(b)
CALCULATED

FIG.1.

experimentally observed level at 2426 KeV whose spin-parity assignment has yet to be determined. Thus in addition to the ground state, K = 0, rotational band a k = 2, γ-vibrational band is indicated for this nucleus.

TABLE I

The rotational constant A and B in KeV obtained by fitting the 2^+ and 4^+ states of the ground state rotational band in various nuclei.

Nucleus	Ne^{20}	Mg^{24}	Si^{28}	Fe^{56}	Kr^{82}	Sm^{152}	Th^{228}
A	298	237	323	157	146	21	10
B	4.3	1.6	4.6	2.6	2.75	0.14	0.02

REFERENCES

1. K. Alder, A. Bohr, T. Huus, B. Mottelson, and A Winther, Rev. Mod. Phys. 28, 432 (1956).

2. N.P. Heydenburg & G.M. Temmer, Ann. Revs. Nucl. Sc. 6, 77 (1956).

3. Raj K. Gupta and P. C. Sood, Prog. Theo. Phys. 31, 509 (1964); R.K. Sheline, T. Sikkeland and R. N. Chanda, Phys. Rev. Lett. 7, 446 (1961); E. Marshalek, L. W. Person and R.K. Sheline, Rev. Mod. Phys. 35, 108 (1963).

4. N.P. Heydenburg, G.F. Pieper, C.E. Anderson, Phys. Rev. 108, 106 (1957).

5. L. Simons, S. Bergstrom & A. Anttila, Nucl. Phys. 54, 683 (1964); T.J. Kennett, I.B. Webster and W.V. Prestwick, Nucl. Phys. 58, 56 (1964).

SHELL MODEL CALCULATIONS FOR LEVELS IN Nb^{91}

S. D. Sharma, Raj K. Gupta and
P.C. Sood
Department of Physics, Panjab University, Chandigarh-3

The calculations for energy levels of nuclei with or near closed shells are normally carried on the jj coupling model. Several investigators have done such calculations for the nucleus Zr^{90} with considerable success. These and the results for other nuclei with similar configurations suggest that 38 protons may be taken to constitute a fairly stable core along with 50 neutrons. Further it is well known that the matrix elements of the two-body interaction do not change appreciably from one nucleus to a neighbouring one. Based on these considerations we have carried out the calculations of the energy levels of the nucleus Nb^{91} using the study of Zr^{90} levels by Thankappan, Waghmare and Pandya (1) (hereafter referred to as TWP) and the discussion of this nucleus by Sood and Waghmare (2).

In the present report we have not included the configuration mixing effects which are still under investigation. Thus the ground state configurationis taken as $(p_{\frac{1}{2}})^2\ (g9/2)^1$ proton added to the 50 neutrons- 38 protons core. The excited levels are obtained when one or both of the protons from the $p_{\frac{1}{2}}$ orbit are excited. Single proton excitation resulting in the configuration $(p_{\frac{1}{2}})^1\ (g9/2)^2$ leads to the negative parity states and the excitation of both the protons from $p_{\frac{1}{2}}$ orbit gives $(g9/2)^3$ configuration and positive parity states. For our calculations we assume that the ground state of Nb^{91} is reached by adding one $g_{9/2}$ proton to the $(p_{\frac{1}{2}})^2$ ground state of Zr^{90} and similar is the case for the excited levels.

The central two-body nuclear interaction assumed by TWP (1) is a Gaussian potential of the type

$$H_{12} = (V_t \Pi_t + V_s \Pi_s)\, exp(-r/r_0)^2 \tag{1}$$

with $\Pi_t = \frac{1}{4}(3+\bar{\sigma}_1\cdot\bar{\sigma}_2)$; $\Pi_s = \frac{1}{4}(1-\bar{\sigma}_1\cdot\bar{\sigma}_2)$

The energy levels are calculated as a function of the parameter $\lambda = r_0/r_l$ where r_0 is the range of the Gaussian potential (1) and r_l that of the harmonic oscillator wave functions chosen to describe the particle states. When two equivalent particles are coupled to a non-equivalent particle, the matrix elements of the two body nuclear interaction can be written as (2)

$$\langle (j)^2_x\, j' : J | H_{12} | (j)^2_y\, j'' : J \rangle = \delta_{xy}\, \delta_{j'j''} \langle (j)^2_x | H_{12} | (j)^2_x \rangle + 2[xy]^{1/2} \times (-)^{x+y} \sum_{x'} [x'] W(jjJj';xx') W(jjJj'';yx') \langle jj':x' | H_{12} | jj'':x' \rangle \tag{2}$$

where different terms have their usual meaning. If all the three particles are equivalent, then we have the well known relation in terms of the fractional parentage coefficients

$$E_J[(j)^3] = 3 \sum_x \langle (j)^3 : J | (j)^2 : x \rangle^2 E_x[(j)^2] \tag{3}$$

We assume the singlet and the triplet potential strengths V_s and V_t derived by TWP for Zr^{90}. The single particle energy $\Delta = E(p_{\frac{1}{2}}) - E(g_{9/2})$ is taken to be 0.915 MeV from the data on Y^{89}. Since the ground state may not be a pure configuration, we normalise our results to the $1/2^-$ state. The level spectrum calculated for Nb^{91} as a function of the parameter λ is shown in Fig. 1(a). The spin values higher than 9/2 have been left out. Fig. 1(b) gives the experimental energy levels (3,4) and 1(d) and 1(e) show the results from other investigators (5,6) along with our best fit results shown in 1(c).

First we notice that our results are very similar to those of other investigators (5,6) and the agreement will improve with the inclusion of configuration mixing in our calculations, although the approach is basically

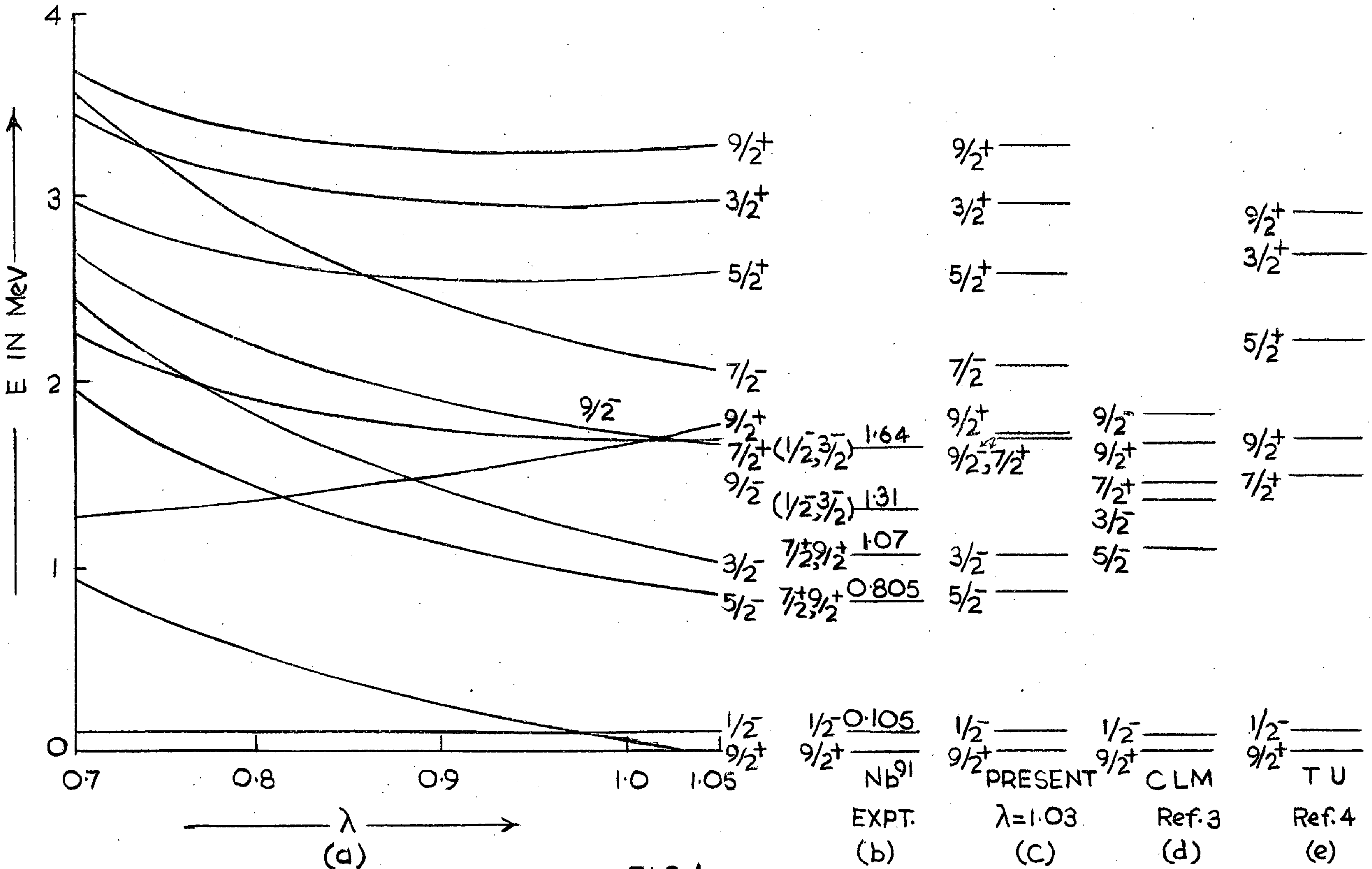

E IN MeV
0
1
2
3
4
0.7
0.8
0.9
1.0
1.05
λ
(a)
9/2+
3/2+
5/2+
7/2−
9/2−
9/2+
7/2+
9/2−
3/2−
5/2−
1/2−
9/2+
(1/2−, 3/2−) 1.64
(1/2−, 3/2−) 1.31
7/2+, 9/2+ 1.07
7/2+, 9/2+ 0.805
1/2− 0.105
9/2+
Nb91
EXPT.
(b)
9/2+
3/2+
5/2+
7/2−
9/2+
9/2−, 7/2+
3/2−
5/2−
1/2−
9/2+
PRESENT
λ=1.03
(c)
9/2−
9/2+
7/2+
3/2−
5/2−
1/2−
9/2+
CLM
Ref. 3
(d)
9/2+
3/2+
5/2+
9/2+
7/2+
1/2−
9/2+
T U
Ref. 4
(e)

FIG. 1

different. We start with an explicit form of the two body interaction and seek out its verification through these calculations whereas others treat the two-body interaction matrix elements (and not the interaction itself) and single particle binding energies as independent parameters. The agreement of the results obtained via the two approaches - the analytical approach of our type and the one using high speed computers like CDC 3600 -strengthens one's faith in simple mindéd approach of investigators with limited facilities.

Now let us compare our results with the available experimental information. We have chosen the best fit values as shown in 1(c) to agree with the observed $9/2^+$ — $1/2^-$ separation. In addition two negative parity states at 1.31 MeV and 1.64 MeV are observed with the possible spin assignments ($1/2^-$, $3/2^-$) for both. Shell model considerations suggest only one $3/2^-$state with the other member of the doublet as $5/2^-$. However core-excitation, i.e., excitation of one proton from the $p_{3/2}$ orbit to $g_{9/2}$ orbit can give us a $3/2^-$ state. Thus both these levels may be assigned spin parity $3/2^-$ arising from the configuration $(p_{1/2})^1$ $(g_{9/2})^2$ and $(p_{\frac{1}{2}})^2$ $(g_{9/2})^2$ $(p_{3/2})^{-1}$ respectively. This is in agreement with the suggestion of Lobkowicz and Marmier (3). Further these investigators (3) report two positive parity levels at 0.805 MeV and 1.07 MeV both with suggested spin parity assignment ($7/2^+$, $9/2^+$). Our calculations show these levels at higher excitation energy, and it is expected that, with the inclusion of the configuration mixing, their separation can be correctly predicted.

We are, at present, investigating the effect of configuration mixing and also the core excitation process. Meanwhile further definite experimental information can be very useful in determining the nuclear interaction parameters.

REFERENCES

1. V.K. Thankappan, Y.R. Waghmare and S.P. Pandya; Prog. Theo. Phys. (Japan) 26, 22(1961).
2; Y.R. Waghmare; Ph.D. Thesis, University of Bombay, 1962; P.C. Sood and Y.R. Waghmare, Nucl. Phys. 46, 181 (1963).
3. B. Lobkowicz and P. Marmier; Helv. Phys. Acta. 34, 85 (1961).
4. Nuclear Data Sheets, 1960.
5. S. Cohen, R.D. Lawson and M.H. Macfarlane; Phys. Lett. 10, 195 (1964).
6. I. Talmi and I Unna; Nucl. Phys. 19, 225 (1960).

ALPHA -DECAY OF AMERICIUM - 241

M. Rama Rao
Saha Institute of Nuclear Physics, Calcutta

Most of the available information on the excitation levels of Np^{237} has been derived through experiments based on : (i) β-decay of U^{237}, (ii) Electron capture in Pu^{237}, and (iii) Coulomb excitation of Np^{237}.

However, relatively much less was known about the excitation levels of Np^{237} from direct measurements on alpha transitions in the decay of Am^{241}. Our knowledge of the alpha decay of Am^{241} was limited to only six or seven fine structure alpha groups until 1963 when working with a high resolution magnetic spectrograph, Baranov et al (1) showed the existence of at least 18 fine structure alpha-ray groups. A study of the alpha decay of Am^{241} would hence be of considerable interest both from the view point of excited levels of Np^{237} as well as of the alpha decay characteristics of Am^{241}.

This study has been undertaken with the help of a low pressure expansion cloud chamber (2). The alpha-tracks are photographed in a stereo set-up. Range and energy measurements are made after stereo projection of the photographs. Table I, summarises the results based on the evaluation of 40,000 tracks.

TABLE I

Finstructure of Am^{241} alpha groups

Alpha particle energy (MeV)	Intensity %	Energy levels above the ground state (KeV)
5.540	0.25	0
5.508	0.13	32
5.482	85.00	59
5.438	12.70	103.7
5.383	1.45	159
5.317	1.2×10^{-2}	226

In general, agreement has been obtained with the results of most previous work. Hitherto, the experimental evidence for the excitation level of Np^{237} at 226 KeV arises mainly through the results of alpha spectrometry of Am^{241}. Recently, the low energy gamma ray transitions in Np^{237} following alpha decay of Am^{241} have been studied by examination of the internal conversion spectrum, using $\pi\sqrt{2}$ beta-ray spectrometer and the existence of level at 226 KeV has been revealed (3). We, in our own cloud chamber studies, have been able to identify and substantiate the existence of this low intensity 226 KeV level.

REFERENCES

1. S.A. Baranov et al; JETP 16, 562 (1963) and JETP. 18, 1241(1964).
2. M.Rama Rao, Indian Journal of Physics. 35, 92 (1960).
3. J.L. Wolfson and J.J.H. Park, Canadian Journal of Physics 42, 1387 (1964).

DISCUSSIONS

P. Mukherjee: What is the effect of straggling on your energy resolution?

M. Rama Rao : We have used Bethe's range-energy relations for estimation of energies. This sets an energy resolution limit to 20 KeV for alphas.

P.Mukherjee: Did you take into account the self absorption of the alpha's in the target?

M.Rama Rao : We have used in our investigations Am^{241} source prepared and imported from ORNL. They have quoted the energy spread to be 3 KeV compared to limitations on the range-energy relations utilised, the contribution arising from the energy spread of the source itself is negligible.

P. Mukherjee: How uniform is your chamber pressure?

M.Rama Rao: The constancy of pressure in the cloud chamber has been tested from time to time by obtaining photograhs of Po^{210}-α's with Am^{241}-α's. This is achieved by using a electro-magnetically operated shutter arrangement.

CROSSSECTION MEASUREMENTS OF (p,p'γ) RADIATIONS FROM Ni^{60} & Ni^{62}*

by

P.N. Trehan and N.C.Singhal

Department of Physics, Punjab University
Chandigarh - 3

The experiment was to measure the yield of (p,p'γ) radiations from isotopically enriched Ni^{60} and Ni^{62} targets for proton bombarding energy ranging from 3.4 MeV to 5.0 MeV. The target was mounted at 90° to the proton beam direction in a target chamber of the type discussed by Trehan(1). The gamma ray measurements were carried out with a 3" x 3" NaI crystal counter (connected to 400 channel analyser) at 55° to the beam direction. Table I gives all the gamma rays observed in Ni isotopes.

TABLE I

Target	Gamma rays observed (in MeV)				
Ni^{60}	0.67^{+}	0.83^{*}	0.96^{*+}	1.33^{*}	
	1.56^{+}	1.79^{*}	2.16^{+}		
Ni^{62}	0.68^{+}	0.88^{*}	0.96^{+}	1.17^{*}	1.33^{+}
	1.42^{+}	1.72^{*}	1.86^{+}	2.30^{*}	

* γ -rays observed from (p,p'γ) reaction

\+ γ -rays observed from (p,γ) reaction in Ni or Cu^{63} contaminant.

The assignment of gamma rays to either (p,γ) or (p,p'γ) reaction was made on the basis of observed threshold energy and the rate of the variation of production cross-section with proton energy. Figure 1 shows

* This work was done in collaboration with Dr. D.M. Van Patter, Bartol Research Foundation under the sponsorship of U.S. Air Force Office of Scientific Research.

the decay schemes of Ni^{60} and Ni^{62} along with the observed $(p,p'\gamma)$ radiations in the present measurements.

To get the production crosssection of various gamma rays, their yields were corrected for summing effects and the gamma ray efficiencies given by Heath (2). Correction to these gamma-rays were made due to absorption of γ -rays in the Platinum backing, target chamber walls and crystal housing. After applying these corrections, γ -ray yields were used to calculate $(p,p'\gamma)$ production crossections.

Figure 2 shows the level excitation crossections as a function of proton energy for some levels in case of Ni^{60} and Ni^{62}. For the levels 2.16 and 2.29 MeV in Ni^{60}, for which spin and parity assignments were not definite, theoretical calculations were made (using Hauser and Feshbach method (3) and suitable optical potential for the expected spins and are shown in fig. 2 (a). In case of 2.16 MeV level the experimental crossection is higher than that expected theoretically. This could be explained if we consider the possibility of contribution to this level from some higher energy levels. In case of 2.29 MeV level, the experimental crossections are corrected for Ni^{60} (p,γ), Cu^{63} (p,γ) contribution (Cu^{63} is present as contamination in Ni^{60} target) and are shown with the expected theoretical crossection (calculated with 0^+ or 2^+ spin). It is observed that 0^+ spin assignment is most suitable.

For the levels 2.05 and 2.30 MeV in Ni^{62} experimental and theoretical crossections are shown in Fig. 2(b). In case of 2.05 MeV level 0^+ assignment is most suitable which agrees with that done by Sen Gupta et al (4). In case of 2.30 MeV level, the experimental crossection is lower than that expected theoretically. This is expected as we could not observe 1.13 MeV

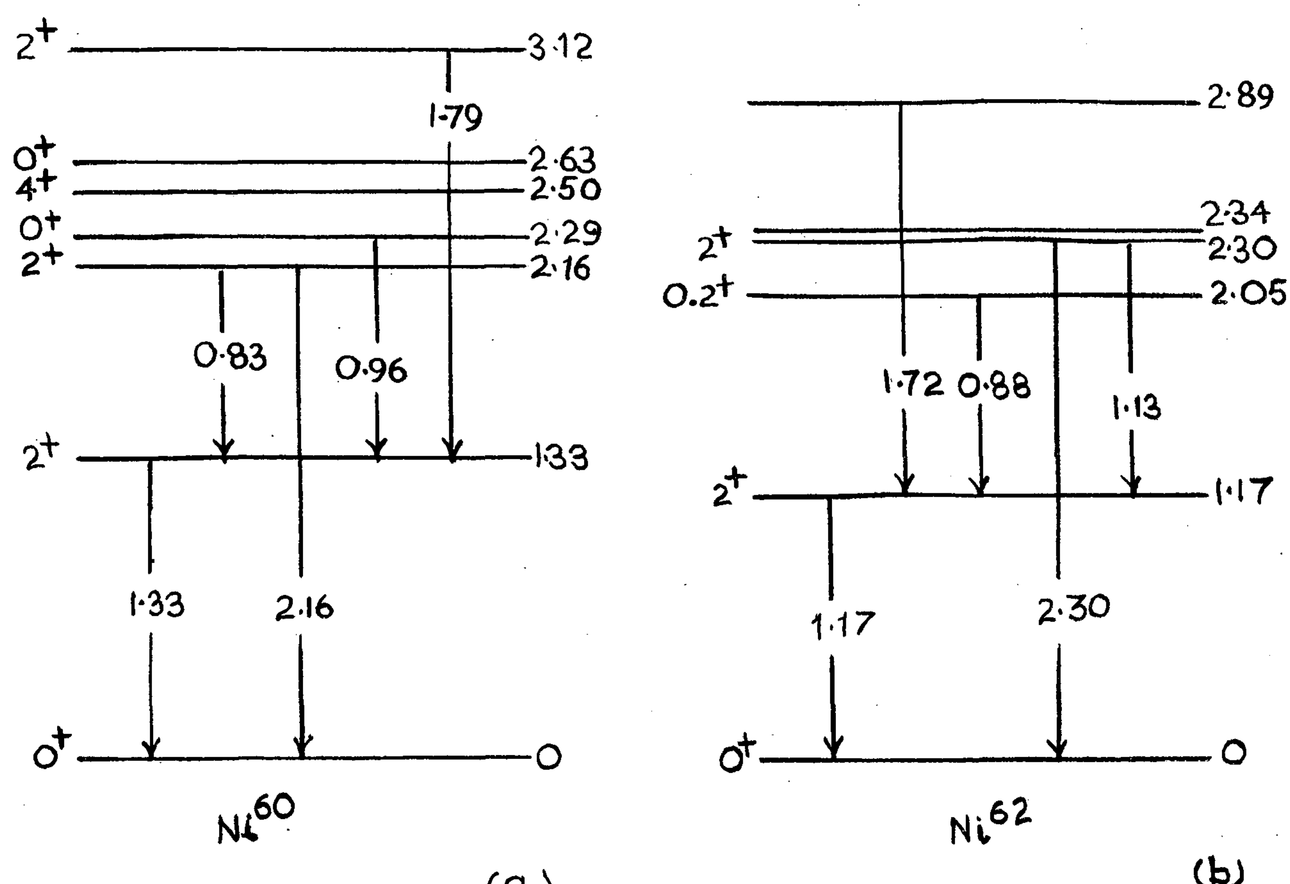

2+
3·12
1·79
0+
2·63
4+
2·50
0+
2·29
2+
2·16
0·83
0·96
2+
1·33
1·33
2·16
0+
0
Ni60
(a)
2·89
2·34
2+
2·30
0.2+
2·05
1·72
0·88
1·13
2+
1·17
1·17
2·30
0+
0
Ni62
(b)

FIG·1

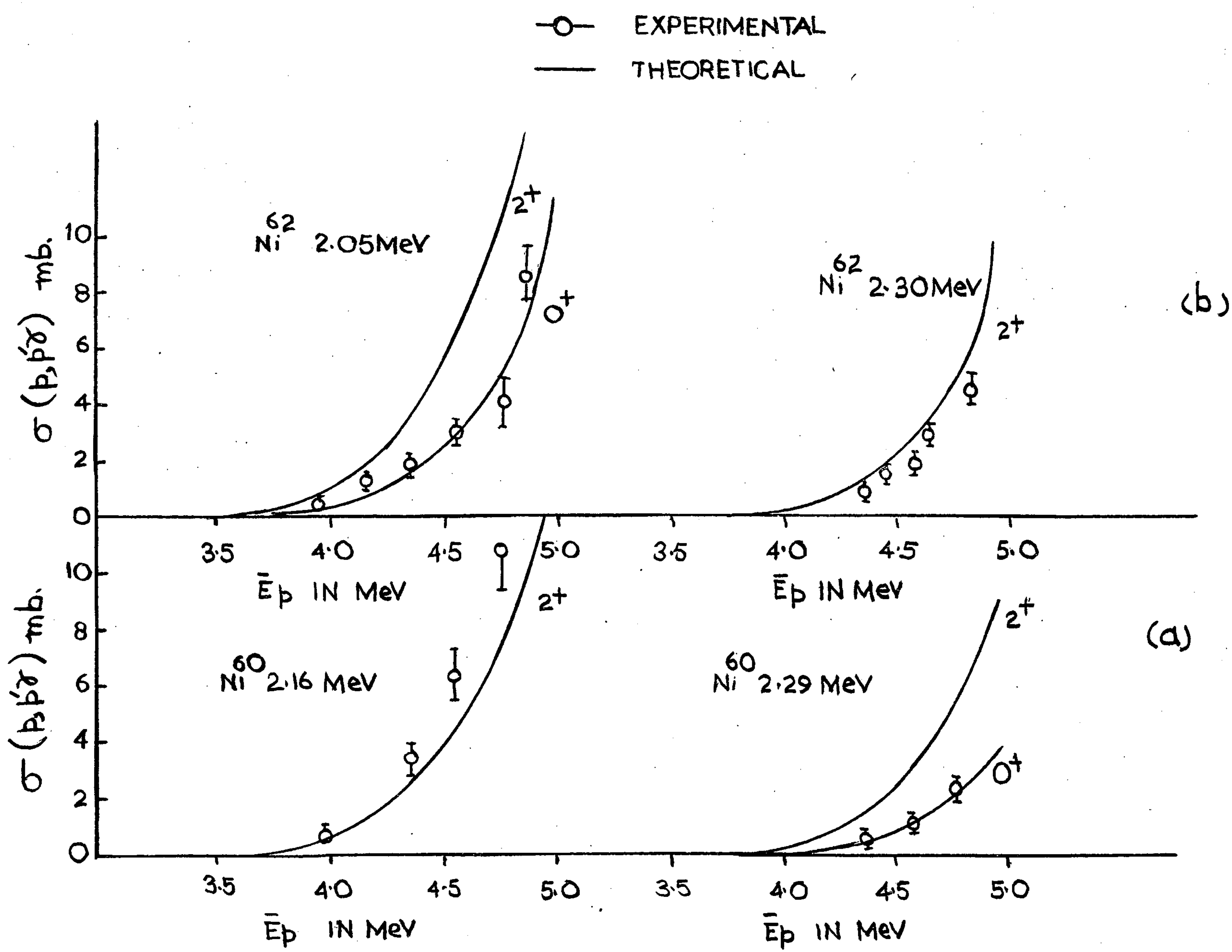
EXPERIMENTAL
THEORETICAL
Ni^{62} 2·05MeV
Ni^{62} 2·30MeV
Ni^{60} 2·16 MeV
Ni^{60} 2·29 MeV
(b)
(a)
2^+
0^+
σ (p, p'γ) mb.
$\bar{E}_p$ IN MeV
0
2
4
6
8
10
3·5
4·0
4·5
5·0

FIG. 2

gamma ray for the 1.13 - 1.17 MeV cascade and thus could include its yield in the crossection calculation for 2.30 MeV level. This gamma ray has been observed recently by Sen Gupta and Van Patter (5), in coincidence measurements. Thus we expect that the experimental crossection for 2.30 MeV level will be raised to lead to a fair agreement with the theoretically expected value. Thus we conclude that 2.30 MeV level is 2^+ level.

REFERENCES

1. P.N. Trehan, Proceeding Nuclear Physics Symposium, 8, (1964)
2. R.L. Heath, Phillips Petroleum Report I.D.O. 16408 (July 1, 1957) unpublished.
3. W. Hauser and H.Feshbach, Phys. Rev. 87, 366 (1962)
4. A.K. Sen Gupta, P.N. Trehan and D.M. Van Patter, Bull. Am.Phys. Soc. 7 81 (1962); A.K. Sen Gupta and D.M. Van Patter, Physics Letters 3, 355 (1963)
5. A.K. Sen Gupta and D.M. Van Patter private communication.

DISCUSSION

E. Kondaiah : Did you make any p - γ coincidence measurements? In view of the unobserved cascade decays and other complications, the yields of γ- rays by themselves may not uniquely determine the spins of the levels.

P.N. Trehan: There are ways by which we could decide about the assignment of γ-rays to (p,p'γ) reaction in $Ni^{60, 62}$.

1) Firstly from the threshold of observation of a particular γ- ray e.g. (p,p'γ) radiations will start showing at higher energies as compared to (p,γ) radiations.

2) The yield of (p,γ) radiations will show a relatively less increase as we go to higher and higher proton energies whereas $(p, p'\gamma)$ radiations will show a constant increase starting from threshold.

3) Coincidence measurements have been done which also help us in deciding about the origin of γ-rays.

"INELASTIC NEUTRON SCATTERING CROSSECTIONS IN In^{115}"

N. C. Singhal and P. N. Trehan
Physics Department, Panjab University
Chandigarh-3

Significant improvement in the experimental techniques of measuring inelastic neutrons scattering data has been made ever the last few years. This has made possible a precise a nalysis of experimental data in terms of the Hauser-Feshbach theory (1). We have calculated the inelastic neutron scattering crossection in In^{115} from the method of Hauser and Feshbach making use of transmission coefficients from the diffused surface potential of Campbell et al (2). A comparison has been made between the theoretically calculated values and the experimental data of Lind and Day (3). The spin assignment of two levels at 1125 KeV and 1290 KeV in In^{115} is discussed in the light of the above comparison.

Several investigators have studied the level scheme of In^{115} from the beta decay of Cd^{115m} and Cd^{115} using scintillation and coincidence techniques (4) and also from the measurements of inelastic scattering of neutrons by sharp et al (5) and Lind and Day (3). The level scheme of Lind and Day (3) established from their study of inelastic scattering of neutrons has been adopted for the present calculations and is shown in Fig.1.

Fig. 2. shows the results of our calculations for the excitation crossections for 1125 KeV and 1290 KeV levels in In^{115} as a function of neutron energy. The experimental values as obtained by Lind and Day(3) are also shown. For the present calculations, the levels at 935, 1420 have been included with the accepted spin assignments of $7/2^+$ and $9/2^+$ respectively. The spin values

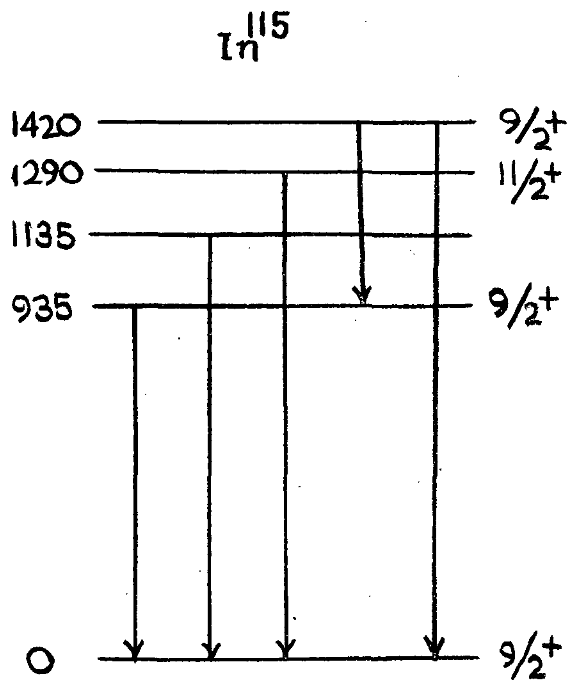

FIG. 1

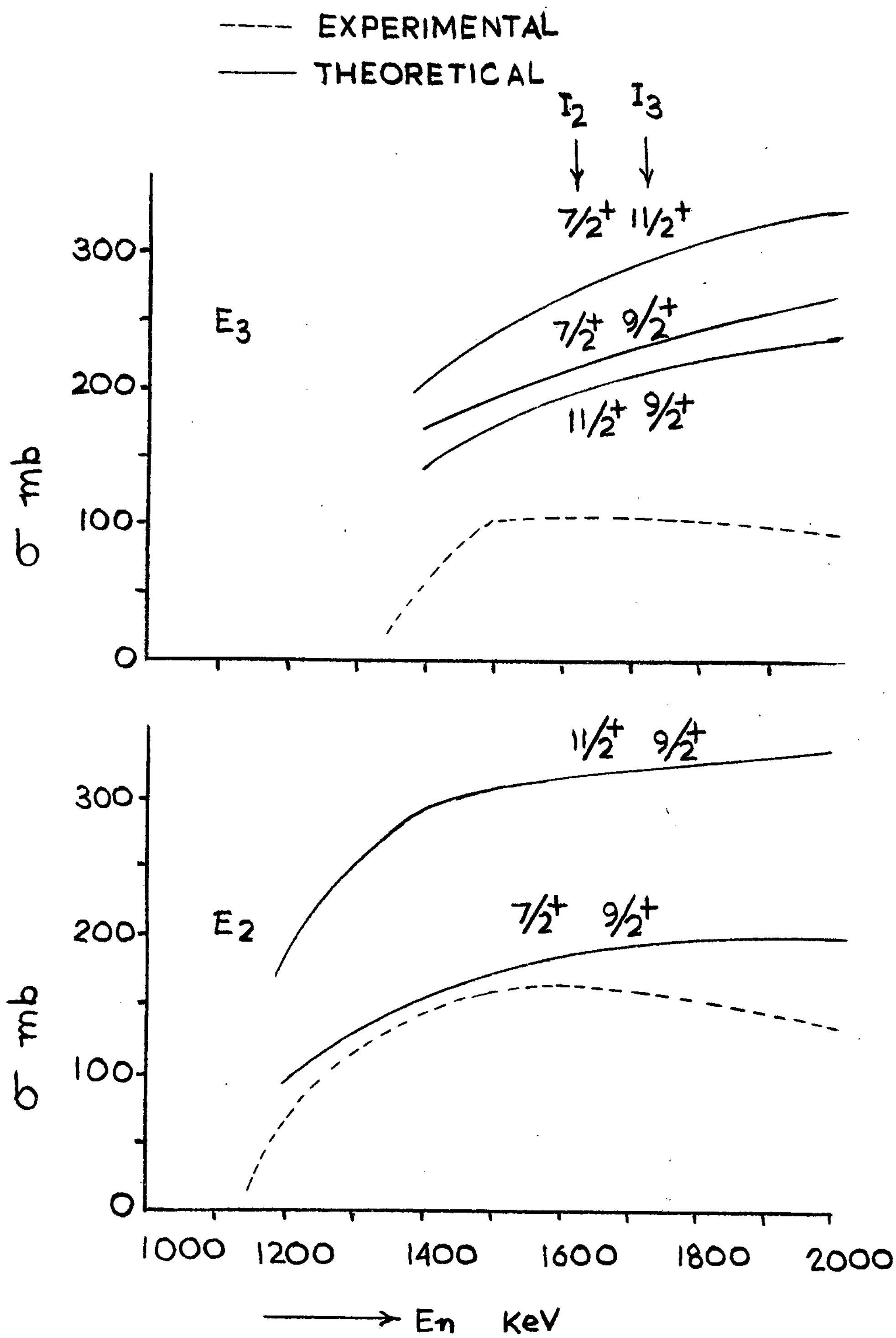
EXPERIMENTAL
THEORETICAL
I_2
I_3
7/2+ 11/2+
7/2+ 9/2+
11/2+ 9/2+
E_3
300
200
100
0
σ mb
11/2+ 9/2+
7/2+ 9/2+
E_2
300
200
100
0
σ mb
1000 1200 1400 1600 1800 2000
En KeV

FIG. 2

to 1125 KeV and 1290 KeV levels are not known definitely and thus various expected spin values ($7/2^+$, $9/2^+$, $11/2^+$, $13/2^+$) and ($9/2^+$, $11/2^+$) have been tried for these two levels. The levels at 650 KeV (recently reported by Sharma et al (4) and Rao et al (4) and 1560 KeV have not been included for these calculations because these levels are not excited in the inelastic neutron scattering process.

From Figure 2(a) we find that the theoretical inelastic neutron scattering crossection for 1290 KeV level are higher as compared with the experimentally measured values of Lind and Day (3) for both the spin assignment of $9/2^+$ and $11/2^+$. It can be observed the theoretical values of crossections for this level do not differ much when a spin change of $11/2^+$ in place of $7/2^+$ is made for 1125 KeV level. Therefore,we cannot select between these two spin assignments for this level.

For 1125 KeV level we have shown two theoretical curves (figure 2 (b) for two different spin values $7/2^+$ and $11/2^+$ (as suggested by Sharma et.al. from their study of angular correlation work(6)) to this level. From the comparison of experimental and the theoretically calculated values of excitation crossections we find the theoretical values are rather too high when a spin assignment of $11/2^+$ is made to 1125 KeV level. There is, in general, quite a good agreement between the theoretical and the experimentally observed values both qualitievely and quantitatively when a spin value of $7/2^+$ is assigned to 1125 KeV level. We also find from the figure 2(b) that the theoretical curve starts deviating towards higher values around about 1700 KeV. This may be explained on the ground that we are not taking into account the contribution of 1560 KeV level and also some high levels might be missing which we are not including in our calculations. More work on these lines is contemplated. It is also proposed to make these calculations taking into account the effect of spin-orbit coupling term in the optical model.

REFERENCES

1. W.Hauser and H. Feshbach, Phys. Rev. 87, 366 (1952).

2. E. J. Campbell, H. Feshbach, C.E. Porter and V.F. Weisskopf M.I.T. , L.N.S. Technical Report No. 73, (February, (1960).

3. D.A. Lind and R.B. Day Ann. of Phys. 12, 485 (1961).

4. R.P. Sharma H.G. Devare Phys. Rev. 131, 384 (1961); V.V. Rao, V. Lakshminarayana, and S. Janananda, Nucl. Phys. 51, 442 (1964); J.B. Vander Koi, H.J. Vanden Bold, and P.M. Endt., Physica 29, 140 (1963).

5 R.D. Sharp and W.W. Buechner Phys. Rev. 116, 992 (1959).

6. V.R. Pandharipande, R.P. Sharma, Girish Chandra, Phys. Rev. 136, 346 (1964).

COMPLEX REFRACTIVE INDEX OF A MAGNETOPLASMA

J.Basu
Saha Institute of Nuclear Physics, Calcutta

INTRODUCTION

In microwave diagnostics of a magnetoplasma, using the free-space method(1), the basic quantities measured are the complex reflection and transmission coefficients of a microwave beam incident normally on the plasma. These quantities can easily be related to plasma parameters, such as N, ν and H, by plotting the complex refr-active index n on a Smith chart. Results are reported in the paper, giving n on a Smith chart for a few typical values of ν and for two orientations of H that are generally found in laboratory experiments on plasma, -viz., longitudinal and transverse to the direction of wave propagation.

COMPLEX REFRACTIVE INDEX

n is given by the well - known appleton-Hartree formula (2) based on the magneto-ionic theory. The same formula follows from the conductivity tensor of a magnetoplasma (3), derived from Boltzmann's equation, assuming that collision frequency of electrons is independent of electron velocities.

Since the permeability of the medium can reasonably be taken to equal to that of free space, n plotted on a Smith chart gives directly, as shown in Fig. 1(a), ρ and τ for an electromagnetic wave incident normally from free space on to a semi-infinite magneto-plasma and vice versa (4). The coefficients for a finite plasma can be interpreted in terms of those for a semi-infinite one (5)

REFLECTED, TRANSMITTED AND ABSORBED POWER

For a semi-infinite magnetoplasma the power reflected, normalized with respect to the incident power, is

$$p_r = \frac{(1-n')^2 + n''^2}{(1+n')^2 + n''^2} \tag{1}$$

The normalized transmitted power in the magnetoplasma at a distance d from the boundary is given by

$$p_t = 4n' e^{-2\beta_0 n'' d} \Big/ (1+n')^2 + n''^2 \tag{2}$$

where β_0 is the phase-change coefficient in free space.

The power absorbed by the medium between any two distances d_1 and d_2 from the boundary is, when normalized,

$$p_a = \frac{4n'}{(1+n')^2 + n''^2} \left(e^{-2\beta_0 n'' d_1} - e^{-2\beta_0 n'' d_2} \right) \tag{3}$$

ZERO COLLISION FREQUENCY

For the ordinary (O-) wave in both the longitudinal (L) and Transverse (T) cases n is confined to the contour ONQM in Fig. 1(a).

For the extra-ordinary (E-) waves, n may be extended to the line OM as well, when the magnetoplasma acts like an ordinary dielectric. This happens if $\omega_c \geqslant \omega$ in L case and if $1-(\omega_c/\omega)^2 \leq N/N_c \leq 1$ (or, in other words, $\omega_c^2 + \omega_p^2 \geqslant \omega^2 \geqslant \omega_p^2$) in T case. The magnetoplasma acts not only as a high-pass filter but also as a low-pass filter in the first case, the cut - off frequency being $\omega = \omega_c$, and as a band-pass filter in the second case, the cut-off frequencies being $\omega = \frac{1}{2}[\sqrt{(\omega_c^2 + 4\omega_p^2)} - \omega_c]$ and $\omega = \sqrt{\omega_c^2 + \omega_p^2}$. There are two interesting features of n, illustrated in Figs.1 (b) and (c), which do not appear to have been pointed out in the past.

FINITE COLLISION FREQUENCY

If ν is very high so that $\nu \gg \omega$ and $\nu \gg \omega_p$, n can, to a good approximation, be represented by the point O in Fig. 1(a).

For an intermediate frequency n lies somewhere in the upper half of the Smith chart. n has been plotted on simplified versions of this half for

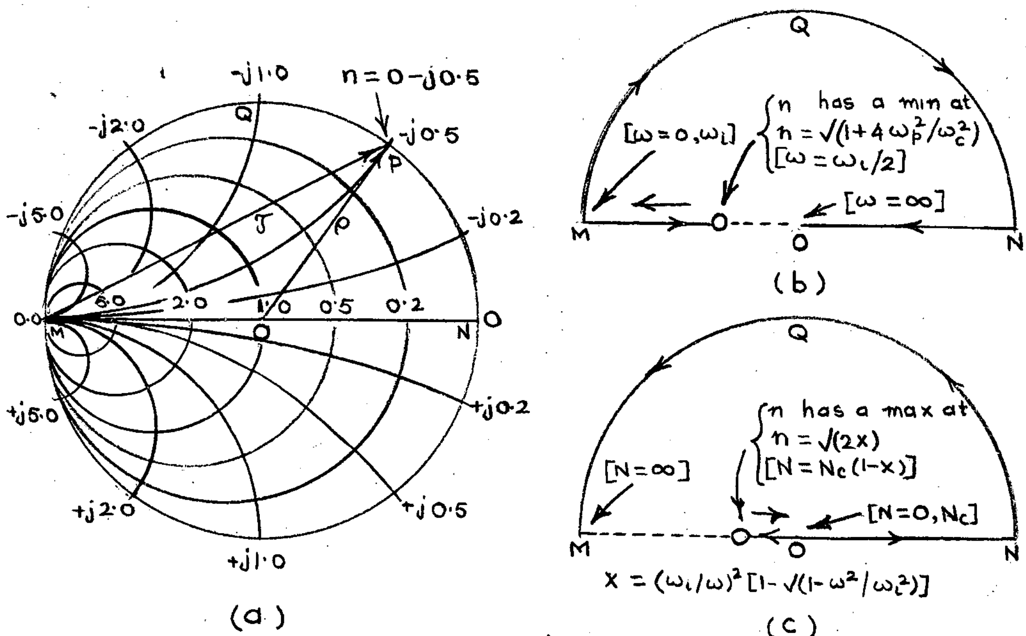

-j1·0
n = 0-j0·5
-j2·0
Q
-j0·5
P
-j5·0
-j0·2
5·0
2·0
1·0
0·5
0·2
0·0
M
O
N
O
+j5·0
+j0·2
+j2·0
+j0·5
+j1·0
(a)
Q
n has a min at
[ω = 0, ω_i]
n = √(1+4 ω_p²/ω_c²)
[ω = ω_i/2]
[ω = ∞]
M
O
N
(b)
Q
n has a max at
n = √(2x)
[N = ∞]
[N = Nc (1-x)]
[N = 0, Nc]
M
O
N
x = (ω_i/ω)² [1 - √(1- ω²/ω_i²)]
(c)

Fig. 1.

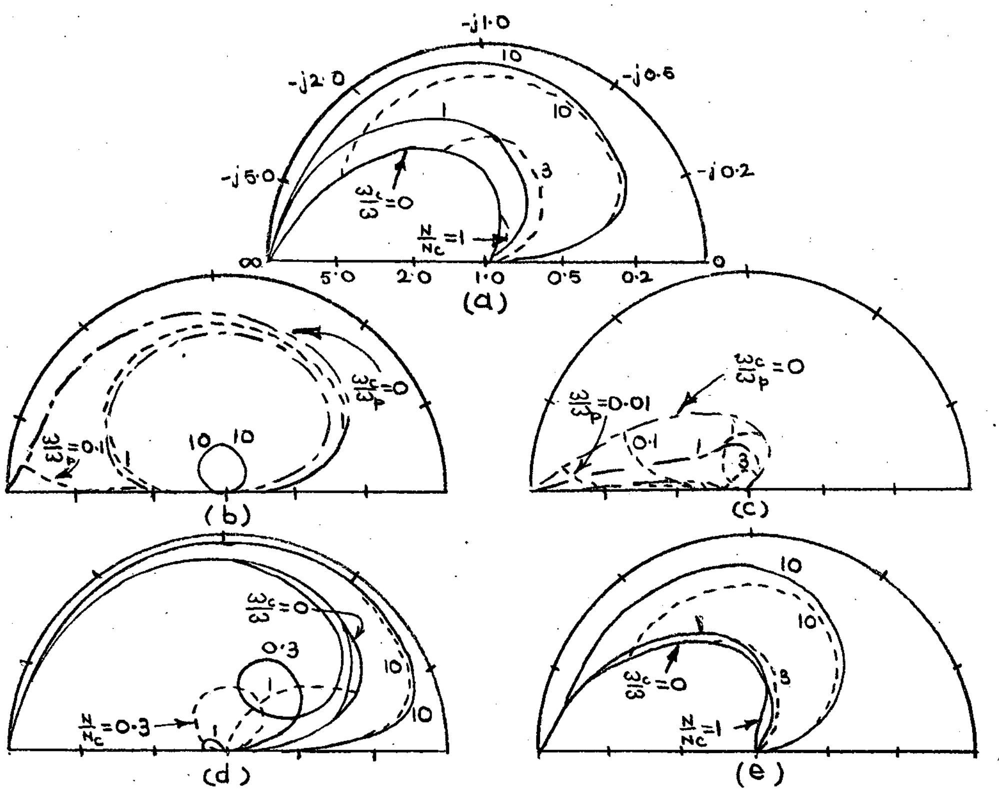

-j1·0
10
-j2·0
-j0·5
10
1
-j5·0
3
-j0·2
ωc/ω = 0
N/Nc = 1
∞
5·0
2·0
1·0
0·5
0·2
0
(a)
ωc/ωp = 0
ω/ωp = 0.1
1
10
10
(b)
ωc/ωp = 0
ω/ωp = 0·01
0·1
1
3
(c)
ωc/ω = 0
0·3
1
10
N/Nc = 0·3
10
1
(d)
10
10
1
3
ωc/ω = 0
N/Nc = 1
(e)

Fig. 2.

a few typical values of ν. The selected loci shown in Fig. 2 are obtained by varying one of the parameters N, H and ω, from zero to infinity while the other two are kept fixed. For O-wave, T case, n is given by the curves corresponding to $\omega_c = 0$. A few interesting features of the loci are noted below.

Consider O-wave, L case. As the magnetic field is increased, there is a decrease in n", indicating thereby that the attenuation in the plasma is reduced.

Referring to E-waves, each of n" and $|\rho|$ has a maximum at cylotron resonance in L case while each has a dip at plasmaresonance in T case. These are appreciable if ω_c is of the same order as ω_p (or ω_c) and $\nu < \omega_p$ (or ω).

CONCLUDING REMARKS

If any plane wave is incident normally on a magnetoplasma in a direction longitudinal or transverse to the static magnetic field, it can be resolved into components corresponding to the characteristic waves, and the plasma can then be studied with the help of the results given in the paper.

The refractive index, as used, was derived on the assumption that the electron motion is damped only due to collisions. Other causes of damping may also be taken into account by replacing ν by $\nu + \delta$, where δ is the damping factor due to causes other than collision. (1).

The effect of ion cyclotron resonance is neglected in the derivation of n. This introduces an error, which, however, is inappreciable except very near the resonant condition.

LIST OF PRINCIPAL SYMBOLS

H = Static magnetic field of a magnetoplasma.

N = Number density of electrons.

N_c = Critical number density.

n = $n' - jn''$ = Complex refractive indx

ν = Electron collision frequency.

ρ = Complex reflection coefficient.

τ = Complex transmission coefficient.

ω = Angular wave-frequency.

ω_c = Cyclotron frequency for an electron.

ω_p = Plasma frequency.

REFERENCES

1. J.E., Drummond, 'Plasma Physics' (McGraw-Hill, 1961), p.307.
2. J.A. Ratcliffe, 'The Magneto-Ionic Theory and Its Applications to the Ionosphere' (Cambridge University Press, 1959), p.19.
3. D.C. Kelly, Phys. Rev., Vol. 119, 1960 p.32.
4. G.R., Nicoll, and J. Basu, Proc. I.E.E. Vol. 109, Part C, 1962, p 335.
5. J. Basu, Indian J. Physics., Vol. 38, 1964, p.435.

LOSS OF THE FAST NEGATIVE IONS IN ATOMIC COLLISIONS

S. B. Karmohapatro
Saha Institute of Nuclear Physics, Calcutta

A negative ion may lose electrons in the following ways:

$$A^- + B \rightarrow A + B^- \qquad (1)$$

$$A^- + B \rightarrow A^+ + 2e + B \qquad (2)$$

$$A^- + B \rightarrow A + e + B \qquad (3)$$

where A and B are atoms or molecules with a positive electron affinity.

In the present work, we have calculated the cross sections of process (1) for the negative chlorine ion in atomic chlorine, e.g.

$$Cl^- + Cl \rightarrow Cl + Cl^- \qquad (4)$$

in the energy range between 25 ev and 90 KeV by the inpact parameter method similar to that used by Gurnee and Magee (7). The method has been applied by different authors to the similar processes (8-12) involving positive ions and excitation transfer processes.

METHOD

The impact parameter method differs from the wave treatment in atomic collision problems in the way that in the impact parameter treatment the internal motion of the associated electron is considered wave mechanically and the external motion or the motion of the heavier particles are considered classically; whereas both the motions are wave mechanical in wave treatments. In impact parameter treatment it is possible for

$$\lambda \ll a_0 \qquad (5)$$

where λ is the de Broglie wave length and a_0 is the Bohr radius.

The conditions assumed in the treatment are

$$R_0 M v \gg \hbar \qquad (6)$$

$$R_0 \Delta p \gg \hbar \qquad (7)$$

where M is the mass and ϑ the velocity of the ion. Δp is the momentum transfer in collision. $\Delta p \sim \frac{V}{\vartheta}$, where V is the effective potential energy of interaction. The paths of the ions are assumed tobe straight, so that

$$v\,dt = dx \tag{8}$$

in the direction of the fast beam.

The transition probability for the reaction (4) in the impact parameter method, is given by (7)

$$P(R_0) = \sin^2 \int_{-\infty}^{+\infty} 1/\hbar\vartheta \cdot H'_{fi} \cdot dx \tag{9}$$

and the total cross section is given by

$$Q = 2\pi \int_0^{\infty} P(R_0)\, R_0\, dR_0 \tag{10}$$

In this model, to evaluate the exchange integral H'_{fi}, we use the interaction Hamiltonial

$$H' = \frac{1}{R} - \frac{1}{r_l} \tag{11}$$

where R is the distance between the nuclei of Cl^- and Cl, r_l is the distance between the nucleus of the chlorine atom and the electron of Cl^- ion.

H' operated on

$$\Psi_{if} = A_1 \exp(-a_1 r_{ab}) \tag{12}$$

gives

$$H'_{fi} = \frac{S(R)}{R} - J(R) \tag{13}$$

where the matrix elements

$$S(R) = \langle a|b\rangle,\ J(R) = \langle a|\frac{1}{r_b}|b\rangle$$

and $A_1 = 0.9958$, $a_1 = 0.13472$

Suffixes a, b are for the initial and final states.

We have used the first one term of the analytical wave function of Cl^- given by Lowdin and Appel (13) as give above

The integral (13) is solved in the usual way and we have

$$H'_{fi} = \sum_{\nu=-1}^{5} A_\nu R_0^\nu \left(\frac{2\pi R_0}{a_1}\right)^{1/2} \exp(-a_1 R_0) \tag{14}$$

RESULTS

For different values of the velocity of Cl^- ions, $P(R_0)$ is computed from (9). Q is calculated by solving (10) by graphical method. Fig. 1 shows the values of Q in units of $A^{\circ 2}$ for the reaction (4) in the energy range between 25 ev to 90 KeV.

DISCUSSION

So far no experimental data are available to compare our theoretical results. From Fig. 1, it is evident that the variation of Q with energy shows a symmetrical resonance behaviour predicted by the adiabatic hypothesis and this agrees to the nature of the similar curve for H^- in H given by Dalgarno and McDowell (5). Again values of Q are higher than those of similar reactions involving positive ions. It may be attributed to the diffuse structure of the negative ion. In case, where copious negative ions can be produced, this type of reaction seems to be a good source for producing fast neutral atoms, required in some experiments (14) because of the high cross section of the present type of reaction. For the present reaction of Cl^- in Cl, the cross sections are even higher than those (13) for H^- in H for the same energy. Generally, for similar reactions involving positive ions, the cross sections increase with decreasing ionization potential (16) of the system. But it is otherwise for Cl^- in Cl reaction which has a higher cross section value than H^- in H for the same energy, though the electron affinity for H^- is much lower than that of Cl^-. As regards the nature of the electrons forming negative ions, these results show departure from the nature of the binding of electrons in atoms, in general. More such data on negative ion-atom collisions will determine this difference in the nature of the binding of the electrons in the formation of the negative ions.

However, for experimental verification of the reaction (4) the method used by Hummer et al (3) may be applied. More such experimental results

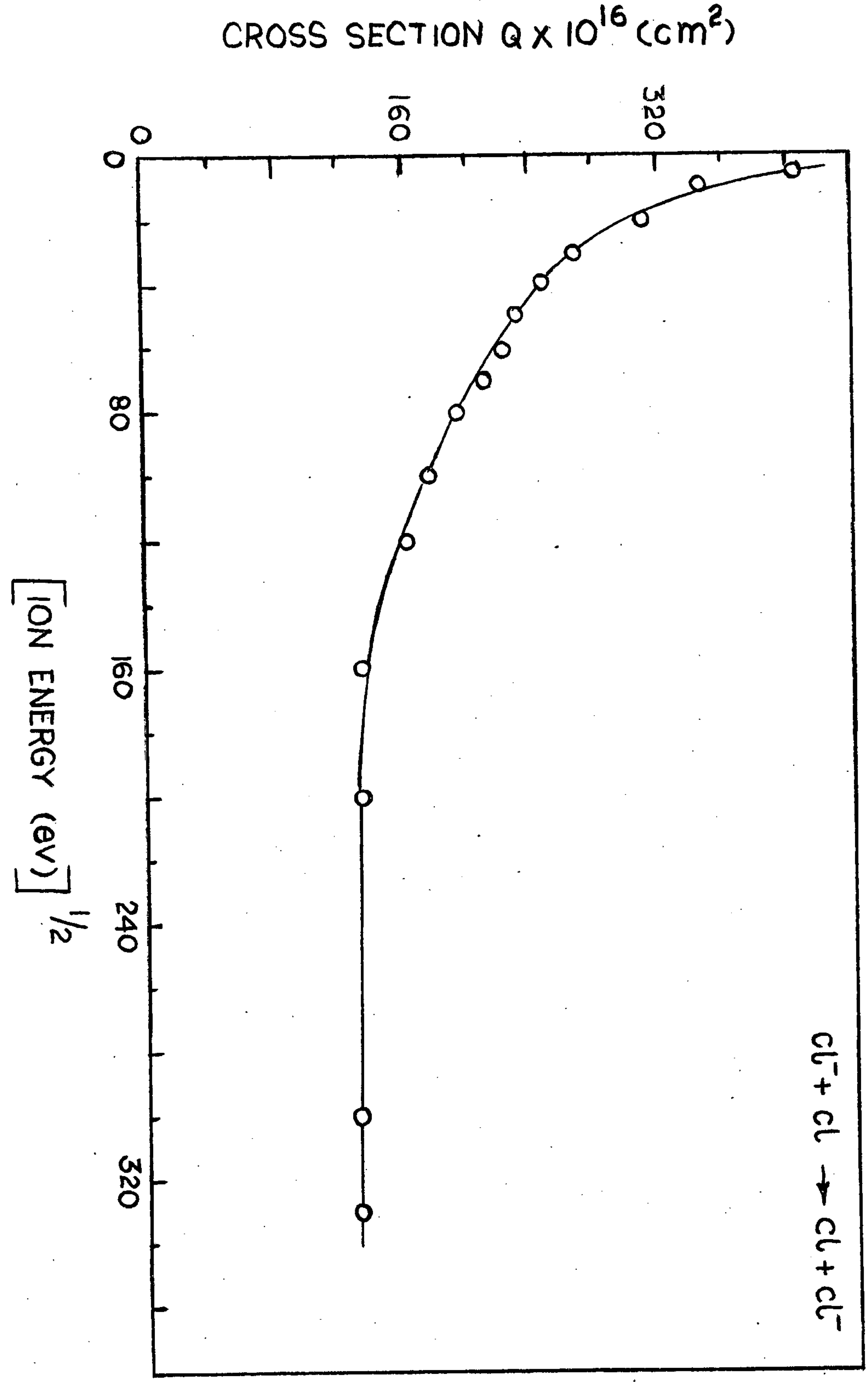

CROSS SECTION Q x 10^16 (cm^2)
0
160
320
0
80
160
240
320
[ION ENERGY (ev)]^1/2
Cl⁻ + Cl → Cl + Cl⁻

will evidently explain the general trend of the negative ions.

REFERENCES

1. V.M. Dukelskii, and N.V. Fedorenko, Soviet Physics - JETP 2, 307 (1955). Fogel et al-Zh. eksper. Teor. Fiz. 32, 453 (1957).
2. J.B. Hasted, Proc. Roy. Soc. A 212, 235 (1952). Y.F. Bydin and V.M. Dukelskii -Zh. eksper Teor. Fiz. 31, 474 (1957).
3. David G. Hummer, R.F. Stebbings, W.L. Fite, L.M. Branscomb, Phys. Rev. 119, 668 (1960).
4. M.R.C. McDowell and G. Peach, Proc. Phys. Soc. 74, 463 (1959).
5. A. Dalgarno and M.R.C. McDowell, Proc. Phys. Soc. 69A 615 (1956). D.W. Uida, Proc. Phys. Soc. 68A 240 (1955).
6. C.D. Moak, Nucl. Inst. Meth., 28, 155(1964).
7. E.F. Gurnee and J.L. Magee, J. Chem. Phys. 26, 1237 (1957).
8. D. Rapp and W.F. Francis, J. Chem. Phys. 37, 2631 (1962).
9. D. Rapp and I.B. Otenburger, J. Chem. Phys. 33, 1230 (1960).
10. S.B. Karmohapatro and T.P. Das, J. Chem. Phys. 29, 240 (1958).
11. S.B. Karmohapatro, J. Chem. Phys. 30, 583 (1959); Proc. Phys. Soc. (London) 76, 416 (1960).
12. M. Mori, T. Wantbe and K. Katsuura. J. Phys, Soc. (Japan) 19, 380 (1964).
13. P.O. Lowdin and K. Appel, Phys. Rev. 103, 1746 (1956).
14. P.H. Rose, Nucl. Inst. Meth. 28, 146 (1964).

DISCUSSIONS

A.K. Saha: Is not there a possibility of a real Cl_2^- molecule being formed? What is the Probability?

S.B. Karmohapatro: Probability will be very very small.

A.K. Saha: In the cross section calculations ~~there~~ is a possibility that a intermidiate virtual state of Cl_2^- contributing. In that case molecular wave functions with charge shielding will be necessary?

S.B.K: In the present two-state approximation method we have neglected it.

PROBE MEASUREMENTS OF A COLD CATHODE PENNING DISCHARGE

D.K. Bose, B. D. Nagchaudhuri and S.N. Sen Gupta
Saha Institute of Nuclear Physics, Calcutta.

It has long been recognised that the usual Langmuir probe when applied to a gas discharge plasma produces plasma disturbance which may affect the quantities intended to be measured with the help of the probe. In order to make probe measurements more dependable Johnson and Malter(1) have deviced a double probe technique in which two nearly identical Langmuir-type probes are kept floating with respect to the discharge voltage and are fed by a separate voltage source. The double probe does not require to draw any part of the discharge current for its operation and hence it causes less plasma disturbance. By making use of the floating double probe technique we have studied the plasma parameters, electron temperature Te, electron and ion densities ne, ni, etc., in a cold cathode Penning discharge. The Penning tube was operated with argon at different pressures and in magnetic field of different strengths. In what follows we give a brief account of some of the results of our probe study.

The double probe current voltage (i_d vs. V_d) characteristic curves for various values of gas pressure and magnetic field were obtained in the usual manner. From each characteristic curve a corresponding plot of $\ln\left(\frac{\sum i_p}{i_e} - 1\right)$ vs. V_d (where $\sum i_p$ is the total ion current in the two probes and i_e is the electron current in one probe for the voltage V_d) was obtained. The slope of the semi logarithmic plot then gave the corresponding electron temperature Te. Table I gives our experimental values of Te in different discharge conditions. It appears from the table that the electron temperature increases slowly with the increase of magnetic field and gas pressure. Using the measured values of Te in the expressions for ion and electron currents (2) collected by the probe the values of ne, ni were then obtained.

TABLE I

Experimental values of electron temperature Te for different magnetic field and gas pressure

Magnetic field (Gauss)	1000	1400	1700
Electron Temp. Te (eV)	2.8	3.6	4.5
Pressure of argon ($\times 10^{-4}$ mm.Hg)	4	6	10
Electron Temp. Te (eV)	3.6	4.1	5.8

In determining the plasma parameters, Te, ne and ni from the double probe data it was necessary to assume a Maxwellian form of energy distribution for the discharge electrons. This assumption may not be valid for the case of Penning discharge as in that case there may appear a radial electric field which together with the applied magnetic field may cause the electron distribution to differ from the Maxwellian form. To determine the nature of the electron distribution in the Penning discharge, we have carried out a Druyvesteyn-type analysis (3) of current voltage data obtained by means of a single Langmuir probe. Druyvesteyn has derived the following expression for the electron distribution function:

$$f(V) = K V^{1/2} \, d^2 i / dV^2 \tag{1}$$

where $d^2 i/dV^2$ is the second derivative of the current-voltage characteristic, V is the probe potential with respect to the plasma K is a constant depending

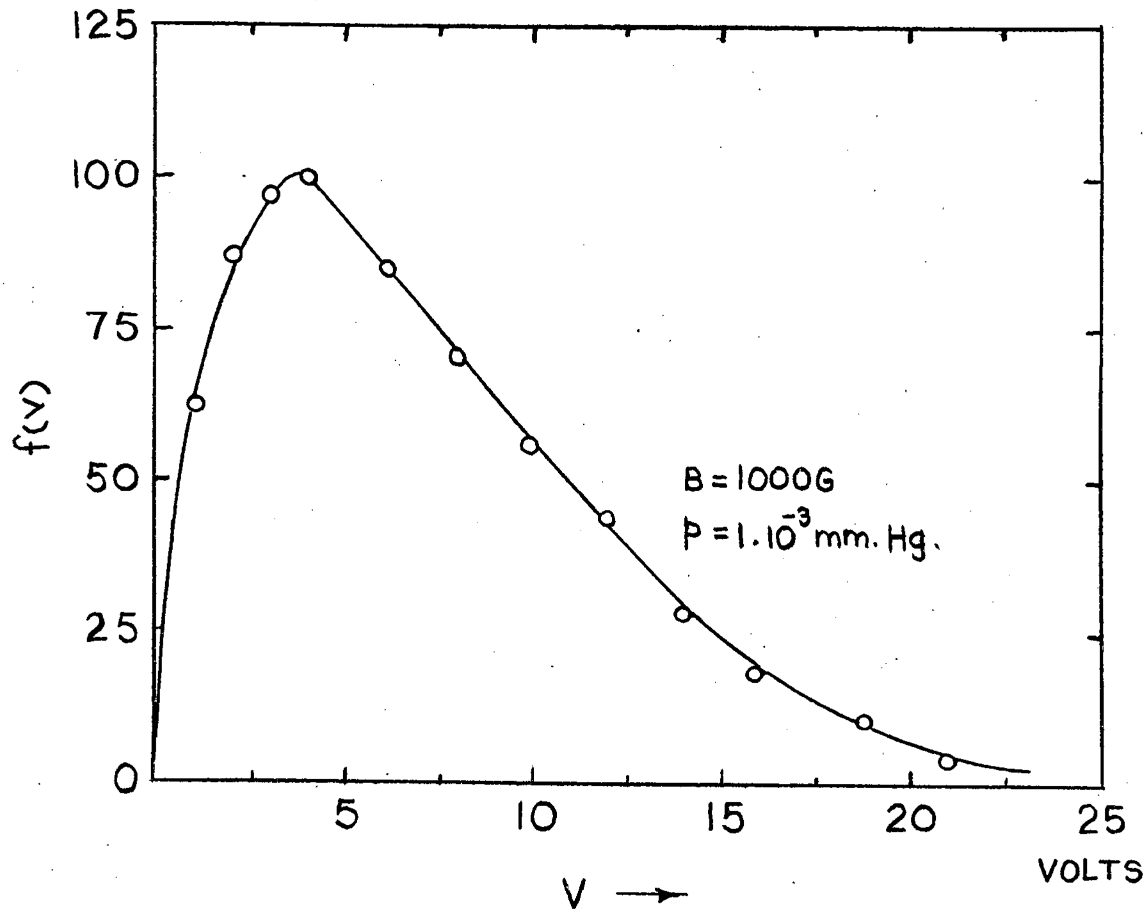

Fig. 1. ELECTRON ENERGY DISTRIBUTION.

on the probe area. We have computed the values of d^2i/dV^2 from the probe characteristic data by a procedure of double graphical differentiation as given by Aisenberg (4). In Fig.1 is shown the electron energy distribution in the case of Penning discharge. The points in Fig. 1 indicate the experimental distribution using Eq. (1) and the continuous curve gives the corresponding Maxwellian distribution . The experimental distribution agrees satisfactorilly with the expected Maxwellian distribution. It appears, therefore, that in the ranges of gas pressure and magnetic field in which we have operated the Penning discharge the electron energy distribution is Maxwellian and our procedure of evaluation of the plasma parameters, Te, ne and ni, is satisfactory.

REFERENCES

1. E.O. Johnson and L. Malter, Phys. Rev. 80, 58 (1950).

2. David Bohm, E.H.S. Burhop and H.S.W. Massey, in "The Characteristics of Electrical Discharge in Magnetic Field" Ed. by A. Guthrie and R.K. Wakerling, p.13, (1949).

3. M.J. Druyvesteyn, Zeit. f.Phys. 64, 790 (1930).

4. S. Aisenberg, Jour. Appl. Phys. 35, 130 (1964).

ON THE SET-UP OF DUOPLASMATRON FOR AN INTENSE ION BEAM

D.K.Bose, N.K. Majumdar and B.D. Nagchaudhuri

INTRODUCTION

Duoplasmatron is a sophisticated type of ion source (1-5) which can give a hundred milli-ampers of proton current or more from an emission aperture of 1-2 m.m. diameter, and reaching almost 100% efficiency in gas ionisation.

DESCRIPTION

It is essentially a low pressure arc discharge in a magnetic field parallel to the electric field. The extracted ion current density J^+ follows the proportionality $\vec{J}^+ \propto n^+$ where n^+ is the ion density in plasma and in turn the rate of production of n^+ is given by

$$\frac{dn^+}{dt} \propto \vec{J}_e$$

$\vec{J}_e$ is the electron current density in the Source Chamber. Here the discharge burns between a large area filament and the water-cooled anode through a capillary - 4.m.m. diameter. There is an axial inhomogeneous magnetic field which not only traps the electrons but constrains them to oscillate back and forth in the inter-anodic space. Recently this oscillation has been shown by Popov (6) to be the cause of the high degree ionisation as also high percentage of monatomic ions (40-80%) in this source. Extremely high density plasma, leaks through the emission aperture to the extraction chamber.

EXTRACTION

For the extraction of 100 ma of proton current the discharge level

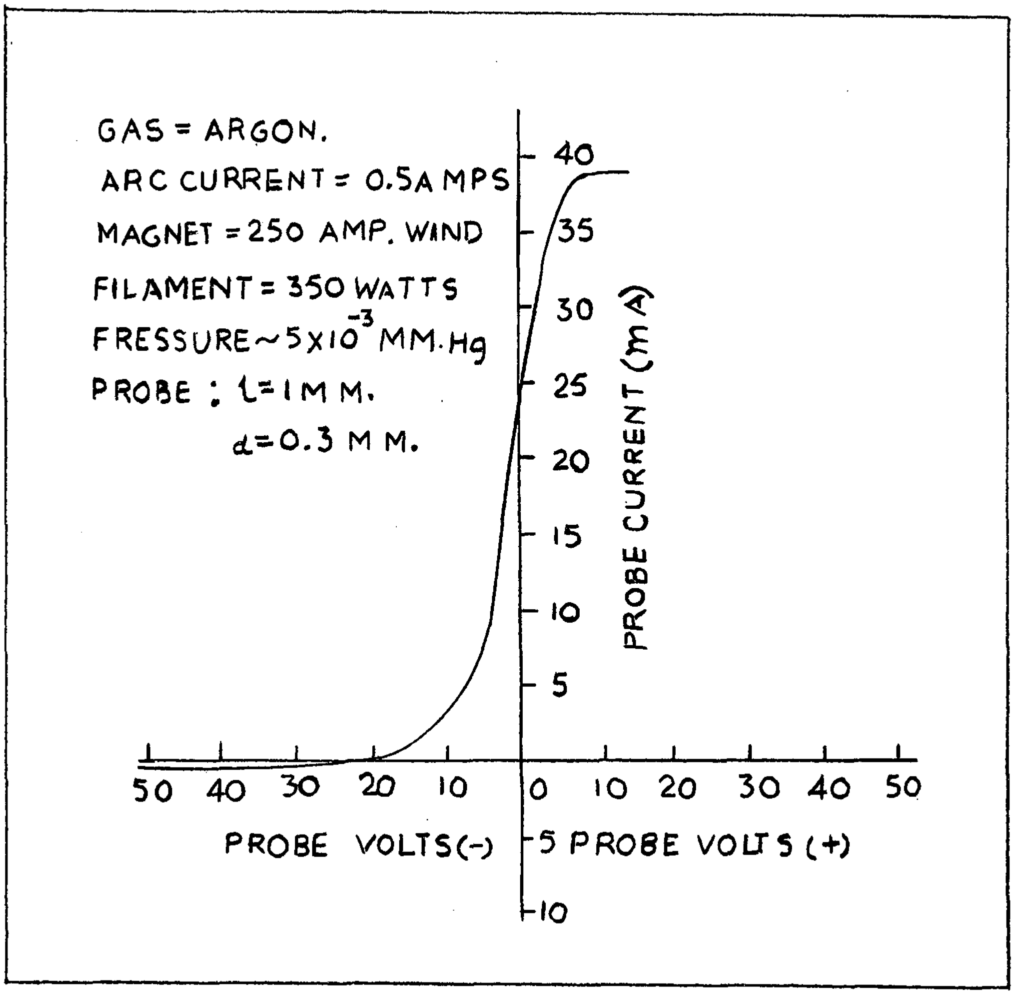
GAS = ARGON.
ARC CURRENT = 0.5AMPS
MAGNET = 250 AMP. WIND
FILAMENT = 350 WATTS
FRESSURE ~ 5X10^-3 MM.Hg
PROBE : l = 1 MM.
d = 0.3 MM.
40
35
30
25
20
15
10
5
PROBE CURRENT (mA)
50 40 30 20 10
0 10 20 30 40 50
PROBE VOLTS(-)
5 PROBE VOLTS (+)
10

Fig. 1.

is maintained at $n_e \simeq 10^{14}$ and a high extraction field given by-60 Kv across 3 mm is prescribed according to conventional extraction principle. This high value is required to over-come space charge effects in the ionic beam, which has a natural dispersion in a field free space. Further, it expands the plasma emission surface by giving it a concave shape. This high potential gradient obviously limits the dimension of emission opening that can keep the difference of vacuum and hence the ultimate beam current obtainable.

The conditions of extraction and focussing as adopted by Lamb et al (7), Gabovich (8), Demikharnov (9) etc. are less stringent. Here the plasma is allowed to emerge out through a larger opening or a ring of openings and ions are extracted from the expanded plasma surface by an application of a moderate value of electric field gradient and collimated by a magnetic lens system.

We have used for extraction a voltage supply of -12 KV which would satisfy the field requirement of the latter method of extraction. But while the source is operated at n_e less than 10^{14}, this value may be quite sufficient to overcome the existing space charge dispersive forces. This has been sampled by a series of runs with the source at different levels of arc current. The results are given in the following table.

Gas : Argon

Pressure $p = 5 \times 10^{-3}$ Tor.

Acceleration voltage = - 8 K.V. acc.

3 m,m. gap.

TABLE

Arc. Current amps	Extractor current mA	Extracted current mA
0.5	0*	2.5
1.0	3	2.5
1.5	5	2.5
2.0	6.5	2.5

We find that at arc current 0.5 amp ($n_e \simeq 10^{13}$), the extractor loss is negligible. But for increase of n_e with higher values of arc current, the extraction field is in-sufficient and extractor loss increases. We note that argon current of 2.5 ma is about equivalent to 15 ma of proton.

DETERMINATION OF ELECTRON TEMPERATURE Te AND ELECTRON DENSITY n_e AND ION DENSITY n^+.

A probe has been inserted just below the emission opening. The current collected by the probe corresponding to its voltage applied is plotted (Fig .1).

Assuming Boltzmann distribution it is known that

$$i_e = i_{re} \exp(-eV/kT_e)$$

i_e = electron current collected by probe

i_{re} = random electron current in plasma

T_e = average electron temperature

V = p.d. between the plasma and the probe

e = electronic charge. Hence Te can be calculated and from Te

* Meter scale calibration - 0.5 amp per division.

n_e and n^+ can be determined. We obtained.

Te $\gtrsim$ 10 e.v. and $n_e \gtrsim 6 \times 10^{12}$ per cc. and $n^+ \gtrsim 8 \times 10^{12}$ per cc.

Probe method (10, 11) will be utilised to find further informations of the plasma.

REFERENCES

1. New development in applied ion and nuclear physics by Manfred Von Ardenne, AERE, Harwell, Report No. 758.
2. Manfred Von Ardenne, A.E. R.E., Harwell, Vol. 39, Report No. 898.
3. Tabellenbuck Electronenphysik, Ionen, Physik, Ubermikroskopie, Vol. 1, Deutscher Verlaz der Wissenschaften, Berlin, (1956).
4. C.D. Moak, et al, R.S. I. 30, 694 (1959).
5. J. Kistemaker, Nucl. Instr. and Methods, 11, 179 (1961).
6. S.N. Popov, Pribori i teknika eksperimenta, No. 4 , p. 20-24, (1961).
7. William A.S. Lamb and Edward J. Lofgren, R.S.I., 27, 907 (1956).
8. Gabovich et al, Sov. Tek. Phys. 31, 87 (1961).
9. R.A. Demirkhanov et al, Instruments & Experimental techniques No. 2 March -April, (1964).
10. Langmuir and H-Mall, Gen. Elec. Rev., 27, 449, 538, 616, 762, 810 (1924).
11. D. Bohm, E.H.S. Burhop, H.S. W. Massey in the "Characteristics of Electristics of Electrical discharges in magnetic fields" by A. Guthrie and R.K. Wakerling (1949).